

Copyright © and Moral Rights for this thesis and, where applicable, any accompanying data are retained by the author and/or other copyright owners. A copy can be downloaded for personal non-commercial research or study, without prior permission or charge. This thesis and the accompanying data cannot be reproduced or quoted extensively from without first obtaining permission in writing from the copyright holder/s. The content of the thesis and accompanying research data (where applicable) must not be changed in any way or sold commercially in any format or medium without the formal permission of the copyright holder/s.

When referring to this thesis and any accompanying data, full bibliographic details must be given, e.g.

Thesis: Author (Year of Submission) "Full thesis title", University of Southampton, name of the University Faculty or School or Department, PhD Thesis, pagination.

Data: Author (Year) Title. URI [dataset]

UNIVERSITY OF SOUTHAMPTON

FACULTY OF OCEAN AND EARTH SCIENCE

Discerning the interacting effects of phytoplankton blooms and temperature anomalies on the relationship between algal symbionts of the genus *Symbiodinium* and their reef coral hosts in the Arabian Gulf

by

Dawoud A. Sheail

Thesis for the degree of Doctor of Philosophy

August 2017

UNIVERSITY OF SOUTHAMPTON

ABSTRACT

FACULTY OF NATURAL AND ENVIRONMENTAL SCIENCES

OCEAN AND EARTH SCIENCE

Thesis for the degree of Doctor of Philosophy

Discerning the interacting effects of phytoplankton blooms and temperature anomalies on the relationship between algal symbionts of the genus *Symbiodinium* and their reef coral hosts in the Arabian Gulf

Dawoud Ajeel Sheail

Coral reefs are among the most threatened ecosystem worldwide, partly due to the sustained and continuing effects of global climate change. The coral from the Arabian/Persian Gulf (hereafter “the Gulf”) are exposed to several extreme environmental factors. This thesis reports on the understanding of how local climate factors modulate the tolerance of the algal symbionts to thermal stress in the Gulf. *In situ* measurements, remote sensing data and meteorological variables were used as tools to determine anomalies and trends of different environmental factors focusing on three regions within the southern Gulf, Delma (latitude 24.5208/longitude 52.2781), Saadiyat (lat. 24.599/long. 54.4215) and Ras Ghanada (lat. 24.8481/long. 54.6903) over the period from 1982 to 2015. A severe bleaching event affected coral communities off the coast of Abu Dhabi, UAE in August and September, 2012. In Saadiyat and Ras Ghanada reefs ~40% of the corals showed signs of bleaching whereas, only 15% of the corals were affected on Delma reef. The work presented in this thesis shows that, in spite of their proximity, there were differences in the severity of local bleaching between the sites (Ras Ghanada=34.48 °C, Saadiyat=34.55 °C, Delma= 35.05 °C). The result also suggests that phytoplankton density in Saadiyat during 2012 bleaching event might have temporarily reduced certain nutrients, such as nitrate and phosphate, below average levels leading to a reduced availability of these essential nutrients to the corals. In the study regions, the seasonal chl-*a* cycle was characterised with

a summer maximum and a winter minimum. The results also show that positive anomalies of dust are likely to be observed one to two months before the emergence of a phytoplankton bloom. This study shows that the combination of satellite observations and *in situ* measurements can help generate detailed insights into coral bleaching events. The 2010 bleaching event was accompanied by a phytoplankton anomaly that spread over a wider Gulf area. The thesis highlights the needs of integrating different observation platforms to establish an integrated monitoring water quality system in the Gulf, in particular around coral reefs.

Table of Contents

ABSTRACT	i
Table of Contents	iii
List of Tables	vii
List of figures	viii
DECLARATION OF AUTHORSHIP	xii
Acknowledgements	xiii
Abbreviations	xiv
Chapter 1: Introduction	1
1.1. Introduction	1
1.2. Thesis hypothesis	2
1.3 Scientific background	3
1.3.1 Coral reefs	3
1.3.2 Relationship between the coral and its algal symbiont	4
1.3.3 Environmental factors influencing the algal symbiont and the coral host ..	4
1.3.3.1 Water temperature	5
1.3.3.2 Phytoplankton bloom	6
1.3.3.3 Wind	8
1.3.3.3.1 Dust storms	9
1.3.3.3.1.1 Dust composition	12
1.3.3.4 Water currents	14
1.3.4 The study region	15
1.3.4.1 Water temperature	17
1.3.4.2 Phytoplankton blooms	19
1.3.4.3 Wind patterns	21
1.3.4.3.1 Dust storms in the Arabian Peninsula	22
1.3.4.4 Water circulation	24
1.3.5 Coral diversity in the Southern Gulf (Abu Dhabi)	25

1.3.6	Coral bleaching events in the Gulf	26
1.4	Study sites	35
1.4.1	Delma	36
1.4.2	Saadiyat	37
1.4.3	Ras Ghanada	37
1.5	Reference sites	38
1.5.1	Kuwait	38
1.5.2	Kingdom of Saudi Arabia (KSA)	39
1.5.3	Bahrain	39
1.5.4	Qatar	40
1.5.5	Iran	40
1.5.6	Oman	41
1.6	Remote sensing as a monitoring tools for coral reef environment	41
Chapter 2: Local bleaching thresholds established by remote sensing techniques vary among reefs with deviating bleaching patterns during the 2012 event in the Arabian/Persian Gulf		49
2.1	Introduction	50
2.2	Material and methods	53
2.2.1	Measuring SST using remote sensing products	53
2.2.2	Reconstruction of daily temperature maxima <i>in situ</i>	54
2.2.3	Reconstruction of daily temperature maxima using remote sensing..... data.....	54
2.2.4	Calculation of bleaching threshold temperatures	56
2.2.5	Field surveys	56
2.3	Results	58
2.3.1	Local temperature thresholds of coral bleaching	58
2.3.2	Site-specific severity of the 2012 bleaching event	62
2.4	Discussion	64
2.5	Conclusion	66

2.6 Acknowledgments	67
Chapter 3: The role of temperature, phytoplankton, and nutrients on 2012 coral bleaching event in Abu Dhabi	69
3.1. Introduction	70
3.2. Material and methods	72
3.2.1. Study sites	72
3.2.2. Thermal stress analysis	73
3.2.3. Remote sensing analysis of chlorophyll- <i>a</i>	75
3.2.4. <i>In situ</i> and meteorological data measurements	76
3.3. Results and discussion	78
3.3.1. Regression analysis of the remote sensing data	78
3.3.2. Thermal stress during bleaching and non-bleaching years	78
3.3.3. Interannual anomalies of remote sensed chl- <i>a</i>	84
3.3.4. Comparative analysis of environmental condition in Saadiyat reefs in..... 2012 and 2015	84
3.4. Conclusions	90
Chapter 4: Long-term changes in the environmental factors surrounding coral reef..... sites in Abu Dhabi.....	91
4.1 Introduction	92
4.2 Material and methods	97
4.2.1 Study sites	97
4.2.2 Environmental data acquisition	98
4.2.2.1 Chlorophyll- <i>a</i>	98
4.2.2.2 Sea surface temperature (SST)	100
4.2.2.3 Aerosol optical thickness (AOT)	100
4.2.2.4 Water current speed (WCS)	101
4.2.2.5 Water turbidity	103
4.2.2.6 Meteorological data	104

4.2.2.7	Dipole mode index (DMI) and the El Niño Southern Oscillation (ENSO)	104
4.2.3	Regression analysis of the remote sensed data	105
4.2.4	Seasonality and interannual anomalies	106
4.2.5	Cross-correlation analysis	107
4.2.6	Regional coral bleaching thresholds	107
4.3	Result and discussion	109
4.3.1	Regression analysis of the remote sensed data	109
4.3.2	Seasonal variation	109
4.3.2.1	Chlorophyll- <i>a</i>	109
4.3.2.2	Diffusion attenuation coefficient (K_d490)	113
4.3.2.3	Sea surface temperature (SST)	114
4.3.2.4	Water current speed (WCS)	116
4.3.2.5	Aerosol optical thickness (AOT)	118
4.3.2.6	Air temperature	121
4.3.2.7	Horizontal visibility	123
4.3.2.8	Wind speed and direction	124
4.3.2.9	Precipitation	127
4.3.3	Interannual anomalies	128
4.3.4	Coral bleaching thresholds	146
4.3.5	Conclusion	148
Chapter 5:	Summary, conclusions and future research	149
5.1.	Summary and conclusions	149
5.2.	Recommendations for future work	151
Appendices	153
List of References	167

List of Tables

Table 2.1. Calculated bleaching threshold temperatures for the hottest weeks of the..... year.....	59
Table 2.2. Statistical analysis of site-specific differences in bleaching susceptibility. χ^2 = Chi-square value, df = degrees of freedom, P-value <0.05 indicates that the recorded proportion of bleached, partially bleached and non-bleached colonies is significantly dependent on the region	63
Table 2.3. Numbers of adult <u>Porites</u> spp. and <u>Platygyra</u> corals recorded along the transects in the different study sites	64
Table 2.4. Numbers of juvenile corals recorded along the transects in the different study sites.....	64
Table 3.1. Pearson correlation analysis between the <i>in situ</i> nutrients (nitrate, phosphate, iron, silicate), remote sensed chl=a (Saadiyat), meteorological visibility and wind. The underline correlation coefficient values (r) are significant with $p < 0.05$	86
Table 4.1. Summary of properties and sources of environmental data used in this study.	98
Table 4.2. Descriptive statistics for the environmental parameters in Delma, Saadiyat..... and Ras Ghanada obtained by remote sensing analysis	110
Table 4.3. Descriptive statistics for the meteorological parameters in Kuwait airport, Bahrain airport and Abu Dhabi airport	111
Table 4.4. Pearson correlation between the remote sensed parameter in Delma, Saadiyat and Ras Ghanada	115
Table 4.5. Pearson correlation between the meteorological data from Abu Dhabi airport	116
Table 4.6. Pearson correlation between the meteorological data and the environmental parameters obtained by remote sensing in Delma, Saadiyat and Ras Ghanada.....	116

Table 4.7. Cross-correlation analysis between of the environmental parameter against the chl-a in all study sites. R is the correlation coefficient	116
---	-----

List of Figures

Figure 1.1. The major dust sources in the world, including the Sahara Desert, the Taklamakan and Gobi deserts in East Asia and the Arabian Peninsula. Source: http://oceancolor.gsfc.nasa.gov	9
Figure 1.2. Dust fluxes to the world oceans based on studies that match satellite optical depth, <i>in situ</i> concentration, and deposition observations (Ginoux et al., 2001; Mahowald and Luo, 2003; Tegen et al., 2004). Source: Jickells, (2005)	10
Figure 1.3. Countries surrounded the Arabian Gulf. Including: Iraq, Kuwait, Saudi Arabia, Bahrain, Qatar, United Arab Emirates, Oman and Iran. Source: https://lance3.modaps.eosdis.nasa.gov	16
Figure 1.4. Sea surface water temperatures (SST) of the world during the summer period of 2010, 2011 and 2012. Show that the Arabian Gulf SST reaching 32-34 °C regularly during the summer period. Source: https://oceancolor.gsfc.nasa.gov/cgi/l3	18
Figure 1.5. Bloom events occurs in the Arabian Gulf during 2008. have been reported from Abu Dhabi, Dubai, Ajman, Fujairah, Iran and Oman during August 2008–May 2009. The picture of the right is MODIS-Aqua 1km resolution image showing remote sensed chl-a levels during August 2008 during the algal bloom event. Source : https://oceancolor.gsfc.nasa.gov	19
Figure 1.6. HAB incidents outbreaks since 2002 in Abu Dhabi. HAB have increased since 2002, according to observation and subsequent sample analysis by the MWQ Team. Source: EAD marine water quality report 2014	20
Figure 1.7. Major dust sources in the Arabian Peninsula. Including the Tigris and Euphrates Rivers, the alluvial plain in Iraq and Kuwait, and the Ad Dahna and the Rub Al Khali deserts. Source: https://lance3.modaps.eosdis.nasa.gov	22
Figure 1.8. General water circulation in the Arabian Gulf. Adopted from Riegl and Purkis, 2012	24

Figure 1.9. Study sites in UAE (Abu Dhabi) are Delma (lat. 24.5208/long. 52.2781), Saadiyat (lat. 24.599/long. 54.4215) and Ras Ghanada (lat. 24.8481/long. 54.6903)	36
Figure 1.10. Reference sites around the Arabian Gulf. Including: Kuwait, the Kingdom of Saudi Arabia (KSA), Bahrain, Qatar, Iran and the Gulf of Oman	38
Figure 1.11. Examples of Chl-a satellite images from the MODIS-Aqua sensor showing the average global distribution of chl-a during September 2012. Showing rich chl-a areas along the coasts and continental shelves. Moderate chl-a concentrations are found along the equator in the Atlantic and Pacific region, and in the subtropical convergence zone (red circle). Source: http://oceancolor.gsfc.nasa.gov	45
Figure 2.1. In situ temperature data recorded in hourly intervals at ~7m depth at the Saadiyat site. The graph shows the average temperatures and standard deviations calculated from the values obtained for the last week of August from the years 2013 and 2014	54
Figure 2.2. MODIS-Aqua data and the corresponding in situ temperature. Values were plotted against each other and the coefficient of determination (R^2) for a linear regression fit was calculated. Equations are given in the graphs	55
Figure 2.3. Time series of regional SST in the southern IRSA. SST values were obtained from MODIS-Aqua imagery from 2002-2014 for (a) Delma, (b) Saadiyat and (c) Ras Ghanada. The local bleaching thresholds (Delma: 35.05°C, Saadiyat: 34.55°C and Ras Ghanada: 34.48°C	55
Figure 2.4. Study sites and bathymetric map of the southern IRSA. Numbers identify the three study sites: (1) Delma, (2) Saadiyat and (3) Ras Ghanada. The map was constructed using Sea-viewing Wide Field-of-view Sensor (SeaWiFS) Ocean Color Data provided by NASA Ocean Biology (OB.DAAC). Gray-level scale defines the depth in meters	57
Figure 2.5. Variations in heat stress exposure during the 2012 bleaching event in the southern IRSA reconstructed from MODIS-Aqua imagery. a) Number of days during which the site-specific bleaching threshold temperatures (Delma: 35.05 °C,	

Saadiyat 34.55 °C, Ras Ghanada: 34.8 °C) were exceeded in each of the study sites.	
b) Days at which the site-specific local bleaching threshold was exceeded in the corresponding study sites, indicating also the length of the positive temperature anomaly	60
Figure 2.6. Site-specific composition of the coral community. a) Total number of juvenile (species indicated in the panel legend) and b) adult (<i>Porites</i> spp. and <i>Platygyra</i> spp.) corals recorded along the transects in the three study sites	60
Figure 2.7. Representative photographs of corals from the bleaching categories used in this study. (Image credits: J. Wiedenmann)	61
Figure 2.8. Site-specific severity of bleaching. Comparison of the percentage of the total numbers of juvenile and adult <i>Porites</i> spp. colonies and other species affected by bleaching	63
Figure 3.1. Remote sensing data comparison at Saadiyat site. Including a) AVHRR SST with in situ water temperature, b) MODIS-Aqua SST with AVHRR SST, c) MODIS-Aqua chl- <i>a</i> with the in situ chl- <i>a</i>	77
Figure 3.2. Thermal stress in Delma, Saadiyat and Ras Ghanada during 2009-2015. a) Days above the local thresholds, b) degree heating days (DHD), and c) Heating rates (HR)	79
Figure 3.3. Characteristics of environmental condition in Saadiyat reefs between 2009 and 2015. Including a) Air temperature anomalies, b) SST anomalies, c) MODIS-Aqua chl- <i>a</i> anomalies. Red lines indicate bleaching events and blue line indicate thermal stress, but no bleaching witnessed	83
Figure 3.4. Comparative analysis of environmental parameters in Saadiyat in 2012 and 2015, a) monthly mean SST, b) Monthly mean chl- <i>a</i> mg/m ³ . Symbols show average values calculated from 15 data points determined per months in each year. Error bars represent the standard deviation	85
Figure 3.5. Comparative analysis of environmental parameters in Saadiyat in 2012 and	

2015, a) monthly mean SST, b) Monthly mean chl-a mg/m ³ . Symbols show average values calculated from 15 data points determined per months in each year. Error bars represent the standard deviation	86
Figure 3.5. Meteorological data from Abu Dhabi Airport. Showing seasonality of a) visibility climatology (2009-2015) and b) wind speed climatology (2009-2015). And a comparison between monthly averages between c) 2012 and 2015 visibility, and d) 2012 and 2015 wind speed	89
Figure 4.1. Countries surrounded the Arabian Gulf. Including: Iraq, Kuwait, Saudi Arabia, Bahrain, Qatar, United Arab Emirates, Oman and Iran. Source: https://lance3.modaps.eosdis.nasa.gov	97
Figure 4.2. Samples of a major dust storms passing over the Arabian Gulf in the right panel (source: https://lance3.modaps.eosdis.nasa.gov/), matched with MODIS-Aqua AOT (111km ² resolution) in the left panel. source: http://giovanni.gsfc.nasa.gov	102
Figure 4.3. Study sites in the Arabian Gulf. A) Kuwait (Qaro island), b) Saudi Arabia (Abu Ali island) (KSA), C) Bahrain, D) Qatar, E) Delma, F) Saadiyat, G) Ras Ghanada, H) Iran, and I) Oman	108
Figure 4.4. Validation of data obtained by remote sensing analysis of a) diffusion attenuation (K_d490), and b) Aerosol optical thickness (AOT) at 550nm, c) chlorophyll-a (chl-a)	110
Figure 4.5. Comparing chl-a climatology obtained by MODIS-Aqua in Delma, Saadiyat and Ras Ghanada. Symbols shows average values during 1997-2015, error bars display standard deviation	112
Figure 4.6. Comparing the diffusion attenuation coefficient (K_d490) climatology obtained by MODIS-Aqua in Delma, Saadiyat and Ras Ghanada. Symbols show average values during 1997-2015, error bars display standard deviation	114
Figure 4.7. Comparing the sea surface temperature (SST) climatology obtained by MODIS-Aqua in Delma, Saadiyat and Ras Ghanada. Symbols show average values during	

1997-2015, error bars display standard deviation	115
Figure 4.8. Comparing the climatology of water current speed obtained by OSCAR in Delma area and Saadiyat/Ras Ghanada area. Symbols show average values during 1992-2014, error bars display standard deviation	118
Figure 4.9. Comparing the climatology of Aerosol optical thickness in Delma and area, Saadiyat/ Ras Ghanada area. Symbols show average values during 1997-2015, error bars display standard deviation	120
Figure 4.10. Comparing air temperature climatology from Abu Dhabi, Kuwait and Bahrain airports. Symbols show average values during 1983-2015, error bars display standard deviation	122
Figure 4.11. Comparing horizontal visibility climatology from Abu Dhabi, Kuwait and Bahrain airports. Symbols show average values during 1983-2015, error bars display standard deviation	123
Figure 4.12. Comparing wind speed climatology from Abu Dhabi, Kuwait and Bahrain airports. Symbols show average values during 1983-2014, error bars display standard deviation	124
Figure 4.12. Comparing wind speed climatology from Abu Dhabi, Kuwait and Bahrain airports. Symbols show average values during 1983-2014, error bars display standard deviation	126
Figure 4.14. Comparing precipitation climatology from Abu Dhabi, Kuwait and Bahrain airports. Symbols show average values during 1983-2015, error bars display standard deviation	127
Figure 4.15. Long-term anomalies of environmental parameters in <u>Delma</u> site, calculated from remote sensing data. Including a) temperature, b) chl-a, c) water current speed, d) attenuation coefficient (K_d490), and f) aerosol optical thickness (AOT). The vertical red lines indicate the bleaching events, the broken line curves display a fourth order polynomial trend. The equations and R^2 values of the regression	

curves obtained are shown in each graph	129
Figure 4.16. Long-term anomalies of environmental parameters in <u>Saadiyat</u> site, calculated from remote sensing data. Including a) temperature, b) chl-a, c) water current speed, d) attenuation coefficient (K_d490), and f) aerosol optical thickness (AOT). The vertical red lines indicate the bleaching events, the broken line curves display a fourth order polynomial trend. The equations and R^2 values of the regression curves obtained are shown in each graph	130
Figure 4.17. Long-term anomalies of environmental parameters in <u>Ras Ghanada</u> site, calculated from remote sensing data. Including a) temperature, b) chl-a, c) water current speed, d) attenuation coefficient (K_d490), and f) aerosol optical thickness (AOT). The vertical red lines indicate the bleaching events, the broken line curves display a fourth order polynomial trend. The equations and R^2 values of the regression curves obtained are shown in each graph	131
Figure 4.18. Long-term meteorological anomalies in Abu Dhabi a) SST values calculated by remote sensing analysis at Saadiyat site, b) air temperature, c) visibility, d) wind speed, and e) precipitation. The vertical red lines indicate the bleaching events, the broken line curves display a fourth order polynomial trend. The equations and R^2 values of the regression curves obtained are shown in each graph	132
Figure 4.19. Temperature parameters related to the ENSO and Indian ocean dipole anomalies. a) Long term temperature anomalies of El Niño–Southern Oscillation (ENSO) in the Niño 3.4 region (5°N-5°S, 120°-170°W) extracted from the NOAA nationalweatherservice(http://www.cpc.ncep.noaa.gov/products/analysis_monitoring/ensostuff/ensoyears). b) Dipole Mode index (DMI), which represents the Indian Ocean Dipole (IOD), extracted from the state of the ocean climate (http://stateoftheocean.osmc.noaa.gov)	133
Figure 4.20. Chl-a concentration in Abu Dhabi between 2002 and 2009. Averages values were calculated from the data corresponding to the month of September of each year, extracted from MODIS-Aqua level 3 OCI images (4km resolution) from ocean colour web site (www.oceancolor.com). The bar at the top of the figure indicates	

the minimum and maximum colour scale of chl-a concentration. The area where a phytoplankton bloom occurred in 2008 is marked with a black lined oval139

Figure 4.21. Chl-a concentration in Abu Dhabi between 2010 and 2015. Averages values were calculated from the data corresponding to the month of September of each year, extracted from MODIS-Aqua level 3 OCI images (4km resolution) from ocean colour web site (www.oceancolor.com). The bar at the top of the figure indicates the minimum and maximum colour scale of chl-a concentration 140

Figure 4.22. Coral bleaching thresholds from coral reef regions within the Arabian Gulf region calculated as 1°C over the average summer from 33 years (1982-2015). Showing different local bleaching thresholds, with the highest found at Delma island (southern Gulf) and the lowest in the northern Gulf (Kuwait) and Gulf of Oman 147

DECLARATION OF AUTHORSHIP

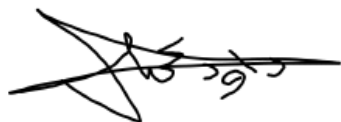
I, Dawoud Sheail declare that this thesis “Discerning the interacting effects of phytoplankton blooms and temperature anomalies on the relationship between algal symbionts of the genus *Symbiodinium* and their reef coral hosts in the Arabian Gulf” and the work presented in it are my own and has been generated by me as the result of my own original research.

I confirm that:

1. This work was done wholly or mainly while in candidature for a research degree at this University;
2. Where any part of this thesis has previously been submitted for a degree or any other qualification at this University or any other institution, this has been clearly stated;
3. Where I have consulted the published work of others, this is always clearly attributed;
4. Where I have quoted from the work of others, the source is always given. With the exception of such quotations, this thesis is entirely my own work;
5. I have acknowledged all main sources of help;
6. Where the thesis is based on work done by myself jointly with others, I have made clear exactly what was done by others and what I have contributed myself;
7. Parts of this work have been published as:

Shuail, D., Wiedenmann, J., D'angelo, C., Baird, A.H., Pratchett, M.S., Riegl, B., Burt, J.A., Petrov, P. and Amos, C., 2016. Local bleaching thresholds established by remote sensing techniques vary among reefs with deviating bleaching patterns during the 2012 event in the Arabian/Persian Gulf. *Marine pollution bulletin*, 105(2), pp.654-659.

Signed:



Date: **29/10/17**

Acknowledgements

First and foremost, I would like to thank God Almighty for providing me with this PhD opportunity and for facilitating the companionship of people who have enabled me to complete it.

I would like to offer my sincere gratitude to my supervisors Prof. Joerg Wiedenmann, Prof. Carl Amos and Dr. Cecilia D'Angelo who has supported me throughout my PhD with their knowledge, guidance and patience. Thank you for introducing me to the world of Coral reefs. Your valuable time, advice, and encouragement are highly appreciated.

I would like to thank Prof. Peter Petrov for his wisdom and advice, and for the tremendous help and support that he given me. Thank you for your involvement in the field work and for helping me analyze a problem from a different perspective.

I would also like to mention a word of gratitude to the National Oceanography Centre (NOC) for allowing me the use of their facilities and library.

I would also like to thanks Dr. Anil Kumar and Dr. Anuja Puthuppallil Vijayan at the Environmental agency Abu Dhabi (EAD) for allowing me the use of their in situ data.

Special thanks go to my friend Hachem Kassem. Thank you for taking the time of your own PhD to offer your technical and nontechnical support. I cannot thank you enough for your thoughtfulness and encouragement. Also, my friends Dr. Thamer Al-Rashidi, Dr. Fahad Al-Awadi, have provided invaluable support and encouragement -thank you.

To my officemates, my little brothers and sisters, thank you for your kindness and your much-needed support. You made the office a cheerful place to work in, in spite of all the stress we go through.

I am very appreciative to my family, especially my dear wife - Ms. Ream al-Dawai for their great encouragement and patient throughout my study. You made me laugh when I was down and you pushed me when I felt like I could not do it anymore. I am grateful to have you in my life.

Finally, to my loving mother, who put their lives on hold to be my side, thank you for being there for me when I needed you the most, your love and support kept me going. I wouldn't have been able to be where I am now without you by my side.

Abbreviations

Km	Kilometer
m	Meter
cm	Centimeter
%	Percentage
°C	Degrees Celsius
g	Grams
AOT	Aerosol optical thickness
Chl- <i>a</i>	Chlorophyll <i>a</i>
SST	Sea surface temperature
WS	Wind speed
WCS	Water current speed
K _d 490	Light attenuation coefficient
N	North
S	South
W	West
E	East
mm	Millimeter
nm	Nanometer
H	Hours

min	Minutes
Sec	Seconds
RMSE	Root mean square error
GMT	Greenwich Mean Time
MODIS	Moderate Resolution Imaging Spectroradiometer
AVHRR	Advanced Very High Resolution Radiometer
SeaWiFS	Sea-Viewing Wide Field-of-View Sensor
SD	Standard deviation
l	Liter
Turb.	Turbidity
D. O.	Dissolve oxygen
pxl	Pixel
Temp	Temperature
±	variation of different
DMI	Dipole Mode index
ENSO	El Niño–Southern Oscillation
NOAA	National Oceanic and Atmospheric Administration

Chapter 1: Introduction

1.1.Introduction

Coral reefs are among the most diverse and critically important marine ecosystems. They are economically important to humanity (Spalding et al., 2001). Yet, climate change threatens their survival, particularly due to the increase in episodes of coral bleaching that are often followed by coral mass mortality (Riegl and Purkis, 2015a). Coral bleaching refers to the loss of symbiotic algae (zooxanthellae) that live within the coral tissue, leaving visible the pale white colour of the coral skeleton (Baker, 2001; Fitt et al., 2001; Douglas, 2003; Dubinsky and Stambler, 2010). Apart from extreme temperature fluctuation, other factors such as phytoplankton blooms, local dust storms, water currents and turbidity can modulate the coral susceptibility to bleaching (Bauman et al., 2013b; D'Angelo and Wiedenmann, 2014a). In addition, biological factors, such as densities of microbes and grazers play an important role in the health of the coral population and define their susceptibility to climate change (Moriarty et al., 1985; Knowlton and Jackson, 2008; Riegl et al., 2012a). About 30% of the Earth's coral reefs are already severely damaged, and an estimated 60% may be lost by 2030 (Hughes, 2003). However, it is difficult to give accurate projections of climate change impacts on coral reef structure and function (Dawson et al., 2011). Because many predictive models do not consider the capacity of corals to cope with the changing environment and the effect of environmental factors other than temperature remains insufficiently understood (Logan et al., 2014).

1.2. Thesis Hypothesis

Coral bleaching within an affected region is not always uniform, but often exhibits a patchy distribution between centimetres to kilometers in scale (Berkelmans and Willis, 1999; Loya et al., 2001). Previous research studies (West and Salm, 2003; Baker et al., 2008; Wiedenmann et al., 2013; D'Angelo and Wiedenmann, 2014a; Riegl and Purkis, 2015b) suggest that such variability may not only be the result of water temperature, but also that other environmental conditions may modulate bleaching susceptibility. At the present, there are not enough data to understand how environmental factors, such as phytoplankton, nutrient concentrations, dust, wind and water currents are enhancing bleaching susceptibility of corals in natural reef systems. The Gulf was chosen as a natural laboratory for this research because of its distinct environmental extremes that exceed the tolerance limits of most corals around the world (Sheppard, 1993; George and John, 2000; Wilkinson, 2008). Furthermore, *in situ* data exists from this region that can be combined with results from remote sensing. Therefore, the aim of this thesis is to discern how local and global environmental factors modulate the thermal stress tolerance of algal symbionts in reef corals and to test the central hypothesis:

“Concentrations of dissolved inorganic nutrients, modulated by phytoplankton blooms, affect the bleaching susceptibility of reef corals in the southern Gulf.”

This research hypothesis was to be tested through identifying possible causes of local differences in bleaching severity observed among coral communities in the southern Gulf off the coast of Abu Dhabi. *In situ* measurements, remote sensing data and meteorological

variables were used to determine anomalies and trends of different environmental factors surrounding three study regions off the coast of Abu Dhabi: Delma (lat. 24.5208/long. 52.2781), Saadiyat (lat. 24.599/long. 54.4215) and Ras Ghanada (lat. 24.8481/long. 54.6903). However, the central hypothesis is tested (chapter 3) only in Saadiyat study site due to the availability of *in situ* nutrient and chl-a data.

1.3. Scientific background

1.3.1. Coral reefs

Corals are classified as members of the animal kingdom, under the phylum Cnidaria (Latin term for “nettle organisms”), which includes also organisms such as jellyfish, sea anemones, hydrozoans and corals (Claereboudt, 2006). Shallow water coral reefs are among the most biologically diverse and productive ecosystems that are generally found in tropical and subtropical regions (Connell et al., 1978). They provide coastal protection as well as offering aesthetic, economic and cultural benefits (Connell et al., 1978; Ahmed et al., 2007; Ahmed et al., 2007). There are four general types of coral communities, fringing reefs, barrier reefs, atolls and platform reefs. All of these reefs types have functional differences, and are connected to other ecosystems, such as mangrove forests, seagrass beds, and the open ocean. Globally, approximately 0.1–0.5% of the seafloor is covered by coral reefs (Spalding and Grenfell, 1997). The reef’s framework creates a three-dimensional complex habitat that embraces a diversity of fishes and other reef organisms, such as encrusting coralline algae, foraminifera, molluscs, and echinoderms (McAllister, 1991). The wide variety of mutualistic associations between the coral reef and the surrounding biota are essential for reef health. But these are not as important as the

relationship between corals and their symbiotic algae of the genus Symbiodinium (Taylor, 1974; McAllister, 1991 Trench, 1993; Rowan, 1998) that are described below.

1.3.2. Relationship between the coral and its algal symbiont

A close look at coral polyps shows that most of the endodermal cells are harbouring unicellular dinoflagellates of the genus Symbiodinium called “zooxanthellae” (Trench, 1979). These unicellular algae supply up to 95% of photosynthetic products, including sugars, lipids, and amino acids to the coral host (Muscatine, 1990; Lesser, 2004). In return, zooxanthellae obtain essential nutrients such as ammonium, phosphate, as well as carbon dioxide from the metabolic wastes of the coral (Trench, 1979; Muller-Parker et al., 2015). However, the symbiosis between corals and their zooxanthellae is sensitive to changes in environmental conditions (Riegl et al., 2012a; Bauman et al., 2013b). This symbiosis requires sufficient light and good water circulation, and can flourish best in water temperature range of 25°-29° C and within a salinity range of 34-36 parts per thousand, preferably with low nutrient and sedimentation loads (Moberg and Folke, 1999; Muller-Parker et al., 2015a)

1.3.3. Environmental factors affecting the algal symbiont and the coral host

A variety of environmental stressors can disrupt the coral’s symbiotic relationship and cause bleaching due to the loss of zooxanthellae or their photosynthetic pigment (West and Salm, 2003). Temperature has been identified as a major environmental factor influencing the survival/capability of corals to thrive in a particular region. However,

additional environmental parameters, including phytoplankton presence, turbidity, water currents, winds and dust are shown to be important factors affecting the survival of the reefs (Kendall et al., 1985; Baker et al., 2008; Sheppard et al., 2010; Riegl and Purkis, 2012b; Bauman et al., 2013a; D'Angelo and Wiedenmann, 2014a; Howells et al., 2016a). These are discussed in turn below.

1.3.3.1 Water Temperature

Coral bleaching has been most frequently associated with elevated seawater temperature and so global warming (Coles and Brown, 2003). Both field and laboratory studies have established a causal link between temperature stress and bleaching (Hoegh-Guldberg, 1999; Lesser, 2004; Bauman et al., 2013a). The first documented observations of high temperature-related coral mortality was by Cary (1911) following several days of hot, calm weather in the Dry Tortugas, Florida (in Mayer, 1914). Water temperatures between 23-27°C are generally considered the normal range for coral growth (Coles and Jokiel, 1978). But at temperatures between 30 to 32°C or above, damage to the photosynthetic apparatus of symbiotic algae can occur (zooxanthellae) (Lesser et al., 1990; Glynn and D'Croz, 1990). Photodamage can occur as a result of the malfunctioning of the photosynthetic electron transport chain, along with a continued absorption of light energy. This can lead to the increased production of reactive oxygen species (ROS), such as singlet oxygen [$^1\text{O}_2$] superoxide radicals [O_2^-], hydrogen peroxide [H_2O_2], and hydroxyl radicals [OH] (Lesser, 2004). These different types of ROS affect numerous cellular sites including photosystem II and the primary carboxylating enzyme, Rubisco, in zooxanthellae (Lesser, 1996; 2006). However, there are protective mechanisms in the coral host that involves the

breakdown of these harmful active oxygen radicals, for example by the enzyme superoxide dismutase (SOD) (Gardner et al., 2016). However, elevated levels of the active oxygen can overpower the host defense system and consequently destabilize the symbiosis and result in the loss of zooxanthellae (Muller-Parker et al., 2015b). Coral health is also affected adversely at or below 18 °C (Porter et al., 1982). In laboratory experiments by Mayer (1914), it was shown that temperatures between 13.3 °C and 15 °C for nine hours were enough to cause mortality of *Acropora* species. Below 16 °C, coral metabolic activity and feeding cease (Crossland, 1984). Therefore, this latter temperature is considered the long term lower thermal limit for coral reef development (Jokiel and Coles, 1977; Coles and Fadlalallah, 1991).

1.3.3.2 Phytoplankton Blooms

When conditions are favorable, such as optimal light, water temperature and elevated levels of nutrients, phytoplankton cells divide rapidly and develop into a bloom (Glibert et al., 2002; Landsberg, 2002). These blooms can potentially help corals to survive temperature and light stress through blocking, absorbing and scattering radiation reaching corals, (West and Salm, 2003; Maina et al., 2008). However, phytoplankton blooms are undoubtedly a significant worldwide problem resulting in several negative impacts on a broad range of marine organisms including coral reefs (Benito and Haag, 2004). For example, these impacts can be through shading, toxin production, oxygen depletion and nutrient alteration (Al-Ansi et al., 2002; Wiedenmann et al., 2013; D'Angelo and Wiedenmann, 2014). About 300 (7%) of the estimated 3,400-4,100 phytoplankton species have been linked to harmful algal blooms known also as red tides including diatoms,

dinoflagellates, silicoflagellates, prymnesiophytes, and raphidophytes (Theodore J Smayda, 1997). An incident of bloom harmful shading was witnessed in the Red Sea following the eruption of Mount Pinatubo in the Philippines during spring 1992. It was caused by strong vertical mixing in the Gulf of Eilat (Aqaba) resulting in increased supply of nutrients to surface waters inducing a rapid algal bloom. This bloom resulted in thick mats of filamentous algae covering broad sections of the benthic reefs causing extensive coral death (Genin et al., 1995). Some phytoplankton blooms can grow so dense and consequently affect the health of the benthic organisms through oxygen depletion. Phytoplankton bloom occasionally use up all nutrients needed for their growth causing some or even all of the bloom to die back temporarily. These phytoplankton then are decomposed by microflagellates, protozoans, rotifers, and small crustaceans, which leads to oxygen removal from the water body (Taft et al, 1980; Malone et al., 1988; Conley and Malone, 1992; Theodore J. Smayda, 1997). Examples of these phytoplankton includes: dinoflagellates *Gonyaulax polygramma*, *Noctiluca scintillans*, *Scrippsiella trochoidea*, cyanobacterium *Trichodesmium erythraeum* (Hallegraeff, 1993). They usually develop in summer, at low wind speeds, good light condition and sufficient nutrient levels (Glibert et al., 2002). Several types of phytoplankton blooms can endanger marine organisms by damaging and clogging their respiratory system (e.g. diatom *Chaetoceros convolutus*, dinoflagellate *Gymnodinium mikimotoi*, prymnesiophytes *Chrysochromulina*, *C. leadbeateri*, *Prymnesium parvum*, *P. patelliferum*, raphidophytes *Heterosigma akashiwo*, *Chattonella antiqua*) (Hallegraeff, 1993). Other phytoplankton species can release toxic chemicals or inhibitory substances that can harm zooplankton, finfish, shellfish, coral,

birds, marine mammals and humans (Hallegraeff, 1993; Chattopadhyay, 2002; Roy et al., 2007).

Elevated phytoplankton densities in a coral reef environment can alter the nutrient balance surrounding the corals (Wiedenmann et al., 2013; D'Angelo and Wiedenmann, 2014). Phytoplankton can rapidly deplete nutrients in the water column, impacting the entire benthic ecosystem (Furnas et al., 2005). Furthermore, phytoplankton might temporarily reduce nitrogen compounds, phosphate below average concentrations, which can result in a reduced availability of these essential nutrients for benthic corals (Wiedenmann et al., 2013; D'Angelo and Wiedenmann, 2014). In coral reef waters, Nitrate: Phosphorous ratios were found ranging from 4.3:1 to 7.2:1 (Smith et al., 1981; Crossland et al., 1984; Furnas et al., 1995) which is lower than the known Redfield ratio of 16:1, considered optimal to sustain phytoplankton growth (Redfield, 1958). Consequently, many processes in coral reefs tend to be nitrogen limited (Furnas et al., 2005). The limitations of these nutrients are known to disrupt the symbiotic relationship and increase the susceptibility of zooxanthellae to external stressors and subsequently promote coral bleaching (Wiedenmann et al., 2013; D'Angelo and Wiedenmann, 2014). Phytoplankton load can also stimulate the proliferation of filter feeders and bioeroders that can represent space competitors for corals or endanger their structural integrity (Fabricius et al., 2012).

1.3.3.3 Wind

Wind impacts on coral reefs through wave action-inflicted mechanical damage, deposition of aeolian dust, the resuspension of sediment, and water column mixing (Riegl and Purkis, 2012; Islam, 2015; Sabine et al., 2015). Particularly, in arid climates, a strong

wind can pick up dust from the unprotected surfaces of desert regions, creating local dust storms that subsequently deposit their contents downwind into the sea (Reynolds, 1993; Hamza et al., 2011). Winds, above 8 m/s, are considered the most important mechanism for wave-generating and water current flow strength (Clemens et al., 1991; Sheppard, 1993). They also cause intensive water column mixing, reaching to about 30 m, which reduce stratification and resulting thermal stresses to benthic coral communities (Nishino et al., 2015).

1.3.3.3.1 Dust storms

Most dust storms are generated in desert and semi-desert areas and transported across local-to-global scales. The major global dust sources are the African and Asian deserts, which is called the “dust belt” (Prospero et al., 1987, Arimoto et al., 1989; Pye, 2015). The dust belt comprises the Sahara Desert, arid and semiarid regions, Central Asia, the Taklamakan and Gobi deserts in East Asia and the Arabian Peninsula (Figure 1.1; 1.2).

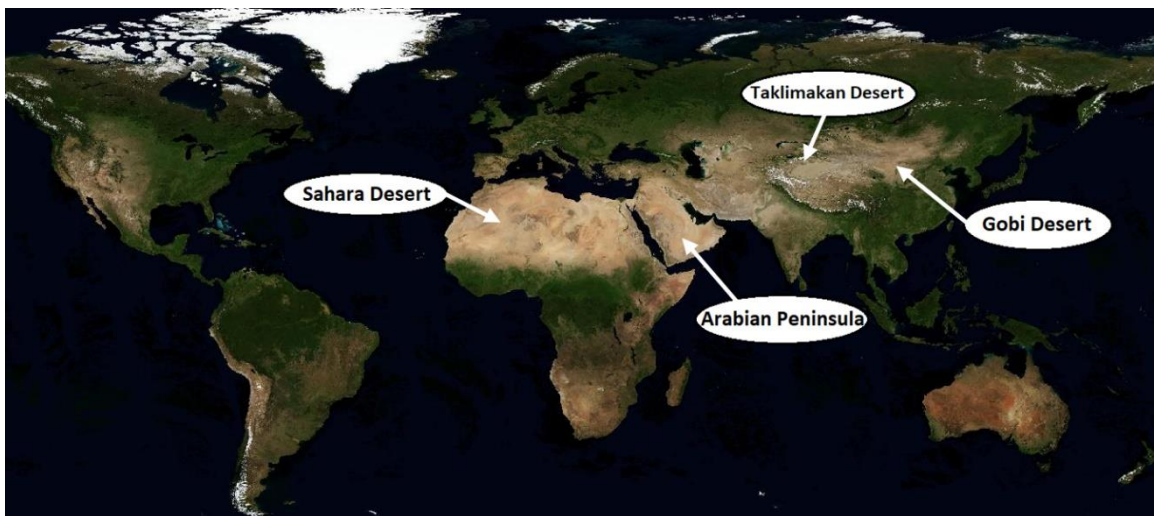


Figure 1.1. The major dust sources in the world, including the Sahara Desert, the Taklamakan and Gobi deserts in East Asia and the Arabian Peninsula. Source: <http://oceancolor.gsfc.nasa.gov>.

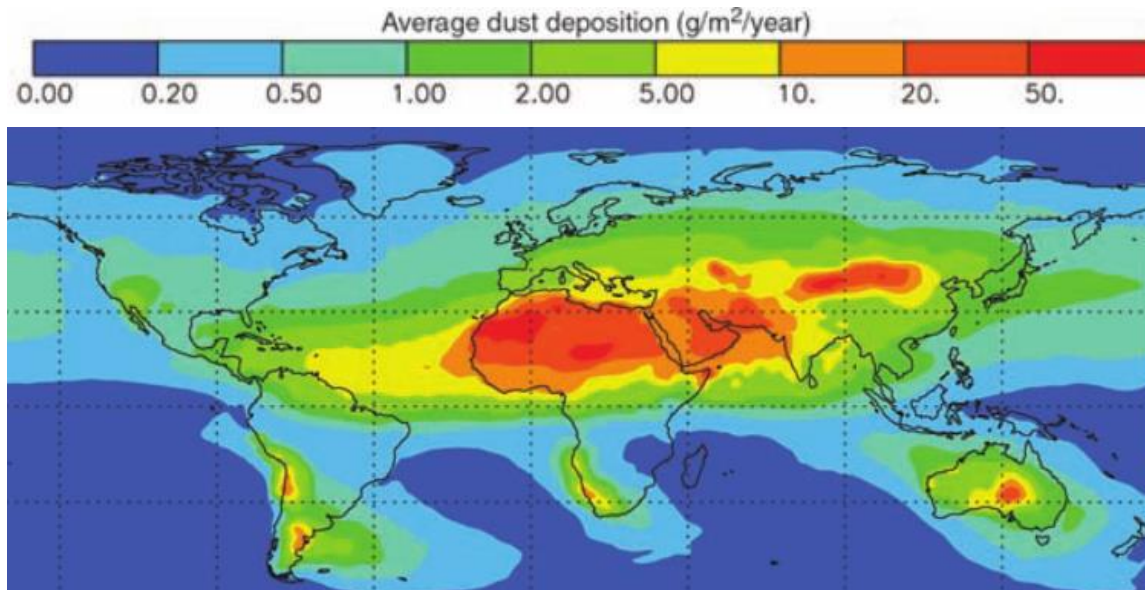


Figure 1.2. Dust fluxes to the world oceans based on studies that match satellite optical depth, *in situ* concentration, and deposition observations (Ginoux et al., 2001; Mahowald and Luo, 2003; Tegen et al., 2004). Source: Jickells, (2005).

Dust transport are strong most of the year, but during the summer season, dust transport is the most intense. The winds in the North Sahara region are remarkably active in summer, transporting strong bulk of dust, via vigorous wind systems that are found in the middle troposphere, across the Mediterranean to Europe and the Middle East as well as across the Atlantic to the Caribbean, Central and North America (Prospero, 1996). Nonetheless, dust storm activity is also quite strong in the winter and spring in the sub-Saharan region (Glantz, 1994). It has been shown that dust concentration can be corelated with rainfall scarcity as it is interpreted by Prospero (1996), showing that the increase dust is coincided with the increase droughtnes. Moreover, Asian dust has two large sources, the Taklimakan and Gobi Deserts. The Asian dust has a strong impact on Asian atmospheric radiation and air quality. Dust from the Gobi desert has the most attention from dust observer and modeling researcher because it is located near large urban areas, such as

Beijing, Seoul, and Tokyo (Park and In 2003; Gong et al. 2003; Uno et al. 2001; Wang et al. 2000). During severe dust storms, dust from East Asia can be transported beyond the continent, drifting over the Pacific ocean to the west coast of North America (Husar et al., 2001; Tratt et al., 2001). The Arabian Peninsula, as well, is one of the largest desert areas in the world, characterized by its arid conditions with a large areas of sand dunes, and strong monsoon winds in spring and summer (March-August). It promote dust storms over the Arabian Gulf area, more detailed background on the Arabian Peninsula dust storms will be discussed in section 1.3.4.3.2 of this thesis.

Dust storms can transport huge amount of dust into the atmospheric boundary layer, which is the region of the lower troposphere (from 50m-1000m) where the Earth's surface is strongly influenced temperature, moisture, and wind through the transfer of air mass (Kaimal and Finnigan, 1994). These large quantities of dust can cause air pollution, reduce visibility, cause airports shutdown, and increase road traffics and aircraft accidents (Morales, 1979; Hagen and Woodruff, 1973; Middleton and Chaudhary, 1988; Dayan et al., 1991). Other environmental impacts of dust include crop damage and reduced soil fertility, reduced solar radiation on the surface, which decreases the efficiency of solar energy appliances. Dust storms can damaged telecommunications and mechanical systems, increased respiratory diseases and other impacts on human health (Hagen and Woodruff, 1973; Mitchell, 1971; Fryrear, 1981; Bennion et al., 2007). Additionally, Shinn et al. (2000) and Garrison et al. (2003), suggested that dust storms can transport anthropogenic pollutants, synthetic chemicals, pathogenic microorganisms, and other toxic constituents from land and deposited in the oceans. Dust storms can have a cooling effect during the summer months, which benefits marine organisms, by blocking solar radiation reaching

the water surface through “solar dimming” (Stanhill and Cohen, 2001; Al-Ghadban and El-Sammak, 2005). However, some types of dust known as “absorbing aerosols” characterised by heating effects to the atmosphere and subsequently to the water body by absorbing solar radiation (Lau and Kim, 2006; Wang, 2013; Devara and Manoj, 2013). These absorbing aerosols include desert dust and the anthropogenic black carbon (Devara and Manoj, 2013). The black carbon aerosols are the dust particles containing black carbon (BC), which is a strong absorber of sunlight, and are mainly anthropogenic (Wang, 2013). It comes from a partial combusted fossil fuel or biofuel, and from the vehicle and industrial emissions to biomass burning events (Lau and Kim, 2006; Wang, 2013).

1.3.3.3.1.1 Dust composition

The chemical composition of dust is dependent on the origin (Duce et al. 1976; Arimoto et al. 1995; Perry et al. 1997; Hamza et al., 2011). Sahara and Asian dust consists mainly of clay soil minerals such as quartz, illite, chlorite, kaolinite, plagioclase, microcline, and calcite (Prospero 1981). In addition to some elements, such as iron, manganese, cobalt, scandium, occur on Sahara dust particles in concentrations similar to average crustal abundance. Whereas elements, such as selenium, mercury and lead, accumulate at concentrations three times greater than mean crustal abundance (Duce et al. 1976). Detailed background on the Arabian Peninsula dust composition will be discussed in section 1.3.4.3.1 of this thesis.

Several studies during the last decades have been concerned with the major chemical element of atmospheric dust, and its effects on marine ecosystems (Prospero, 1996; Paerl, 1997; Guerzoni et al., 1999; Markaki et al., 2003; Jickells et al., 2005; Hamza,

2008). Particularly the inputs of elements such as nitrogen (N), phosphorus (P) and iron (Fe), which are essential for the biological activity of marine living organisms. According to Martin (1990) these micronutrients are considered a source of ocean enrichment, which can trigger either harmful or non-HAB phytoplankton blooms (Zhuang et al., 1992; Arimoto, 2001; Anderson et al., 2002; Al-Shehhi et al., 2012). The nutrient input from the Asian dust is reported to fuel phytoplankton productivity in the northern Pacific (Young et al. 1991). Walsh and Steidinger (2001) linked African dust to the red tides developments in the Gulf of Mexico. The nitrogen (N), phosphorus (P) and iron (Fe), elements are vital to marine life overall, but iron is essential for all life on Earth and is particularly important for oceanic plant nutrition in the oligotrophic waters, because atmospheric nitrogen cannot be fixed, nor can chlorophyll be synthesized, or nitrate be reduced without it (Jickells, 1999). Dust deposition is thought to be the dominant source of iron in the photic zone of the ocean (Duce and Tindale, 1991). Marine organisms have a variety of means for acquiring iron that differ from those of terrestrial organisms (Butler, 1998). However, iron has to be in the form of Fe (II), which is a biologically available and soluble species to phytoplankton and other marine organisms in order for it to be beneficial (Garrison et al., 2003). Dust from the African Sahara and Asian deserts is transported long distances in extreme physical and chemical environmental conditions where the small particles are exposed to high levels of solar radiation, multiple freezing cycles, and relatively acidic conditions (Jickells, 1999). It has been suggested that during this atmospheric transport iron is reduced through photoreduction from Fe (III) to Fe (II), which is biologically available and soluble iron (Graedel et al. 1986, Duce and Tindale 1991). Turner et al. (1996), showed that iron deposition to the oceans leads to the biotic production of

dimethylsulfide (DMS) and its release into the atmosphere. Subsequent oxidation of DMS and formation of sulfate in turn produces sulfuric acid, which with atmospheric mixing could increase the solubility of iron (in the form Fe [III]) in the mineral aerosols. Sayadam and Senyuva (2002), proposed that oxalate released by fungi in desert dust facilitates photoreduction of Fe (III). Moreover, Fe (III) can form a stable complexes with siderophores, which are a small iron-chelating compounds secreted by microorganisms such as bacteria and fungi, facilitating the uptake by microorganisms and phytoplankton (Butler, 1998). Young et al. (1991) also suggested the smaller the dust particle, the longer the residence time in the photic zone and therefore the greater the amount of iron that could be released and made available for phytoplankton and microbes.

1.3.3.4 Water Currents

Water motion and currents are caused by variable combinations of tidal forcing, wind stresses (barotropic) and/or density gradients (baroclinic) (Reynolds, 1993). Several metabolic processes of coral and its symbionts are affected by current flow, probably due to diffusion via mass-transfer-limited processes (Jokiel, 1978; Dennison and Barnes, 1988; Patterson, 1992; Lesser et al., 1994; Nakamura and Van Woesik, 2001; Nakamura et al., 2005). Water movement can influence the degree to which corals can tolerate elevated temperatures and irradiance (Nakamura and Van Woesik, 2001; Nakamura et al., 2003). Accelerated water motion resulting from a wind gust, can reduce the boundary layers surrounding corals thus increasing mass transfer, which supports dissipation of heat and the removal of toxic compounds from the corals (Nakamura et al., 2005). ROS radicals that build up within corals during high temperatures and irradiance may damage adjoining

tissue. They may become less concentrated during high current flow conditions (Nakamura et al., 2005).

Strong water motion enhances the circulation caused by waves, tides, and currents (Jokiel, 1978). Therefore, it can modify several important environmental parameters, such as plankton, dissolved nutrients and gasses, seabed sediment, water clarity, substrate stability, salinity and temperature, all which affect corals (Jokiel, 1978). Water motion influences corals by controlling the rate of exchange of material across the interface between the sea water and the coral tissue (Jokiel, 1978). It is now clear that high water flow rates (50 to 70 cm s⁻¹) reduce bleaching susceptibility in corals (Nakamura and Van Woesik, 2001; Nakamura et al., 2003). Therefore, abnormally high water temperatures (26.22 to 33.65°C) coupled with low water flow (2 to 3 cm s⁻¹), can potentially cause coral mortality (Nakamura and Van Woesik, 2001; Nakamura et al., 2003; Riegl and Purkis, 2012a).

1.3.4 The study region

The Gulf is a shallow, semi-enclosed water body, approximately 1,000 km in length, 200-300 km wide and is relatively shallow (average 35m) (Sheppard et al., 1992). The Gulf at its deepest point in the southeast region, reaches about 100 meters (Spalding et al., 2002). It is surrounded by eight countries (Iraq, Kuwait, Saudi Arabia, Bahrain, Qatar, United Arab Emirates, Oman and Iran) (Figure 1.3). Seawater in the Gulf circulates in a counter-clockwise direction. Oceanic water enters the Gulf through the Strait of Hormuz and moves northwestward along the Iranian Coast. Then it moves southeastward along the Saudi Arabian coastline, eastward passing along the United Arab Emirates

(UAE), where it finally leaves the Arabian Gulf as deep water current through the Strait of Hormuz (Hunter, 1983; Coles and Riegl, 2013). Although temperature has previously been cited as the major environmental factor influencing corals around the region, additional environmental parameters, including phytoplankton blooms, turbidity, water currents, winds and dust are shown to be important (Kendall et al., 1985; Baker et al., 2008; Sheppard et al., 2010; Riegl and Purkis, 2012b; Bauman et al., 2013a; D'Angelo and Wiedenmann, 2014; Howells et al., 2016a). This makes the Gulf a valuable area to study the effect of environmental factors on the survival of coral communities.



Figure 1.3. Countries surrounded the Arabian Gulf. Including: Iraq, Kuwait, Saudi Arabia, Bahrain, Qatar, United Arab Emirates, Oman and Iran. Source: <https://lance3.modaps.eosdis.nasa.gov>.

1.3.4.1 Water Temperature

Gulf corals are routinely exposed to annual ranges of water temperature that exceed the temperature extremes for other reefs in the world (Sheppard, 1993). Water temperature fluctuations can exceed 20°C throughout the year. Corals in the Gulf are regularly exposed to water temperatures reaching 32-33 °C during summer (Sheppard et al., 1992; Coles, 2003; Sheppard et al., 2010b) (Figure 1.4). Since corals adapt to the temperature of their local environment, Gulf corals can endure temperatures up to 35°C for a limited amount of time (Riegl and Purkis, 2012a). Bleaching thresholds vary among and within different regions of the Gulf (Berkelmans, 2009). The thermal threshold for coral bleaching in coral reefs of the southern Gulf is considered to be 35.5°C (Riegl and Purkis, 2012a; Shuail et al., 2016), and is between 33.5 °C to 34 °C in the northern Gulf (Kavousi et al., 2014).

Reef development in the Gulf is patchy and shows the best growth in the offshore. However, the increasing frequency, severity and diversity of disturbances are likely to cause marked shifts in community composition (Bauman et al., 2014). After the 1996/1998 temperature anomalies, six species of *Acropora* species disappeared mainly from the shallow areas of Dubai (Riegl, 1999a). The more resilient taxa, Faviids and *Porites* are now achieving spatial dominance in most mid-depth areas (>3m), shifting the nature and overall structure coral reef communities of the southern Gulf (Sheppard et al., 2010b). A new species of Symbiodinium (Symbiodinium thermophilum) has been identified in *Porites* corals and other anthozoan species in the southern Gulf (Hume et al., 2015; D'Angelo et al 2015; Hume et al., 2016).

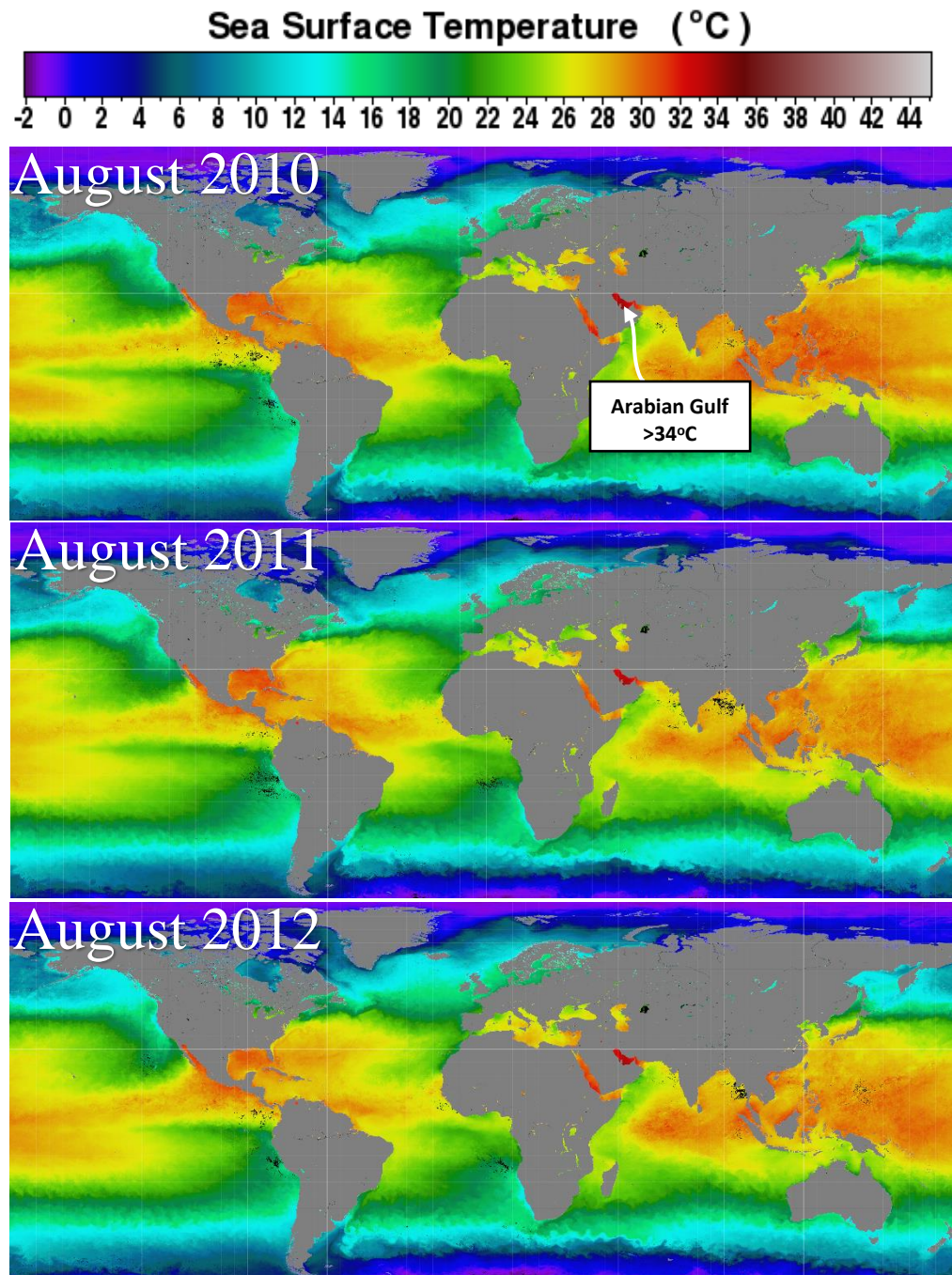


Figure 1.4. Sea surface water temperatures (SST) of the world during the summer period of 2010, 2011 and 2012. Show that the Arabian Gulf SST reaching 32-34 °C regularly during the summer period. Source: <https://oceancolor.gsfc.nasa.gov/cgi/13>

1.3.4.2 Phytoplankton blooms

Over the last several decades algal blooms have been recorded from almost all areas of the Gulf (Al-Yamani et al., 2000). Countries throughout the Gulf have experienced an escalating trend in the incidence of problems termed “harmful algal blooms” (HABs) (Zhao and Ghedira, 2014a; Abuelgasim and Alhosani, 2014). Three harmful algal blooms have been witnessed in Kuwait during 1999, 2001 and 2017 (Al-Yamani et al., 2000; Heil et al., 2001, Al-Enezi, 2017). All of these incidents coincided with a massive mortality of both mariculture and wild fishes, the HAB species were *Karenia selliformis* and *Prorocentrum rathymum* (Al-Yamani et al., 2000; Heil et al., 2001). A possible cause of this event may be attributed to the deteriorating water quality through the rise in nutrient levels around fish cages and the discharge of approximately 30,000 m³ of untreated sewage water into Kuwait Bay (Sheppard et al., 2010b). Other bloom events in the Gulf have been reported from Abu Dhabi, Dubai, Ajman, Fujairah, Iran and Oman during August 2008–May 2009 (Sheppard et al., 2010b) (Figure 1.5).

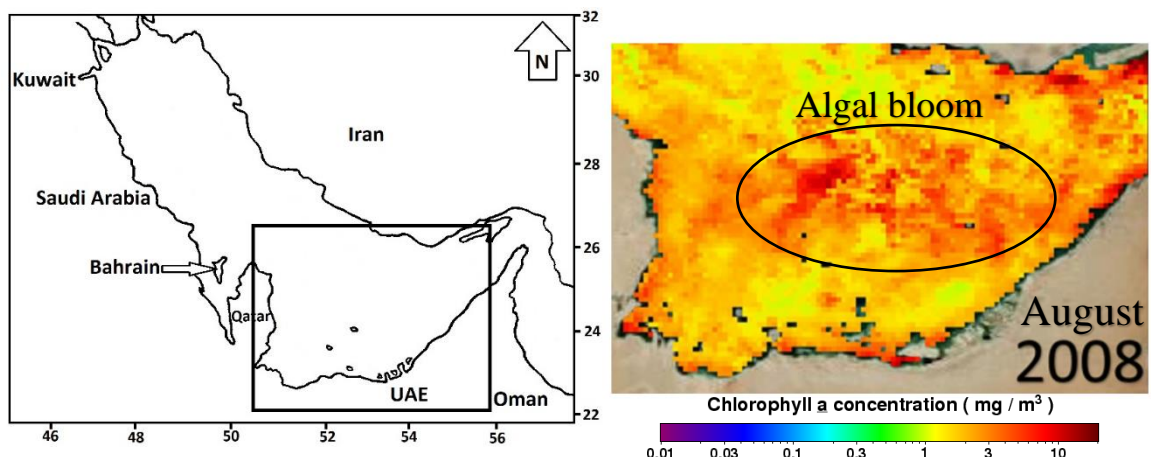


Figure 1.5. Bloom events occurs in the Arabian Gulf during 2008. have been reported from Abu Dhabi, Dubai, Ajman, Fujairah, Iran and Oman during August 2008–May 2009. The picture of the right is MODIS-Aqua 1km resolution image showing remote sensed chl-*a* levels during August 2008 during the algal bloom event. Source : <https://oceancolor.gsfc.nasa.gov>.

This bloom changed the water colour and coincided with wide spread fish and coral deaths, threatening coastal tourism and blocking desalination plant water intakes (Richlen et al., 2010). The main species causing the bloom is *Cochlodinium polykrikoides* (Naser, 2014). Moreover, several fish-kill incidents have been recorded, in the South Mussafah channel since 1998 (EAD, 2008). Water quality analyses have routinely shown that the Mussafah South Channel (southern Gulf, UAE) is impacted by nutrient enrichment, low DO concentrations in bottom waters, and phytoplankton blooms throughout the year (EAD, 2008). These outbreaks have increased over the past decade and are likely associated in part with the eutrophic conditions caused by discharges into the marine environment (EAD, 2015) (Figure 1.6).

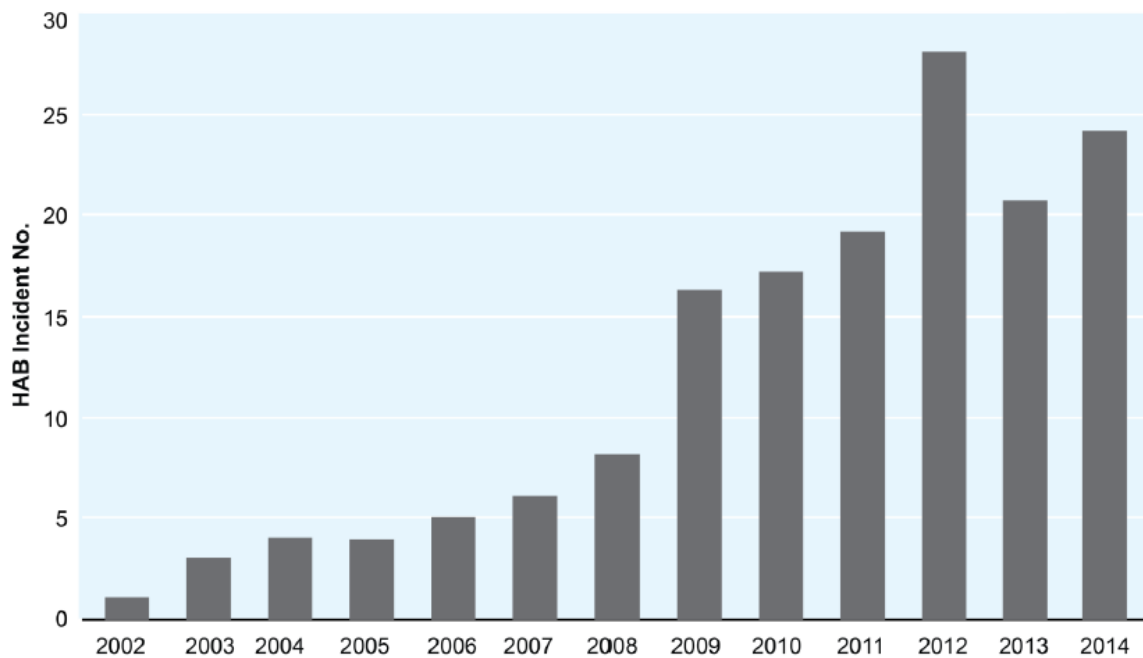


Figure 1.6. HAB incidents outbreaks since 2002 in Abu Dhabi. HAB have increased since 2002, according to observation and subsequent sample analysis by the MWQ Team. Source: EAD marine water quality report 2014.

1.3.4.3 Wind patterns

The Gulf's wind circulation patterns are mostly affected by the Indian Ocean monsoon, which is one of the Earth's most dynamic interactions between atmosphere, ocean, and continents (Clemens et al., 1991; Reynolds, 1993). In the Arabian Gulf, two well documented, weather phenomena include the Shamal and Kaus winds (Perrone, 1979; Murty and El-Sabh, 1984; Reynolds, 1993; Thoppil and Hogan, 2010a; Riegl and Purkis, 2012a; Apel et al., 2015). The Shamal blows from a northwestern direction, and brings some of the strongest winds to the region (Chao et al., 1992; Riegl and Purkis, 2012a). This is particularly apparent during winter when it has a rapid and abrupt onset and reaches speeds of up to 100 km/h (John et al., 1990). The Shamal wind is formed because of the orographic control surrounding the Gulf, including the Taurus and Pontic mountains of Turkey, the Caucasus mountains of Iran, and the Hejaz mountains of the Arabian Peninsula together with the Tigris-Euphrates Valley (Perrone, 1979). A southwesterly wind known as Kaus often precedes the Shamal and increases in intensity as the Shamal-bearing cold fronts approach (Vishkaee et al., 2012). Kaus is strong on the eastern side of the Gulf adjacent to the Zagros mountains in western Iran. Like the Shamal it has the potential to generate high wind reaching up to 62–74 km/h (Murty and El-Sabh, 1984; Riegl and Purkis, 2012a).

Both the Kaus and the Shamal winds are considered to be equal to Caribbean hurricanes in the impacts on reef-building corals (Kendall et al., 2003; Shinn, 1973; Fadlallah et al., 1995). Some of these impacts are the deposition of dust, water current modification and water mixing (Riegl and Purkis, 2012). These winds can pick up dust and sand from the unprotected surfaces of the desert regions around the Gulf, which is blown

up into the atmosphere creating dust storms in both southeasterly and northeasterly direction (Reynolds, 1993; Hamza et al., 2011).

1.3.4.3.1 Dust storms in the Arabian Peninsula

The Arabia Peninsula is among the major sources of dust storms worldwide (Zender, 2003; Hamza, 2008; Hamza and Munawar, 2009, Jish Prakash et al., 2014). There are up to 15 to 20 dust storms per year, which may affect all aspects of human activity and natural processes in this region. Dust storms in the north are more frequent in spring, while they occur mainly in summer (May-August) along the southern parts (Jish Prakash et al., 2014). The estimated sediment deposition in the Arabian Gulf during sandstorm events is around 60 to 200 x 10⁶ tonnes/year (Riegl and Purkis, 2012b). This region has been severely under-sampled and there are few available in-situ observations, and very few international research campaigns have been conducted in this area compared with the Sahara and the Asian deserts. The major dust sources are the Tigris and Euphrates Rivers, the alluvial plain in Iraq and Kuwait, and the Ad Dahna and the Rub Al Khali deserts (Figure 1.7) (Kutiel and Furman, 2003; Shao, 2008).



Figure 1.7. Major dust sources in the Arabian Peninsula. Including the Tigris and Euphrates Rivers, the alluvial plain in Iraq and Kuwait, and the Ad Dahna and the Rub Al Khali deserts. Source: <https://lance3.modaps.eosdis.nasa.gov>.

The peak of dust storm activity is reached usually during day time, when intense solar heating of the ground generates turbulence and local pressure gradients (Middleton, 1986a, 1986b). Dust emitted from southern Iraq, Iran and the eastern Arabian Peninsula was mainly deposited in the Persian Gulf and the Arabian Sea. Dust emitted from the western coast of the Arabian Peninsula was mostly deposited in Red Sea (Jish Prakash et al., 2014). In an analysis done by Hamza et al. (2011), on the dust composition along the UAE coasts, during an intensive dust storm documented in summer 2009, showed that Silica and calcium were the major chemical elements in the samples, accounting for a combined 60–80%. The analysed results also show high percentages of iron (2-18 %), aluminum (2-8%), magnesium (2-10%), and sulphur (0.5-7%) along the samples station in the UAE. These elements are essential nutrients for phytoplankton growth and activity in the marine environment if they exist in a soluble form (Graedel et al. 1986; Duce and Tindale 1991; Young et al., 1991; Garrison et al., 2003).

The solubility of iron compounds and other trace metals in the marine environment is known to be dependent on the sediments acidity, in that the binding capacity of sediments decreases at acidic pH allowing mineral dissolution (Parekh et al., 2004; Jickells et al., 2005). Both rainwater and photochemical reactions have the potential to be of great importance in dissolving elements carried by dust storms over the Arabian Gulf. Rain water in the Gulf area is scarce, however, as a consequence of intensive sulfur rich oil production, mixing with high sulphur concentrations in the atmosphere may make the rain water acidic enough to dissolve other minerals such as iron (Walker and Brimblecombe, 1985). On the other hand, light intensity in the Arabian Peninsula is high enough to promote photochemical processes at the sea surface micro-layer (Sayadam and Senyuva, 2002;

Almazroui et al., 2012). Khan et al., (2002), shows that the Arabian Gulf highly productive body of water, reflected through the efficient assimilation of nutrient by primary producers. Despite the limited freshwater sources (Hamza and Munawar, 2009), the Arabian Gulf ecosystem appears to receive additional nutrients inputs, especially Fe, P and N, from other sources. One of these extra sources could be the upwelling of waters charged with dissolved nutrients derived by recycling of marine sediments (Kampf and Sadrinassab, 2006). Another source is surely the annual dust and aerosol deposition onto its waters (Hamza, 2008).

1.3.4.4 Water circulation

A cyclonic circulation develops in the central Gulf, and dissociates into 3–4 cyclonic eddies called the Iranian Coastal Eddies (Thoppil and Hogan, 2010b). These eddies might be necessary for coral and other planktonic larva transportation from Iran to the southeastern Gulf (Riegl and Purkis, 2012c). When the water flow reaches Shatt El Arab, it increases in density due to cooling and evaporation, becoming dense enough to sink and flow southeast toward the Strait of Hormuz where it exits as a bottom current with a velocity of about 10 cm/s (Figure 1.8) (Hunter, 1982; Sheppard et al., 2010a)

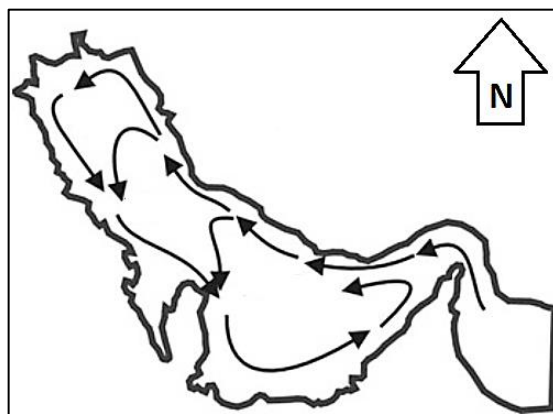


Figure 1.8. General water circulation in the Arabian Gulf. Adopted from Riegl and Purkis, 2012.

1.3.5 Coral diversity in the Southern Gulf (Abu Dhabi)

Abu Dhabi, located at the southern margin of the Arabian Gulf, is the largest emirates of the United Arab Emirates (UAE). It covers about 226,000 km² of the territorial seas of the United Arab Emirates (Purser and Seibold, 1973). A variety of habitats occurs in the marine and coastal environment of Abu Dhabi. These include sand dunes, beaches, seagrass beds, mangrove stands, tidal inlets and coral reefs (Environment Agency, 2008).

Coral reefs are among the UAE's most diverse habitats and are beneficial for fisheries and coastal protection. The shallow coastal waters of the Abu Dhabi Emirate encompass an abundance of fringing and patch reefs harbouring coral taxa, such as *Acropora*, *Porites*, *Platygyra* and faviids (George and John, 2000). Both patch reefs and fringing reefs dominate shallow waters between 1-4m depth in the coastal areas. Branching corals, mainly *Acropora* species, are found in these areas, with an underlayer of *Porites*, *Platygyra*, and smaller faviids. At depths of about 6-8m, species of the dendrophylliid coral *Turbinaria* are often seen, particularly when the reefs meet the surrounding sand (Kinsman, 1964; George and John, 1998 & 2000; Sheppard and Loughland, 2002; Burt et al., 2011). Coral reefs in the region are rarely found at depths greater than 10m (George and John, 1998).

Knowledge about the diversity and changes in the coral reefs of Abu Dhabi in the last decades is enhanced by the first coral habitats map in the southern Arabian Gulf. The outcome of using both Landsat satellite imagery and ground-truthing (Zanter, 2005). The habitat map was prepared during 2005 as a collaboration among the biodiversity management of Abu Dhabi (Marine Sector), Dolphin Energy, the World Wildlife Fund (WWF), Emirates Wildlife Society (EWS), and the National Coral Reef Institute (NCRI).

The map highlights some of the most important coral reefs around the islands and banks of Abu Dhabi Emirate and Qatar's harbour (see <http://uae.panda.org>). It shows the species density of coral reefs in the Gulf that had already been affected by three temperature-related bleaching events in 1996, 1998 and 2002 (Riegl, 2002; Sheppard and Loughland, 2002; Riegl, 2003). As a result, Abu Dhabi's coral population was reduced from 90% to about 22%. *Acropora* species were most affected in the area and six of them went locally extinct. Thus the total number of coral species in the region was reduced from 34 to 27 species (Riegl, 2002).

Coral reefs have suffered consecutive bleaching events in 2009, 2010, 2011 and 2012 (Riegl and Purkis, 2015a). These have increasingly reduced overall cover by 10% in 2009, 20% in 2010, 20% in 2011 and 15% in 2012 (Riegl and Purkis, 2015a). *Acropora* species have suffered almost 100% mortality in western Abu Dhabi including Delma, and overall 60–80% mortality in eastern Abu Dhabi (Saadiyat and Ras Ghanada) (Riegl and Purkis, 2012b). Other species, such as Montipora, Pocillopora, Goniopora, fungiids, agariciids, oculinids, alcyonaceans and hydrozoans were notably absent from the UAE fauna.

1.3.6 Coral bleaching events in the Gulf

Coral reef bleaching events reported in the Gulf are considered to be driven mainly by water temperature anomalies, the frequency of which has increased since the early 1980s. The frequency and scale of coral bleaching events in the Gulf during the past few decades have been studied thoroughly (Shinn, 1976; Sheppard et al., 1992; Riegl, 2002; Sheppard, 2003). Details of these reports are available online in various databases

maintained by agencies such as the World Fish Center (www.worldfishcenter.org), NOAA (www.noaa.gov), and Great Barrier Reef Marine Park Authority (www.gbrmpa.gov.au).

1964

The first coral mortality event in the Gulf was reported by Shinn (1976) around the Qatar coastlines. The paper presents the result of onshore transect surveys from the eastern and northern part of the peninsula, extending to a depth of approximately 7.6m. The initial survey in May 1965 was followed by further studies in 1965 and 1966. In 1965, the studied areas contained dead *Acropora* communities covered with soft green and brown algae as well as encrusting coralline algae. The mortality of these corals appeared to have been the result of an unusually severe Shamal wind, which had occurred during the previous year (1964). The wind started on January 19th, 1964 and reached full force on January 20th at around 65 k/h velocity. The water temperature at 18 m depth was 14.1 °C, and the air temperature was 0.5 °C, which was the lowest temperature ever recorded in Qatar. However, after an 18-month period from May 1965 to September 1966, the small *Acropora* colonies, 1-2 cm in height, were found attached to the dead coral branches and other hard substrates. By September, 1966 abundant *Acropora* colonies ranging in height from a few centimeters to around 20 cm were found. Shinn (1976) concluded that these newly growing corals constituted a population that had grown from coral larvae transported from distant sources of living coral such as Halul Island and the reefs near Bahrain Island, which were the closest source available.

1981

According to Holt-Titgen (1982), a second coral mass mortality occurred near Jebel Ali in Dubai between July 1979 and February 1981. In fact, 1980 had the highest positive summer water temperature anomaly of the period 1969–1987 was followed by a cold winter, and subsequently by an even hotter summer in 1981. In this event, the majority of *Acropora* species was affected. The primary cause of this event was probably the fluctuation of a hot summer followed by a cold winter (Riegl and Purkis, 2012a).

1988

A series of cold fronts passing over the western Arabian Gulf, in Saudi Arabia from Manifa area to Tarut Bay (Coles and Fadlalallah, 1991b) from December 1988 to March 1989 produced the longest period of sustained low water temperatures ever recorded in any coral reef area around the Gulf. Water temperatures reached 11.4 °C on 19-20 January at Manifa area, and 12.0 °C on 19 January at Tarut Bay. Water temperatures stayed below 16 °C for 62 days at Manifa compared to 35 days in Tarut.

Severe mortality at those sites was restricted to *Acropora* and *Platygyra*, whereas severe stress was observed in most species, such as *Porites lutea*, *Psammocora contigua*, *Pavona varians*, *Coscinarea monile*, *Leptastrea purpurea*, *Cyphastrea microphthalma*, *Favia pallida*, *F. speciose*, *F. favus*, *Farites pentagona*, and *Tubinaria crater* (Coles and Fadlalallah, 1991b).

1996

In 1996, an abnormally elevated water temperature was recorded in the UAE, reaching 35°C, southern Gulf (Riegl, 1999b). It was the most severe mass mortality in the Arabian Gulf region and the world widespread event ever recorded (Riegl and Purkis, 2012a). This coincided with a large El Nino event, switching over to a strong La Nina in mid-1998 (Wilkinson, 1998). Positive water temperature anomalies in the Gulf started in April and lasted until September 1996. During June, July, and August the anomalies reached 1.5–2.5 °C above normal (Riegl, 2002). The water temperature reached 35°C, which is about 2°C above the normal maximum in that region. About 95% of *Acropora* community bleached at Abu Dhabi and Dubai, mainly between Jebel Ali and Ras Haysan. Six species of *Acropora* disappeared after the mass mortality, including *Acropora pharaonis*, *Acropora horrida*, *Acropora valenciennesi*, *Acropora arabensis*, *Acropora florida*, and *Acropora valida*. The dominant populations left were poritid and faviid species (Riegl, 1999b). Only one viable population of *Acropora clathrate* remained in the region, found 30 km east of Abu Dhabi, in Deira Corniche, Dubai. Other coral communities that survived the event were distributed in deeper water, such as *Pseudosiderastrea tayamai*, *Porites mayeri* and *Coscinarea monile* (Riegl, 1999b). The overall species richness in the UAE went from 34 to 27 species, and healthy coral cover was reduced from 90% to about 26% (Riegl, 1999; Riegl, 2002).

The 1996 bleaching event was not restricted to the UAE, but affected also the Kingdom of Saudi Arabia, Bahraini, Oman, Madagascar, parts of the Great Barrier Reef, parts of Indonesia and the Philippines, Taiwan, Palau, French Polynesia, Galapagos, Bahamas, Cayman Islands, Florida, Bermuda, and Brazil coastlines (Wilkinson, 1998; Goreau et al.,

2000). However, across certain areas of the world such as the Red Sea, southern Indian Ocean, eastern Andaman Sea, most of Indonesia, large parts of the Great Barrier Reef, most of the central Pacific and many parts of the southern and eastern Caribbean, bleaching was less pronounced or even insignificant (Wilkinson, 1998; Goreau et al., 2000).

Along the Bahrain and Saudi Arabia coastline over 90% of the same species also bleached (Wilkinson, 1998). *Acropora* species, considered to be most temperature sensitive, had been the dominant habitat forming coral in this area (Coles, 2003).

1998

The Gulf was not only affected by a temperature anomaly in 1996 but also in 1998. In UAE, coral cover was further reduced from 26% to 22% (Riegl, 2002). However, in 1998 the Gulf did not experience coral bleaching and mortality comparable to the Indo-Pacific coral systems. Seawater temperature exceeded 34°C for 14 continuous weeks, and reached 36°C for three weeks in August 1998 when bleaching started (Riegl, 2002; George and John, 2000). This unusual rise in sea surface temperature was the greatest since 1870 (Sheppard and Rayner, 2002) and it also coincided with a severe EL Niño- La Niña event during late 1997 and early 1998, which was the largest of this type ever recorded (Wilkinson, 1999, 1998; Goreau et al., 2000; Sheppard and Loughland, 2002b; Sheppard, 2003). Although in most regions *Acropora* was the most affected species. Only small populations of *Acropora* survived in the UAE at Ras Ghantoot, Deira, and Sir Abu Nuair (Riegl, 2003). Massive *Porites lutea* and *Siderastrea savigniana* colonies had the highest spatial extension and did not suffer bleaching during either 1996 or 1998 events (George and John, 1999, 2000; Goreau et al., 2000; Riegl, 2002). In 1998, bleaching was also

documented in Madagascar, Tanzania, Kenya, Comores and Reunion. No bleaching was recorded in South Africa (Wilkinson, 2004).

2002

During summer 2002, water temperature reached 37 °C in the southern Gulf area (Jebel Ali and Ras Hasyan in Dubai). This event, which may have also been linked to the Pacific El Niño/Southern Oscillation (ENSO) (Riegl, 2003), had only negligible effects on the remaining coral communities in the area (Riegl, 2003). *Acropora* sp. bleached at Jebel Ali and Ras Hasyan, but not at Sir Abu Nuair, whereas most *Porites lutea*, *Porites solida*, and *Porites lobata* bleached. However, all of these species had fully recovered by November 2002 (Riegl, 2003; Coles and Riegl, 2013), possibly as a consequence of their previous exposure to extreme temperatures in 1996 and 1998 (Riegl, 2002, Coles and Brown, 2003). This scenario is supported by the adaptive hypothesis, according to which reefs that recovered from stress might show an increased resistance to subsequent bleaching events likely due to changes in coral symbiont communities (Baker, 2001; Baker et al. 2002)

2007

According to Foster et al. (2012), seawater temperature in August 2007 reached 37 °C in Qatar and Abu Dhabi. Still, only mild bleaching was observed in these areas, In contrast, corals, mainly *Acropora*, in Iran were suffered notable bleaching and subsequent mortality in that year (Baker et al., 2008; Shuail et al., 2016).

2008

Extreme-temperature-related bleaching events were absent during 2003-2009. In fact, coral species, such as *faviids* and *Porites* spp. showed strong signs of recovery in between 2002 and 2010 (Riegl and Purkis, 2012a). However, reports have documented two bleaching events that were linked to environmental factors other than temperature. The first event was caused by a harmful algal bloom (HAB) that was sustained from August 2008 to May 2009 (Richlen et al., 2010). It resulted in mass mortality of corals, such as *Pocillopora* and *Acropora* sp., as well as of wild and farmed fish in the area (Bauman et al., 2010). It also stopped the operation of most desalination plants in Oman and the UAE (Richlen et al., 2010). News from the Emirates Diving Association (EDA) also reported 95% damage to coral reefs in the Dibba Marine Protected Zone in Fujairah (Landais, 2009). This harmful algal bloom was related to the dinoflagellate species *Cochlodinium polykrikoides*, the first time this species was reported in the region (Naser, 2014). The western parts of the Gulf, including Dubai and the Abu Dhabi Emirates, did not witness any coral bleaching related to this bloom (Riegl et al., 2012).

2009

During the summer of 2009, a second bleaching event, unrelated to temperature anomalies, occurred in Abu Dhabi. It was driven by diseases, which caused an overall mortality of about 10% of the corals (Riegl and Purkis, 2015b). The event started from May and persisted till September, but the onset of the event occurred in the last week of August or early September (Riegl and Purkis, 2015b).

2010

In the summer of 2010, corals in the Arabian Gulf were influenced by prolonged exposure to temperatures between 33°C and 36°C (Riegl et al., 2011; Guest et al., 2012; Riegl and Purkis, 2015a). From the beginning of August, bleaching was observed in eastern Abu Dhabi and Qatar, where local temperatures reached 36.4°C (BuTinah, Abu Dhabi) and 36.1°C (Fasht el Hurabi, Qatar) (Riegl et al. 2012). In Abu Dhabi most coral species including *P. harrisoni* and *A. downingi*, and *D. pallida* bleached (Riegl and Purkis, 2015a). According to the observations of Riegl et al. (2011), Acropora sp. colonies had a bleaching percentage of 70% and 50–90% mortality from disease outbreak. Porites sp. colonies had 60% bleaching. 15-18% of the massive and encrusting Porites, Cyphastrea, Favia, Favites, and Platygyra colonies bleaching ranged from 15 to 80%. *Coscinaraea*, *Turbinaria*, *Anomastrea* had 50 to 100% bleaching. The overall mortality was specific to the Acropora species in the western Abu Dhabi (Dalma, Bu Tinah, Al Heel), which suffered almost 100% mortality. In contrast only 60 to 80% mortality of Acropora was witnessed in eastern Abu Dhabi (Ras Ghanada) (Bernhard and Riegl et al., 2012; Coles and Riegl, 2013).

Considerable numbers of *Acropora* and *Porites* were able to withstand the thermal stress and had recovered by the end of September (Riegl and Purkis, 2012a). Mortality coincided with the occurrence of a coral disease known as White Syndrome (WS) disease, a growing threat to coral reef ecosystems (Riegl et al., 2012a). WS is responsible for the demise of a significant number of coral reefs worldwide, such in the Great Barrier Reef (Kvennefors and Blackall, 2007). The occurrence of such a coral disease in this year might have possibly been related to the temperature stress (Riegl and Purkis, 2015a). Comparable

incidents have also been reported in the Great Barrier Reef, the Florida Keys and the Caribbean region (Bruno et al., 2007, Brandt and McManus, 2009, Eakin et al., 2010).

2011

Bleaching occurred across the eastern Abu Dhabi region in summer 2011, from August to November, along with a new major disease outbreak, known as the Black Band Disease (BBD). This resulted in significant mortality for all corals in this area (Riegl et al., 2012). Moreover, similar to 2010, this BBD outbreak coincided with high water temperature that reached 35-36 °C for six consecutive weeks (Coles and Riegl, 2013). Overall, there was 20% decline of total cover in the southern Gulf (Riegl and Purkis, 2015a). It is important to note that the occurrence of BBD and WS was new in the southern Gulf region (Korrubel and Riegl, 1998) and it affected several species including *Acropora downingi*, *A. clathrata*, *A. pharaonis*, *A. valida*, *Favia pallida*, *F. speciosa*, *Platygyra daedalea*, *P. lamellina*, *Cyphastraea microphthalma* and *Dipsastrea pallida* (Riegl and Purkis, 2012a; Riegl and Purkis, 2015a).

2012

A severe bleaching event affected the coral population off the coast of Abu Dhabi, UAE between August and September 2012 (Riegl and Purkis, 2015a; Shuail et al., 2016; Howells et al., 2016a). In the southern Gulf (Abu Dhabi), the corals experienced a higher number of warm days (about 20 days of temperature above 35 °C) than the remaining Gulf sites (Howells et al., 2016a). In the Oman Sea, summer temperatures rarely exceeded 33 °C, and no bleaching was observed in 2012 (Howells et al., 2016a). According to Shuail et al.

(2016), coral communities in the western parts of Abu Dhabi had less relative heat stress than in the eastern regions. Specifically, coral communities endured 16 days above local thresholds in Ras Ghanada reefs and 15 days in Saadiyat reefs. In contrast, in Delma Island reefs, the temperatures were higher than the local bleaching threshold for only 10 days. In Saadiyat and RasGhanada reefs ~40% of the corals showed signs of bleaching, while only 15% of the corals were affected on the Delma reef (Shuail et al., 2016). The 2012 event caused the least decline (15%) in the southern Gulf, but the cover was already low due to the back to back bleaching events (2009, 2010, 2011 and 2012) (Riegl and Purkis, 2015a).

2017

Following the 2012 event, there were no records of bleaching in the southern Gulf until summer 2017, a severe coral bleaching witnessed in August 2017 on nearshore reefs in Qatar, Bahrain, and all nearshore reefs along the coast of the UAE. More severe impacts appear to be experienced towards eastern parts of Abu Dhabi city, with >95% coral bleaching, >70% coral mortality, than towards the west (30-40% bleaching in Delma island). The normally stress-tolerant *Porites* seem to have been hardest mortality in Abu Dhabi, with >90% of *Porites* now dead at Saadiyat reef (Burt and Wiedenmann, 2016).

1.4 Study sites

This study will focus on the coral communities at three sites in the southern Gulf in Abu Dhabi Emirate. The sites are Delma (latitude 24.5208/longitude 52.2781), Saadiyat (lat. 24.599/long. 54.4215) and Ras Ghanada (lat. 24.8481/long. 54.6903) (Figure 1.9). These sites were selected for their coral cover and their pronounced difference in their

bleaching patterns during 2012 bleaching event (Shuail et al., 2016). The majority of the coral communities in these sites were composed of four common families, poritids, faviids, acroporids, and siderastreeids (Burt et al., 2011; Foster et al., 2012).

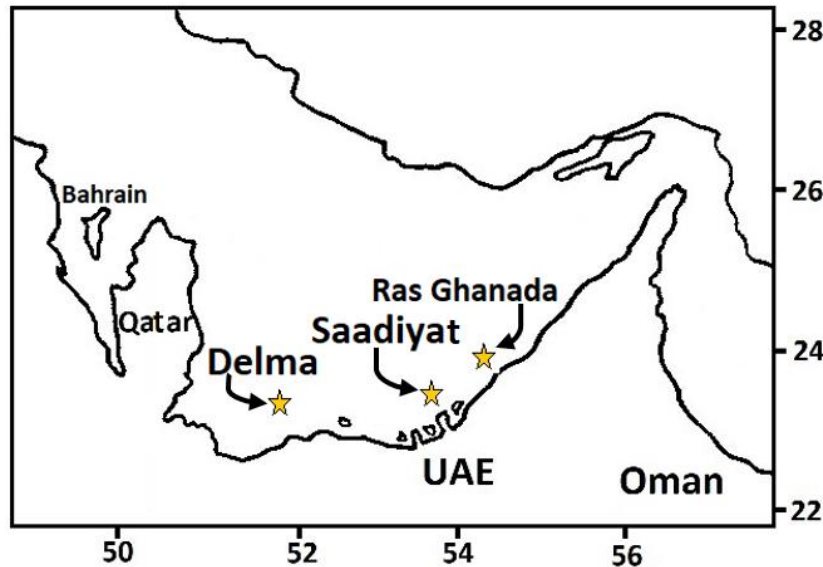


Figure 1.9. Study sites in UAE (Abu Dhabi) are Delma (lat. 24.5208/long. 52.2781), Saadiyat (lat. 24.599/long. 54.4215) and Ras Ghanada (lat. 24.8481/long. 54.6903).

1.4.1 Delma

Delma is a diapiric island found offshore the west of Abu Dhabi coastal area, surrounded by remnants of incipient coral fringes (Ben-Romdhane et al., 2016). Coastal modification has affected several extensive reef areas around the island. For example, Delma airport, which is located on the eastern coast of the island, lies on top of a fringing reef. However, the tidal areas yielded large suitable areas for coral framework development (Riegl and Purkis, 2012a). Delma is one of the islands that is located southeastern of the Qatar peninsula. This area is known to have an overall higher water temperature than the eastern parts of the Gulf, which is more exposed to winds (Sheppard and Loughland,

2002b). It is mostly dominated by more resilience species such as nodular *Porites*, faviids and *Platygyra* spp, with *Acropora* being rare or completely absent (Riegl and Purkis, 2012b; Shuail et al., 2016).

1.4.2 Saadiyat

Saadiyat is a 27 km² island 500m off the coast of Abu Dhabi. According to Foster et al. (2012), it is moderately populated with live coral cover ranging from 12.5 to 16.9 corals per m². However, this region is threatened by a major coastal development and discharges from industrial facilities including power generation, iron and steel works, which are concentrated in Industrial Cities Abu Dhabi (ICADs), Mussafah Industrial Area and Khalifa Industrial Zone Abu Dhabi (KIZAD) (EAD, 2015).

1.4.3 Ras Ghanada

Ras Ghanada is a headland, extending out into the water, located near the border with Dubai, about 90 kilometres northwest Abu Dhabi. It has one of the largest and yet least impacted high-diversity habitats in the UAE (Sheppard et al., 2010). Around this headland, there are mangroves, seagrass beds and an extensive coral reef, more than 24 corals per m² (Sheppard et al., 2010; Foster et al., 2012). Despite the nearby coastal construction at the Khalifa Port and Industrial Zone (KPIZ), coral reefs remain in good health.

1.5 Reference sites

Other coral reef regions of the Gulf were analysed for comparative purposes, including remote sensed sea surface temperature (SST) and meteorological data. These areas include Kuwait, the Kingdom of Saudi Arabia (KSA), Bahrain, Qatar, Iran and the Gulf of Oman (Figure 1.10).

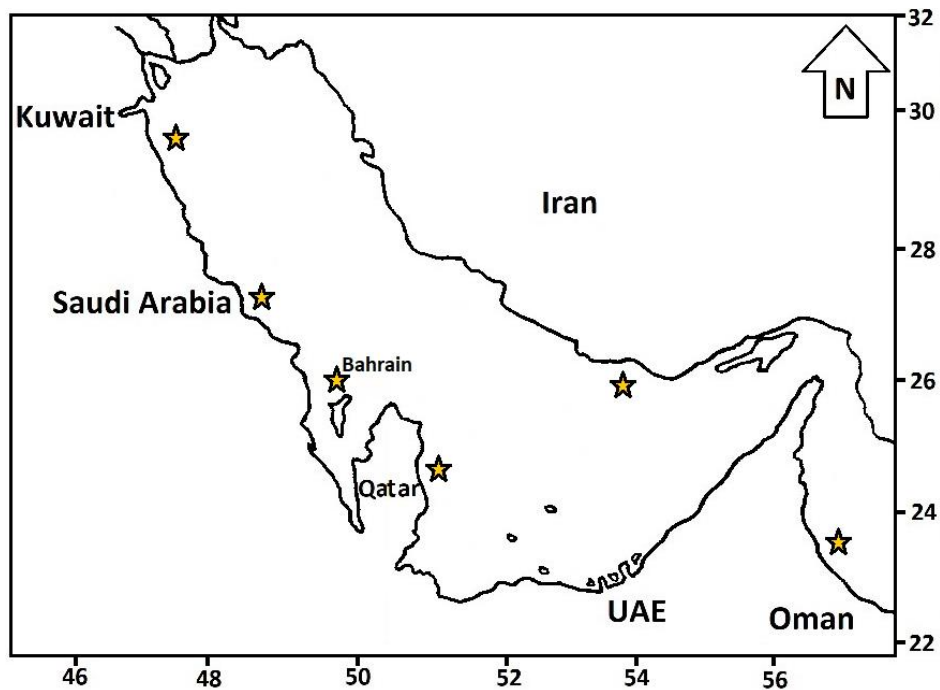


Figure 1.10. Reference sites around the Arabian Gulf. Including: Kuwait, the Kingdom of Saudi Arabia (KSA), Bahrain, Qatar, Iran and the Gulf of Oman.

1.5.1 Kuwait

Kuwait's coral reefs are located mostly in its southern part and around some offshore islands, mainly the islands of Kubbar, Qaru and Um Al-Maradim (Hodgson and Carpenter, 1995; Rezai et al., 2004). Coral communities are found as patches of fringing reefs and the most dominant species are *Porites harrisoni*, *Acropora arabensis* and *A. downingi* (Rezai et al., 2004). There are considerable impacts on these reefs from various

human activities, such as overfishing, solid waste disposal, such as paper, glass, metal and plastic containers, and widespread anchor damage (Wilkinson, 2008). These reefs were also among those most directly impacted by the oil spills from the Gulf War (Downing and Roberts, 1993). The reefs in Kuwait are exposed to a very heavy load of particles due to the shallow water environment and input from the Shatt Al-Arab (Wilkinson, 2004).

1.5.2 Kingdom of Saudi Arabia (KSA)

Corals along the Saudi coastline are mostly limited to small patch reefs between Ras Al-Mishab, Saffaniyah and Abu Ali, and between Abu Ali and Ras Tanura (Wilkinson, 2008). The most extensive and diverse reefs are around 6 offshore islands, particularly Jana and Karan. However, bleaching and mortality has impacted the majority of the live corals around these sites (Rezai et al., 2004). For example, around Karan Island, the population of the healthy corals was 33% in 1992, but declined to 23% in 1994 and 1% in 1999 after the Gulf-wide mass mortality in 1996 and 1998 events. Corals at Abu Ali island, which is part of Jubail area in the Eastern Province of KSA, also suffered about 99% mortality. None of the colonies of the extensive Acropora communities on the eastern of the peninsula were found alive in 1999 (Rezai et al., 2004).

1.5.3 Bahrain

Coral reefs in Bahrain are mainly distributed around the northern and eastern coastlines. Including Fasht Al Adhom; west Fasht Al Dibal; Khwar Fasht; north Jabari; Fasht Al Jarim; Samahij; and Abul Thama (Rezai et al., 2004). Following widespread mortality in 1996 and 1998, coral cover in Bahrain is very low. The only population of

living coral in Bahrain surrounds Abul Thama, a small raised area surrounded by 40 m deep water, about 72 km north of the main island (Wilkinson, 2008).

1.5.4 Qatar

The best coral growth conditions for Qatar are on its northern and eastern coasts, while the western coast is subject to extremes of temperature and salinity (Wilkinson, 2008). The best coral growth is found on the offshore islands, including Halul Island. However, the island contains oil and gas marine terminals and is subject to notable human impacts (Wilkinson, 2008). There has been very high coral mortality in the past 10 years from bleaching and human impacts. For example, several *Acropora* and *Porites* beds east of Doha suffered nearly 100% mortality in 1996 and 1998 (Spalding et al., 2002). Before 1998, there was heavy siltation from the construction of a breakwater and land reclamation for the new Doha International Airport that severely stressed these communities (Rezai et al., 2004).

1.5.6 Iran

Fringing reefs are known to occur along parts of the mainland and particularly around some of the offshore islands, including Kharg, Kharko in the northern coast, and Kish and Qeshm Islands in the southern region (Wilkinson, 2008). Around 35 coral species have been documented surrounding Hormuz Island (Rezai et al., 2004). Anthropogenic impacts are found in the main industrial areas in the northwest and around Kish and Qeshm (Rezai et al., 2004). These include sedimentation and pollution, together with solid waste and anchor damage (Spalding et al., 2002). Around Kish Island, algal overgrowth of corals

in the late 1990s was attributed to increased nutrient levels (Mohammadizadeh et al., 2013). The narrow waters around the Straits of Hormuz are among the busiest tanker lanes in the world, representing an ongoing threat to the southernmost reefs (Rezai et al., 2004).

1.5.7 Oman

The Omani shoreline is around 1700 km, and the healthiest coral areas are found along the Musandam Peninsula, Daymaniyat Islands, the Gulf of Masirah, Dhofar coast, and Al Hallaniyat Islands (Rezai et al., 2004). Around 107 species of reef-building corals have been documented in the Gulf of Oman, and an additional 20 species occur on Oman's Arabian Sea coast (Claereboudt, 2006). The most common species along the Omani coasts are *Montipora* sp., *Porites* sp. *Pocillopora* sp. and *Acropora* sp. The impact of the 1998 bleaching event Oman's corals was minor, the most affected area was the southern Oman, along the Arabian Sea coast, 95% of the more sensitive species (*Acropora*) showed partially bleaching symptoms. No mortality had been witnessed further north of the Arabian Sea coast or in Gulf of Oman (Coles, 2003).

1.6 Remote sensing as a monitoring tools for coral reef environment

Remote sensing is defined as the collection of information about an object without making physical contact with it (Schowengerdt, 2006). Remote sensing covers measurements using the electromagnetic spectrum characterising the properties of a landscape (Barrett and Curtis, 1992). Over the years remote sensing techniques have extended to provide the capability of measuring the entire electromagnetic spectrum (Colwell, 1983). Different sensors can be used to collect unique information about the

properties of the Earth's surface layers. For example, measurements of reflected solar radiation give information on albedo, which is the fraction of energy reflected from the Earth's surface back into space (Brest and Goward, 1987). Thermal sensors measure surface temperature, and microwave sensors measure the properties of soil or snow surface (Engman and Gurney, 1991). The challenge for the user is to interpret these remotely sensed properties in a way that can be used for effective management and monitoring.

The potential of remote sensing applications to deliver essential information has been highlighted by many researchers (Franz et al., 2005; Liu et al., 2014; Pettorelli et al., 2014; Blondeau-Patissier et al., 2014; Zhao and Ghedira, 2014; Sahay et al., 2014). There is clearly an urgent need to access global, long-term, reliable information on spatial and temporal fluctuations in the distribution of direct and indirect environmental and anthropogenic pressures to the biological environment. This is particularly true for coral reefs ecosystems. As mentioned in the previous sections, mass mortality of coral populations in the Gulf has increased in frequency and severity over the last two decades, leading to the demise of the overall population density as well as coral species diversity (Riegl and Purkis, 2012b; Riegl and Purkis, 2015a). Several environmental factors are shown to be responsible for this deterioration in coral reef conditions, such as thermal stress and phytoplankton blooms (Riegl et al., 2012a; Riegl and Purkis, 2012b; Bauman et al., 2013a; Bauman et al., 2013b; D'Angelo and Wiedenmann, 2014).

Since the late 1970s, a variety of operational satellite sensors and algorithms have been developed to fulfill the requirements of coral reef managers and researchers (Bernstein and Stevens, 1986; Blondeau-Patissier et al., 2014). Spatial resolutions across all satellite sensors range from 50 cm to 100 km, with either daily, monthly or annual

information available for several sensors. Some of the widely used ocean colour sensors for the ocean biological activity are Coastal Zone Colour Scanner (CZCS), the Sea-viewing Wide Field-of-view Sensor (SeaWiFS) and two Moderate Resolution Imaging Spectroradiometers (MODIS-Aqua and MODIS-terra).

The first ocean colour data set derived from a spaceborne sensor was provided by the Coastal Zone Color Scanner (CZCS), onboard the National Aeronautics and Space Administration (NASA) Nimbus-7 spacecraft, (Hovis et al., 1980). It had five near infrared bands (443, 520, 550, 670, and 750 nm), and one thermal infrared band (10.5-12.5 μm). The satellite was in a sun-synchronous orbit with ascending node near local noon with a ground resolution of 825 m (Hovis et al., 1980). Feldman et al. (1989), were able to provide the first monthly global maps of the photosynthetic pigment (chlorophyll a) from this sensor. Following the success of CZCS, NASA launched an additional ocean colour capable sensors, the Sea-viewing Wide Field-of-view Sensor (O'Reilly et al., 1998; Wang, 1999; Stumpf et al., 2003). The SeaWiFS is a multi-spectral radiometer, synchronising the Earth's equator daily during the noon time (12:00) from August 1997 until December 2010 (O'Reilly et al., 1998; Franz et al., 2005). SeaWiFS views the planet's surface in eight spectral bands covering the visible and near-infrared (NIR) range from 400-900 nm. It has a global area coverage (GAC) resolution of 4.5km.

Another ocean color sensor MODIS instrument is currently on both the Aqua (MODIS-aqua) and Terra (MODIS-terra) platforms of the Earth Observing System (EOS). MODIS-terra was launched in December 1999 into a daily sun-synchronous orbit at 10:30 am, but it begins its operation from February 2000. MODIS-aqua platform was launched in May 2002 into a daily sun-synchronous orbit at 13:30 MODIS-Aqua has been in

continuous operation since June 2002 to the present (Alexandridis et al., 2009). Both MODIS sensors measure radiance in 36 spectral channels covering the range from 400 nm to 14.4 μm , supporting land, ocean, and the atmosphere. The bands of primary interest to ocean colour applications are the nine channels covering the spectral range from 400-900 nm. Both platforms (SeaWiFS and MODIS) collect data over a wide swath of a pixel resolution ranging from 1 km for SeaWiFS and from 250 m, 500 m to 1km for MODIS (Hu et al., 2001; Franz et al., 2005; Zhang et al., 2006; Gregg and Casey, 2007).

The remote sensing tool is considered a primary source of information for the monitoring of abiotic conditions, such as temperature, winds, rainfall and bathymetry (Kidder and Vonder Haar, 1995; Rees, 2013; Martin, 2014). Biotic factors, as well, can be acquired from the several ocean colour sensors, such as detection, mapping and monitoring of phytoplankton blooms (Al-Yamani et al., 2006; Mol et al., 2007; Nezlin et al., 2007).

The above-mentioned ocean colour sensors are designed to retrieve the spectral information of the upwelling radiance above the sea surface that is referred to as the water-leaving radiance or $L_w(\lambda)$. This radiance can be used to estimate a number of geophysical data parameters, such as the concentration of chlorophyll *a*, which is the direct proxy for phytoplankton biomass (Cullen, 1982; Alexandridis et al., 2009). Chlorophyll-*a* (chl-*a*) global distribution (Figure 1.11) of shows that the rich chl-*a* areas are located along the coasts and continental shelves, mostly because of a strong nutrient supply (Rabalais et al., 1996). Moderate chl-*a* concentrations are found along the equator in the Atlantic and Pacific regions, which is caused by the upwelling of deep, nutrient-rich, cool waters from the divergence of the ocean water masses along the equator (Lyle et al., 1992). Moderate chl-*a* are also found in the subtropical convergence zone, where cool, nutrient-rich sub-

Antarctic water masses mix with warm, nutrient-poor subtropical waters (Butler et al., 1992).

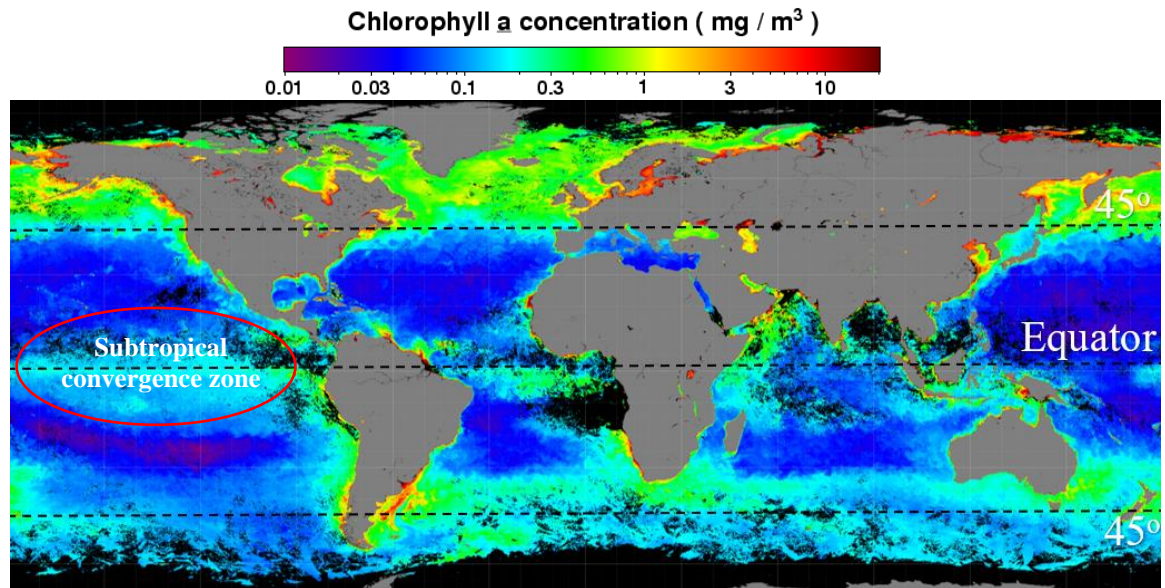


Figure 1.11. Examples of Chl-*a* satellite images from the MODIS-Aqua sensor showing the average global distribution of chl-*a* during September 2012. Showing rich chl-*a* areas along the coasts and continental shelves. Moderate chl-*a* concentrations are found along the equator in the Atlantic and Pacific region, and in the subtropical convergence zone (red circle). Source: <http://oceancolor.gsfc.nasa.gov> .

Over the past decades, most of the research in algorithm development was driven by the need for accurate retrievals of chl-*a* concentrations in open and coastal ocean waters from ocean color data. The empirical blue–green (440–550 nm) spectral band-ratios are the most common types of ocean color algorithms used for chl-*a* retrievals, because most of the phytoplankton absorption occurs within this visible spectrum region (Gordon et al., 1983; Feldman et al., 1984). However, most reflectance band-ratios are designed for global applications over optically deep ocean waters and the use of visible wavelengths can be unreliable in coastal waters (Odermatt et al., 2012). The blue–green (440–550 nm) of the spectrum region become less sensitive to changes in chl-*a* concentrations due to the increase in the concentrations of color dissolved organic matter (CDOM) and total

suspended matter (TSM) (Bowers et al., 1996). Additional limitations in the use of the blue–green ratios are regional differences in optical properties. In other words, the generalized global characteristics of some algorithms can be inapplicable in some of the world's ocean regions (Claustre and Maritorena, 2003; Volpe et al., 2007). Thereby, development of more sophisticated atmospheric corrections and constituent retrieval algorithms, are required for both improved retrieval accuracy for water quality variables and algal bloom detection in coastal ocean waters.

However, different strategies can be used to overcome these limitations and improve the quality of retrieved ocean colour information, such as the comparison of field data with *in situ* or ground-truth measurements. In the Arabian Gulf, there has been an increase in peer-reviewed publications on the study of phytoplankton using ocean color satellite data. Data Acquired from SeaWiFS and MODIS by Alsahli, (2007) were used as input to models for predicting ocean chlorophyll concentrations in the Kuwait coastal waters. The author showed that *in situ* chl-*a* measurements above 2.0 mg/m⁻³ in Kuwait Bay (10m max depth) had a good match with satellite chl-*a*, whereas in the southern coastal area, all *in situ* chl-*a* concentrations exceeding 1.20 mg/m⁻³ had a good relationship with satellite chl-*a*. The accuracy of assessment of phytoplankton biomass based on remote sensed chl-*a* can be limited by vertical distribution of phytoplankton (Nezlin et al., 2010). In the Gulf, vertical profiles of phytoplankton are characterized by low concentration in the upper 5–10 m layer (Sheppard, 1993; Subba Rao and Al Yamani, 1998), which may result in underestimating of total phytoplankton biomass from remote sensed chl-*a*. Nezlin et al. (2010) analysed the chl-*a* seasonal variability in different regions of the Arabian Gulf, and showed that in the deeper parts of the open Gulf water (50-80m deep) chl-*a* is

characterised by winter maximum ($1\text{-}1.5\text{ mg/m}^{-3}$) and summer minimum ($0.6\text{-}0.9\text{ mg/m}^{-3}$), while shallow coastal regions had a higher concentration with a minimum chl-*a* in spring ($0.7\text{-}1.5\text{ mg/m}^{-3}$) and the maximum in late summer and autumn ($1.5\text{-}3\text{ mg/m}^{-3}$).

The aim of this thesis is to combine a suite of remote sensing data and in situ measurements to establish long-term trajectories in environmental conditions in the Gulf to identify anomalies prevailing during recent coral bleaching events. These data sets will be used to test the central hypothesis of this thesis as defined in section 1.1.

Chapter 2: Local bleaching thresholds established by remote sensing techniques vary among reefs with deviating bleaching patterns during the 2012 event in the Arabian/Persian Gulf

Abstract

A severe bleaching event affected coral communities off the coast of Abu Dhabi, UAE in August/September 2012. In Saadiyat and Ras Ghanada reefs ~40% of the corals showed signs of bleaching. In contrast, only 15% of the corals were affected on Delma reef. Bleaching threshold temperatures for these sites were established using only day time remotely sensed sea surface temperature (SST) data recorded by MODIS-Aqua. The calculated threshold temperatures varied between locations (34.48 °C, 34.55 °C, 35.05 °C), resulting in site-specific deviations in the numbers of days during which these thresholds were exceeded. Hence, the less severe bleaching of Delma reef might be explained by the lower relative heat stress experienced by this coral community. However, the dominance of Porites spp. that is associated with the long-term exposure of Delma reef to elevated temperatures, as well as the more pristine setting may have additionally contributed to the higher coral bleaching threshold for this site.

This chapter is based on the publication: Shuail, D., Wiedenmann, J., D'angelo, C., Baird, A.H., Pratchett, M.S., Riegl, B., Burt, J.A., Petrov, P. and Amos, C., 2016. Local bleaching thresholds established by remote sensing techniques vary among reefs with deviating bleaching patterns during the 2012 event in the Arabian/Persian Gulf. *Marine pollution bulletin*, 105(2), pp.654-659 – Appendix A

2.1. Introduction

Warm water coral reefs are among the most productive and biologically diverse ecosystems on Earth. Many of these reefs are in decline due to the impact of a variety of global and local stressors (Sheppard, 2003, Baker et al., 2008, Logan et al., 2014, van Hooidonk et al., 2013, D'Angelo and Wiedenmann, 2014). Among them are heat stress episodes during which temperatures exceed a regional threshold and induce the breakdown of the coral/alga symbiosis which manifests as coral bleaching (Baker et al., 2008, Goreau and Hayes, 1994). The globally highest bleaching thresholds are found among corals of the southern Arabian/Persian Gulf, hereafter IRSA (Inner ROPME Sea Area) where they survive peak temperatures above 35 °C (Coles, 2003; Sheppard et al., 1992). However, these corals can fall victim to bleaching. Coral bleaching linked to unusually warm temperatures has been shown to affect the IRSA at least since 1996 contributing to the loss of coral cover (Riegl and Purkis, 2015; Riegl, 2002). The variability of bleaching susceptibility between among different species resulted in shifts of the coral community structure in the aftermath of bleaching events in the IRSA (Riegl and Purkis, 2015).

According to Riegl et al., (2011) and Riegl and Purkis, (2012), coral bleaching was observed in summer (August-October) 2010. In this year a positive SST anomaly of 1-3°C was witnessed over the Gulf region with the maximum heat found in the southern part of the Gulf, particularly Abu Dhabi and Qatar offshore island, reaching an hourly maxima of 36.4°C in Abu Dhabi and a daily average of 35.72°C in Qatar (*in situ* measurements), which exceeded the long-term summer means by 2.5°C. The 2010 bleaching event showed that Gulf corals bleach when daily mean temperatures remain above 34°C for a total of 8 weeks (Abu Dhabi 67 days, Qatar 57 days) during which more than 3 weeks are spent above 35°C

(Abu Dhabi 23 days, Qatar 33 days). These values exceeded, not only considerably higher than for corals within the Indo-Pacific and Caribbean generally, but the highest ever recorded (Hoegh-Guldberg et al., 2007; Berkelmans, 2009).

The IRSA is a shallow basin at high latitude and the thermal properties of the waterbody respond quickly to local factors. Rapid cooling by winds (Thoppil and Hogan, 2010; Cavalcante et al., 2016) or preferential heating/cooling in shallow areas or regions protected by headlands is common (Riegl and Purkis, 2012). Correspondingly, small scale excursions of thermal stress with consequent variation in the severity of coral bleaching and mortality events have been observed. A severe bleaching event recorded in 2007 off the Iranian coast (Baker et al., 2008) was absent or had negligible impact in the south-eastern IRSA. Bleaching was observed in 2013 in Qatar, but not in eastern Abu Dhabi (B. Riegl pers. obs.). In general, coral stress events in the northern IRSA (Iran) often do not coincide with those in the southern IRSA, and the Western IRSA (Kuwait, KSA, Bahrain) appears to have suffered fewer, or at least differently-timed, events than the south-eastern IRSA. Hence, strong regional variability in the frequency and severity of bleaching events seem to be characteristic for the region. Bleaching events are frequently characterized by high variability. On an individual level, the within-colony bleaching response can strongly vary depending on light exposure (Coles and Jokiel, 1978; Brown et al., 1994; Hoegh-Guldberg, 1999). Further variability can also arise from the bleaching susceptibility of different zooxanthellae clades/species (Baker, 2001; Pettay et al., 2015). Among them, the year-round prevalent algal partner of corals in the southern IRSA, Symbiodinium thermophilum, can be considered to be one of the most thermo- tolerant symbionts (D'Angelo et al., 2015; Hume et al., 2015). Marked regional variability is commonly

encountered during bleaching events and may be caused by small-scale water-dynamics and flow patterns (Nakamura and Van Woesik, 2001; Davis et al., 2011), by greater adaptation/ acclimatization due to previous stress episodes (Brown et al., 2002; Guest et al., 2012) or by differences in the species assemblage of the affected sites (Marshall and Baird, 2000). The onset of bleaching is often not synchronous across several, even nearby, reefs and neither is the severity or the effects of bleaching (Baker et al., 2008). Additional stressors, such as the disturbance of the nutrient environment, can have significant impacts on bleaching susceptibility (Wiedenmann et al., 2012; D'Angelo and Wiedenmann, 2014). In this context, the mean water column productivity, besides mean temperatures, was the best predictor of the variability of coral reef recovery across the Indo-Pacific (Riegl et al., 2015). Also, local adaptations to environmental factors other than temperature can have strong influences on the temperature tolerance of corals. D'Angelo et al. 2015, have shown that IRSA corals are characterized by a pronounced local adaptation to the high salinity of their habitat and that their superior heat tolerance is lost when they are exposed to normal oceanic salinity levels (D'Angelo et al., 2015). Global warming will expose the world's reef to positive temperature anomalies with increasing frequency (Logan et al., 2014). The prerequisite for knowledge-based coral reef management that aims to regionally mitigate the effects of climate change is a thorough understanding of how local factors modulate the response to temperature stress. Therefore, I set out to identify the causes for local differences in bleaching severity observed among coral communities in the southern IRSA off the coast of Abu Dhabi. Since remote sensing platforms offer valuable tools to reconstruct environmental conditions prevailing during coral reef disturbance events

(Andréfouët et al., 2014), we used satellite data to establish the local bleaching thresholds in the study sites.

2.2. Materials and methods

2.2.1. Measuring SST using remote sensing products

The SST (°C) data was extracted from the Aqua\Terra Ocean Colour 3 (OC3) Moderate Resolution Imaging Spectroradiometer (MODIS) imagery downloaded from the NASA ocean colour data website (<http://oceancolor.gsfc.nasa.gov/>) and by the Regional Organization for the Protection of the Marine Environment (ROPME) archived in Kuwait. MODIS data are recorded by two instruments. The first is integrated in the Terra satellite (MODIS-Terra), launched in December 1999. The second instrument is installed on the Aqua satellite (MODIS-Aqua), and was launched in May 2002. Both satellites are in sun synchronous orbits: Terra crosses the equator in a descending node at 10:00, and Aqua crosses in an ascending node at 12:00 noon. Satellite imagery was used for the periods between February 2000 to December 2014 (MODIS-Terra) and from July, 2002 to December, 2014. (MODIS-Aqua). Level-2 images were used for which the sensors were calibrated, geo-located with atmospheric corrections and bio-optical algorithms had been applied. Temperatures were determined for 1 km² areas covering the study sites, the highest spatial resolution provided by the MODIS product. Images were analyzed using the SeaWiFS Data Analysis System (SeaDAS) software program Version 7.2 and VISAT BEAM software Version 4.10.3. Images in which the SST signal was affected by cloud cover or high amounts of dust in the air were excluded from the analysis. The time of recording of the respective imagery was extracted from file names.

2.2.2. Reconstruction of daily temperature maxima *in situ*

In situ water temperature timeseries were recorded at ~7 m depth for the Saadiyat and Delma sites using Hobo temperature loggers (Tempcon, UK) at hourly intervals from January to December 2013. Using this data set and data from August 2014, typical daily temperature variations were calculated by averaging the corresponding hourly values for the last week of August, commonly one of the hottest weeks of the year. This temperature record revealed considerable variations of the temperature over the course of the day with temperatures differing by >0.25 °C between the early morning hours and the daily temperature maximum at ~17:00 (Figure. 2.1).

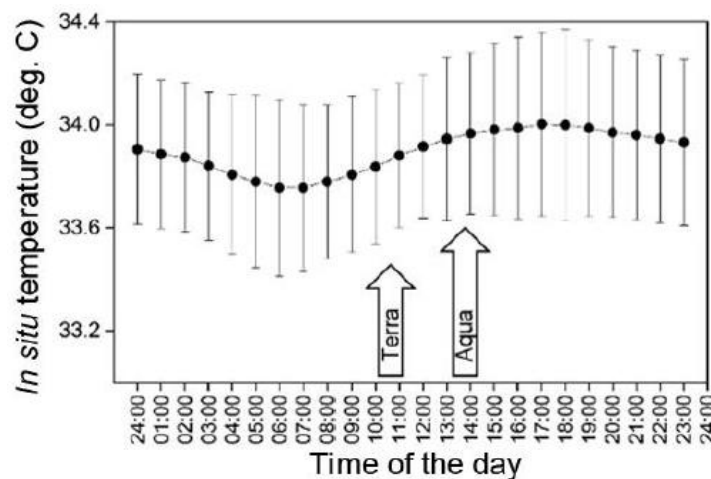


Figure 2.1. In situ temperature data recorded in hourly intervals at ~7m depth at the Saadiyat site. The graph shows the average temperatures and standard deviations calculated from the values obtained for the last week of August from the years 2013 and 2014.

2.2.3. Reconstruction of daily temperature maxima using remote sensing data

The recording times of the analyzed MODIS Terra and Aqua imagery show considerable deviations due to the different flight paths of the satellites. Terra data were recorded between 09:30–11:45 (median 10:50) whereas Aqua images were taken in the period 12:05–14:20 (median 13:50). The Terra data provided values that can be ~ 0.15 °C

below the daily SST maximum due to their early recording time. By contrast, MODIS Aqua records close to the *in situ* temperature maximum and its data are therefore best suited to reconstruct the SST of the IRSA. To verify this method, we selected >250 pairs of MODIS-Aqua values and corresponding *in situ* measurements (14:00 data points), from days distributed over all seasons of 2013. Then, the corresponding temperature values were plotted against each other and the coefficient of determination (R^2) for a linear regression fit was calculated (Figure. 2.2).

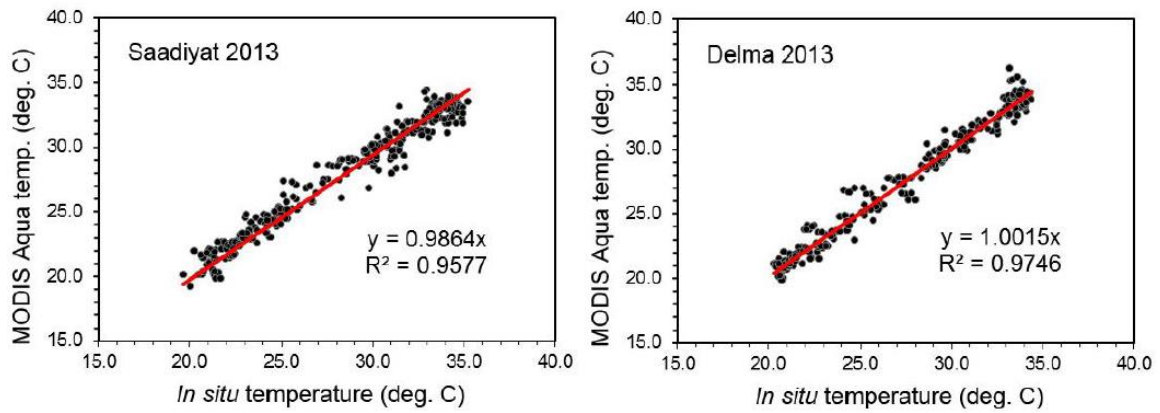


Figure 2.2. MODIS-Aqua data and the corresponding *in situ* temperature. Values were plotted against each other and the coefficient of determination (R^2) for a linear regression fit was calculated. Equations are given in the graphs.

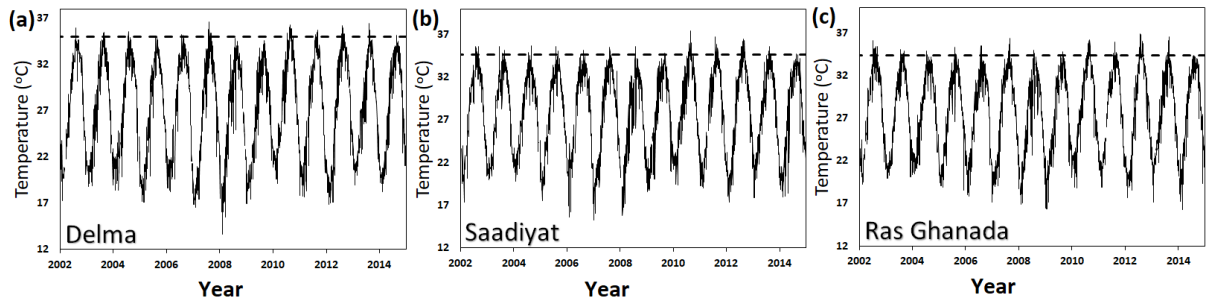


Figure 2.3. Time series of regional SST in the southern IRSA. SST values were obtained from MODIS-Aqua imagery from 2002-2014 for (a) Delma, (b) Saadiyat and (c) Ras Ghanada. The local bleaching thresholds (Delma: 35.05°C, Saadiyat: 34.55°C and Ras Ghanada: 34.48°C).

2.2.4. Calculation of bleaching threshold temperatures

The MODIS-Aqua SST data set was used to calculate the local threshold temperature of coral bleaching, defined as the temperature 1 °C higher than the highest monthly mean temperature (Glynn and D'Croz, 1990). Since the SST peaks are mostly in August in the southern IRSA (Figure. 2.3), we used this period to determine the highest 4-weekly mean temperature using the Aqua data set for the years 2002 to 2014. However, since temperatures are also high in the first two weeks of September, the period from 15th August to 15th September was analyzed for comparison.

2.2.5. Field surveys

Coral communities were surveyed at three sites in the southern IRSA in UAE, Delma (lat. 24.5208/long. 52.2781), Saadiyat (lat. 24.599/long. 54.4215) and Ras Ghanada (lat. 24.8481/long. 54.6903) (Figure. 2.4). At each of these sites, bleaching was recorded along three replicate transects during the period from 17th to 19th September 2012. Transects were arranged radially around a central origin, extending for 10 m with 120 degrees separating each transect. Corals were classified to genus level on the basis of Veron (2000), with taxonomic updates from Budd et al. (2012). The genus of juvenile corals (>5 cm diameter) within a 1 m wide band were included in the dataset. The analysis of adult corals was restricted to Platygyra spp. and Porites spp. as these corals were represented in large numbers in all sites. Porites spp. were represented by species with massive growth forms (Porites cf. lutea, lobata and harrisoni). Underwater color scales were used to assign the degree of bleaching to three categories: 1) Bleached: The whole colony was white, 2) Partially bleached: Larger parts of the colony (>20%) lost their normal colour and 3)

Unbleached: The colonies showed their typical variety of colours. Chi-square statistic (χ^2) was used to test whether the percentage of bleached, partially bleached and non-bleached coral colonies recorded in August 2012 in Delma, Saadiyat and Ras Ghanada was region-specific.

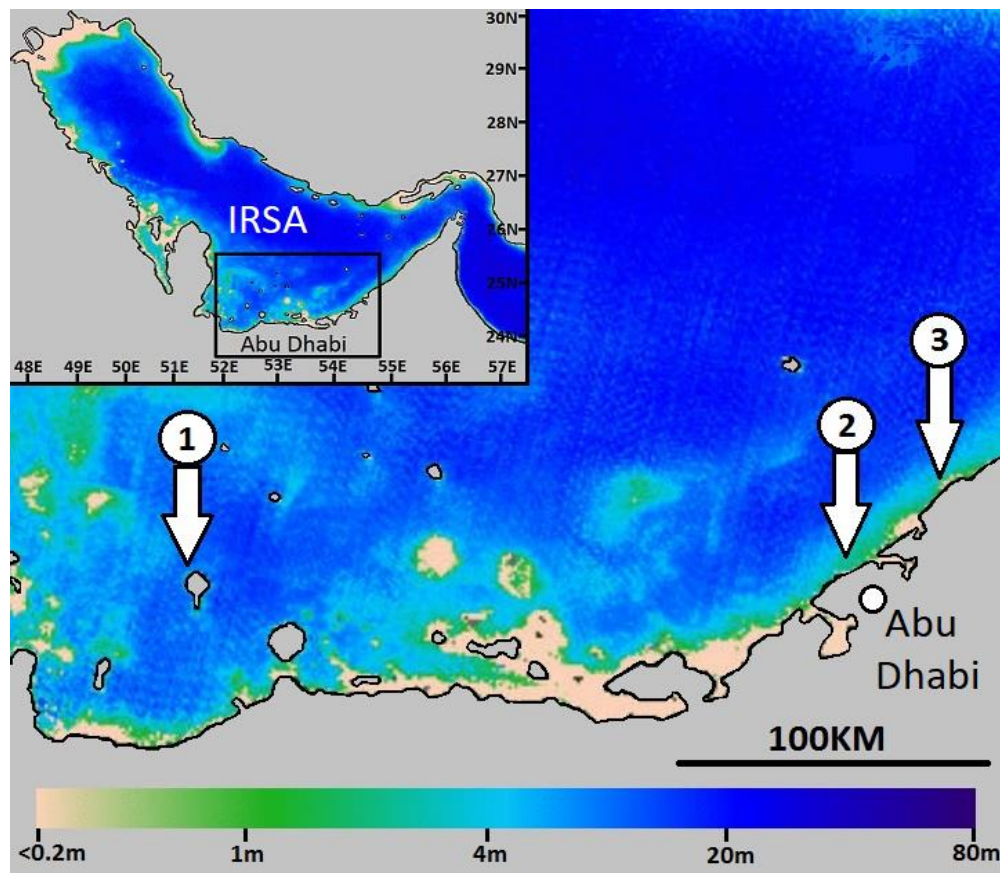


Figure 2.4. Study sites and bathymetric map of the southern IRSA. Numbers identify the three study sites: (1) Delma, (2) Saadiyat and (3) Ras Ghanada. The map was constructed using Sea-viewing Wide Field-of-view Sensor (SeaWiFS) Ocean Color Data provided by NASA Ocean Biology (OB.DAAC). Gray-level scale defines the depth in meters.

2.3. Results

2.3.1. Local temperature thresholds of coral bleaching

Using the MODIS Aqua data, the local threshold temperatures for coral bleaching (defined as 1 °C above the long-term average of the mean temperature of the 4 hottest weeks of each year) was calculated for the time period 2002–2014. Comparably high threshold temperatures were obtained for the 4 weeks of August and for the period from the 15th of August to the 15th of September, signifying the length of time over which IRSA corals are exposed to elevated temperatures (Table 2.1). My analysis revealed marked differences in the local temperature history of the study sites which are reflected in bleaching threshold temperatures ranging from 34.48 °C (Ras Ghanada) over 34.55 °C (Saadiyat) to 35.05 °C (Delma) (Figure. 2.5; Table 2.1). In summer 2012, the number of days during which temperatures exceeded 35.05 °C was comparable for the three sites (Figure. 2.5a). Around Delma reef, temperatures above 34.48 and 34.55 °C were recorded more frequently than for the other two sites within the same time period. However, due to the site-specific deviations of the bleaching threshold temperatures, the three locations showed considerable differences in the number of days during which their regional thresholds were exceeded (Figure. 2.5b). Specifically, coral communities had to endure above-threshold temperatures for 16 days in Ras Ghanada reefs and for 15 days in Saadiyat reefs. In contrast, in Delma Island reefs, the temperatures were higher than the local bleaching threshold for only 10 days (Figure. 2.5a). Also, the period of time between the first and the last day at which the threshold temperatures were exceeded was longer in Saadiyat and Ras Ghanada (~60 days) compared to Delma (~25 days). These data suggest

that similar relative heat stress levels were experienced by corals in Saadiyat and Ras Ghanada and that these were higher than in Delma.

Other methods of measuring coral thermal thresholds were used by Riegl and Purkis, 2012) (Method of Berkelmans (2002a, b)) in the southern Gulf area, particularly in the offshore islands of Abu Dhabi (Ras Ghanada, Al Heel, Delma and Bu Tina). These measurements have suggested that temperature threshold for the Gulf corals are between 35.7 and 36.0°C, above which bleaching is triggered. A mean bleaching curve was also evaluated by the author and shows that corals are likely to bleach if they are exposed to more than 3 weeks at daily mean temperatures at or above 35°C and between 8 and 9 weeks at or above 34°C (Riegl and Purkis, 2012). These thermal thresholds differences between this study and Riegl and Purkis, (2012), might be due to either the difference in the type of data used to construct the thermal thresholds, between the remote sensed data (1km resolution), which is used in this thesis, and the *in situ* logger used by Riegl et al., (2011) and Riegl and Purkis, (2012). Or due to the difference in the length of the time series used in the measurements of both studies. Riegl et al., 2011 and Riegl and Purkis, 2012 used an *in situ* logger's timeseries from 2007 to 2010, while in this study I used a timeseries from 2002 to 2014 to construct the coral thermal threshold.

Table 2.1. Calculated bleaching threshold from the remote sensed, MODIS-Aqua, SST for the hottest weeks of the year, including all August (first row) and 15-August to 15-September, compared to other studies in the same region (Riegl et al., 2011).

	Delma	Saadiyat	Ras Ghanada
Bleaching threshold temperature (remote sensed SST) (1-31 Aug. 2002-2014)	34.99 °C	34.55 °C	34.37 °C
Bleaching threshold temperature (remote sensed SST) (15 Aug.-15 Sep. 2002-2014)	35.05 °C	34.53 °C	34.48 °C
Bleaching threshold temperature (in situ) (1-31 Aug. 2007-2010)(Riegl et al., 2011)			35.72 °C

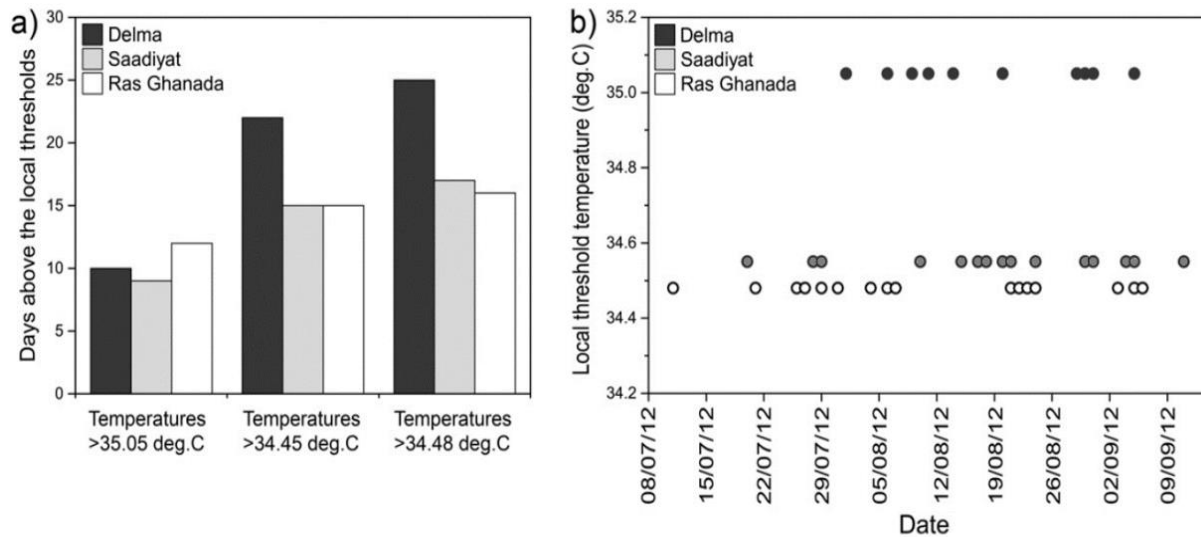


Figure 2.5. Variations in heat stress exposure during the 2012 bleaching event in the southern IRSA reconstructed from MODIS-Aqua imagery. a) Number of days during which the site-specific bleaching threshold temperatures (Delma: 35.05 °C, Saadiyat 34.55 °C, Ras Ghanada: 34.8 °C) were exceeded in each of the study sites. b) Days at which the site-specific local bleaching threshold was exceeded in the corresponding study sites, indicating also the length of the positive temperature anomaly.

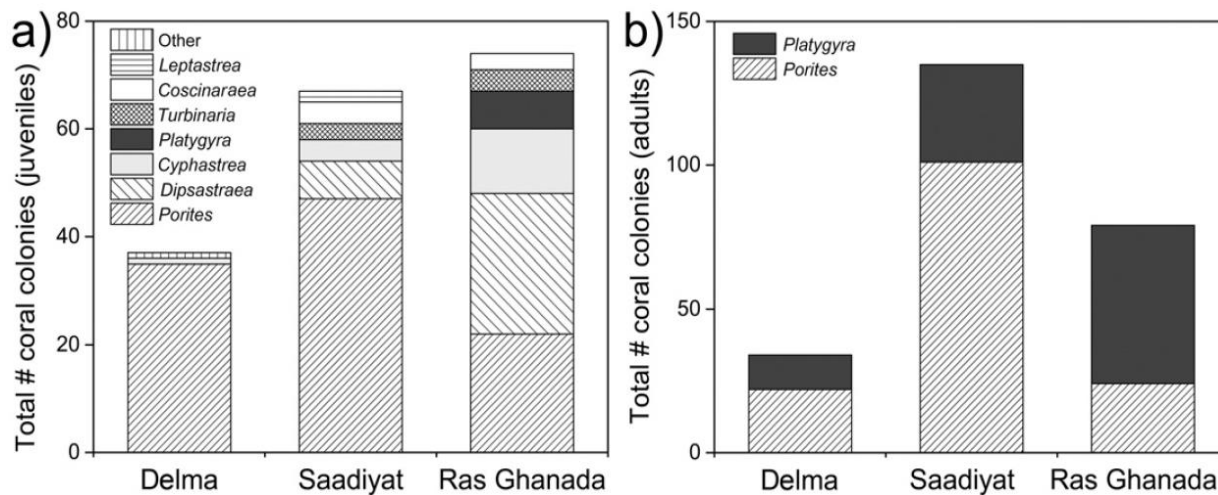


Figure 2.6. Site-specific composition of the coral community. a) Total number of juvenile (species indicated in the panel legend) and b) adult (Porites spp. and Platygyra spp.) corals recorded along the transects in the three study sites.

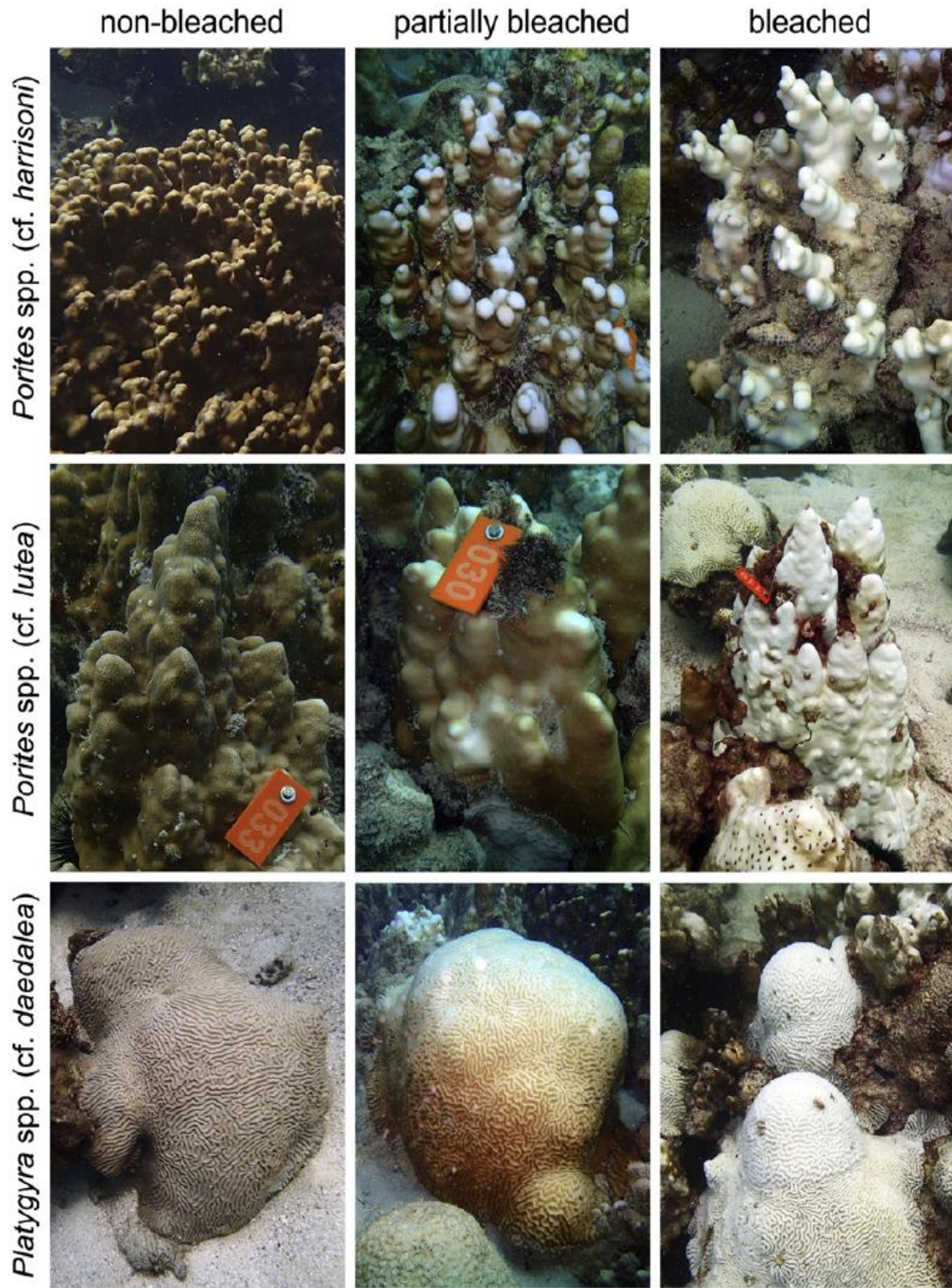


Figure 2.7. Representative photographs of corals from the bleaching categories used in this study. (Image credits: J. Wiedenmann).

2.3.2. Site-specific severity of the 2012 bleaching event

Three coral reef sites in the southern IRSA was surveyed to document the bleaching event that took place in August/September 2012. The three sites revealed pronounced differences in the abundance of genera and genus richness of juvenile corals (Figure. 2.6a). The overall abundance of juveniles was similar in Saadiyat and Ras Ghanada and numbers were higher than in Delma. Species richness of juvenile corals decreased from Ras Ghanada to Saadiyat and Delma, with Porites spp. becoming increasingly dominant. Similarly, the number of adult Porites spp. and Platygyra spp. recorded along the transects was higher in Ras Ghanada and Saadiyat than in Delma (Figure. 2.6b).

Within the sites, corals of the same taxonomic group were affected to variable degrees by bleaching, ranging from unaffected to partially bleached and completely bleached (Figure. 2.7). Partially bleached corals lost their pigmentation often in the upper, most light-exposed parts of the colonies. In Ras Ghanada and Saadiyat reefs, >40% of the analyzed corals (juvenile and adult Porites, adult Platygyra) were affected by bleaching (Figure. 2.7; Table 2.2). An exception where juvenile Porites among which no partially bleached individuals were encountered in Ras Ghanada and the overall percentage of colonies showing signs of bleaching was accordingly lower. In all analyzed groups, between 20 and ~30% of the corals were completely bleached in Saadiyat and Ras Ghanada. By contrast, the corals in the Delma site were less affected and no more than 15% of the corresponding groups showed signs of bleaching. For both species, statistical analysis identified the lower bleaching severity in Delma as a significant site-specific effect (Table 2.2). Similar bleaching levels were observed for the combined numbers of recorded juveniles from other species (Figure. 2.6). It has to be noted, however, that the data for

Delma reef need to be considered with caution due to low number of non-*Porites* spp. juveniles encountered in this site.

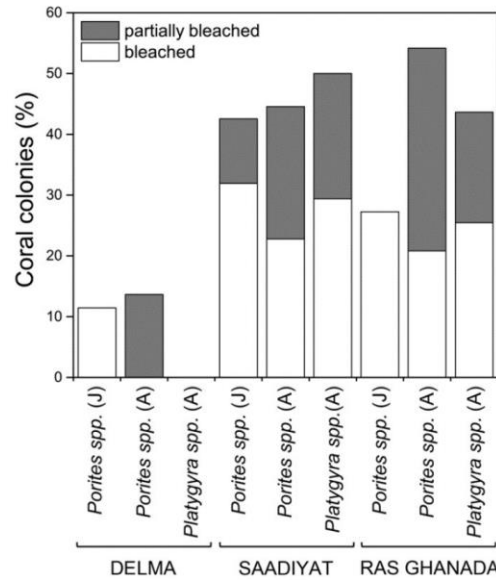


Figure 2.8. Site-specific severity of bleaching. Comparison of the percentage of the total numbers of juvenile and adult *Porites* spp. colonies and other species affected by bleaching.

Table 2.2. Statistical analysis of site-specific differences in bleaching susceptibility. χ^2 = Chi-square value, df = degrees of freedom, P-value < 0.05 indicates that the recorded proportion of bleached, partially bleached and non-bleached colonies is significantly dependent on the region.

Juvenile <i>Porites</i> spp.	Bleached	Partially bleached	Non bleached	Total
Dalma	4	0	31	35
Saadiyat	15	5	27	47
Ras Ghanada	6	0	16	22
Total	25	5	74	104
$\chi^2 = 12.42867066$, df = 4, P-value = 0.014437				
Adult <i>Porites</i> spp.	Bleached	Partially bleached	Non bleached	Total
Dalma	0	3	19	22
Saadiyat	23	22	56	101
Ras Ghanada	5	8	11	24
Total	28	33	86	147
$\chi^2 = 10.75273216$, df = 4, P-value = 0.029497				
Juvenile <i>Platygyra</i> spp.	Bleached	Partially bleached	Non bleached	Total
Dalma	0	0	12	12
Saadiyat	10	7	17	34
Ras Ghanada	14	10	31	55
Total	24	17	60	101
$\chi^2 = 9.659601028$, df = 4, P-value = 0.046569				

Table 2.3. Numbers of adult Porites spp. and Platygyra corals recorded along the transects in the different study sites.

Corals	Delma	Saadiyat	Ras Ghanada
<i>Porites</i> sp. (adults) (<i>Porites</i> cf. <i>lobata</i> / <i>lutea</i> / <i>harrisoni</i>)	22	101	24
<i>Platygyra</i> sp. (adults)	12	34	55
Total (adults)	34	135	79

Table 2.4. Numbers of juvenile corals recorded along the transects in the different study sites.

Species	Delma			Saadiyat			Ras Ganada		
	Non-bleached	Bleached	Partially Bleached	Non-bleached	Bleached	Partially Bleached	Non-bleached	Bleached	Partially Bleached
<i>Porites</i>	31	4	0	27	15	5	16	6	0
<i>Dipsastraea</i> (<i>Favia</i> *)	0	0	0	4	3	0	18	8	0
<i>Cyphastrea</i>	1	0	0	2	0	2	5	7	0
<i>Platygyra</i>	0	0	0	0	0	0	3	3	1
<i>Turbinaria</i>	0	0	0	0	3	0	1	3	0
<i>Coscinaraea</i>	0	0	0	1	3	0	0	3	0
<i>Leptastrea</i>	0	0	0	2	0	0	0	0	0
other	1	0	0	0	0	0	0	0	0
Total	33	4	0	36	24	7	43	30	1

*The genus *Favia* was replaced by *Dipsastrea* by: Budd, A.F., Fukami, H., Smith, N.D., Knowlton, N. 2012, Taxonomic classification of the reef coral family Mussidae (Cnidaria: Anthozoa: Scleractinia). Zoological Journal of the Linnean Society 166, 465-529.

2.4. Discussion

Three sites in the IRSA region were studied regarding their experience in different levels of bleaching during the 2012 bleaching event. The purpose of this study is to establish potential causes for the patchiness of bleaching that is frequently observed during mass bleaching events. Bleaching levels for two common taxa, Porites spp. and Platygyra spp., were analyzed. Additionally, we recorded the site-specific degree of bleaching among juvenile Porites spp. and other less abundant corals. Reefs in Saadiyat and Ras Ghanada were severely affected by bleaching whereas corals in Delma showed little or no signs of bleaching despite their relatively close geographic proximity and exposure to a comparable temperature regime in August–September 2012. This trend was comparable for all the

monitored species and developmental stages. Since light exposure is known to promote heat-stress mediated bleaching (Coles and Jokiel, 1978; Brown et al., 1994, 2002; Hoegh-Guldberg, 1999; Fitt et al., 2001), the observation, that partial bleaching of adult colonies was frequently found in the upper part of the colonies, suggests that light stress was also influential in 2012 bleaching event. In Ras Ghanada, a higher percentage of adult Porites spp. showed signs of bleaching compared to juveniles from the same taxon. This observation is in line with previous studies that found juvenile corals to be less affected by bleaching than adults (Mumby, 1999; Nakamura and Van Woesik, 2001; Loya et al., 2001). However, this trend was not observed in the other sites where comparable numbers of adults and juveniles suffered from bleaching.

A possible explanation for the different bleaching susceptibility across the three study sites is that the local bleaching threshold of ~35 °C at Delma reef is ~0.5 °C higher than in the other sites. Consequently, the corals experienced less relative heat stress, indicated by the smaller number of days during which the local bleaching threshold was exceeded. Still, the threshold temperature was exceeded for 10 days at Delma with little effect on the corals, setting this site among the most temperature tolerant reefs of the world (Riegl et al., 2011). The resilience of Delma reef is further underlined by the fecundity of its corals in the aftermath of the 2012 bleaching event which was significantly higher compared to those from Saadiyat and Ras Ghanada reefs (Howells et al., 2016). Previous observations from elsewhere found massive Porites spp. to be among the taxa with a high survival rate after bleaching events (Loya et al., 2001; Sheppard and Loughland, 2002). Therefore, the dominance of massive Porites spp. at Delma (Burt et al., 2011) that is reflected by the species composition of juvenile corals presented in this study, may be considered as an

additional potential reason for the exceptional heat tolerance of this reef site (Marshall and Baird, 2000; Loya et al., 2001). Also, the history of increased temperature stress levels in Delma may have increased the bleaching threshold of the community by a long-term selection of more resilient genotypes and/or acclimatization of corals (Brown et al., 2002). Furthermore, Delma reef is situated ~50 km off the coast in a relatively pristine environment whereas the other two sites are under the direct influence of a densely populated urban area and intense coastal construction (Sale et al., 2011; Van Lavieren et al., 2011). Since the water quality, in particular the nutrient levels, can affect bleaching thresholds (Wooldridge, 2009; Wiedenmann et al., 2012; D'Angelo and Wiedenmann, 2014), the influence of the water chemistry at the different sites should be investigated as another potential cause for the observed differences in their bleaching tolerance.

2.5. Conclusions

Different bleaching threshold temperatures and the composition of the coral communities at the study sites offer likely explanations for the “patchiness” of the 2012 bleaching event in the southern IRSA, but other parameters such as the water quality and light stress should also be considered. Our results suggest that the bleaching threshold of the Porites-dominated Delma site is only 0.5 °C higher than in the more diverse Saadiyat and Ras Ghanada sites. Hence, a long-term increase of the mean temperature of the hottest weeks in the same order of magnitude may lead to a considerable loss of coral diversity in the latter reefs.

2.6. Acknowledgment

The study was funded by NERC (Grant no. NE/K00641X/1 to JW) and the European Research Council under the European Union's Seventh Framework Program (FP/2007–2013) ERC Grant Agreement no. 311179 to JW and a scholarship by the Public Authority for Education and Training of the State of Kuwait to DS. We are grateful to NYU Abu Dhabi Institute for supporting the 2012/2013 field workshops during which data for this study were collected. We also thank Tropical Marine Centre (London) and Tropic Marin (Wartenberg) for sponsoring the NOCS Coral Reef Laboratory and acknowledge NASA Ocean Biology (OB.DAAC) for Sea-viewing Wide Field-of-view Sensor (SeaWiFS) Ocean Color Data. We extend our appreciation to ROPME for the access to their remote sensing database.

Chapter 3: The role of temperature, phytoplankton, and nutrients on the 2012 coral bleaching event in Abu Dhabi

Abstract

Coral communities off the coast of Abu Dhabi, UAE were affected by severe bleaching in 2010, 2011, and 2012. These events were assessed considering fluctuations in phytoplankton biomass (chl-*a*), temperature stress (SST) and nutrient availability, including nitrate, phosphorus, iron and silicate, to assess primary causes of the algal symbiosis breakdown and subsequent bleaching. These analyses were undertaken only in Saadiyat study sites due to *in situ* (nutrient and chl-*a*) data availability. The period of analysis (2009-2015) includes both bleaching and non-bleaching years. The thermal methods used in this period (number of days above threshold, DHD and HR) gave a significant prediction of the onset of bleaching in Delma, Saadiyat and Ras Ghanada. The number of days above local threshold results suggest that a coral bleaching event, of a severity comparable to that of 2012 was expected in the summer of 2015. While the DHD and HR results do not uphold the year 2015 to be a bleaching year, particularly in Saadiyat and Ras Ghanada. However, in 2015 coral bleaching did not occur in any of the study sites. The bleaching events in 2010 and 2012 coincided not only with local elevated temperature but also with high concentrations of chl-*a* (reaching 4.66 mg/m³) in the water. It is then possible that in these two years, both environmental factors contributed to triggering a bleaching response. In the summer of 2015 a lower intensity of chl-*a* (0.8 mg/m³) was detected. The result also indicate that phosphorous levels were completely depleted from the water body in the summer of 2012. While in 2015, the concentrations of 100-350 µg/L of this element were detected during the same period. The depletion of phosphorus might be attributed to the rapid assimilation by phytoplankton in 2012. Thus, it is reasonable to suggest that the absence of phosphorus in the water during the summer months of 2012 might have promoted coral bleaching in response to the elevated temperature.

3.1. Introduction

Coral reefs are critically important marine ecosystems. They are declining due to climate change and numerous forms of anthropogenic impacts (Hoegh-Guldberg et al., 2007). A variety of environmental stressors including extreme water temperature, phytoplankton blooms and turbidity can disrupt the symbiotic relationship between the zooxanthellae and the coral host. For example, extreme water temperature, phytoplankton blooms, and turbidity, which consequently lead to coral bleaching (Hoegh-Guldberg, 1999; Wiedenmann et al., 2012; Bauman et al., 2013; D'Angelo and Wiedenmann, 2014; Kavousi et al., 2014). The resulting phenomenon is known as coral bleaching since after the loss of symbiotic algae (zooxanthellae) the white skeleton is visible through the coral tissue.

Corals in the southern Gulf region thrive under exceptionally high water temperature fluctuations (Burt et al., 2008), characterised by exceptionally hot conditions during summer (reaching 35°C), and cold temperatures during winter (18°C) (Coles and Fadlallah, 1991; Richlen et al., 2010). These temperature extremes surpass the tolerance limits of most corals in the world (30-32°C) (George and John, 2000; Sheppard and Loughland, 2002). Coral in the Gulf can survive daily summer temperature of 34 to 35°C for several weeks, and display the highest documented bleaching thresholds (Riegl et al., 2012; Shuail et al., 2016). However, since the 1980's, the Gulf has experienced significant heat-related coral bleaching events: For example, during the major El Niño Southern Oscillation (ENSO) events of 1996 and 1998 that affected coral reefs worldwide (Goreau et al., 2000, Wilkinson, 2000, Riegl, 2003, Al-Rashidi, 2009). More recently, back-to-back mortality events in the Gulf (in 2009, 2010, 2011 and 2012), have been caused by bleaching and disease and have altered the community structure of the reefs, particularly in the southern Gulf (Riegl and Purkis, 2015a).

Other factors that have been linked to coral reef degradation are phytoplankton and eutrophication (Benito and Haag, 2004; Wiedenmann et al., 2013; D'Angelo and Wiedenmann, 2014). In coastal waters, anthropogenic eutrophication can increase the concentration of dissolved inorganic nutrients, such as ammonium, nitrate and phosphate (Brodie et al., 2011). The enrichment with elevated amount of dissolved inorganic nitrogen (DIN) and phosphate can trigger phytoplankton growth in the water (Davis et al., 2015). Phytoplankton eventually deplete, either dissolved inorganic nitrogen (DIN) or phosphate from the water body (D'Angelo and Wiedenmann, 2014). Imbalanced levels of DIN to phosphate can increase the susceptibility of the reef corals to suffer stress. Wiedenmann et al. (2013) have shown that increased levels of DIN combined with limited phosphate concentrations could result in an increased susceptibility of corals to temperature and light-induced bleaching. High concentrations of DIN in the water is known to increase zooxanthellae cell density in the coral body, which results in phosphate starvation particularly when the phosphate availability is low (Wiedenmann et al., 2013; D'Angelo and Wiedenmann, 2014; Rosset et al., 2017).

Since 1999, several algal blooms have been recorded in the Gulf (Heil et al., 2001; Richlen et al., 2010; Naser, 2014). The first algal bloom event was documented in Kuwait coastal waters during summer 1999, which resulted in massive fish mortality (Heil et al., 2001). The most recent incident was reported in the southern part of the Gulf between August 2008 and May 2009. This bloom, caused mainly by *Cochlodinium polykrikoides*, changed the water colour and coincided with widespread fish and coral mortality, threatening coastal tourism and blocking the water intakes of desalination plants (Richlen et al., 2010; Naser, 2014).

The aim of the present work was to test the hypothesis that phytoplankton blooms can change the balance of nutrients in the coral environment, thereby increasing the susceptibility of corals to heat stress and subsequent bleaching. Remote sensing tools were used to calculate the concentration of chlorophyll-*a* (chl-*a*) and thus estimate the phytoplankton density in the southern Gulf area, Abu Dhabi. The data was complemented by *in situ* measurements of nutrients (phosphorus, nitrate, iron, and silicate) provided by the Environmental Agency Abu Dhabi (EAD). The thermal stress during bleaching and non-bleaching years is determined by the analysis of remote sensed sea surface temperature (SST) (Shuail et al., 2016). The heat stress were tested in two ways: 1) as the number of days exceeding a local threshold, and 2) the degree heating days, which Maynard et al., (2008) and Riegl and Purkis, (2012) have shown to be a useful thermal stress indicator. The period of analysis ranged from 2009 to 2015, and include both bleaching and non-bleaching years. The documented coral bleaching events in Abu Dhabi were assessed considering fluctuations in phytoplankton biomass (chl-*a*), temperature stress (SST) and nutrients availability to assess primary causes of the breakdown of the algal symbiosis and subsequent bleaching.

3.2. Material and methods

3.2.1. Study sites

Coral communities were surveyed at three locations in the southern Arabian Gulf area in UAE, Delma (lat: 24.5208°/long: 52.2781°), Saadiyat (lat: 24.599°/long: 54.4215°) and Ras Ghanada (lat: 24.8481°/long: 54.6903°) (Shuail et al., 2016). Detailed information

about the survey areas and site-specific severity of the 2012 bleaching event are found both in the introductory chapter of this thesis and in Shuail et al., (2016).

3.2.2. Thermal stress analysis

Local bleaching thresholds and the cumulative thermal days exceeding the local bleaching threshold during the 2012 bleaching year were presented in Chapter 2 of this thesis (Shuail et al., 2016). In this chapter, the accumulation of thermal stress was calculated during 2009 to 2015 using three stress indices; these are the ‘degree heating days’ (DHD) and the heating rate (HR). Specifically, DHD is the summed positive deviations of the daily SST (T_{heating}) from the local long-term mean summer temperature (LMST).

$$\text{DHD} = \sum (T_{\text{heating}} - \text{LMST})$$

According to Maynard et al., (2008), the DHD, shows mild bleaching responses at sites that incurred 60 or less DHD. DHD of 61 to 100 would show a moderate to severe bleaching categories (mild, moderate and severe bleaching is described in Figure 2.7, p61). HR would prompt a mild bleaching response to sites that experienced values below between 1.7, moderate between 1.7-2.4, and severe bleaching above 2.4. Daily summer temperatures from 15th July to 15th September over the study period (2009-2015) were used according to published papers (Maynard et al., 2008 and Riegl and Purkis, 2012). The LMST was calculated as the SST average of 15th August to 15th September from 33 summers including 2015 (1982-2015). The LMST for Delma=33.79°C, Saadiyat=33.55°C and Ras Ghanada=33.33°C. According to Maynard et al., (2008), DHD does not

differentiate between a broad range of heat stresses. For example, three weeks at 1°C above the local LMST has similar results as one week at 3°C. For this reason, heating rates (HR), which is the DHD divided by the number of days in which T_{heating} have exceeded the LMST, were calculated for each study site during the same study period (2009-2015). In other words, the HR is the rate at which DHD have accumulated throughout the summer. The DHD and the HR were used according to published papers (Maynard et al., 2008 and Riegl and Purkis, 2012), and were used by the *ReefTemp* application, which was developed specifically to monitor conditions conducive to coral bleaching on the Great Barrier Reef and Coral Sea (<http://www.bom.gov.au/environment/activities/reeftemp/reeftemp.shtml>). SST anomalies were also calculated for all study sites, during the period of 2009-2015, but only Saadiyat SST anomalies were included in this chapter to compare it with the in situ measurements, which is obtained only from Saadiyat site.

The SST data (in °C) from 2002 to 2015 was extracted from the Moderate Resolution Imaging Spectroradiometer onboard Aqua platform (MODIS-Aqua). Images of the sea SST were the standard level-2 (netCDF4) downloaded from the NASA ocean color data website (<http://oceancolor.gsfc.nasa.gov/>), and by the Regional Organization for the Protection of the Marine Environment (ROPME) archived in Kuwait. These level-2 images were calibrated and geolocated with atmospheric corrections applied (<http://oceancolor.gsfc.nasa.gov/cms/format/l2nc.html>). Temperatures were determined for 1 km² areas covering the study sites, which is the highest spatial resolution provided by the OC3 MODIS product. The 1 km² resolution help in detecting temperature variability on reefs at local scales (Maynard et al., 2008). Images were analyzed using the SeaWiFS Data Analysis System (SeaDAS) software program Version 7.2. Images in which the SST

signal was affected by cloud cover or high amounts of dust in the air were excluded from the analysis. The SST data prior to the availability of MODIS-Aqua in 2002 were collected from the daily Level 4 SST analysis from the Group for High-Resolution Sea Surface Temperature (GHRSSST). This dataset is produced daily with 4 km spatial resolution using the access server of the Pacific marine environment laboratory (<https://podaac-tools.jpl.nasa.gov/las/UI.vm>). This product uses optimal interpolation data (OI) from the Advanced Very High-Resolution Radiometer (AVHRR). For the validation of the data from MODIS-Aqua, *in situ* water temperature measurements were used as described previously (Shuail et al. 2016). AVHRR SST data were matched with the *in situ* temperature data from the EAD, spanning days distributed over all seasons of 2009. A linear regression coefficient with the root mean square error (RMSE) was calculated for the AVHRR data and the *in situ* (Figure 3.1a). AVHRR SST and MODIS-Aqua SST were also compared during a three years period, from 2003-2005, to calculate the RMSE and the R^2 (Figure 3.1b).

3.2.3. Remote sensing analysis of chlorophyll-*a*

Remote sensed chlorophyll-*a* concentrations (chl-*a* mg/m⁻³) in the surface water of Saadiyat area were acquired from MODIS-Aqua from January 2009 to December 2015. The MODIS-Aqua platform was launched in May 2002 into a daily sun-synchronous orbit at 12:00 p.m. and it has been in continuous operation from June 2002 to the present (Franz et al., 2005). The sensor measures 36 spectral channels covering the range from 400 nm to 14.4 μ m, supporting land, ocean, and atmosphere. The bands of primary interest to ocean colour applications are the nine channels covering the spectral range from 400-900 nm

(Behrenfeld et al., 2008). Daily images were retrieved from NASA ocean colour data website (<http://oceancolor.gsfc.nasa.gov/>) with a spatial resolution of 1 km. The image format was the standard Ocean color (OC) level-2 (netCDF4), as it is generated from the MODIS standard atmospheric correction algorithm developed by NASA.

Data was examined within an average area of 5x5 pixel for MODIS-Aqua centered at Sadiyaat study site using SeaDAS v.7.2. The 5x5-pixel region of interest was used to minimize the consequences of residual miss-registrations (Cannizzaro and Carder, 2006). MODIS-Aqua Chl-*a* values were matched with the *in situ* chl-*a* provided by the Abu Dhabi EAD. Both values were plotted to examine the differences between the two data sets and to calculate the simple linear regression coefficient (R^2) and the RMSE (Figure 3.1c).

3.2.4. *In situ* and meteorological data measurements

In situ water temperature data of Saadiyat sites from 2009 to 2013 were obtained as discussed in chapter two of this thesis (Shuail et al., 2016). Monthly *in situ* chl-*a* and nutrient values (phosphate $\mu\text{g/l}$, nitrate $\mu\text{g/l}$, iron $\mu\text{g/l}$ and silicate $\mu\text{g/l}$) were acquired from the Abu Dhabi EAD, marine water quality program MWQMP, from January, 2011 to December, 2015. The MWQMP has set a recommended thresholds levels for the chl-*a* ($0.7 \mu\text{g/l}$), Nitrate ($220 \mu\text{g/l}$), and phosphorus ($150 \mu\text{g/l}$), exceeding these values would indicate a potential public health issue (EAD, 2015). The MWQMP monitoring has 20 stations distributed throughout the territorial waters of the Emirate. The selected site in this chapter is located offshore Saadiyat Island site (lat. 24.533°N /long. 54.285°E) due to nutrient availability data. Detailed laboratory sampling methods used by the MWQMP have been previously published (EAD, 2014, 2015). Air temperature, wind and horizontal visibility

data were obtained from Abu Dhabi International Airport, which is near the Saadiyat site, from 2009-2015 through the Weatherspark Beta database (<https://weatherspark.com/>). Weatherspark utilises the data from NOAA site (www.noaa.gov).

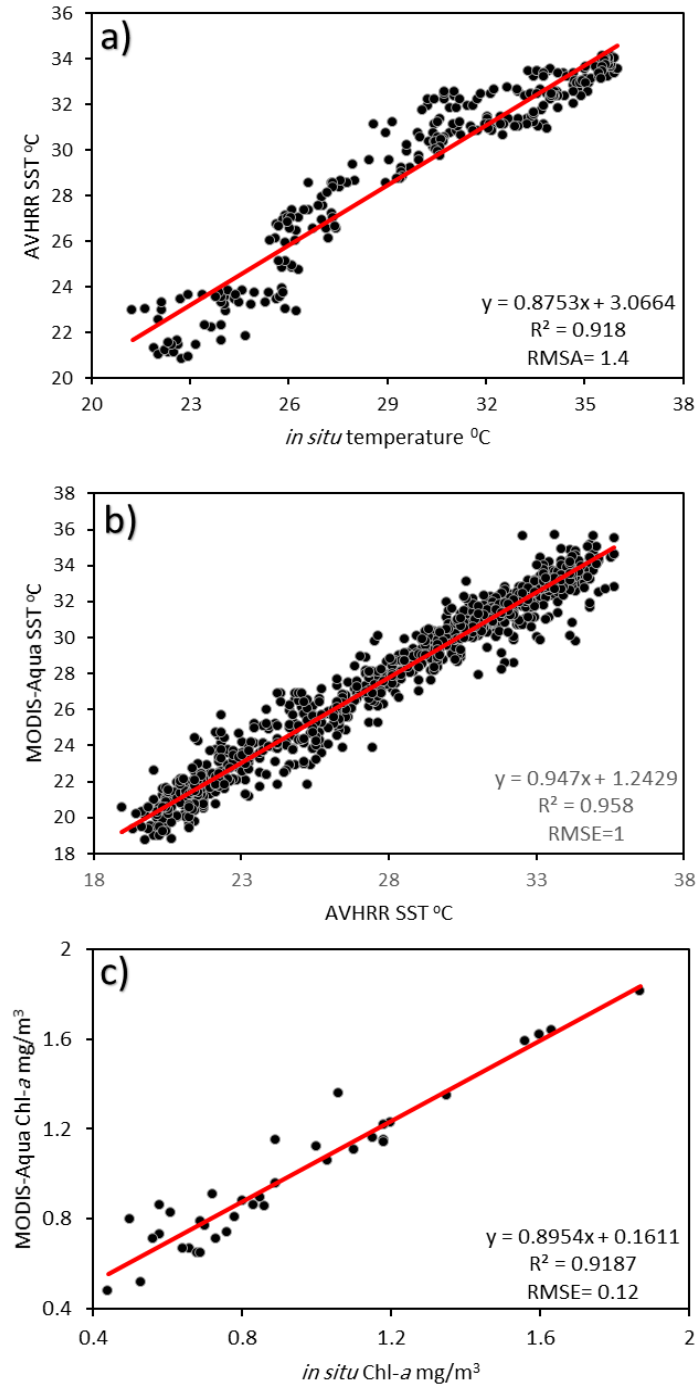


Figure 3.1. Remote sensing data comparison at Saadiyat site. Including a) AVHRR SST with in situ water temperature, b) MODIS-Aqua SST with AVHRR SST, c) MODIS-Aqua chl-*a* with the in situ chl-*a*.

A Pearson correlation was run to assess the relationship in between the remote sensed chlorophyll, *in situ* nutrients and the meteorological data. The Pearson correlation is a measure of the strength and direction of the relationship that exists between two continuous variables.

3.3.Results and discussion

3.3.1. Regression analysis of the remote sensing data

Linear regression along with RMSE was used to compare parameters estimated by remote sensing, such as SST and chl-*a* with the *in situ* water temperature and chl-*a* measurement. The regression coefficient for the AVHRR with the *in situ* measurements shows an $R^2=0.918$ and RMSE=1.4, indicating that the differences between the two data sets are minor (Figure 3.1a). The results also show a strong positive regression coefficient between both AVHRR and MODIS-Aqua SST, $R^2= 0.958$, with RMSE=1 (Figure 3.1b). Additionally, the comparative analysis of MODIS-Aqua chl-*a* and the *in situ* chl-*a* values from Abu Dhabi EAD is also reveals a regression coefficient $R^2= 0.9187$, RMSE=1.2 (Figure 3.1c).

3.3.2. Thermal stress during bleaching and non-bleaching years

As temperature stress is a primary cause of mass coral bleaching on the global scale (Muscantine et al., 1989, Szmant, 2002, Wooldridge, 2009), we tested the impact of increased temperatures stress and the influence of eutrophication on corals in Abu Dhabi. The number of days exceeding the local thresholds, the DHD and the HR, established by remote sensed data, were used as three parameters to quantify thermal stress during the

period 2009-2015 in all study sites. The air temperature from Abu Dhabi airport was also used as a reference to the environmental conditions during the study period.

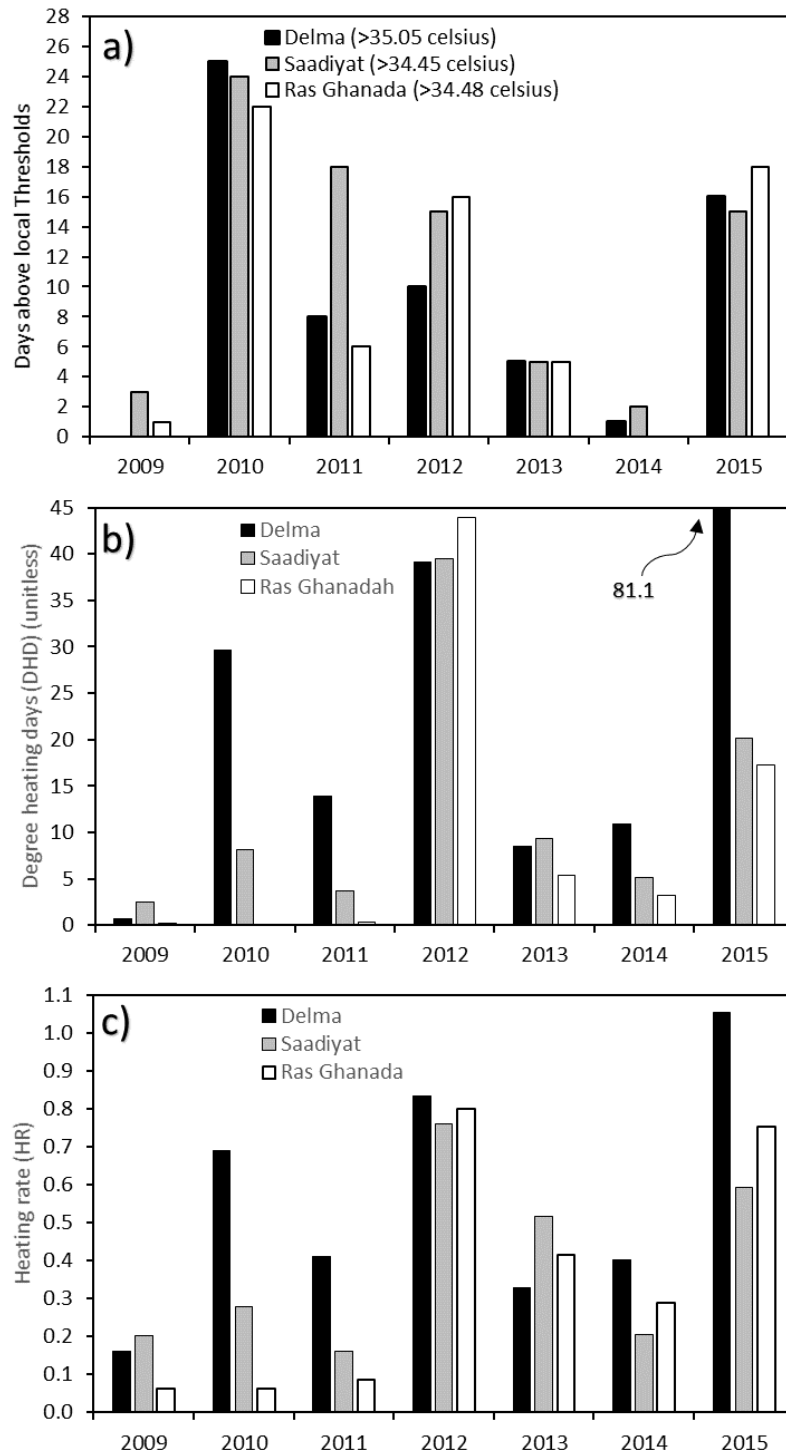


Figure 3.2. Thermal stress in Delma, Saadiyat and Ras Ghanada during 2009-2015. a) Days above the local thresholds, b) degree heating days (DHD), and c) Heating rates (HR).

Both the degree heating days (DHD) and the number of days above thresholds methods show similar profile during the study period (2009-2015) (Figure 3.2a, b). In 2009, the local threshold was exceeded for only three days and one day in Saadiyat and Ras Ghanada respectively, whereas it remained below that value at the Delma reefs. Likewise, the DHD was lower in Delma (0.65) and Ras Ghanada (0.19), followed by Saadiyat (2.44). The HR also shows negligible values at Delma (0.16), Saadiyat (0.2) and Ras Ghanada (0.06). In agreement with these results, a bleaching event that was observed in the region in the summer of 2009 was reportedly the consequence of a disease outbreak that lasted until November-2009 and was not related to a thermal stress (Riegl and Purkis, 2015).

During the back-to-back bleaching events (2010, 2011 and 2012), the three thermal parameters (number of days above threshold, DHD and HR) gave a notable prediction of the onset of bleaching during this period. In the summer of 2010, when the bleaching events were observed, the number of days above the local threshold shown a better predictor of bleaching severity than DHD and HR, as it recorded 25 days in Delma, 24 in Saadiyat, and 22 in Ras Ghanada, representing the highest values during the study period (Figure 3.2a). These results are in agreement with Riegl and Purkis, (2012b), as the western parts of Abu Dhabi (Delma, Bu Tinah and Al Heel) suffered 20% mortality higher than the eastern Abu Dhabi (Ras Ghanada) in this year. The DHD and HR only showed an increase of thermal stress at Delma sites reaching DHD=29.7 and HR=0.7, but there is only a slight increase in Saadiyat, and there was no significant temperature stress in Ras Ghanada.

During the summer of 2011, Delma and Ras Ghanada showed relatively lower counts of days exceeding the threshold (8 and 6 days, respectively) compared to Saadiyat (18 days). As determined by the three methods all sites experienced lower thermal stress than

in 2010. During the 2012, bleaching event, coral communities were exposed over 10 days to temperature above the local threshold in Delma, whereas this value increased to 15 days in Saadiyat, and 16 days in Ras Ghanada (Shuail et al., 2016). In agreement with the data, both DHD and HR show increased thermal stress for Delma (DHD=39.11, HR=0.83), Saadiyat (DHD=39.5, HR=0.76) and Ras Ghanada (DHD=44, HR=0.8). DHD and HR values below 60 and 1.7 respectively is considered to show only a mild bleaching response as observed by Maynard et al. (2008) through the *ReefTemp* application on the Great Barrier Reef (GBR) and in the Coral Sea. However, in this study DHD between 14-43 and HR between 0.4-0.8 predicted major bleaching events at the three study sites. These deviations in DHD and HR between this study and Maynard et al. (2008) may be related to the species composition between the GBR and the southern Gulf and the overall ecosystem.

Coral mortality in 2010, 2011 and 2012 has been suggested to be linked to heat stress and subsequent disease outbreak, causing a persistent decline in coral cover in the southern Gulf (Riegl and Purkis, 2012, Guest et al., 2012, Riegl and Purkis, 2015, Riegl and Purkis, 2015a; Shuail et al., 2016). A low level of heat stress was indicated by all valuation methods in 2013 and 2014 in the three sites (Figure 3.2). This supports the suggestion that during the summer of 2013 strong winds may have caused cooling of shallow waters, consequently reducing the severity of the summer heat (Riegl and Purkis, 2015b). This strong wind may have reduced the air temperature of the Abu Dhabi Emirate, as observed in Figure 3.3a where the air temperature anomalies in this year reached -2.4°C below the summer average.

In 2015, the number of days exceeding the bleaching threshold in Delma, Saadiyat, and Ras Ghanada were high and comparable to years in which bleaching was recorded (in

particular 2010 and 2012 (Figure 3.2a). Also, the calculated DHD and HR showed that in 2015 the thermal stress was elevated at the Delma reefs (DHD=81.1, HR=1.05), with a noticeable increase also in Saadiyat (DHD=20.1, HR=0.6) and Ras Ghanada (DHD=17.31, HR=0.75) (Figure 3.2b). However, the increase in DHD and HR levels in Saadiyat and Ras Ghanada was lower than the levels observed in 2012 (Saadiyat 2012: DHD=39.48 HR=0.76; 2015: DHD=20.14 HR=0.59) (Ras Ghanada 2012: DHD=43.92, HR=0.8; 2015: DHD=17.31, HR=0.75). Air temperature of Abu Dhabi airport, along with the MODIS-Aqua SST in Saadiyat site (3.3 a&b), indicates clear positive anomalies during the summer years in which bleaching events are documented (2010, 2011 and 2012), and negative anomalies in the summer of non-bleaching years (2009, 2013 and 2014) (Figure 3.3 a&b). Both SST and air temperature showed a positive anomaly during summer in 2015, when compared to the summer temperatures of other bleaching years. Taken together these results suggest that a coral bleaching event, of a severity comparable to that of 2012 was expected in the summer of 2015. However, in this year coral bleaching did not occur in any of the study sites (Burt, J.A. and Wiedenmann, J 2016, pers. com.).

There are several possible explanations for this result. First, the coral community in Delma is known to be dominated by *Porites* spp. This genera is known to contain species of corals that are more heat tolerance than those more prevalent in other location in Abu Dhabi (Hume et al., 2013). The representation of *Porites* in Delma might actually be the consequence of the demise of less resistance species in previous bleaching events (2010, 2011, and 2012), and further supported by the recovery and growth of the thermal tolerant taxa during the non-bleaching periods in 2013 and 2014 (Shuail et al., 2016). Historical bleaching events in this region may have also induced acclimatization and adaptation of

the coral community by incorporation of more thermally tolerant symbionts (Maynard et al., 2008).

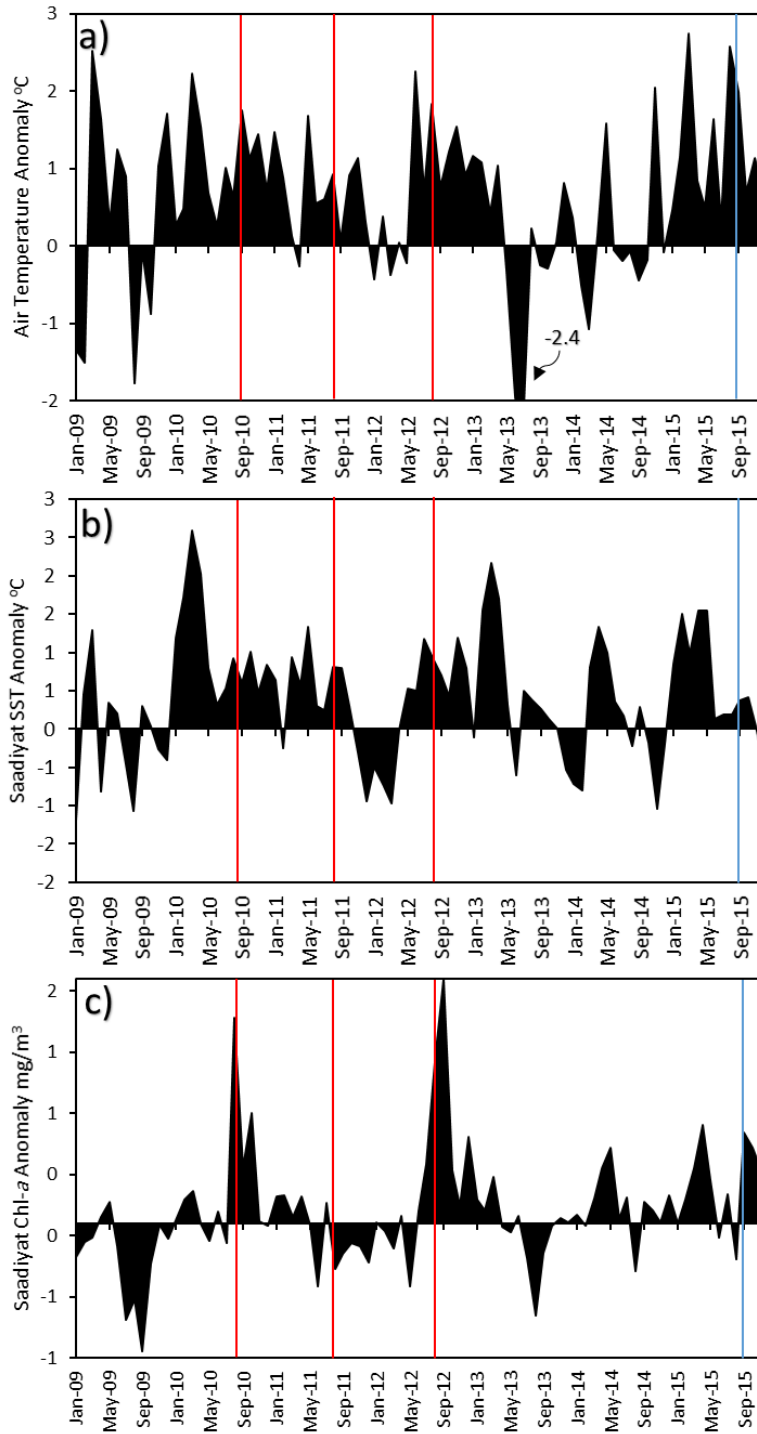


Figure 3.3. Characteristics of environmental condition in Saadiyat reefs between 2009 and 2015. Including a) Air temperature anomalies, b) SST anomalies, c) MODIS-Aqua chl-*a* anomalies. Red lines indicate bleaching events and blue line indicate thermal stress, but no bleaching witnessed.

3.3.3. Interannual anomalies of remote sensed chl-*a*

Three summer chl-*a* anomalies were observed between 2009 and 2015 in Saadiyat area (Figure 3.3 c). The first two occurred in the summers of 2010 and 2012 ($>1.5 \text{ mg/m}^3$), and both coincided with the bleaching events in those years. Particularly in September 2012 when chl-*a* was higher (4.6 mg/m^3) than the average monthly value by $>1.8 \text{ mg/m}^3$. In those two years, the SST also presented positive anomalies during the summer (2010: Aug= Sep=, 2012: Aug= Sep=)(Figure 3.3b). Therefore, the bleaching event in 2010 and 2012 coincided not only with locally elevated temperature but also with high concentration of chl-*a* in the water. It is then possible that in these two years, environmental factors contribute to the triggering of a bleaching response. In agreement with the hypothesis, in the summer of 2015 when high temperature stress did not result in a visible bleaching of the coral communities in Saadiyat, a lower intensity (0.8 mg/m^3) of chl-*a* was detected (Figure 3.3c). Increased concentration of chl-*a* might be an indicator of the development of phytoplankton blooms, which may have several impacts on coral reefs, including shading, release of toxins, oxygen depletion, and alteration of the water chemistry (Al-Ansi et al., 2002, Furnas et al., 2005, Fabricius et al., 2013, Wiedenmann et al., 2013; D'Angelo and Wiedenmann, 2014).

3.3.4. Comparative analysis of environmental condition in Saadiyat reefs in 2012 and 2015

A comparison of environmental parameters (SST, chl-*a* and nutrient conditions) between the bleaching year of 2012 and the non-bleaching year of 2015 was conducted to evaluate potential reasons for the different bleaching responses of the same coral

communities and comparable levels of heat stress. The monthly mean SST of 2012 and 2015 showed comparable values throughout the seasons. In contrast, during 2012 chl-*a* reached a maximum monthly average of 3.91 mg/m³ during August and 4.66 mg/m³ in September. These high values persisted for approximately four months (Figure 3.4b), and was ~1-2 mg/m³ higher than the chl-*a* measured during the same period in 2015. These findings indicates differential impact to the reefs during 2012 as compared to 2015.

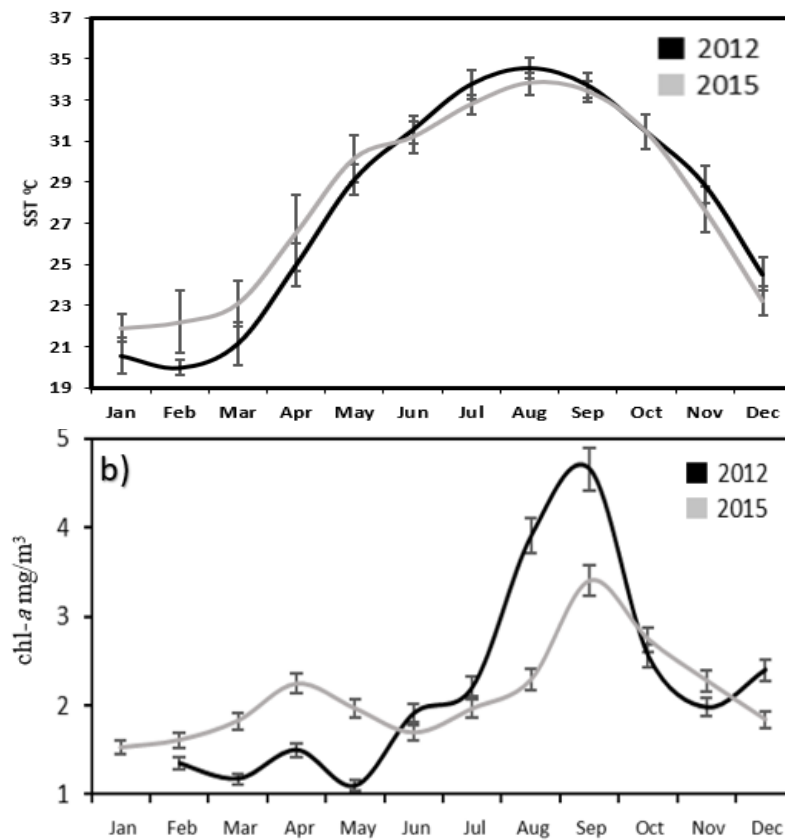


Figure 3.4. Comparative analysis of environmental parameters in Saadiyat in 2012 and 2015, a) monthly mean SST, b) Monthly mean chl-*a* mg/m³. Symbols show average values calculated from 15 data points determined per months in each year. Error bars represent the standard deviation.

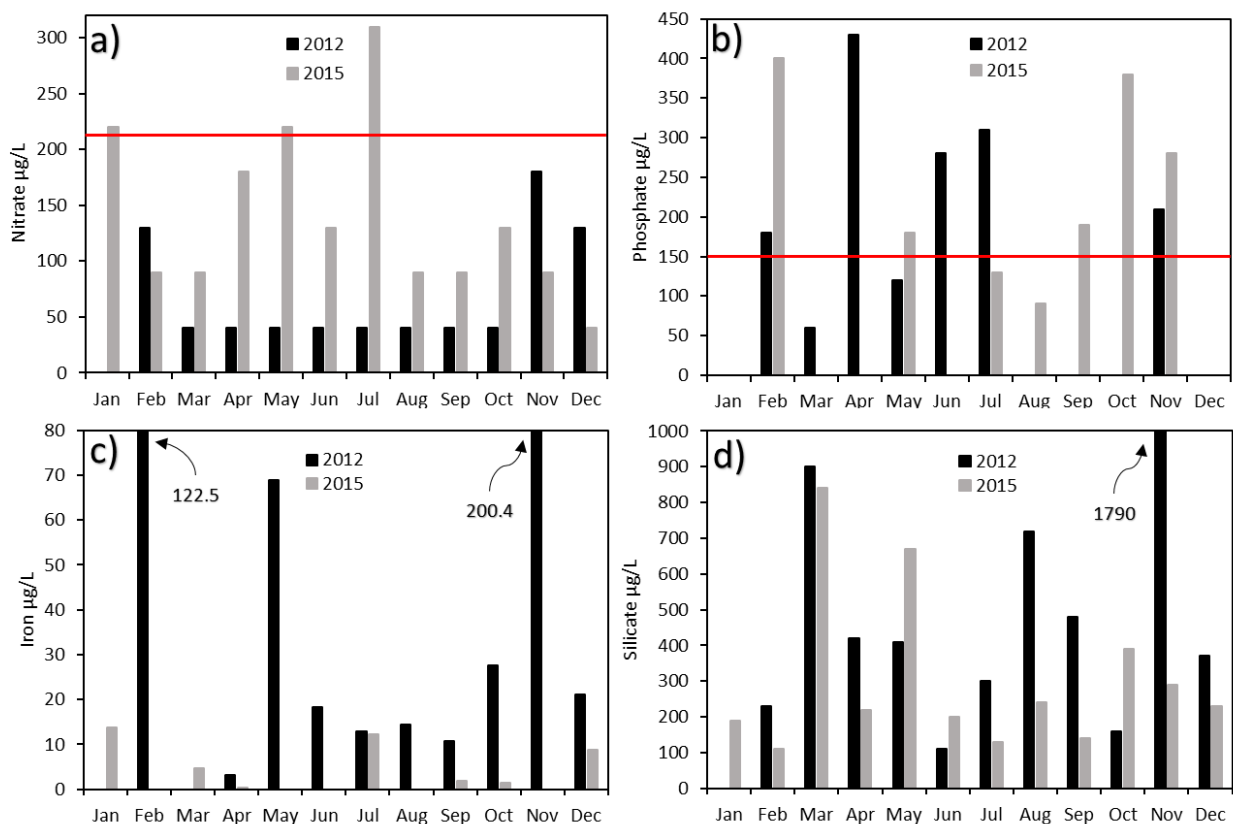


Figure 3.5. Comparative analysis of environmental parameters in Saadiyat in 2012 and 2015, a) monthly mean SST, b) Monthly mean chl-a mg/m^3 . Symbols show average values calculated from 15 data points determined per months in each year. Error bars represent the standard deviation.

Table 3.3. Pearson correlation analysis between the *in situ* nutrients (nitrate, phosphate, iron, silicate), remote sensed chl-a (Saadiyat), meteorological visibility and wind. The underline correlation coefficient values (r) are significant with $p < 0.05$.

	Chl-a	Iron	Nitrate	Phosphate	Silicate	Visibility	Wind
Chl-a	100%	1%	<u>-27%</u>	-18%	8%	-9%	<u>-30%</u>
Iron	1%	100%	-8%	1%	17%	7%	-11%
Nitrate	<u>-27%</u>	-8%	100%	11%	-4%	11%	9%
Phosphate	-18%	1%	11%	100%	2%	0%	-6%
Silicate	8%	17%	-4%	2%	100%	10%	-18%
Visibility	-9%	7%	11%	0%	10%	100%	<u>-35%</u>
Wind	<u>-30%</u>	-11%	9%	-6%	-18%	<u>-35%</u>	100%

Nitrate levels in the water during 2012 were lower than in 2015 throughout the summer period (**Error! Reference source not found.a**). This may indicate the consumption of this macronutrient by the high phytoplankton densities that was estimated due to the high chl-*a* levels. The pearson correlation in table 3.1 also show that nitrate has a significant negative correlation (-27%) with the chl-*a* (Table 3.1). This result further support the association between the increase in phytoplankton biomass and the consumption of nitrate levels. Nitrate plays a major role in the physiological functioning of phytoplankton cells, including its photosynthetic efficiency and the ability to react to different environmental stresses (Parkhill et al., 2001). Therefore, high phytoplankton biomass in the water column may lower the nitrate levels, thereby imposing an additional stress to the corals that require this nutrient for optimal biological mechanisms (D'Angelo and Wiedenmann, 2014).

Phosphorous levels were completely depleted from the water body in the summer period (Aug-Sep-Oct) of 2012 (**Error! Reference source not found.b**). This is in stark contrast with the concentrations of 100-350 µg/L of this element that were detected during comparable time period in 2015. Table 3.1 shows that phosphorus has a negative relationship ($r = -18\%$) with chl-*a*, but this correlation was weak and insignificant. The depletion of phosphorus might, as in the case of nitrate, be attributed to the rapid assimilation by phytoplankton in Saadiyat area in 2012, and would have direct consequences for the physiological functioning and heat tolerance of corals. Previous findings have shown that phosphate starvation results in a lower capacity of coral to respond to heat and light induced bleaching (Wiedenmann et al., 2013). Suggested cellular

mechanisms behind this process involve changes in lipid composition of the algal photosynthetic membrane that result from the shift from nutrient-limited to phosphate-starved condition. Thus, it is reasonable to suggest that the absence of phosphorus in the water during the summer months of 2012 might have promoted coral bleaching in response to the elevated temperature.

Iron, an element that can control the rates of phytoplankton productivity and biomass in the ocean (Coale et al., 1996; Martin et al., 1994). It was markedly higher during most of the seasons of 2012 as compared to 2015. This increase in iron may be attributed to the increase in wind speed that occur during the first three months of the year 2012 (figure 3.6d), which may induce water mixing and potentially triggering the development of algal blooms during 2012 in Saadiyat (**Error! Reference source not found.c**). According to Garrison et al., (2003) wind induced mixing could increase the solubility and the bioavailability of iron. The increased concentration of Iron during the summer period could be attributed also to aeolian dust storm inputs, which is generally more frequent during spring and summer months (Kutiel and Furman, 2003). The meteorological wind speed and visibility in Figure 3.6a & b, seem to be in consistence with the finding observed by Kutiel and Furman, (2003). It shows that there is a notable decrease in the visibility during March and July (Figure 3.6a), which is coincided with an increase in wind speed from Feb to August. The Pearson correlation analysis (Table 3.1), also shows a significant negative relationship ($r = -35\%$) between wind and visibility. These results agree with the hypothesis presented by Martin (1990), who suggested that aeolian dust transport is a major ocean fertilization process.

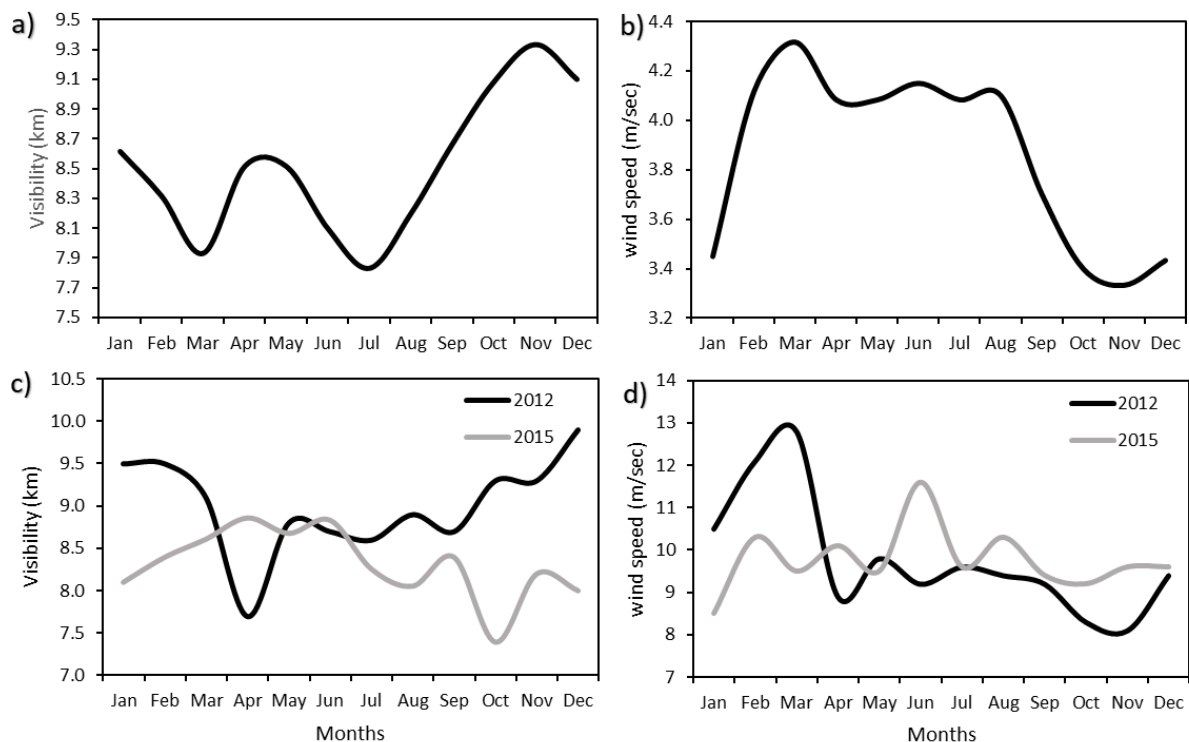


Figure 3.5. Meteorological data from Abu Dhabi Airport. Showing seasonality of a) visibility climatology (2009-2015) and b) wind speed climatology (2009-2015). And a comparison between monthly averages between c) 2012 and 2015 visibility, and d) 2012 and 2015 wind speed.

The dissolved silicate levels were also higher during summer months of 2012, compared to 2015 (**Error! Reference source not found.**d). The dissolved silicon (in the form of orthosilicic acid or "silicate") in natural waters has commonly been assumed as a limiting factor for phytoplankton growth, particularly in the case of diatoms, which require silicon for their shell formation (Paasche, 1973; Brzezinski and Nelson, 1995, Dugdale et al., 1995, Wong and Matear, 1999).

3.4. Conclusion

This chapter presents a detailed characterisation of environmental conditions in coral reef waters off Abu Dhabi, UAE, between 2009 and 2015. The analysis of three parameters, DHD, HR and the number of days above a local threshold, were used to quantify heat stress during episodes of bleaching. As the comparison of heat stress levels in 2012 and 2015 revealed, elevated temperatures are not sufficient to predict local bleaching events. The assessment of other environmental factors suggests that phytoplankton blooms might temporarily reduce certain nutrients, including nitrate and particularly phosphorus, below average levels from the water body. This modification of the local physiochemical conditions of reef water can then act in combination with heat stress to trigger coral bleaching.

Identifying different monitoring methods to detect environmental stressors remains an urgent challenge for the conservation and management of coral reefs worldwide. Remote sensed monitoring techniques could help to meet these challenges by enabling more widespread and continuous monitoring programs. This case study shows how the combination of satellite observations and *in situ* measurements can help to understand the causes of coral bleaching events. It also highlights the needs of integrating different platforms to establish a monitoring system for adverse water quality events.

Chapter 4: Long-term changes in the environmental factors

surrounding coral reef sites in Abu Dhabi

Coral bleaching and mortality events during the period from 1983 to 2015 strongly affected the coral community structure off the coast of Abu Dhabi, UAE. The environmental conditions associated with these events were analysed using satellite observation and meteorological data. Long-term series of phytoplankton (chl-*a*), sea surface temperature (SST), aerosol optical thickness (AOT), water current speed (WCS), diffuse attenuation coefficient (K_d490), air temperature, horizontal visibility, wind speed (WS) and precipitation were acquired and used to characterised the bleaching in the study Delma Island, Saadiyat Island, and Ras Ghanada. The environmental conditions observed around the time of most bleaching events were characterised by dry weather, relatively calm winds and low water currents in addition to elevated air and water temperatures. Notable shifts in the long-term condition include changes in the aerosol regime that started after the 1996 and 1998 El Niño events and shows an apparent intensification of dust storms over the Abu Dhabi area. This increase in dust content in the atmosphere may have been caused by the scarcity of rainfalls and the increase in the wind speed in the region. The dust has the potential to deposit macro and micronutrients in the water and can be considered in addition to anthropogenic nutrient enrichment as a cause of the increasing frequency of phytoplankton blooms after the year 2000. The 2012 phytoplankton bloom has likely resulted in a disturbance of the nutrient environment of the coastal sites, rendering the corals more susceptible to heat stress. In addition, the higher deposition of aeolian dust may have resulted in the introduction of pathogens that might have contributed to the increasing prevalence of coral diseases that has been reported from 2009 onwards.

4.1 Introduction

In recent years, various forms of environmental changes, including elevated water temperature and algal blooms, have impacted coral reef communities in the Arabian Gulf, affecting the symbiotic relationship of corals and leading to coral bleaching (Burt et al., 2008; Bauman et al., 2010; Burt et al., 2011; Burt, 2014; Zhao and Ghedira, 2014). Elevated water temperature has been listed as the major cause of coral bleaching and mortality around the world (Coles and Jokiel, 1978; Glynn and D'Croz, 1990; Sheppard et al., 1992; Baker et al., 2008a; Riegl and Purkis, 2015a). The application of remote sensed SST is widely used around the world as a monitoring tool in estimating and analysing water temperature (Brown et al., 1994; Sheppard, 2003; Logan et al., 2014). In the Arabian Gulf, monitoring water temperature is important because the survival of coral communities is threatened by increased frequency of temperature-related bleaching events (1996, 1998, 2002, 2010, 2011 and 2012) (Riegl and Purkis, 2015a). The consequences of temperature-mediated bleaching events has been varied in the Arabian Gulf, with conditions that have resulted in coral mortality in some regions showing no effect on corals in others (Riegl, 2003; Baker et al., 2008b; Sheppard et al., 2010a; Bernhard M Riegl and Purkis, 2012b; Shuail et al., 2016). This variation may be explained either by the interaction of several environmental factors that can mitigate heat stress or by the adaptation of the corals to their local temperature patterns (Riegl and Purkis, 2012b). It is therefore critically important to establish the differences in local bleaching thresholds among different regions of the Arabian Gulf.

However, a number of other environmental factors can affect coral and their resilience under the impact of temperature stress. Phytoplankton blooms, for instance,

constitute another potentially global threat to coral reefs , as they can impact corals through shading, toxin production, oxygen depletion and alteration of the nutrient balance (Sand-Jensen and Søndergaard, 1981; Landsberg, 2002; Chang et al., 2005; Wiedenmann et al., 2013; D'Angelo and Wiedenmann, 2014; EAD, 2015). Since phytoplankton blooms became more abundant over the last decade in Abu Dhabi (EAD, 2015), monitoring is crucial both in coastal and offshore areas of Abu Dhabi. Since the late 1970s, a wide variety of operational satellite sensors and algorithms have been developed to monitor both biotech and abiotic environmental factors (Hovis et al., 1980). Several ocean colour sensors, such as Coastal Zone Colour Scanner (CZCS) the Sea-viewing Wide Field-of-view Sensor (SeaWiFS) and the Moderate Resolution Imaging Spectroradiometers (MODIS), are capable of mapping and monitoring phytoplankton blooms (Alexandridis et al., 2009). They are designed to retrieve the spectral information of the upwelling radiance above the sea surface that is referred to as the water-leaving radiance or $L_w(\lambda)$. This radiance can be used to estimate the concentration of chlorophyll *a* (chl-*a*), which has been, since the first chl-*a* global maps were published, widely used as phytoplankton bloom indicator (Feldman et al., 1989; Franz et al., 2005; Blondeau-Patissier et al., 2014a; see chapter 3 in this thesis)

Coastline changes and development in Abu Dhabi can influence many intertidal habitats and the overall benthic environment in the region (Sheppard, 1993). Hence, measurements of water clarity can be used to characterise study sites and evaluate whether the increased particle load and potentially associated changes in nutrient levels can be linked to the incidence of phytoplankton blooms. Changes in water clarity can be quantified by measuring the diffuse attenuation coefficient $K_d(\lambda)$ (where λ is the light wavelength in free space) of the spectral solar downward irradiance (Jerlov, 1976; Kirk, 1994). In ocean

colour remote sensing the diffuse attenuation coefficient (K_d) at $\lambda = 490\text{nm}$ is estimated from an empirical algorithm based on the relationship between $K_d(490)$ and the blue-to-green ratio of water-leaving radiance (Austin and Petzold, 1986). It is used to determine the turbidity in the selected sites that serve as an indicator of water clarity (Jerlov, 1976; Kirk, 1994; Wang et al., 2009).

In addition to nutrient enrichment through natural and anthropogenic mechanisms such as upwelling or coastal run-off, dust deposition is considered a triggering factor for phytoplankton blooms through the enrichment of the water body with micronutrients, such as iron (Zhuang et al., 1992; Arimoto, 2001; Anderson et al., 2002; Al-Shehhi et al., 2012). Dust storms are known to be frequent and extreme in the Arabian Gulf, reaching up to 15 to 20 dust storms per year (Kutiel and Furman, 2003) due to the geographical localisation of the Gulf between extensive desert areas (latitudes 24-30°N) (Reynolds, 1993). This vast arid land surrounding the Arabian Gulf (Africa and Asia) is one of the major sources of aeolian dust in the world (Husar et al., 1997). As reported by Kukal and Saadallah (1973), dust storms can reduce the atmospheric visibility of the affected areas to less than 55m in the Arabian Gulf. As suggested by Shinn et al. (2000), dust storms can also potentially transport anthropogenic pollutants, synthetic chemicals, pathogenic microorganisms, and other toxic constituents from land to be deposited in the oceans. According to Underwood (2015), A 2011 study released by the Centre for Naval Warfare Studies, US Naval War College, Rhode Island, found that dust particles tested in Kuwait and Iraq carried very high levels of metals and microbial matter. This study isolated more than 147 different types of bacteria species, including some that showed antibiotic resistance. The isolated samples include the drug resistant Staphylococcus aureus (methicillin-resistant *Staphylococcus*

aureus or MRSA), malaria-causing Neisseria meningitidis and Acinetobacter baumannii, a superbug linked to severely injured soldiers. However, there are lack of direct evidence to support Shinn et al. (2000) hypothesis in the Arabian Gulf.

Moreover, there are only four types of coral diseases found in the Arabian Gulf (white band disease (WBD), black band disease (BBD), yellow band disease (YBD) and pink spot and line disease), compared to the other parts of the world, such as the Caribbean basin where there are over 30 coral disease found (Riegl and Purkis, 2012a). These coral diseases have been potentially linked with thermal anomalies and coral bleaching (Miller et al. 2006; Miller et al. 2009; Bruckner and Hill, 2009). For example, most thermal anomalies and bleaching events in the southern Gulf (e.g. 2010, 2011 and 2012) have being followed immediately by disease outbreaks (Riegl and Purkis, 2015b).

Aerosol optical thickness (AOT) of SeaWiFS and MODIS-Terra satellite sensors and the horizontal visibility at Abu Dhabi airport are used in this chapter as indicators of aeolian dust dynamics surrounding the study sites and potential correlation with phytoplankton blooms. The AOT is a measure of the extinction of the solar beam by dust particles (Chu et al., 2002; Wang and Christopher 2003; Nezlin et al., 2010). The AOT is unit-less number related to the amount of aerosol in the vertical column of atmosphere over the observation location (Lau and Kim, 2006; Wang, 2013; Devara and Manoj, 2013). Abu Dhabi airport's horizontal visibility also served as a direct proxy of dust intensity in the atmosphere. Wind speed and wind angular direction were also acquired in this study from Abu Dhabi Airport. Wind speed is known to be a major factor in dust transport, water current and water vertical mixing, which all play a vital role in stimulating phytoplankton blooms (Arimoto, 2001; Nezlin and Li, 2003; Nezlin et al., 2007; Nezlin et al., 2010; Zhao

and Ghedira, 2014). The water motion resulting from wind gusts has been shown to be beneficial to coral reefs during temperature stress, by thinning boundary layers and accelerating mass transfer (Baker et al., 2008b). It helps in heat dissipation and the removal of toxic oxygen radicals from the water column (Woesik and Koksai, 2006; Baker et al., 2008b). The most significant wind phenomenon in the Arabian Gulf is the 'Shamal' wind. The Shamal (meaning "North" in Arabic), is blown from the Northwester of the Arabian Gulf (Kendall et al., 2003). Although it happens both in winter and in summer seasons, but the winter Shamal has a slightly greater speed, which reaches up to 100 km/h (John et al., 1990). All these environmental factors may direct negative impact on the Gulf coral communities or may affect them through the effect of potentially causally linked phytoplankton blooms. Therefore, it is important to study all these environmental factors in greater detail to determine exactly how, and to what extent, they are related to the increased frequency of coral bleaching witnessed in the last decades.

The purpose of this study is to use remote sensing tools to analyse patterns of environmental factors that are prevalent during documented coral bleaching event in the southern Gulf region (Abu Dhabi). In this work, satellite data, including sea surface temperature (SST), chlorophyll a (chl-*a*), water current speed (WCS), diffuse attenuation coefficient (K_d490) and aerosol optical thickness (AOT), were determined for each region in Abu Dhabi and for control regions elsewhere in the Gulf. These parameters complemented by the analysis of meteorological data, air temperature (AT), horizontal visibility (HV), wind speed (WS) and precipitation obtained from ground measurements, to obtain a comprehensive picture of the environmental conditions in the Southern Arabian Gulf.

4.2 Material and methods

4.2.1 Study sites

The Arabian Gulf is a shallow semi-enclosed water body located within the arid region of the Middle East between latitudes 24 ° and 30 ° N and longitudes 48 ° and 56 ° E. The Arabian Gulf is bordered by Iran and seven Arab countries, namely, Iraq, Kuwait, the Kingdom of Saudi Arabia (KSA), Bahraini, Qatar, Oman, and the United Arab Emirates (UAE) (Figure 4.1) (Robinson and Brink, 2006). The three selected sites are, Delma, Saadiyat, and Ras Ghanada, which are located within the coastal area of the Abu Dhabi Emirate, in the UAE (Purser and Seibold, 1973). These sites were selected based on their coral communities and the difference in their bleaching patterns (Foster et al., 2012). The majority of the coral communities in these sites were composed of four common families, poritids, faviids, acroporids, and siderastreids (Burt et al., 2011; Foster et al., 2012). The three sites were thoroughly discussed in the introductory chapter of this thesis.

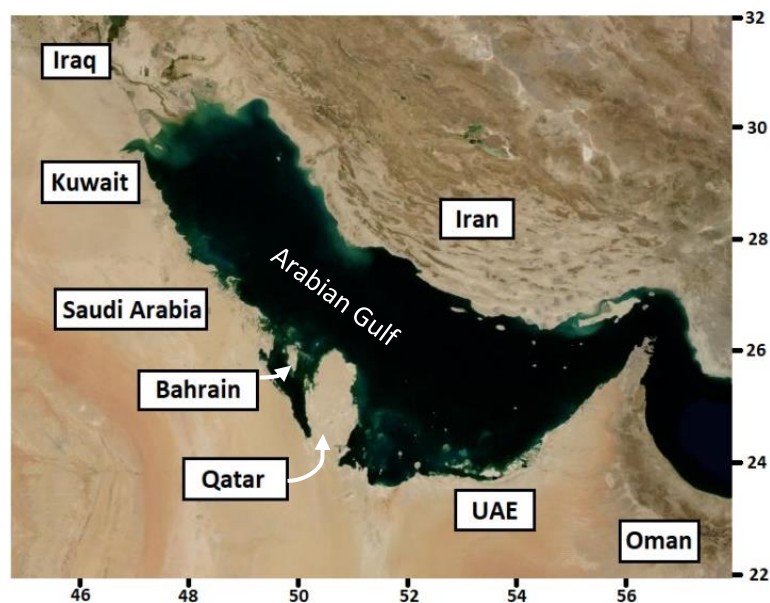


Figure 4.1. Countries surrounded the Arabian Gulf. Including: Iraq, Kuwait, Saudi Arabia, Bahrain, Qatar, United Arab Emirates, Oman and Iran. Source: <https://lance3.modaps.eosdis.nasa.gov>.

4.2.2 Environmental data acquisition

Several environmental factors were used to characterise the environment surrounding the coral reefs of each selected region of this study. These parameters are: 1) Satellite observations, including SST, chl-*a*, water current speed (WCS), diffuse attenuation coefficient (K_d490) and aerosol optical thickness (AOT). In addition to 2) Meteorological data, including air temperature, horizontal visibility, wind speed (WS) and rainfall precipitation. These environmental factors are considered, solely or in interaction with other factors as potential drivers of coral bleaching events documented in the southern Gulf region (Abu Dhabi) (Table 4.1).

Table 4.4. Summary of properties and sources of environmental data used in this study.

Data product	Satellite/model	Spatial resolution	Time Scale	Web site
Sea surface temperature (°C)	AVHRR	4 km	1983-2001	podaac-tools.jpl.nasa.gov
Sea surface temperature (°C)	MODIS-Aqua	1 km	2002-2015	https://oceancolor.gsfc.nasa.gov
Chlorophyll (mg/m ³)	SeaWiFS	4.5 km	1997-2001	https://oceancolor.gsfc.nasa.gov
Chlorophyll (mg/m ³)	MODIS-Aqua	1 km	2002-2015	https://oceancolor.gsfc.nasa.gov
Water current speed (m/sec)	OSCAR	111 km	1992-2014	http://oceanmotion.org
Light attenuation coefficient (K_d490)	SeaWiFS	111 km	1997-2001	https://giovanni.gsfc.nasa.gov
Light attenuation coefficient (K_d490)	MODIS-Aqua	111 km	2002-2015	https://giovanni.gsfc.nasa.gov
Aerosol optical thickness (AOT)	SeaWiFS	111 km	1997-2001	https://giovanni.gsfc.nasa.gov
Aerosol optical thickness (AOT)	MODIS-Aqua	111 km	2002-2015	https://giovanni.gsfc.nasa.gov
Air temperature (°C)	Abu Dhabi Airport	NA	1983-2015	weatherspark.com
Visibility (km)	Abu Dhabi Airport	NA	1983-2015	weatherspark.com
Wind speed (m/sec)	Abu Dhabi Airport	NA	1983-2015	weatherspark.com
Precipitation (mm)	Abu Dhabi Airport	NA	1983-2015	weatherspark.com
Dipole mode index (°C)	Stateoftheocean	NA	1983-2015	stateoftheocean.osmc.noaa.gov
El Nino Southern Oscillation (°C)	Stateoftheocean	NA	1983-2015	stateoftheocean.osmc.noaa.gov

4.2.2.1 Chlorophyll-*a*

Remote sensed chl-*a* data were analysed from the three selected sites in Abu Dhabi Emirate. Chl-*a* images were obtained by the Sea-Viewing Wide Field of View Sensor (SeaWiFS), from September 1997 to February 2009 and the Moderate Resolution Imaging Spectroradiometer (MODIS) Aqua, from July 2002 to December 2015. Both satellites are known as ocean colour sensors that are designed to retrieve the spectral information of the

upwelling radiance above sea surface (water-leaving radiance or $L_w(\lambda)$). This radiance can be used to estimate a number of geophysical data parameters, such as the concentration of chl-*a* (Franz et al., 2005).

SeaWiFS is a multi-spectral radiometer, crossing the earth's equator on a daily basis at noon time, and collecting data since August 1997 (O'Reilly et al., 1998). SeaWiFS views the land in eight spectral bands covering the visible and near-infrared (NIR) range from 400-900 nm. It has a global area coverage (GAC) resolution of 4.5km (Gregg and Casey, 2007). This sensor is considered one of the best tool available to study the planet's biological activity and response to the changes in the environment parameters. However, the OrbView-2 spacecraft that carried the SeaWiFS instrument stopped communicating with Earth-based data stations in December 2010. Therefore, MODIS-Aqua sensor, which has been in operation since June 2002 to the present, was used in this chapter. It has a daily orbit around the earth passing over the equator from south to north in the afternoon (from 12:00 13:30). The overlapped chl-*a* values during the period from July 2002 to February 2009 of each satellite (SeaWiFS and MODIS-Aqua) were plotted against each other, and the coefficient of determination (R^2) for a linear regression fit was calculated to increase the confidence in the comparability of the data.

MODIS sensors measure radiance in 36 spectral channels covering the range from 400 nm to 14.4 μm , to support land, ocean, and atmospheric measurements. The bands of primary interest to ocean colour applications are the nine channels covering the spectral range from 400-900 nm. Both SeaWiFS and MODIS are scanning radiometers, collecting data over a wide swath with a pixel resolution of approximately 1-km x 1-km at the

minimum view angle. Both missions design to operate for global observation on a daily basis (Alexandridis et al., 2009).

4.2.2.2 Sea surface temperature (SST)

Relevant SST data are presented in chapter two of this thesis, within the analysis of the seasonality and interannual variation for the three study sites. The SST data utilised in the present work is a long-term merged data-set from the Very High-Resolution Radiometer (AVHRR) and MODIS-Aqua (1983-2015). According to Marcello et al. (2004), the current SST algorithms applied to Advanced AVHRR and MODIS (Aqua and Terra) can estimate SST with an accuracy of about 0.6°C, which is acceptable for many marine applications. Both chl-*a* and SST were analysed at the three selected sites in Abu Dhabi (Delma, Saadiyat, and Ras Ghanada).

4.2.2.3 Aerosol optical thickness (AOT)

Aerosol optical thickness (AOT) at 550nm of SeaWiFS and MODIS-Aqua obtained from NASA's Giovanni website (<http://giovanni.gsfc.nasa.gov/>), was used to measure dust concentration in the atmosphere (Chu et al., 2002; Wang and Christopher 2003; Nezhlin et al., 2010). Both sensor's data sets were Level 3 (meaning: the variable is mapped on uniform space-time grids (Parkinson et al., 2006) and had 1°×1° (~111 km²) spatial resolution. The dust storms are relevant to this study due to their impact on SST and the radiation budget of the atmosphere (Kaufman et al., 2002). Dust storms also carry micronutrients, which are considered a source of ocean enrichment, which can trigger the development of either HAB or non-HAB, especially the iron element (Zhuang et al., 1992;

Arimoto, 2001; Anderson et al., 2002; Al-Shehhi et al., 2012). Shinn et al., (2000) and Garrison et al., (2003), suggested that dust storms can transport anthropogenic pollutants, synthetic chemicals, pathogenic microorganisms, and other toxic constituents from land to be deposited in the oceans. 2, Figure 4.2 shows examples of Near-Real-Time Images of dust storms trajectory in the Gulf, matched with images of MODIS AOT at 550nm (1°x1°) obtained from Giovanni website (<http://giovanni.gsfc.nasa.gov/>). The Near Real-Time Images were obtained from Rapid Response imagery from the Land, Atmosphere Near Real-time Capability for EOS (LANCE) system (<https://lance3.modaps.eosdis.nasa.gov/cgi-bin/imagery/realtime.cgi>) operated by the NASA/GSFC/Earth Science Data and Information System (ESDIS) with funding provided by NASA/HQ.

4.2.2.4 Water current speed (WCS)

The monthly current speed profiles (1992-2014) in each region were examined using the data available from NASA Ocean Motion website (<http://oceanmotion.org/html/resources/oscar.htm>). This site utilizes the 1°x1° (~111 km²) spatial resolution Ocean Surface Current Analyses Realtime (OSCAR) provided on global grid approximately every five days, from 1992 to December 2014, with daily updates and near-real-time availability (http://www.esr.org/oscar_index.html). Water motion has important control over reef corals in various ways. It enhances the circulation caused by waves, tides, and currents. It can modify several important environmental factors, such as plankton, dissolved nutrients, and gasses, sediment, water clarity, substrata, salinity, and temperature (Jokiel, 1978). It is required to ensure the necessary supply of oxygen and

nutrients to the corals (Kinsman, 1964). It appears to influence corals by controlling the rate of exchange of material across the interface between the sea water and the coral tissue (Jokiel, 1978).

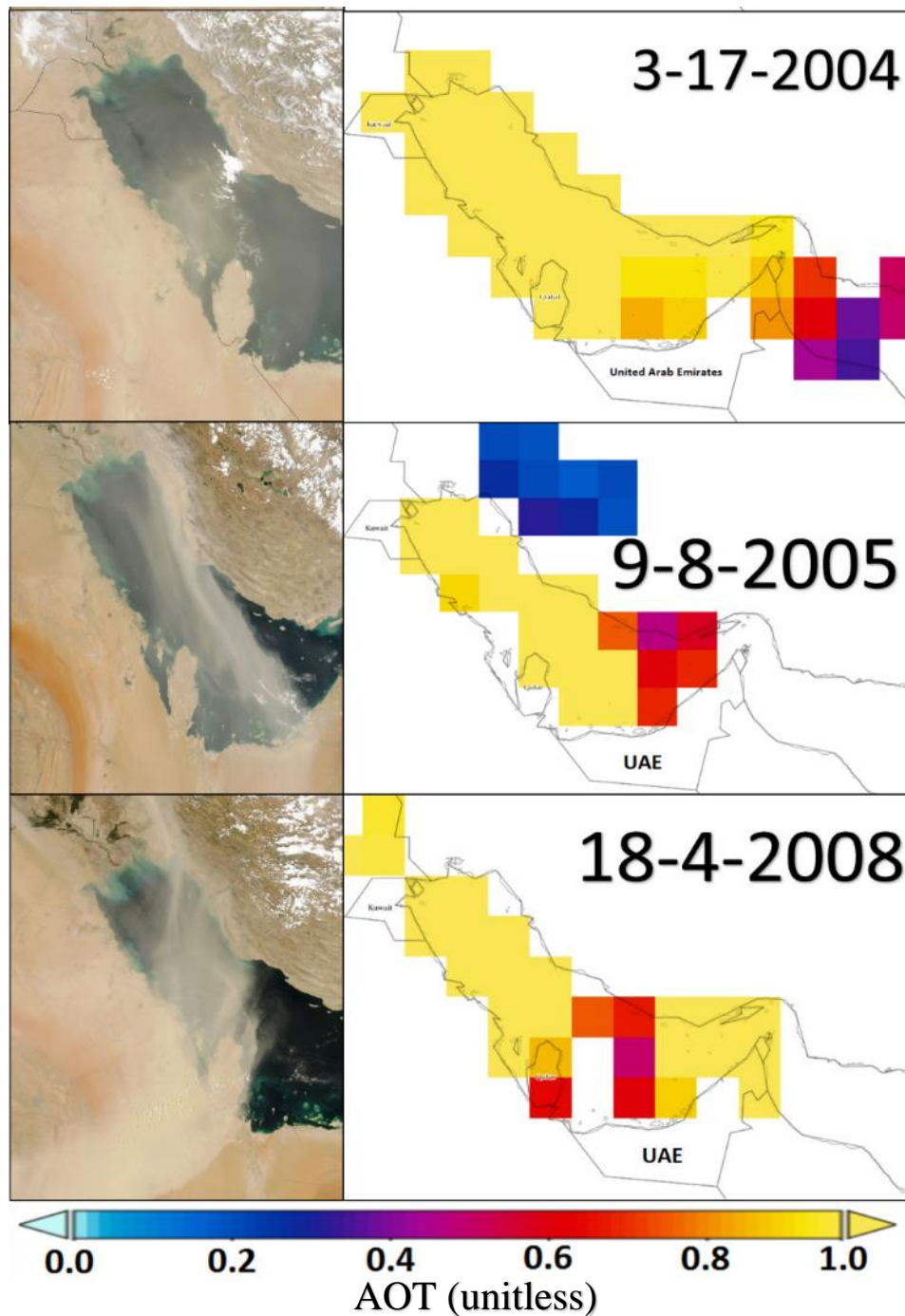


Figure 4.2. Samples of a major dust storms passing over the Arabian Gulf in the right panel (source: <https://lance3.modaps.eosdis.nasa.gov/>), matched with MODIS-Aqua AOT (111km² resolution) in the left panel (source: giovanni.gsfc.nasa.gov).

It is now clear that high water flow rates reduce bleaching susceptibility in corals (Dennison and Barnes, 1988; Nakamura and Van Woesik, 2001). Therefore, abnormally hot and humid summers with very low wind speed and low water flow, most probable cause coral mortality.

Due to the relatively low resolution ($1^{\circ} \times 1^{\circ} = \sim 111 \text{ km}^2$) of AOT acquired through Giovanni website and the water current speed from OSCAR, and the fact that Saadiyat and Ras Ghanada are only $\sim 30 \text{ km}$ apart, two regions were selected to examine the variability of this parameter. The first region is centered at Delma (lat: 24.5208°N /long: 52.2781°E) and the second is centered between both Saadiyat and Ras Ghanada (Lat: $24^{\circ}42'11.8\text{N}$, Long: $54^{\circ}31'06.0\text{E}$).

4.2.2.5 Water turbidity

Water clarity was estimated from remote sensed data using the downwards irradiance of light diffuse attenuation coefficient, $K_d(\lambda)$, at the blue-green band $\sim 490 \text{ nm}$ (K_d490) (Lee et al., 2005). The K_d490 was retrieved from SeaWiFS (9 km pixel resolution) and MODIS-Aqua (4 km pixel resolution) using the Giovanni website (<http://giovanni.gsfc.nasa.gov/>). The K_d490 is the rate at which light intensity at 490 nm is attenuated with depth, as is directly related to the presence of scattering particles in the water column, either organic or inorganic, and thus it is an indication of water clarity (Wang et al., 2009).

4.2.2.6 Meteorological data

Meteorological data were obtained from different airports within the Arabian Gulf region, including Abu Dhabi, Bahrain, and Kuwait through the weatherspark Beta database (<https://weatherspark.com/>). The data acquired include air temperature (degrees celsius), horizontal visibility (km), wind speed (m/sec), wind direction (angular mean) and precipitation (count per day). Although the data is sourced from NOAA, weatherspark facilitates its accessibility. These data were used to analyse the weather and correlate the overall climate conditions in the southern Gulf to the remote sensed parameters studied in this chapter over the study regions.

4.2.2.7 Dipole mode index (DMI) and the El Niño Southern Oscillation (ENSO)

Finally, both the dipole mode index (DMI) and the El Niño Southern Oscillation (ENSO) anomaly indexes were used as a reference to the overall environmental trends and interannual variations. The DMI is a representation of the intensity of the Indian Ocean dipole IOD calculated as the anomalous SST gradient between the western equatorial Indian Ocean (50E-70E and 10S-10N) and the southeastern equatorial Indian Ocean (90E-110E and 10S-0N). It is acquired from the state of the ocean climate (<http://stateoftheocean.osmc.noaa.gov>).

The ENSO is known to be among the strongest natural phenomenon affecting the global climate system (Glantz et al., 1991). ENSO anomalies were obtained from NOAA National Weather service/climate prediction center (http://www.cpc.ncep.noaa.gov/products/analysis_monitoring/). NOAA calculates it as

three-month running mean of ERSST.v4 SST anomalies in the Niño 3.4 region (5°N-5°S, 120°-170°W), based on centered 30-year base periods updated every five years.

4.2.3 Regression analysis of the remote sensed data

A simple linear regression between remote sensed SST and the *in situ* water temperature for MODIS-Aqua and AVHRR platforms in Abu Dhabi is presented in Chapters 2 and 3 of this thesis (Figure 2.3&3.1). The simple linear regression is a statistical method used to study relationships between two continuous (quantitative) variables, and its regression coefficient (R^2) indicates the differences between these variables. For MODIS-Aqua the regression coefficient shows an $R^2=0.96$ in Saadiyat and $R^2= 0.97$ in Delma. This indicates that the differences between the MODIS-Aqua SST and the *in situ* values are small in both Saadiyat and Delma sites. For AVHRR, the linear regression with the *in situ* data shows a strong coefficient $R^2= 0.918$, with RMSE=1.4. Additionally, AVHRR was matched with the corresponding SST values from MODIS Aqua that also reveals a satisfactory regression coefficient $R^2= 0.958$, RMSE=1. The MODIS SST data were also matched with the air temperature acquired from the Abu Dhabi airport ground measurements, which shows again a strong regression relationship result $R^2= 0.927$, RMSE=7.

As detailed in chapter 3 of this thesis, the values of chl-*a* estimated from the analysis of MODIS Aqua data, were also matched with the *in situ* data using the simple regression analysis. The analysis showed a strong regression coefficient $R=0.918$. In this chapter, a 1-pixel value (4.5km) of SeaWiFS chl-*a* were matched an average of 5x5-pixel for MODIS Aqua (to accommodate the spatial difference) centered at the survey location (Sadiyaat).

The chl-*a* values of each satellite were plotted against each other and the coefficient of determination (R^2) for a linear regression fit was calculated.

In this chapter, AOT at 670nm for SeaWiFS (1998-2010) and at 667nm for MODIS-Aqua (2002-2015) were merged in order to extend the time-series of these parameter. Likewise, the K_d490 data extract from SeaWiFS (1998-2010) and MODIS-Aqua (2002-2015) were merged. The overlapping period from both satellites was compared using simple linear regression and the root-mean-square-error (RMSE). The extended time series will help us cover most of the bleaching events that occurs in the Southern Arabian Gulf (1998, 2002, 2010, 2011 and 2012 major bleaching events).

4.2.4 Seasonality and interannual anomalies

Seasonal variations of all previously mentioned variables were analysed from their climatologies, calculated for their monthly averages. To examine interannual variability, seasonal anomalies were extracted for each parameter by subtracting their respective climatic monthly values. chl-*a*, WCS, AOT, and the K_d490 were examined for the time period from September 1997 to December 2015. In the case of SST, the extended time series from January 1982 to December 2015 were used. The meteorological variables, including air temperature, visibility, wind speed, and precipitation, were analysed from January 1983 to December 2015.

Descriptive statistics and one-way ANOVA tests were conducted to discern differences in the remote sensed parameter between the three locations. The Tukey *post hoc* analysis was used to reveal putative significant differences between the sites. The overall yearly variation in the time series for each parameter was fitted to a fourth order

polynomial trend. A Pearson correlation was run to assess the relationship between the remote sensed parameters, and between the remote sensed parameters and the meteorological data. The Pearson correlation is a measure of the strength and direction of association that exists between two continuous variables.

4.2.5 Cross-correlation analysis

Cross-correlation analysis measure the movement and the proximity of alignment among two different time series (Bracewell, 1986; Nikolay P. Nezlin and Li, 2003). This proximity is expressed as a lag time and a correlation coefficient between the two variables, and the maximum correlation has zero time-lag. This will explain how each parameter patterns correlate with the chl-*a* patterns. The cross-correlation analysis will be performed on SST, turbidity (K_d490), aerosol optical thickness (AOT), current speed and wind speed against chl-*a* (phytoplankton bloom) patterns, which will help in understanding which factor is more likely to be the main driver of the phytoplankton development in the region. The cross-correlation analysis in this chapter is based on the monthly average of each parameters, for example one time-lag is equal to one month.

4.2.6 Regional coral bleaching thresholds

Coral bleaching threshold is defined as 1°C higher than the highest monthly mean temperature in a given region (Glynn and D'Croz, 1990). The local bleaching thresholds were calculated for the study sites in Abu Dhabi and are presented in Chapter 2 (Shuail et al., 2016a). To compare these thresholds to the Arabian Gulf region, we calculated the bleaching threshold for six other coral reef areas in the Arabian Gulf (Figure 4.3). These

are Kuwait (Qaru Island: lat: 29° 2'49.22"N long: 48°30'53.76"E), Saudi Arabia (Abu Ali Island: lat: 27°14'10.30"N long: 49°44'9.03"E), Bahrain (offshore Manama area: lat: 26°19'27.51"N long: 50°35'7.19"E), Qatar (Halul Island: lat: 25°40'20.71"N long: 52°21'4.23"E), Oman (Musandam Peninsula: lat: 26°14'25.16"N long: 56°34'38.06"E) and Iran (Siri Island: lat: 25°58'14.45"N long: 54°36'17.05"E). These locations were selected according to their coral reef areas (Rezai et al., 2004), and the extended SST data-set from 1982 to 2015 was used in this analysis.

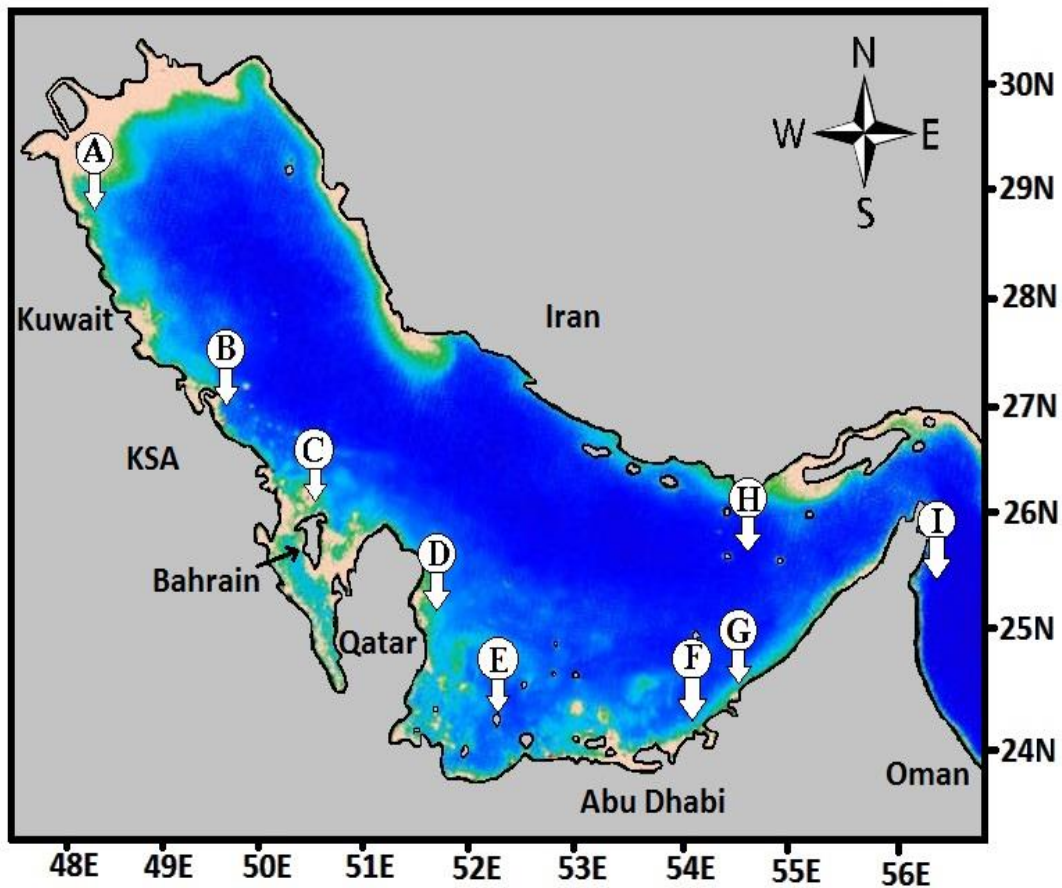


Figure 4.3. Study sites in the Arabian Gulf. A) Kuwait (Qaru island), b) Saudi Arabia (Abu Ali island) (KSA), C) Bahrain, D) Qatar, E) Delma, F) Saadiyat, G) Ras Ghanada, H) Iran, and I) Oman.

4.3 Result and discussion

4.3.1 Regression analysis of the remote sensed data

The regression analysis between the remote sensed platforms, MODIS-Aqua and SeaWiFS, showed a high regression coefficient $R^2=0.9$, RMSE=0.016 for the diffusion attenuation coefficient (K_d490), and $R^2= 0.85$, RMSE=0.105 for the AOT, and $R=0.92$, RMSE=0.19 for the chl-*a* (Figure 4.4). These results justify that a continuous time series can be assembled from the data of both satellites.

4.3.2 Seasonal variations

4.3.2.1 Chlorophyll-*a*

Chl-*a* concentrations in the Gulf varied widely, ranging from the monthly average of 0.12-23.7 mg/m³ in the northern parts of the Gulf (Kuwait), to 0.43-0.67 mg/m³ in the Gulf of Oman (ROPME, 2012). The analyses show that the monthly chl-*a* concentration in the study sites, over the study period (1997-2015) ranges from 0.33-3.88 mg/m³ in Delma, 0.78-3.87 mg/m³ in Saadiyat, up to 0.91-5.15 mg/m³ in Ras Ghanada (Table 4.2). The annual 18 years average is 1.17 mg/m³ in Delma, 1.82 mg/m³ in Saadiyat and 1.75 mg/m³ in Ras Ghanada. Chl-*a* concentration was ~0.5 mg/m³ higher in Saadiyat and Ras Ghanada than in Delma (Figure 4.5). These differences between the regions were statistically significant (one-way ANOVA test, $F(2, 657) = 94.350$, $p < 0.001$. Delma ($M = 1.17$, $SD = 0.52$), Ras Ghanada ($M = 1.76$, $SD = 0.57$) and Saadiyat ($M = 1.82$, $SD = 0.55$)). Further analysis with the Tukey *post hoc* test revealed that chl-*a* values in Delma were significantly lower than in Saadiyat and Ras Ghanada, (-0.58, 95% confidence interval (CI) [-0.71, -0.46]), ($p < 0.001$). The higher chl-*a* concentration in Saadiyat and Ras Ghanada as

compared to Delma could be explained by their proximity to the coastal area, which can potentially introduce different anthropogenic factors that may increases water productivity.

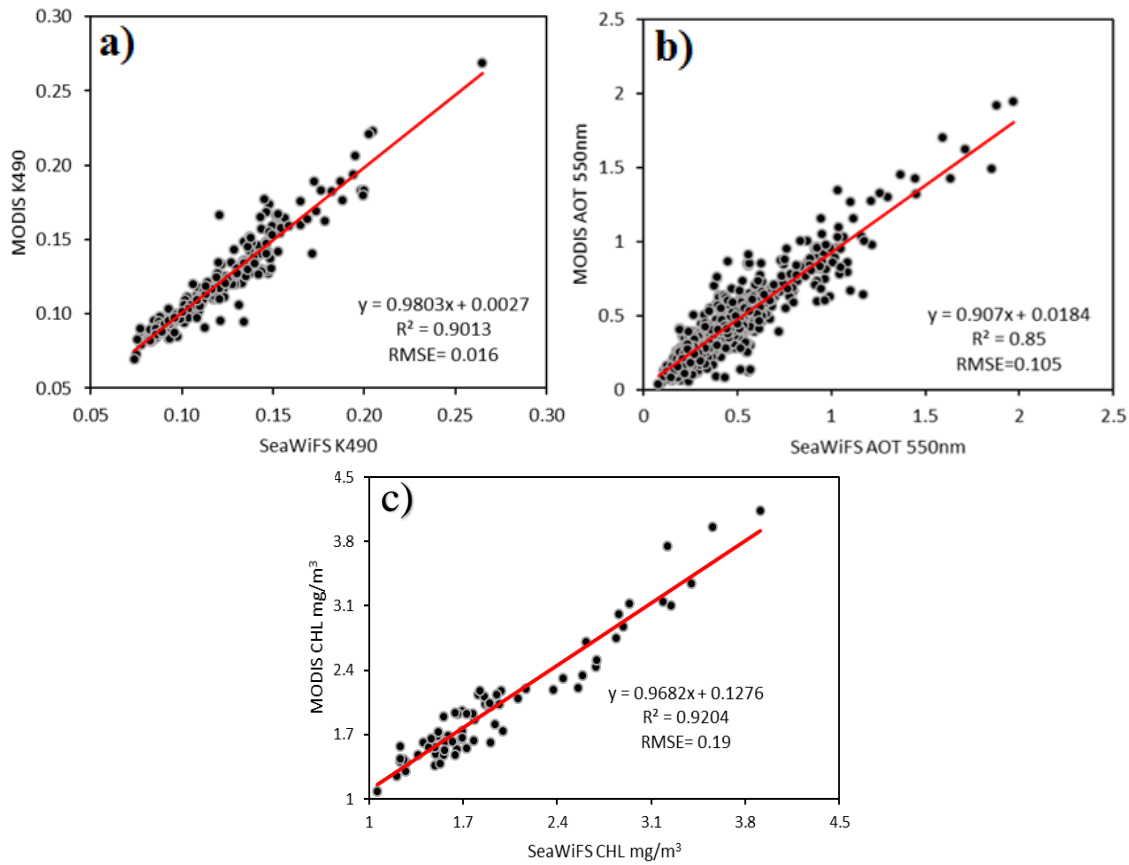


Figure 4.4. Validation of data obtained by remote sensing analysis of a) diffusion attenuation (K_d490), and b) Aerosol optical thickness (AOT) at 550nm, c) chlorophyll-a (chl-a).

Table 4.5. Descriptive statistics for the environmental parameters in Delma, Saadiyat and Ras Ghanada obtained by remote sensing analysis.

	Delma				Saadiyat				Ras Ghanada			
	Mean	Min	Max	Range	Mean	Min	Max	Range	Mean	Min	Max	Range
Chl-a (mg/m^3)	1.17(± 0.5)	0.33	3.88	3.56	1.82(± 0.5)	0.78	4.66	3.87	1.75(± 0.6)	0.91	5.15	4.24
SST ($^{\circ}C$)	27.17(± 5.1)	17.6	36	18.4	27.5(± 4.7)	18.3	35.3	17	27.6(± 4.5)	18.7	34.8	16.2
WCS (m/sec)	0.10(± 0.03)	0.04	0.22	0.18	0.12(± 0.03)	0.06	0.24	0.18	0.12(± 0.03)	0.06	0.24	0.18
AOT (unitless)	0.46(± 0.2)	0.2	1.33	1.13	0.44(± 0.2)	0.15	1.01	0.87	0.44(± 0.2)	0.15	1.01	0.87
K_d490 (m^{-1})	0.11(± 0.03)	0.06	0.23	0.18	0.12(± 0.05)	0.04	0.47	0.43	0.12(± 0.04)	0.06	0.26	0.2

Table 4.3. Descriptive statistics for the meteorological parameters in Kuwait airport, Bahrain airport and Abu Dhabi airport.

	Kuwait				Bahrain				Abu Dhabi			
	Mean	Min	Max	Range	Mean	Min	Max	Range	Mean	Min	Max	Range
Air temp. (°C)	33.11(±10.1)	14.4	47.3	33	30.15(±6.9)	15.7	40.4	24.7	34.04(±6.6)	20.8	45.4	24.6
Visibility (km)	8.5(±1.1)	4.3	15	11	10.35(±1.2)	6.3	13.3	7	9.6(±1.2)	6.1	13.6	7.5
Wind speed (m/s)	7.44(±1.16)	0.5	10.4	10	7.43(±1.01)	1.17	10.4	9.2	7.14(±0.7)	5.4	9.54	4
Precipitation (mm)	0.52(±0.67)	0	3.6	3.6	0.43(±0.7)	0	4.8	4.8	0.2(±0.4)	0	2.7	2.7

Coastal impacts in Abu Dhabi include wastewater discharge, surface runoff, fertilizers from landscape maintenance and agriculture as well as other water-related activity and can potentially introduce excess nutrients into the marine environment (Sheppard et al., 2010b). Other factors that may increase productivity in the coastal sites are the industrial facilities, including power generation, iron and steel works, and several other sectors, which are concentrated in Industrial Cities Abu Dhabi (ICADs), Mussafah Industrial Area, and Khalifa Industrial Zone Abu Dhabi (KIZAD). Effluent discharges from industrial facilities may introduce excess nutrients, sediments, heavy metals, and other potentially toxic chemical contaminants into waterways thereby altering the chemistry levels of the water. Phytoplankton blooms that can develop from this nutrient loading and nutrification can also deteriorate the water quality in this area. Abu Dhabi Environmental Agency has reported an increase in the frequency of HAB incidents in Abu Dhabi during the last decade (EAD, 2015). Abu Dhabi water monitoring program also indicate that Mussafah Channel, which is close to Saadiyat reef, is impacted by nutrient enrichment, low DO concentrations in bottom waters and phytoplankton blooms throughout the year.

The seasonal patterns of chl-*a* were similar among sites (Figure 4.5), characterized by a summer maximum and a winter minimum in all locations. This finding matches those of Moradi and Kabiri (2015) who shows a gradual increase of chl-*a* starting from April, reaching the highest values in late summer (August/September) and start declining from the end of September through to its minimum for Saadiyat and Ras Ghanada in March, and for Delma in April each year. According to Nezlin et al. (2007), the northern river plumes (Shutt al-Arab) constitute the main nutrient-rich waters sources in the Arabian Gulf. In agreement with our findings, the seasonality of chl-*a* in the Gulf is characterised by summer maximum and winter minimum (Moradi and Kabiri, 2015). However, the study area is not under the direct influence of the northern river plumes, which suggest that different factors may control the seasonal chl-*a* fluctuation (Nezlin et al., 2007; Moradi and Kabiri, 2015). The seasonal patterns of the remote sensed chl-*a* in Abu Dhabi are well matched with the *in situ* chl-*a* measured by the environmental agency of Abu Dhabi (Figure 3.1 in chapter 3 of this Thesis).

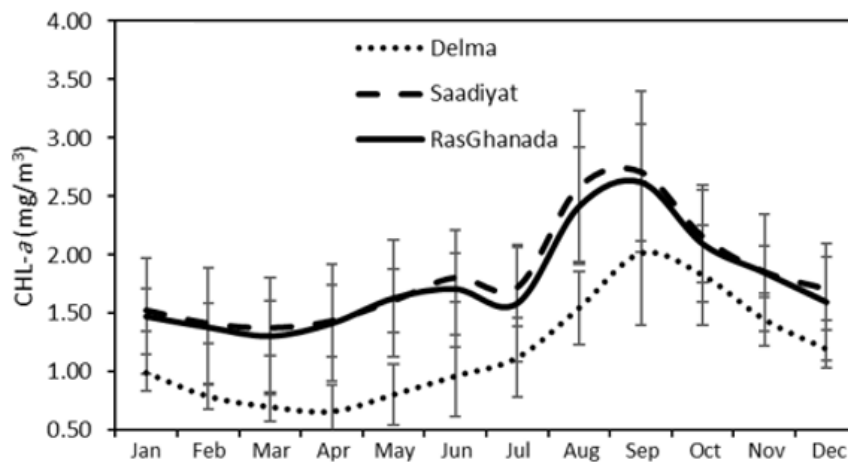


Figure 4.5. Comparing chl-*a* climatology obtained by MODIS-Aqua in Delma, Saadiyat and Ras Ghanada. Symbols shows average values during 1997-2015, error bars display standard deviation.

4.3.2.2 Diffusion attenuation coefficient (K_d490)

The seasonal patterns of both K_d490 (Figure 4.6) and chl-*a* (Figure 4.5) are comparable, showing similar maximum and minimum climatology in all three sites. The K_d490 difference between the three study sites was significant (one-way ANOVA test ($F(2, 657) = 10.839, p < 0.001$)). The Tukey *post hoc* analysis revealed that both Saadiyat and Ras Ghanada were significantly more turbid (K_d490) than Delma (0.009, 95% CI [0.0008, 0.0177]), ($p = 0.028$). The elevated K_d490 in the coastal study sites (Saadiyat and Ras Ghanada), can be, as discussed above, due to their close proximity to the coastal discharges that induce eutrophication (chl-*a*), which in turn reduces water clarity. This result further confirms the hypothesis of Sharifinia et al. (2015), which considered chl-*a* as one of the main components that contribute to turbidity in aquatic ecosystems. Water clarity is not only affected by phytoplankton, but also by the impact of coastal development, as well as the overall benthic environment in the region (Sheppard, 1993). Particularly the large-scale developments near coral reefs areas, such as Khalifa Port may have consequences on the surrounding coastal and offshore ecology. Khalifa Port is a large port in the UAE, dredged between 2008 and 2010, and is in the vicinity of the Ras Ghanada coral reefs. The resuspension plumes of dredged material might have exerted a direct impact on the surrounding seabeds. However, a Marine Infrastructure Impact Assessment (MIIA) was undertaken to analyse and minimise the influence of the port on the surrounding marine environment (Cole and Broderick, 2007). The MIIA reported values of 20 mg/l (± 35 NTU), in areas of total mortality of the coral reef (Bots, 2013), resulted in several unplanned work stoppages at Khalifa Port.

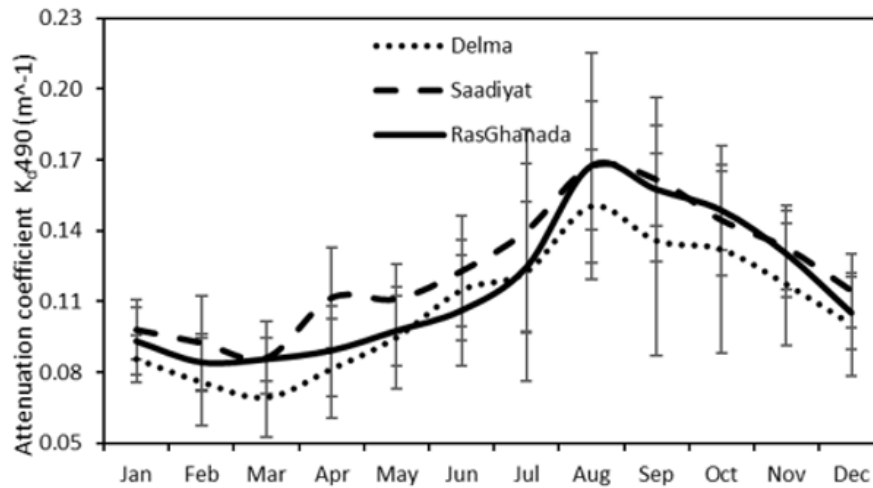


Figure 4.6. Comparing the diffusion attenuation coefficient (K_{d490}) climatology obtained by MODIS-Aqua in Delma, Saadiyat and Ras Ghanada. Symbols show average values during 1997-2015, error bars display standard deviation.

4.3.2.3 Sea surface temperature (SST)

The seasonal variability of SST is characterized by a distinct seasonal cycle with minimum SST in winter and maximum in summer (Figure 4.7), with no significant difference between the sites, $F(2, 657) = 0.459$, $p = 0.632$. However, Delma site is slightly cooler in winter (17.6 °C) and warmer in summer, reaching 36 °C, with a higher SST range (18.4 degrees) than Saadiyat (17 degrees) and Ras Ghanada (16.2 degrees). The summer-winter differences, as seen in Abu Dhabi are remarkably high, and much greater than the Red Sea area, which has a range of 12.5 °C in the northern and only 8°C in the central Red Sea (Sheppard, 1993).

SST has a moderate positive correlation with chl-*a* (Delma=38%, Saadiyat=45%, and Ras Ghanada=39%) and K_{d490} (Delma=42%, Saadiyat=52%, and Ras Ghanada=55%) in all sites (Table 4.4). The cross-correlation analysis in table 4.7 also shows that a lag time of only one month exists between SST and chl-*a* with a *r* value between 60% to 75% in all study sites. These correlation results may indicate an association between phytoplankton

and water temperature in this region, and this association occurs within one-month period. This idea is supported by the fact that certain cellular processes in phytoplankton are temperature dependent, and their biological rates accelerate exponentially with the increase in temperature (Reynolds, 1984). For example, the bloom-forming cyanobacteria *Oscillatoria* sp., dominating most of the algal blooms around Abu Dhabi coastal, was also reported during extreme summer temperature event (EAD, 2015). This species is known for its wide range of temperature adaptability and achieves maximum growth rates at temperatures of 35-40°C (Miami et al., 1983; Robarts and Zohary, 1987).

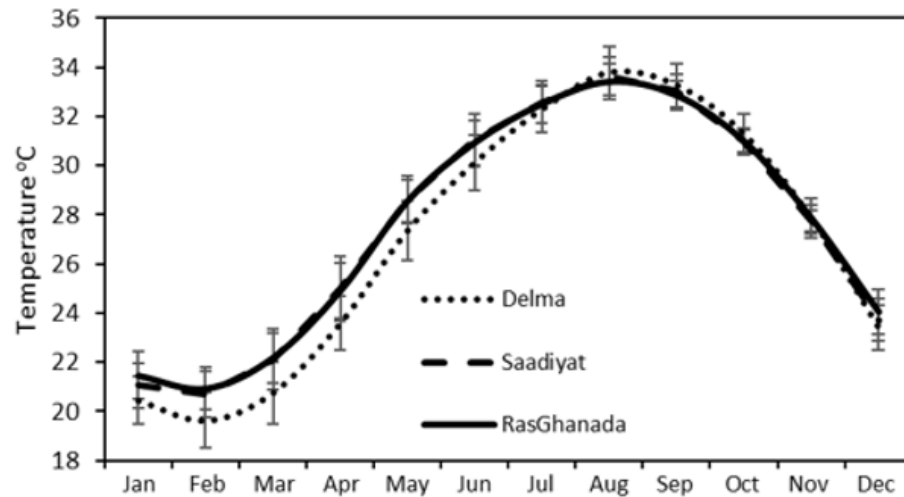


Figure 4.7. Comparing the sea surface temperature (SST) climatology obtained by MODIS-Aqua in Delma, Saadiyat and Ras Ghanada. Symbols show average values during 1997-2015, error bars display standard deviation.

Table 4.4. Pearson correlation between the remote sensed parameter in Delma, Saadiyat and Ras Ghanada

	Delma					Saadiyat					RasGhanada				
	Chl-a	SST	WCS	AOT	K _d 490	Chl-a	SST	WCS	AOT	K _d 490	Chl-a	SST	WCS	AOT	K _d 490
Chl-a	100%	38%	0%	20%	57%	100%	45%	1%	6%	64%	100%	39%	-1%	3%	60%
SST	38%	100%	2%	10%	42%	45%	100%	17%	37%	52%	39%	100%	-5%	40%	55%
WCS	0%	2%	100%	-21%	15%	1%	17%	100%	-3%	17%	-1%	-5%	100%	-3%	0%
AOT	20%	10%	-21%	100%	-6%	6%	37%	-3%	100%	10%	3%	40%	-3%	100%	14%
K_d490	57%	42%	15%	-6%	100%	64%	52%	17%	10%	100%	60%	55%	0%	14%	100%

Table 4.5. Pearson correlation between the meteorological data from Abu Dhabi airport

Meteorological data correlation (Abu Dhabi Airport)				
	Air Temp	Visibility	Wind Spd.	Precipitation
Air Temp	100%	-38%	51%	-49%
Visibility	-38%	100%	-32%	20%
Wind Spd.	51%	-32%	100%	-1%
Precipitation	-49%	20%	-1%	100%

Table 4.6. Pearson correlation between the meteorological data and the environmental parameters obtained by remote sensing in Delma, Saadiyat and Ras Ghanada.

Delma					Saadiyat				RasGhanada			
	Air	Visib.	WS	Precip.	Air Temp.	Visib.	WS	Precip.	Air Temp.	Visib.	WS	Precip.
Chl-a	28%	1%	-19%	-23%	46%	-9%	8%	-21%	41%	-4%	4%	-22%
SST	96%	-27%	44%	-47%	97%	-28%	51%	-46%	97%	-27%	50%	-46%
WCS	-2%	4%	12%	1%	15%	12%	13%	2%	15%	12%	13%	2%
AOT	14%	-32%	35%	3%	40%	-40%	44%	-5%	40%	-40%	44%	-5%
K490	35%	-8%	0%	-20%	54%	-7%	5%	-29%	51%	-6%	1%	-34%

Table 4.7. Cross-correlation analysis between of the environmental parameter against the chl-a in all study sites. R is the correlation coefficient.

VARIABLE	DELMA		SAADIYAT		RAS GHANADA	
	Lag	R	Lag	R	Lag	R
SST	1	75%	1	70%	1	60%
TURBIDITY (K_D490)	0	60%	0	65%	0	60%
AEROSOL (AOT)	5	30%	2	45%	2	45%
WIND (WS)	2	-56%	2	-46%	2	-45%
WATER CURRENT	1	10%	1	25%	1	15%

4.3.2.4 Water current speed (WCS)

The seasonal cycle of water current speed (WCS) was different among the sites (Figure 4.8). As mentioned in the methodology, because of the low resolution acquired ($1^{\circ} \times 1^{\circ}$) from the source, the analysis were divided into two areas (Area 1= Delma (western Abu Dhabi), and Area 2= Saadiyat/Ras Ghanada (eastern Abu Dhabi)). Overall, the water flow along Abu Dhabi's coastal area is characterized by moderate currents at a magnitude of 0.5 m/s with different directions (Bots, 2013). The result of this study, however, shows

much less current speed values (Figure 4.8), which may be related to the low acquired resolution that averages the entire selected regions. Moreover, there was a significant difference in the WCS between area 1 (Delma) and area 2 (Saadiyat/Ras Ghanada), $F(2, 621) = 17.630$, $p < 0.001$. Delma ($M = 0.10$, $SD = 0.03$), Saadiyat/Ras Ghanada ($M = 0.12$, $SD = 0.03$). Tukey *post hoc* analysis showed that Saadiyat/Ras Ghanada have a significantly greater average speed than Delma (-0.02 , 95% CI $[-0.02, -0.01]$, $p < 0.001$). The overall highest peak was seen in June, and another similar increase was observed in January followed by a decreasing slope reaching the minimum in April/May. In Delma, the overall fluctuations were different yet slightly lower. It shows that the maximum peak is seen in January and the minima were during March and May.

A weak, but significant, positive relationship was observed between WCS and turbidity (K_d490) in Delma (15%) and Saadiyat (17%) (Table 4.4), which might be due to the relationship between water mixing and currents (Krissek, 1993). Furthermore, the WCS has a significantly lower positive correlation coefficient ($r=17\%$) with the SST only in Saadiyat. This relationship may not be directly related to temperature, since the main water current drivers in the Gulf are a combination of wind stress, tides, surface buoyancy fluxes, freshwater runoff and water exchange through the Strait of (Hormuz Reynolds, 1993; Thoppil and Hogan, 2010a), which will be discussed later in this chapter. The WCS did not show any relationship with the chl-*a*, even at the coastal study sites (Saadiyat and Ras Ghanada), where the water stream proved to be faster and good mixing can be expected. The cross-correlation analysis (Table 4.7), in the other hand, a one month time-lag between water currents and the chl-*a*, with an increased correlation coefficient toward the coastal areas (Delma= 10%, Saadiyat=25% and Ras Ganada= 20%). This indicate that the increase

of phytoplankton (chl-*a*) could be related to an increase in water currents/mixing within one-month period.

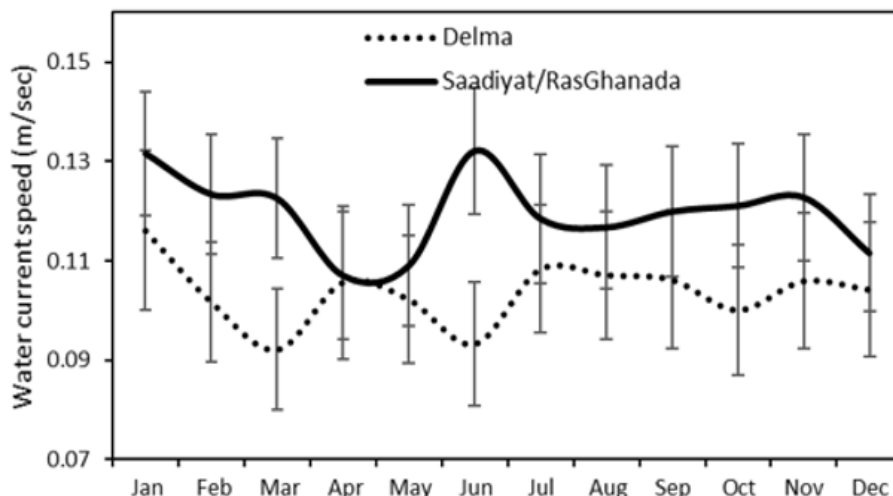


Figure 4.8. Comparing the climatology of water current speed obtained by OSCAR in Delma area and Saadiyat/Ras Ghanada area. Symbols show average values during 1992-2014, error bars display standard deviation.

4.3.2.5 Aerosol optical thickness (AOT)

Similar to the WCS, we divided the study regions to analyse the AOT that is obtained with low resolution $1^{\circ} \times 1^{\circ}$. The seasonal cycle of AOT was almost equal in all sites (Figure 4.9), and it did not show any significant difference between regions, $F(2, 657) = 2.460$, $p = 0.086$. Delma ($M = 0.46$, $SD = 0.02$), and Saadiyat/Ras Ghanada ($M = 0.44$, $SD = 0.02$) show an annual AOT maximum in July, followed by a steady declining slope reaching the minimum seasonal value in winter (November-January) in both locations (Figure 4.9). These results are consistent with the higher frequency (15-20 dust storms) of dust storms during spring and summer months in the Arabian Gulf (Husar et al., 1997; Kutiel and Furman, 2003). Dust is known to have a cooling effect on the earth surface through blocking solar radiation, which has been referred to as the “solar dimming” effect

(Stanhill and Cohen, 2001; Al-Ghadban and El-Sammak, 2005). However, the findings here suggests that period of frequent dust events coincides with significant heating months in the region (Figure 4.7 & 4.9). This may explain the positive correlations between dust (AOT) and SST, specifically at Saadiyat and Ras Ghanada ($r=37\%$ and $r=40\%$, respectively).

The overall seasonal cycle of dust (AOT) is relatively similar to that of *chl-a* (Figure 4.9 & 4.5). The maximum annual peak for AOT was in July-August, whereas that of *chl-a* was in August-September, which is reflected in the significant positive correlation at Delma site ($r=20\%$) (Table 4.4). Moreover, cross-correlation results in table 4.7 also shows that there was a two-month lag between AOT and *chl-a*, indicating that dust input may trigger the development of algal blooms within a two months period. These results would support John Martin (1990) hypothesis, which suggested that aeolian dust transport is a major ocean fertilization process. The estimated sediment deposition in the Arabian Gulf during sandstorm events is around 60 to 200 x 10⁶ tons/year (Riegl and Purkis, 2012b).

The chemical composition of dust depends on the origin. The Gulf is located between the latitudes 24-30°N (Reynolds, 1993), and this vast arid land surrounding the Arabian Gulf (southern Iraq, Iran and the eastern Arabian Peninsula) is one of the primary sources of aeolian dust in the world (Husar et al., 1997). Hamza et al. (2011), showed that silica and calcium were the major chemical elements of dust storms in the UAE coastal areas, accounting for a combined 60–80%. The author also shows a high percentage of iron (2-18%), aluminum (2-8%), magnesium (2-10%), and sulphur (0.5-7%). These elements are essential nutrients for phytoplankton growth and activity in the marine environment if they exist in a soluble form (Graedel et al. 1986; Duce and Tindale 1991; Young et al.,

1991; Garrison et al., 2003). Most of these elements are important to marine life overall, but iron is essential for all life on earth and is particularly important for oceanic plant nutrition because atmospheric nitrogen cannot be fixed, nor can *chl-a* be synthesized, or nitrate be reduced without it (Jickells, 1999). The solubility of iron compounds and other trace metals in the marine environment is known to be dependent on the sediments acidity, in that the binding capacity of sediments decreases at acidic pH allowing mineral dissolution (Parekh et al., 2004; Jickells et al., 2005). Both rainwater and photochemical reactions have the potential to be of great importance in dissolving elements carried by dust storms over the Arabian Gulf. Rain water in the Gulf area is scarce, however, as a consequence of intensive sulfur rich oil production, mixing with high sulphur concentrations in the atmosphere may make the rain water acidic enough to dissolve other minerals such as iron (Walker and Brimblecombe, 1985). On the other hand, light intensity in the Arabian Peninsula is high enough to promote photochemical processes at the sea surface micro-layer (Sayadam and Senyuva, 2002; Almazroui et al., 2012).

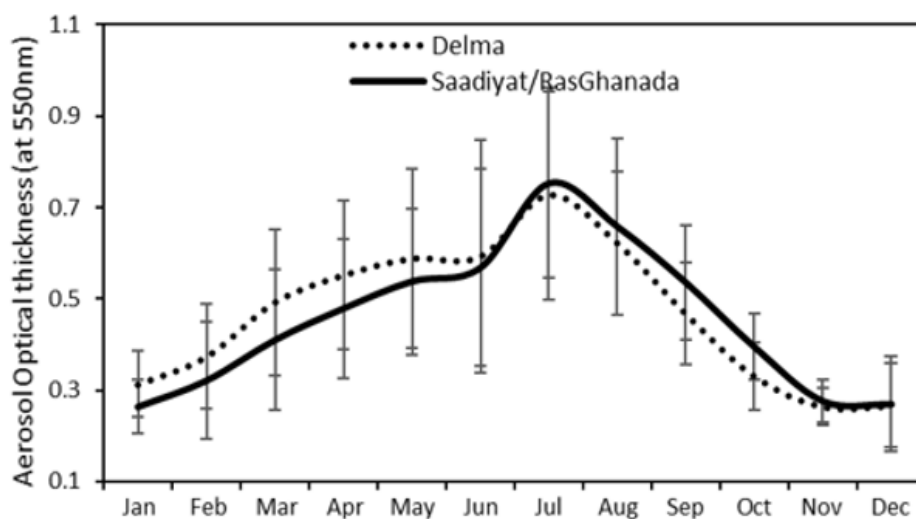


Figure 4.9. Comparing the climatology of Aerosol optical thickness in Delma and area, Saadiyat/ Ras Ghanada area. Symbols show average values during 1997-2015, error bars display standard deviation.

In contrast, not all aeolian dust is beneficial to the marine environment. Anthropogenic pollutants, synthetic chemicals, pathogenic microorganisms, and other toxic constituents are likely to be picked up through dust storms and deposited in the oceans (Shinn et al., 2000) and Garrison et al. (2003). Pathogenic microorganisms can be related to the outbreak of known coral disease. (Smith et al., 1996; Richardson, 1997; Richardson, 1998; Kushmaro et al., 2001; Patterson et al., 2002; Riegl, 2002; Weir-Brush et al., 2004).

In the Arabian Gulf, coral diseases are seasonal, with a higher frequency in the summer months (Riegl et al., 2012; Riegl and Purkis, 2015b). Outbreaks have been detected before mass mortality, such as in the 1996-1998 (Riegl, 2002), or after a bleaching event, for example in 2010, 2011 and 2012 (Riegl and Purkis, 2015a). It might be possible that this seasonality could be linked to the annual maximum of AOT in the region.

The AOT table 4.4, shows a weak, but significant, positive correlation with turbidity (K_d490). This association may be attributed to the dust-inputs in the region that increase light attenuation in the water column. Dust inputs in the Arabian Gulf range between $60\text{--}200 \times 10^6$ tons a year, which is considered high compared to the other area of the world (Sheppard et al., 2010b).

4.3.2.6 Air temperature

The overall air temperature climatology was very similar in different regions around the Arabian Gulf, showing a temperature increase from late February, reaching a maximum value in August, followed by a gradual decline from September to January (Figure 4.10). Kuwait reported the highest air temperature among the airports, and its seasonal maximum was reached in July, which can be due to the shift of the Subtropical Jet Stream northward and the buildup of the ridge of high pressure at the 500 hPa level

(Nasrallah et al., 2004). Abu Dhabi Airports follows the same temporal pattern. The lowest summer average among the locations was measured at Bahrain Airport.

There was a robust resemblance between air temperature and SST seasonal cycles seen in both Figure 4.7 & 4.10. This was reflected in the strong positive relationship between air temperature and SST in all sites (Delma=96%, Saadiyat=97%, and Ras Ghanada=97%) (Table 4.6), indicating that the long-term SST in Abu Dhabi is primarily driven by the surrounding air temperature. Thus, air temperature is considered an important regional driver for the seawater temperature in the area. Due to the strong correlation of these two environmental parameters air temperature shows a comparable positive relationship with chl-*a*, dust (AOT) and turbidity (K_d490) in all study sites.

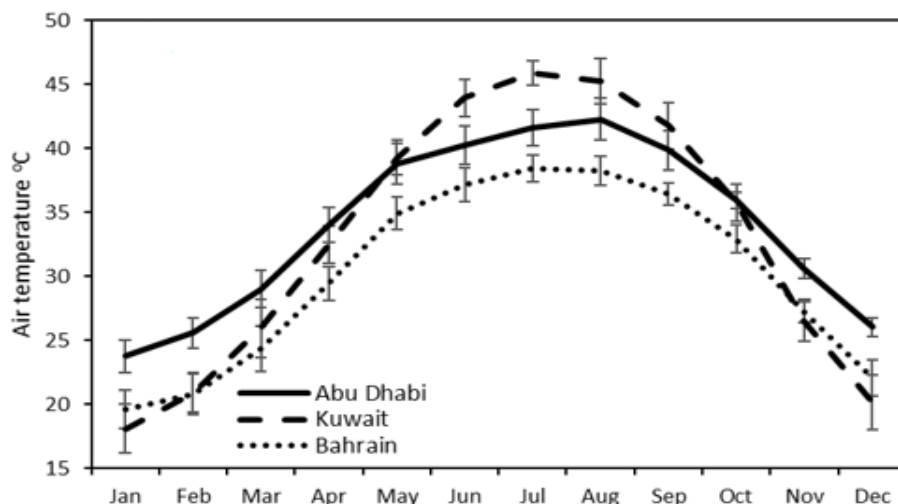


Figure 4.10. Comparing air temperature climatology from Abu Dhabi, Kuwait and Bahrain airports. Symbols show average values during 1983-2015, error bars display standard deviation.

4.3.2.7 Horizontal visibility

The horizontal visibility around the Gulf has a seasonal summer minimum around July and a winter maximum, mostly during November-January (Figure 4.11). This result is likely to be related to the dust climatology (AOT) pattern in the region. In other words, high aerosol content (AOT) in the atmosphere during the summer months (Figure 4.9) is possibly associated with low visibility during the same period in Abu Dhabi (Figure 4.11). The correlation between visibility and AOT (Table 4.6), shows a significant negative correlation in both regions (Delma= -32%, Saadiyat/Ras Ghanada= -40%). The atmospheric impairment in visibility is caused by dust was also reported by McTainsh, (1980); Kavouras et al., (2009) and Esmail et al. (2016). The pattern of visibility in Abu Dhabi and Bahrain is approximately similar. In contrast, Kuwait has slightly shifted visibility minimum (Figure 4.11) that is seen during June.

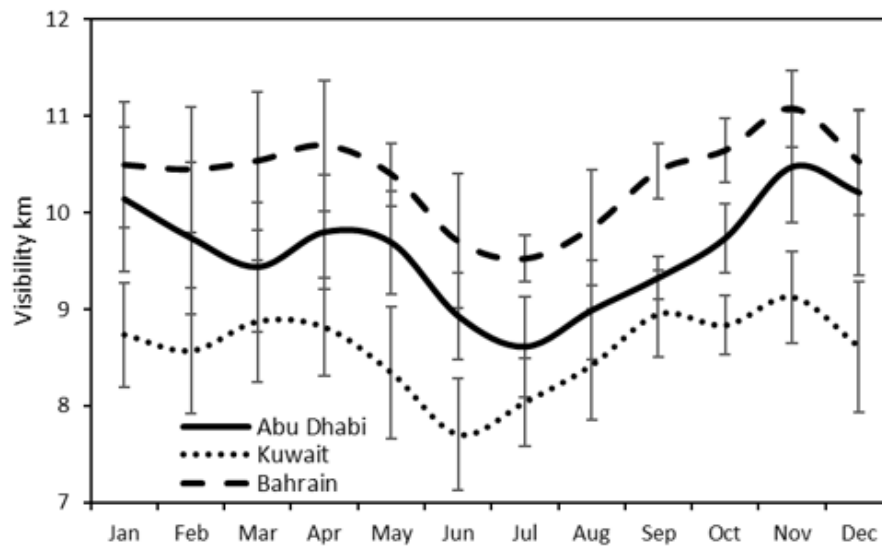


Figure 4.11. Comparing horizontal visibility climatology from Abu Dhabi, Kuwait and Bahrain airports. Symbols show average values during 1983-2015, error bars display standard deviation.

4.3.2.8 Wind speed and direction

The best documented weather phenomenon in the Arabian Gulf is the “Shamal” (Perrone, 1979; Reynolds, 1993; Thoppil and Hogan, 2010a; Riegl and Purkis, 2012a; Apel et al., 2015), which brings some of the strongest winds to the region. This wind is formed because of the orographic control surrounding the Gulf. The Taurus and Pontic mountains of Turkey, the Caucasus mountains of Iran, and the Hejaz mountains of the Arabian Peninsula together with the Tigris-Euphrates Valley (Perrone, 1979). It forms a northwest-southeast axis that strongly influences the tracks of extra-tropical storms to a southeasterly direction (Reynolds, 1993). The wind speed (WS) climatology (Figure 4.12) shows a slight difference between the selected northern (Kuwait and Bahrain) and the Southern (Abu Dhabi) region of the Arabian Gulf. Kuwait and Bahrain had a pronounced maximum peak in June and minimum values during the November-January period. The highest peak in Wind speed of those northern part of the Gulf may be related to the summer Shamal, which starts from early June through July from the northern Arabian Gulf towered the southern regions (Reynolds, 1993).

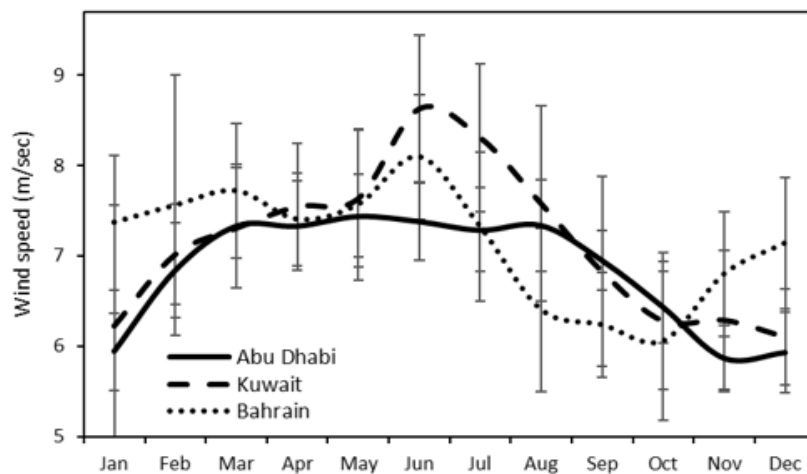


Figure 4.12. Comparing wind speed climatology from Abu Dhabi, Kuwait and Bahrain airports. Symbols show average values during 1983-2014, error bars display standard deviation.

Abu Dhabi WS seasonality was characterised by an extended period of high winds throughout February-August period, which is likely related to both summer and winter Shamal's. The wind speed is slightly reduced from February to August, indicating that the winter Shamal is slightly stronger than the summer Shamal. According to Thoppil and Hogan (2010b) the Shamal winds are predominant throughout the year, and are slightly stronger in winter (November-February) ($\sim 5 \text{ m/s}^{-1}$) than in summer (June-September) ($\sim 3 \text{ m/s}^{-1}$). The wind speed then declines sharply from late August to reach its lowest values in November-January each year

Furthermore, an inverse relationship was observed between seasonal wind speed (Figure 4.12) and visibility (Figure 4.11) with higher wind speeds coinciding with a lower visibility during in all seasons of the year. Additionally, wind speed shows a significant negative correlation with visibility (-32%) and a significant positive relationship with dust (AOT) (Delma=35% Saadiyat/Ras Ghanada=44%). Therefore, the increase in wind speed can be related to the increase in dust (AOT). Figure 4.11 shows that Kuwait has its lowest visibility values in June. This was clearly explained by the wind speed climatology, in figure 4.12, indicating that this reduction in visibility can be related to the strong winds observed in June in Kuwait. The cross-correlation analysis shows a negative cross-correlation coefficient between wind and dust with a two-months' time-lag in all study site sites. This indicate that a low wind speed in correlated with a high chl-*a*/phytoplankton production within two-months period.

The findings suggests that the seasonal wind direction in Abu Dhabi (Figure 4.13), is characterised by southwestern winds during winter and early summer seasons (January-July), and northeastern winds during late summer (August-October). The latter, which

blows from the human-impacted land towards the water, may increase dust particle, thereby introducing additional nutrients in coastal waters and stimulating phytoplankton growth during summer (Singh et al., 2008). In addition, anthropogenically-derived, absorbing aerosols in the atmosphere increase during summer. These originate particularly from industrial facilities along Abu Dhabi coastal area, such as power generation, iron and steel works, which are found within the Industrial Cities Abu Dhabi (ICADs), Mussafah Industrial Area, Khalifa Industrial Zone Abu Dhabi (KIZAD). Thus, increasing these absorbing aerosols frequency during summer (July-September).

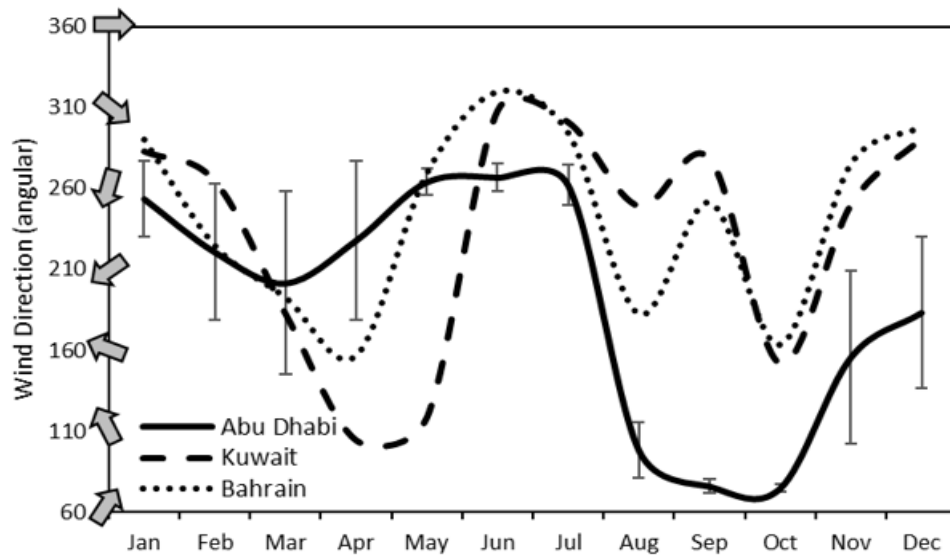


Figure 4.12. Comparing wind speed climatology from Abu Dhabi, Kuwait and Bahrain airports. Symbols show average values during 1983-2014, error bars display standard deviation.

4.3.2.9 Precipitation

The seasonal precipitation patterns, depicted in figure 4.14, show that, in all region, the minimum average rainfall per day is recorded during the summer months, between June-September, whereas highest peaks are seen in the winter, from November to April. These patterns are in agreement with previous reports for this area (Reynolds, 1993; Riegl and Purkis, 2012a). The vegetation-free lands that are caused by insufficient rainfall in summer will leave the sand particles unstabilised. Consequently, these particles will be easily picked up by the accelerated summer winds and blown into the atmosphere, creating dust storms that account for the general reduction in the visibility in various regions of the Gulf (Figure 4.12 & 4.14). This provides a putative explanation for the positive relationship between precipitation and visibility (20%) (Table 4.5). Precipitation has a significant negative correlation coefficient with air temperature (-49%), which is possibly reflecting the inverse seasonality patterns of both variables in the region, as the higher rainfall frequency coincided with lower air temperature and vice versa.

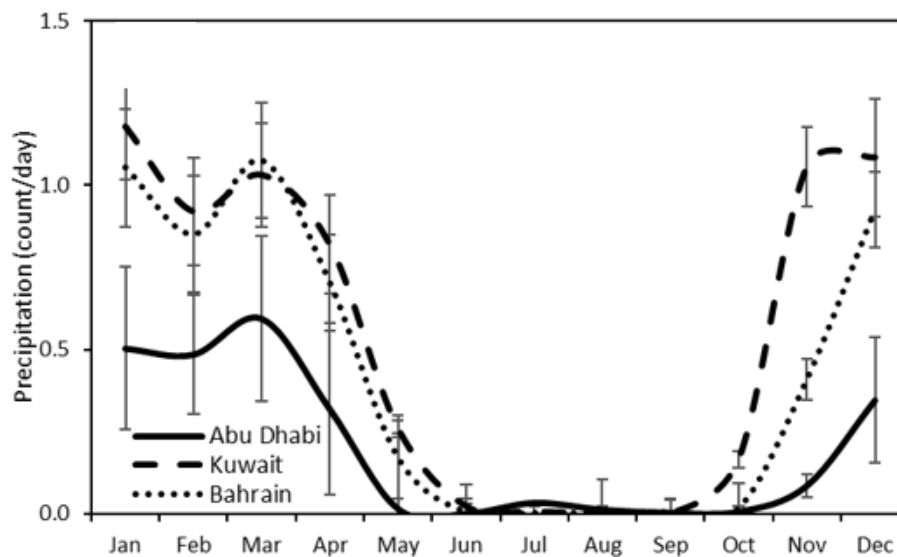


Figure 4.14. Comparing precipitation climatology from Abu Dhabi, Kuwait and Bahrain airports. Symbols show average values during 1983-2015, error bars display standard deviation.

4.3.3 Interannual anomalies

At the interannual scale, all parameters anomalies have been derived from their monthly average. They show a strong seasonal cycle with year-to-year variability during the 18 year period of the remote sensing data, in addition to 32 years of meteorological data. There were five major bleaching events recorded during that period (1998, 2002, 2010, 2011 and 2012), which are highlighted in red lines across all interannual anomalies in Figure 4.7-4.11). Based on the coral bleaching events at all the sites, the long-term interannual anomalies of the environmental data were divided into three transitions periods. The first period from 1996 to 2002, was characterised by an overall dominance of SST anomalies coinciding with three major bleaching events (1996, 1998 and 2002). The first two abnormal heating periods are strongly linked to El Niño events (Figure 4.19), which caused an overall increase in the air and water temperatures (Figure 4.15, 4.16, 4.17, 4.18 & 4.19).

Two major Gulf wide bleaching events during the summers of 1996 and 1998, were reported (Wilkinson, 1998; Wilkinson, 1999; Goreau et al., 2000; Sheppard and Loughland, 2002; Bernhard M Riegl and Purkis, 2012b; Riegl and Purkis, 2015a). Temperatures $>2^{\circ}\text{C}$ above the seasonal average were detected during August/September 1996 and 1998 in all sites. During 1996, about 95% of *Acropora* community bleached at Abu Dhabi and Dubai, mainly between Jebel Ali and Ras Hasyan, and over 90% of this taxon also bleached along the Bahraini and Saudi Arabia coastlines (Wilkinson, 1998b). This event resulted in a drop in the total number of coral species, (from 34 to 27) and the percentage of cover (from 90% to about 26%, Riegl, 1999; Riegl, 2002).

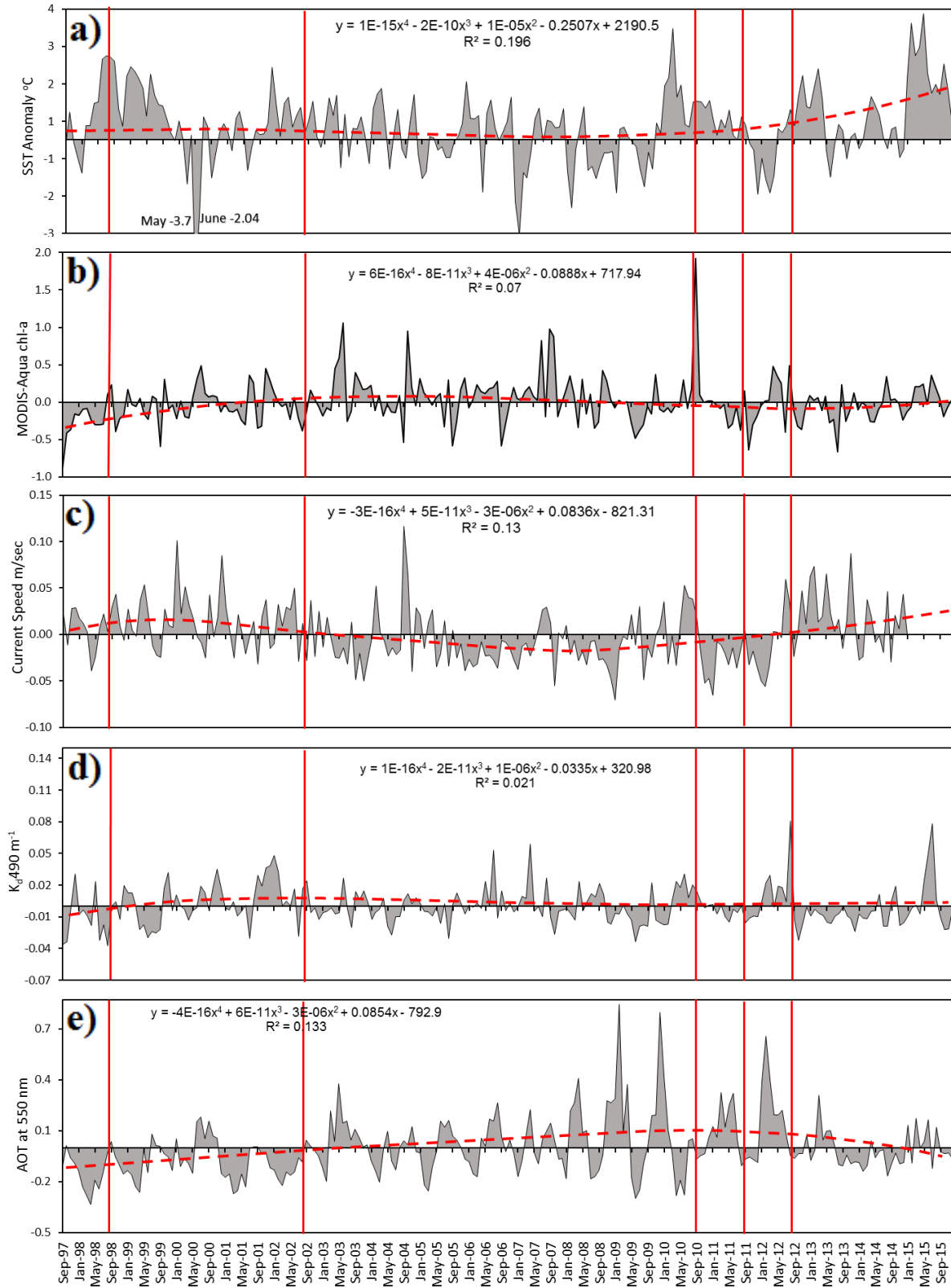


Figure 4.15. Long-term anomalies of environmental parameters in Delma site, calculated from remote sensing data. Including a) temperature, b) chl-a, c) water current speed, d) attenuation coefficient (K_d490), and f) aerosol optical thickness (AOT). The vertical red lines indicate the bleaching events, the broken line curves display a fourth order polynomial trend. The equations and R^2 values of the regression curves obtained are shown in each graph.

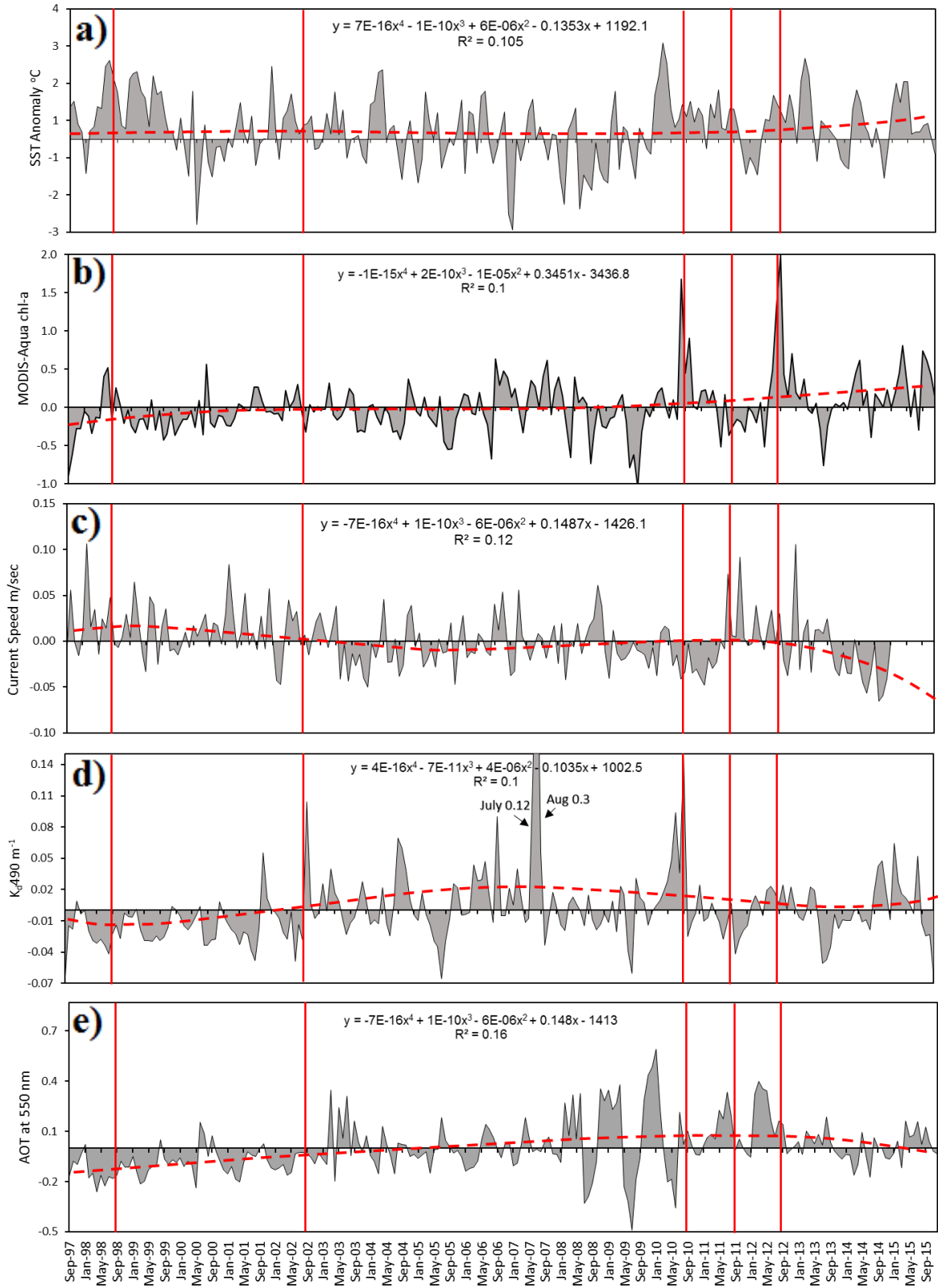


Figure 4.16. Long-term anomalies of environmental parameters in Saadiyat site, calculated from remote sensing data. Including a) temperature, b) chl-a, c) water current speed, d) attenuation coefficient (K_d490), and f) aerosol optical thickness (AOT). The vertical red lines indicate the bleaching events, the broken line curves display a fourth order polynomial trend. The equations and R^2 values of the regression curves obtained are shown in each graph.

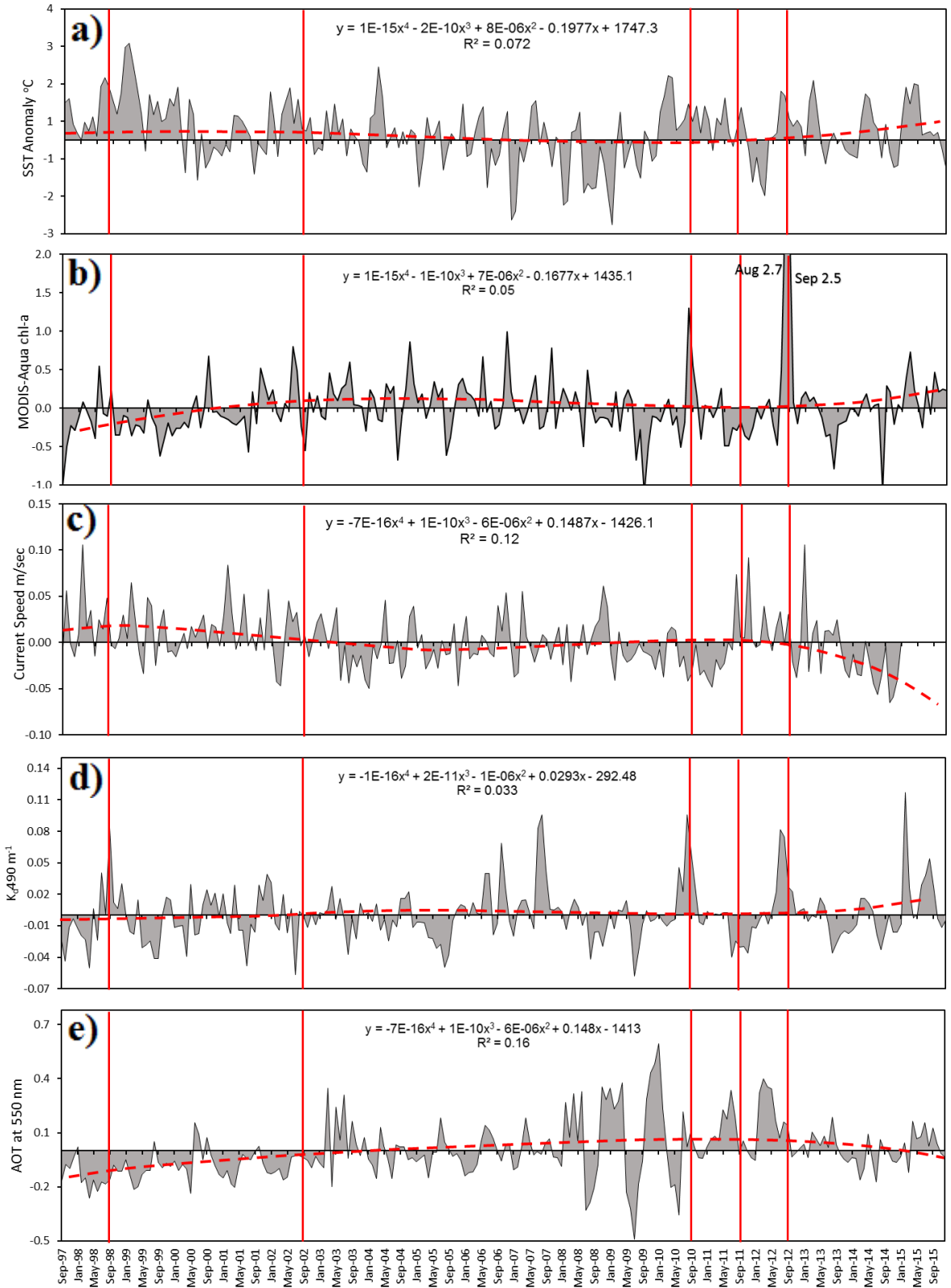


Figure 4.17. Long-term anomalies of environmental parameters in Ras Ghanada site, calculated from remote sensing data. Including a) temperature, b) chl-a, c) water current speed, d) attenuation coefficient (K_{490}), and f) aerosol optical thickness (AOT). The vertical red lines indicate the bleaching events, the broken line curves display a fourth order polynomial trend. The equations and R^2 values of the regression curves obtained are shown in each graph.

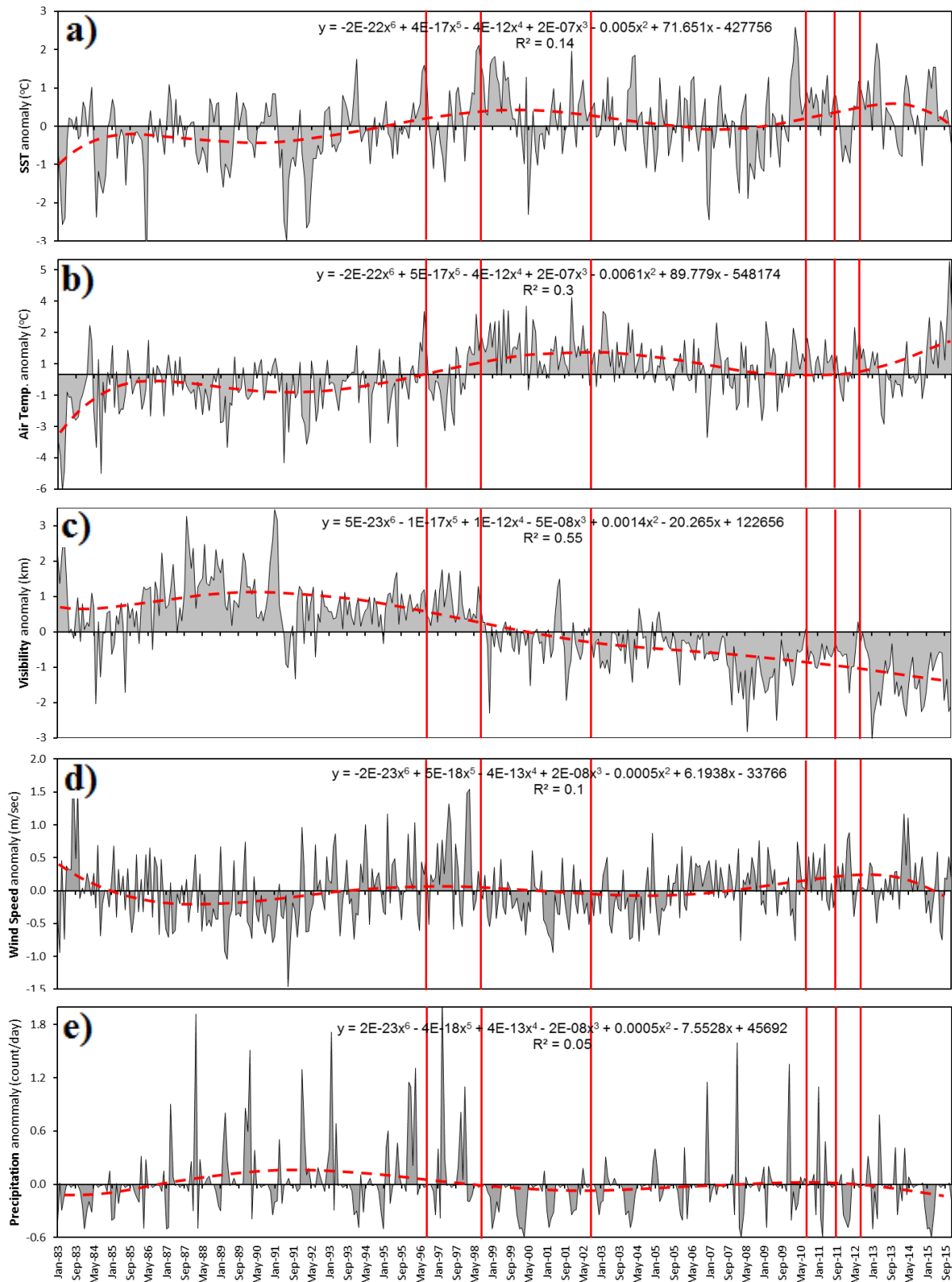


Figure 4.18. Long-term meteorological anomalies in Abu Dhabi a) SST values calculated by remote sensing analysis at Saadiyat site, b) air temperature, c) visibility, d) wind speed, and e) precipitation. The vertical red lines indicate the bleaching events, the broken line curves display a fourth order polynomial trend. The equations and R^2 values of the regression curves obtained are shown in each graph.

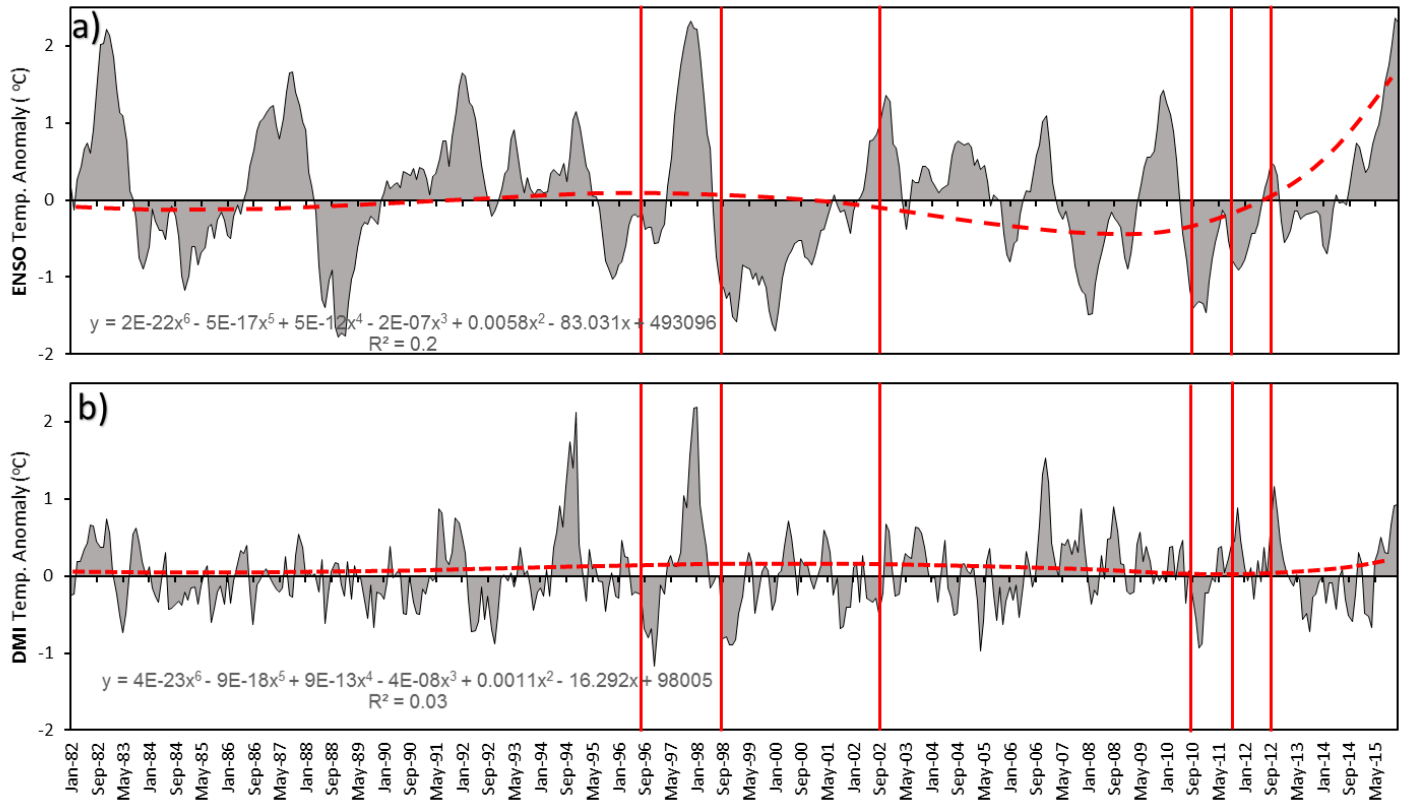


Figure 4.19. Temperature parameters related to the ENSO and Indian ocean dipole anomalies. a) Long term temperature anomalies of El Niño–Southern Oscillation (ENSO) in the Niño 3.4 region (5°N–5°S, 120°–170°W) extracted from the NOAA national weather service (http://www.cpc.ncep.noaa.gov/products/analysis_monitoring/ensostuff/ensoyears). b) Dipole Mode index (DMI), which represents the Indian Ocean Dipole (IOD), extracted from the state of the ocean climate (<http://stateoftheocean.osmc.noaa.gov>).

During 1998, bleaching was even more severe than 1996. According to George and John (2005), water temperature surpassed 34°C for 14 successive weeks in Abu Dhabi and ranging around 36 °C for three weeks. As a consequence, coral cover was further reduced from the remaining 26% to 22%. The EL Niño-La Niña event of 1998 was the largest ever recorded and affected coral reefs worldwide (Figure 4.19) (Wilkinson, 1998; Riegl, 1999; Riegl, 2002; Sheppard and Loughland, 2002).

The third period of anomalously high temperature was throughout the seasons of 2002, as indicated by the SST and air temperature anomalies in Figure 4.18 a & b, and in all the study sites (Figure 4.15a, 4.16a & 4.17a). However, the findings of this study show that the SST and air temperature in this bleaching event were less severe than the previous in 1996 and 1998 El Niño-related events (Figure 4.18 a & b). Temperature of 1°C above the normal monthly average was measured during August in that year, affecting both SST and air temperature (Figure 4.18 a & b). Additionally, positive anomalies in SST and air temperature were seen in the early summer months (May, June, and July) (Figure 4.18 a & b). The highest SST has been observed in May at Saadiyat and Ras Ghanada with 1.2 °C and 1.4 °C above the long-term average, respectively. The maximum air temperature anomalies in Abu Dhabi airport were seen in May (+2.35 °C), June (+1.1 °C), and July (+1.23 °C).

These values slightly deviate from previous studies which have suggested that during the summer of 2002, SST anomalies ranged from +2 to 2.5 °C (Riegl, 2003). However, these high temperatures were recorded mainly in Jebel Ali and Ras Hasyan. This high temperature had only minor effects on the remaining coral communities in the area, including *Acropora* and *Porites*, and mortality was low. In fact, the affected corals had

fully recovered by November of that year (Riegl and Purkis, 2009; Coles and Riegl, 2013). The high survival rate was perhaps possible because these communities had become adapted to the elevated temperatures due to previous exposure to extreme temperature fluctuation in 1996 and 1998 (Riegl, 2002, Coles and Brown, 2003). Alternatively, the moderate severity of the heating event, in addition to the dimming effect of the dust seen from the analysis of the interannual anomalies (Figure 4.18 a, b, c) may have increased resilience. Additionally, Figure 4.18d shows that wind speeds in the period between 1996-2002 were relatively high, with an increased frequency of positive anomalies throughout the relevant time period. These strong winds may explain the similar increase in the water current speed within the same period. This has been argued to be beneficial to coral reefs, through the thinning of boundary layers and acceleration of mass transfer, which in turn supports dissipation of heat and the removal of toxic oxygen radicals (Woesik and Koksai, 2006; Baker et al., 2008b). However, in August 2002 (when bleaching actually occurred), the water current flow was weak. This situation may further increase the probability of bleaching by reducing the ability of corals to remove toxins that could accumulate in the tissue (Baker et al., 2008b).

Furthermore, chl-*a* and turbidity (K_d490) results did not show any prominent peaks during any of the three bleaching events, indicating that phytoplankton/eutrophication did not play a role in these episodes. Accordingly, there were no reports of any algal blooms observed in any of the study sites in this period. It is possible that the increased water currents motion may have played a role in preventing phytoplankton blooms (Woesik and Koksai, 2006; Baker et al., 2008b).

High water motion affects reef corals in various ways. It enhances the circulation caused by waves, tides, and currents. It can modify several environmental factors, such as plankton, dissolved nutrients and gasses, sediment, water clarity, salinity, temperature, all of which influence coral physiology (Jokiel, 1978). It is now clear that high water flow rates reduce bleaching susceptibility in corals. Therefore, abnormally hot and humid summer with very low wind speed and low water flow are the most probable cause of coral mortality (Riegl and Purkis, 2012a) during these years.

The increased wind speed during 1996-1998 (Figure 4.18d) was expected to increase the AOT and in turn reduce the visibility in the region. However, the results for AOT in each site and the horizontal visibility in the area, indicate a dominance of an abnormal clear sky condition throughout this period, which may have increased light stress and the warming of the reef's water during the 1996 and 1998 bleaching events. These unexpected findings may be related to the increased precipitation peaks in this period, which may helped stabilise the loose sand particles in land areas surrounding the study sites and thereby prevented the formation of Aeolian dust.

The second period between 2003-2009, was defined by a significant shift in the visibility from clear weather (positive anomalies) during 1983-1998, to more aerosol-contaminated weather (negative anomalies) (Figure 4.18c). This shift may be caused by the increased wind speed, which coincided with higher recorders of AOT peaks, particularly during the 2004-2009 period (Figure 4.15e, 4.16e & 4.17e). This reduction in visibility, together with increased wind speed and AOT frequency, may explain the overall reduction in the temperature (air and water, Figure 4.18a & b) following the 1996-1998 El Niño event (Figure 4.19) until 2009. This was also reflected by the apparent negative trend

seen in both SST and air temperature on the same time scale (Figure 4.18a & b). The results in this chapter indicates that chl-*a* anomalies, particularly during 2003-2009, show an increase in frequency and magnitude in all sites. Moreover, the long-term anomalies result also shows an increased anomaly rates in the turbidity (k_d490) results during the same period (2003-2009), which may be linked to the phytoplankton abundance in the waters. Another possible explanation for this increase may be attributed to the dust inputs (fertilization load), which possibly triggers phytoplankton growth by the excess nutrient deposition from the land (Hamza et al., 2011).

Furthermore, extreme-temperature-related bleaching events were absent during 2003-2009, which was clearly due to the aforementioned continuous reduction of air and water temperature in that period (Figure 4.18a & b). In fact, species like *Faviids* and *Porites* showed strong signs of recovery between 2002 to 2010 (Riegl and Purkis, 2012a). However, scientific reports have documented two bleaching events that were linked to other environmental factors other than temperature. The first event was caused by a strong harmful algal bloom (HAB) that was sustained from August 2008 to May 2009 (Richlen et al., 2010). Although this bloom caused immense coral damage and fish kills along the UAE and Oman's coastal areas (Richlen et al., 2010), coral bleaching was not witnessed in Abu Dhabi but was mainly observed in the eastern areas of the Gulf, along with the east coast of the UAE to Fujairah and Oman. This was consistent with the chl-*a* maps shown in figure 4.20. The bloom was restricted to the eastern offshore waters of Abu Dhabi, with less impact on the coastal study sites. In contrast, the second bleaching event, during the summer of 2009, also affected Abu Dhabi. This event was driven by diseases, lasted from May to September, and caused an overall coral cover reduction of about 10% (Riegl and

Purkis, 2015a). The meteorological data along with the AOT determined for each site (Delma, Saadiyat, and Ras Ghanada), may help, to some degree, in explaining the reasons behind this event. The results show an abnormal reduction in visibility that continued through 2008-2009 period, which was overlapped with two large and continued peaks of high dust load (AOT) in the sites. Both low visibility and increase AOT anomalies may be linked to the increase in wind speed during the same period (Figure 4.18d). It is reasonable to assume that these unusual dust events may have carried pathogens in the ocean. According to Riegl and Purkis (Riegl and Purkis, 2015a), mortality was mainly caused by white band disease (WBD). The pathogen of this disease was isolated and identified by Denner et al. (2003), as a new genus of gram-negative bacteria, which they considered as one of the dust-associated bacteria. Therefore, dust might have helped to trigger this event (Garrison et al., 2003). The third period of the long-term anomalies can be defined for the period from 2010 to 2015. A close inspection of the interannual anomalies suggests that the weather at this time was extremely stressful to all marine habitats. It was characterised by a positive trend in the air and water temperature (Figure 4.18a and b). Significant chl-*a* anomalies were seen, particularly in the coastal sites (Saadiyat and Ras Ghanada) during August/September in both 2010 and 2012 reaching approximately 2 mg/m³ above average (Figure 4.16b, 4.17b). The phytoplankton bloom (represented by the increase in chl-*a* concentration) that coincided with the 2012 bleaching event was restricted to the coastal areas around the highly urbanised region of Abu Dhabi (Figure 4.21). Delma, situated offshore, was not affected by the bloom and also escaped bleaching. This finding could suggest that the anthropogenic introduction of nutrient might have promoted the development of the phytoplankton bloom and the associated bleaching event

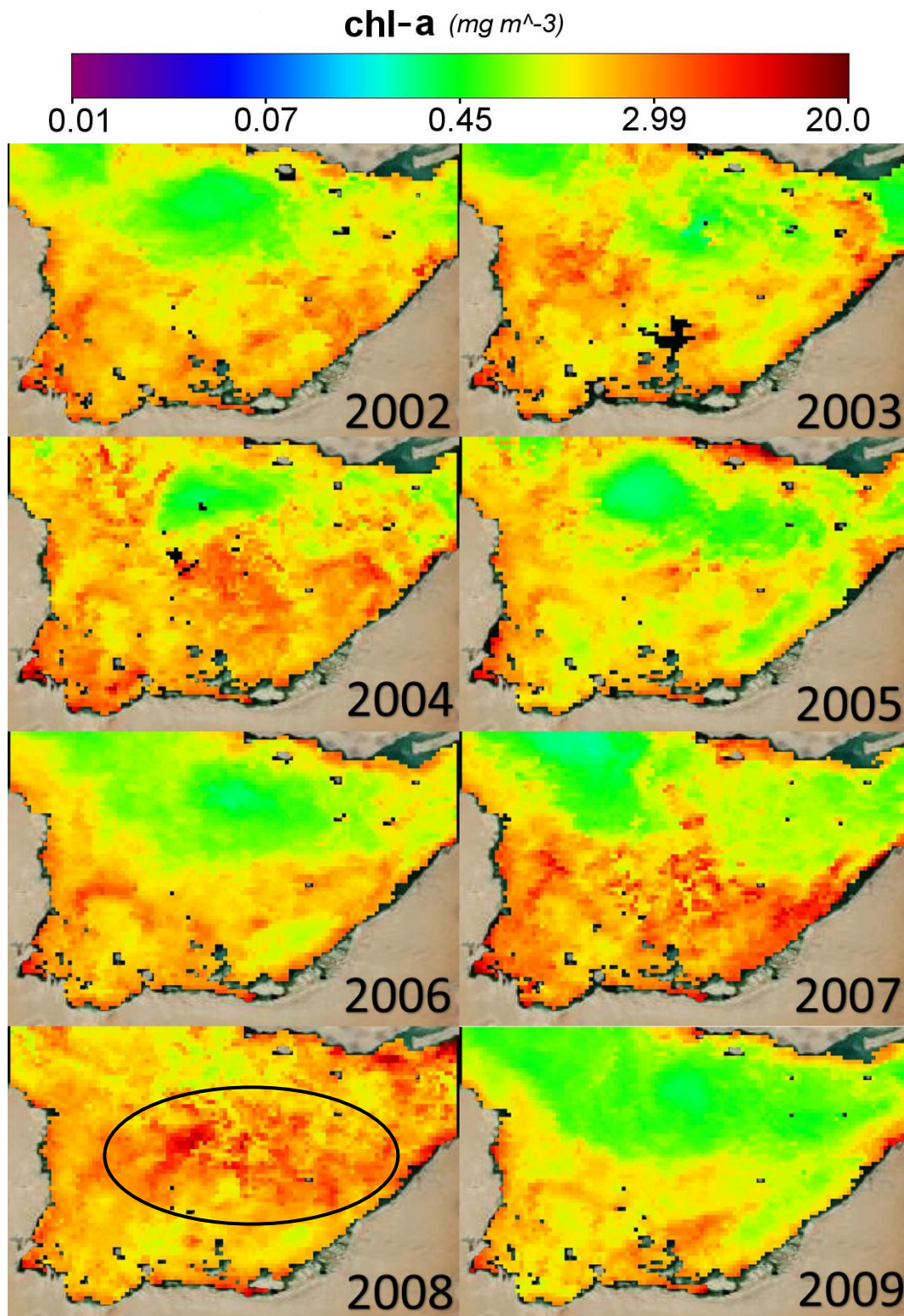


Figure 4.20. Chl-*a* concentration in Abu Dhabi between 2002 and 2009. Averages values were calculated from the data corresponding to the month of September of each year, extracted from MODIS-Aqua level 3 OCI images (4km resolution) from ocean colour web site (www.oceancolor.com). The bar at the top of the figure indicates the minimum and maximum colour scale of chl-*a* concentration. The area where a phytoplankton bloom occurred in 2008 is marked with a black lined oval.

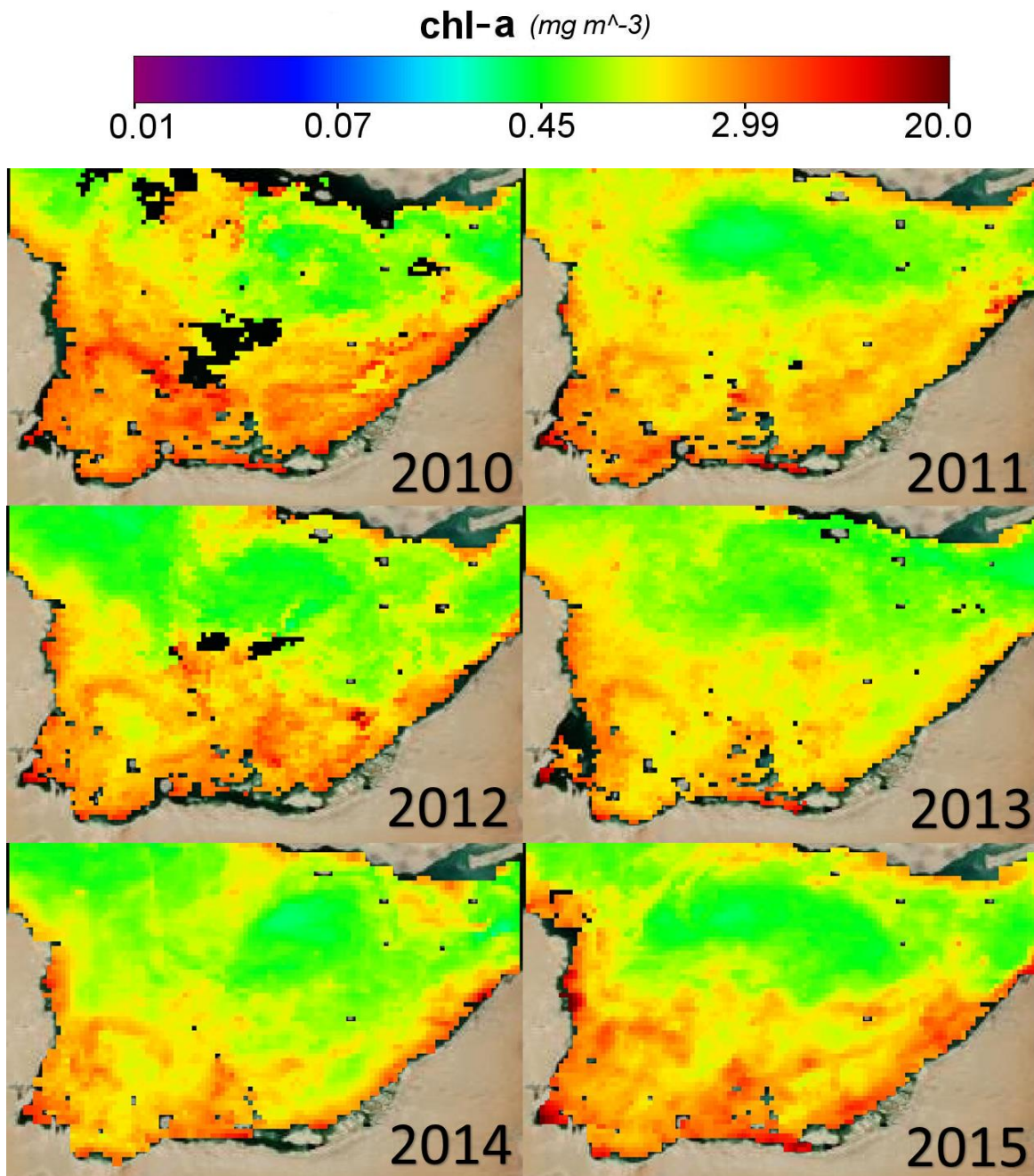


Figure 4.21. Chl-a concentration in Abu Dhabi between 2010 and 2015. Averages values were calculated from the data corresponding to the month of September of each year, extracted from MODIS-Aqua level 3 OCI images (4km resolution) from ocean colour web site (www.oceancolor.com). The bar at the top of the figure indicates the minimum and maximum colour scale of chl-a concentration.

Furthermore, the horizontal visibility in Abu Dhabi continued to deteriorate during 2010-2015 with a clear dominance of negative anomalies and a negative trend throughout the period. This reduction in visibility might have occurred due to the increased frequency of strong winds, showing a positive trend through this period (Figure 4.18d). This stressful environment, prevailing since 2010, may explain three back-to-back bleaching events, which occurred in 2010, 2011 and 2012. These events were thoroughly documented in the literature (Riegl et al., 2011; Bernhard M Riegl and Purkis, 2012b; Riegl et al., 2012; Coles and Riegl, 2013; Riegl and Purkis, 2015a; Shuail et al., 2016b).

The first episode, in the summer of 2010, occurred when the Arabian Gulf was one of the warmest regions in the world's ocean and corals habitats were influenced by prolonged exposure to temperatures between 33°C and 35°C (Riegl et al., 2011). As mentioned in Chapter 3, the thermal threshold in the study sites was exceeded for 25 days in Delma, 24 for Saadiyat and 22 days for Ras Ghanada mostly during August. All of the *Acropora* species were bleached in Abu Dhabi except in Ras Ghanada, where the bleaching was about 60% (Coles and Riegl, 2013). In addition, bleaching in this year was followed by significant mortality even for stress tolerant coral genera, particularly *Favids* (Coles and Riegl, 2013).

Most of the corals were able to recover by the last week of September. The findings indicate that the daily average SST in this year reached maxima of 35.46°C in Delma, 36.12°C in Saadiyat and 35.32°C in Ras Ghanada. Comparable values were reported by Riegl et al. (2012), where the average daily temperatures in Abu Dhabi reached 35.48°C and 35.72°C in August and the monthly mean was 34.44°C in Delma, 34.04 °C in Saadiyat and 33.97 °C in Ras Ghanada. These findings were also consistent with the data obtained

by Riegl et al. (2012), who indicated that the maximum SST was 34.45 °C in Abu Dhabi, which significantly exceeded the thermal tolerance range (25–29°C) for other coral reefs in the world (Buddemeier and Wilkinson, 1994).

Nonetheless, in the summer of 2010 chl-*a* shows some considerable peaks, specifically during August/September (Anomalies in Delma= 2mg/m³, Saadiyat= 1.7mg/m³, and Ras Ghanada 1.3mg/m³). These positive peaks coincided with a similar increase in the light diffusion attenuation (K_d490) seen, in particular, at Saadiyat and Ras Ghanada (Figure 4.15d, 4.16d, 4.17d). This increase in chl-*a* and water turbidity can be attributed to the apparent increase of aeolian dust deposition during this period. Figure 4.7e, 4.8e, 4.9e, show the higher positive anomalies of AOT during summer 2010, that were also confirmed by the negative anomalies in the meteorological visibility illustrated in Figure 4.1c. These changes in the environment during 2010, including extreme water temperature (>36°C), phytoplankton growth, and increased dust deposition, might have affected not only the corals susceptibility to bleaching but also their health by reducing its resistance to infections (Rosenberg and Ben-Haim, 2002; Riegl et al., 2012). After the 2009 WBD mortality event in Abu Dhabi, the frequency of coral diseases had increased (Riegl and Purkis, 2015a). In the aftermath of the 2010 bleaching event, the same disease (WBD) was found again among corals in the UAE (Riegl et al. 2012). Above 30% of all corals in Abu Dhabi were found to show WBD symptoms (Riegl et al., 2012). Also, the mortality of *Acropora* sp. from coral diseases ranged from 50 to 90% (Coles and Riegl, 2013).

Moreover, the environmental conditions in the region has continued to deteriorate since the 2010 event. One year later, in summer 2011, another abnormal increase in the SST during August/September was detected, (Figure 4.15a, 4.16a, 4.17a) (1°C above

average). These summer peaks coincided with a bleaching event (Riegl and Purkis, 2012b; Riegl and Purkis, 2015b) and with a positive anomaly in air temperature corresponding to an abnormally warm year. Horizontal visibility was also low, which is indicated by the continuous negative anomalies seen in Figure 4.18c. In comparison to 2010, chl-*a* peaks were absent in 2011, which may suggest that phytoplankton had a negligible effect on the coral environment in this year. The mortality in this year was similar to 2010, caused by bleaching and subsequent disease. The disease outbreak (black-band disease (BBD)) resulted in a significant reduction in all species particularly in eastern Abu Dhabi areas (Coles and Riegl, 2013; Riegl and Purkis, 2015b).

In the following year 2012, a third consecutive bleaching event was recorded in Abu Dhabi. A large positive anomaly peaks in SST (Delma=0.82°C, Saadiyat=0.92, and Ras Ghanada=1.2 °C), and air temperature (1.2 °C) during August of that year, compared to summer 2011 (Figure 4.18a & b). Coral decline recorded by Riegl and Purkis, (2015b) was 15%, but the coral cover was already low as a result of the bleaching episodes in 2009, 2010, and 2011 (Chapter 2 of this thesis, Shuail et al. (2016)). Bleaching affected >40% of corals in Saadiyat and Ras Ghanada, and 15% in Delma. Increased water temperatures, in summer 2012 (Figure 4.15b, 4.16b, and 4.17b), overlapped with the largest chl-*a* anomalies seen in the entire time series (~2-2.7mg/m³), particularly in the coastal sites (Saadiyat and Ras Ghanada) (Figure 4.21). This may indicate an earlier nutrient enrichment to the water body. The effects of nutrient enrichment and eutrophication beyond certain limits can influence the physiological performance of the coral individual and ecosystem functioning (Cooper et al., 2008). Nutrient enrichment can also contribute to the spread and severity of coral diseases (Bruno et al., 2003), as aspergillosis and yellow band disease, which has

become common in the Arabian Gulf since 1998 (Korrubel and Riegl, 1998). Kuta and Richardson, (2002) statistically confirm the relationships between the black band disease and both increase in water temperature and nutrient enrichment, which is possibly the typical case seen in the summer of 2012 in the Gulf. In fact, the black band disease was indeed seen along with the abundance of cyanobacteria around coral habitats in the aftermath of 2012 bleaching event in Abu Dhabi (Riegl and Purkis, 2015b).

According to the Abu Dhabi environmental agency monitoring reports, the highest number of HAB reports (about 28) around the coast of Abu Dhabi were in 2012 (EAD, 2015) (Figure 1.6 in chapter 1). Phytoplankton growth can alter the nutrient balance surrounding the coral habitats (D'Angelo and Wiedenmann, 2014), consequently affecting the functioning of the coral symbiosis (Wiedenmann et al., 2013). Accordingly, the depletion of phosphate from the water during three consecutive summer months (August, September, and October) in 2012 has likely facilitate bleaching due to phosphate starvation of the corals (See chapter 3 of this thesis)

No positive temperature anomalies were detected throughout the summer months of both 2013 and 2014 (Figure 4.15a, 4.16a, & 4.17a). Similarly, there were no abnormal chl-*a* peaks seen in this period, compared to 2010 and 2012. It is interesting to note that in all six bleaching events along the time-series occurred during a low wind speed conditions (Figure 4.18d), which may have facilitated the increase in water temperatures above tolerance levels for local coral reefs. In contrast, the unusual increase in wind speed in the summers of 2013 and 2014, may explain the reduction of SST and air temperature in these years (Riegl and Purkis, 2015b). Additionally, the visibility in both years (2013 and 2014)

showed considerable larger negative anomalies than any other summer along the time scale since the 80's (Figure 4.18c), which may add up to the solar dimming effect in the region.

High positive anomalies of SST were again measured in May 2015 (Delma=3.4°C, Saadiyat=1.5 °C and Ras Ghanada=1.4 °C) (Figure 4.15, 4.16 & 4.17). In August of that year, the month during which bleaching would have been expected, the peaks were lower, particularly at Saadiyat and Ras Ghanada (0.18 °C and 0.22 °C, respectively). The monthly average was also low in Saadiyat=33.8 °C and Ras Ghanada=33.6 °C. In Delma, the monthly mean 35.28°C was higher than in Saadiyat and Ras Ghanada. Moreover, in Delma area, the positive anomaly in August (1.5 °C) was even higher than the corresponding values measured during the back-to-back bleaching events (2010=1.0 °C, 2011=0.62 °C and 2012=0.82 °C). Although coral reefs in Delma were impacted by high thermal stress in 2015, no bleaching was observed. This might have been due to the dominance of heat tolerant massive *Porites* spp. Within the coral communities at this site. This may, in turn, be the result of the back-to-back bleaching events (2010-2011-2012) resulting in the relative loss of more traditional taxa, plus the recovery and growth of this thermal tolerant genotype in Delma during the non-bleaching years in 2013-2014 (Shuail et al., 2016a). Alternatively, the past bleaching/recovery events may have induced adaptation of the coral community in that region towards the more thermally tolerant symbionts (Maynard et al., 2008).

In agreement with the SST data, air temperature obtained from Abu Dhabi airport shows continuous positive peaks during the summer period, and the highest anomaly was seen in July=2.6 °C /August=2.0 °C period. Visibility was low during the whole year in 2015, and overlapped with positive AOT anomalies (Figure 4.18c), likely due to a high

frequency of dust storms in the region (Figure 4.15e, 4.16e, 4.17e). Wind speed was also high in 2015, specifically during August/September (Figure 4.15d, 4.16d, 4.17d). While there were no records of rainfall during this period (Figure 4.18e). Taken together, these results suggest that higher wind speed, along with the low precipitation conditions may result in greater than normal dust transport over the region. These dust storms may have then triggered the development of phytoplankton growth observed in summer of 2015, as seen by the positive anomalies in chl-*a*, particularly in Saadiyat and Ras Ghanada (Figure 4.16b & 4.17b). However, as discussed in chapter 3 of this thesis, the levels of dissolved inorganic nutrients, in particular, phosphate, remained high compared to the bleaching year 2012. Therefore, the corals may have been more resilient towards the comparable temperature stress.

4.3.4 Coral bleaching thresholds

It has been documented that coral reefs in the Arabian Gulf are living outside the thermal range of the typical tropical reef, with temperatures in the Gulf ranging from 14°C to 36°C. (Shinn, 1976; Sheppard, 1993; Sheppard et al., 2010a; Riegl and Purkis, 2012b). Coral bleaching thresholds for most tropical areas lie between 30–33°C, whereas in the Gulf they can reach up to 34–35°C (Coles and Riegl, 2013; Shuail et al., 2016). Furthermore, significant bleaching and mortality in the Southern Gulf are actually observed when temperatures reach or exceed a threshold of 34°C for more than three weeks (Riegl, 2002; Riegl and Purkis, 2012b). However, recent analyses of long-term SST patterns in three different locations on the coast of Abu Dhabi have shown that the bleaching threshold might also vary among specific sites within a region (Shuail et al., 2016a). In agreement

with that observation, the long-term SST values calculated over 32 years (1983-2015) indicated differences in the local bleaching thresholds across different regions within the Gulf (Figure 4.22). The lowest values were recorded in the northern parts of the Gulf, including Kuwait (33.06 °C) and ascending to 33.76 °C in KSA, and 34.41 °C in Bahrain. The highest bleaching threshold among the other selected coral habitats in the Gulf was found in the southern Gulf, in Delma site 35.05°C (Abu Dhabi) (Shuail et al., 2016a). The thresholds were relatively lower in the southeastern areas of the Gulf, in Iran 34.05 °C and Oman 33.41°C.

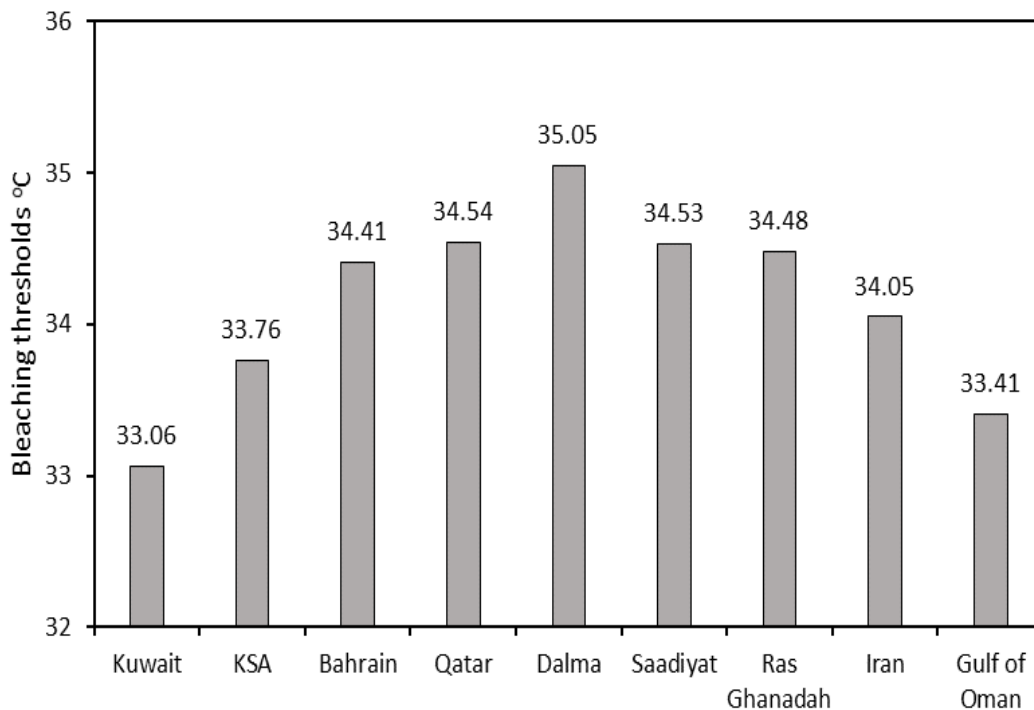


Figure 4.22. Coral bleaching thresholds from coral reef regions within the Arabian Gulf region calculated as 1°C over the average summer from 33 years (1982-2015). Showing different local bleaching thresholds, with the highest found at Delma island (southern Gulf) and the lowest in the northern Gulf (Kuwait) and Gulf of Oman.

4.3.5 Conclusion

The results presented in this chapter illustrates the environmental setting that characterise the habitats of corals in the southern Arabian Gulf over 33 years period. In general, the environmental conditions observed at the exact months of most bleaching events was characterised by dry weather (no rainfall) with an abnormal increase in temperature (air and water), relatively calm wind and slow water currents. The first three bleaching events in the studied time scale (1996, 1998 and 2002), were associated with extreme water temperature, related to El Niño (Figure 4.19). Afterwards, there was a shift in the aerosol properties indicating an elevated level of dust deposition over the Abu Dhabi area. The shift started after the 1996, 1998 El Niño events (Figure 4.19), which may have been facilitated by the scarcity of rainfalls and the increase in wind speed in the region. Since then, new factors were introduced to the complexity of possible causes of coral mortality, such as coral diseases and algal blooms, which may be related to the dust transport and deposition. These conditions were observed during the coral mortality events in during 2009, 2010, 2011 and 2012. The present information calls for continued monitoring of coral reef areas in the Gulf to generate a better understanding the complexity of the ecosystem factors that may affect coral survival.

Finally, the comparison of remotely sensed data and *in situ* measurements is recommended for future monitoring activities in Arabian Gulf, including time series of water temperature, phytoplankton, and nutrient dynamics and their annual variability.

Chapter 5: Summary, conclusions and future research

5.1. Summary and conclusions

Climate change threatens to increase coral mass mortality and accelerate the decline of reefs through coral bleaching. The aim of this thesis was to understand how environmental factors such as phytoplankton blooms modulate the thermal tolerance of the algal symbionts in reef corals in the Gulf. For this purpose, local differences in bleaching severity observed among coral communities in the southern Gulf off the coast of Abu Dhabi were compared and related to the accompanying environmental conditions such as SST, phytoplankton density, wind, dust, water current (WC), diffuse attenuation coefficient (K_d490), aerosol optical thickness (AOT). In addition to the meteorological data, which include air temperature, horizontal visibility, wind speed and precipitation in the Southern Arabian Gulf, Abu Dhabi, UAE.

The key conclusions of this study are:

- Differences in the local bleaching temperatures thresholds and the composition of the coral communities at the study sites offer likely explanations for the “patchiness” of the 2012 bleaching event in the southern Gulf area. The result of this analysis suggests that the bleaching threshold of the *Porites*-dominated Delma site is only 0.5 °C higher than the thresholds in the more diverse Saadiyat and RasGhanada sites. Hence, a long-term increase in the mean temperature of the hottest weeks in the same order of magnitude may lead to a considerable loss of coral diversity in the latter reefs.
- Ground-truthing of SST and chlorophyll-*a* data acquired by remote sensing techniques with data provided by *in situ* measurements revealed that remote sensing is a versatile tool to monitor these environmental parameters in coral reef areas in the southern Gulf.

In particular, remote sensing analysis of the number of days above the local bleaching thresholds temperature was helpful in hindcasting past bleaching events in the southern Gulf. Notably, bleaching did not occur in 2015, despite bleaching thresholds being exceeded in the study sites for a comparable length of time as compared to the bleaching year 2012.

- A key difference between the years 2012 and 2015, in Saadiyat study site, was in the phytoplankton density at the time of the annual temperature maximum. The high chl-*a* levels in the water detected by remote sensing analysis were accompanied by unusual drop in nitrate and phosphate levels in 2012. In particular, phosphate levels were undetectably low in the weeks before and during bleaching. In contrast, the chl-*a* levels were lower in 2015 and the concentration of dissolved organic nutrients were accordingly higher. These findings suggest that the lack of phosphate, likely caused by the phytoplankton bloom, may have rendered the coral more susceptible to thermal bleaching in 2012.
- The environmental conditions observed around the time of most bleaching events were characterised by dry weather (no rainfall), relatively calm wind and water currents, in addition to an unusual increase in temperature (air and water). The notable shift in the aerosol reading that started after the 1996 and 1998 El Niño events, shows an apparent intensification of dust storms over the Abu Dhabi area. This increase in dust content in the atmosphere may have been caused by the scarcity of rainfalls and the increase in the wind speed in the region. Dust could possibly deposit macro and micronutrients in the water, initiate phytoplankton blooms and effect the thermal tolerance of reef corals through the disturbance of their nutrient environment.

In summary, these findings improve the understanding of the role of water temperature and phytoplankton in altering the water chemistry and enhancing the bleaching susceptibility of reef corals. Furthermore, the findings of this thesis suggest that change-related factors such as altered wind and rainfall patterns in addition to anthropogenic nutrient enrichment have the potential to promote phytoplankton blooms and associated risk of coral bleaching.

5.2 Recommendations for future work

The findings of the present study call for future work on possible causes for local differences in bleaching severity among coral communities and to explore opportunities to mitigate the risk of coral bleaching through local management action.

- long-term monitoring of the environmental factors enhancing coral bleaching through remote sensing is recommended for other parts of the Gulf where coral bleaching is witnessed, such as Kuwait, KSA, Bahrain, Qatar, and Oman. In particular, a continued assessment of daily SST and chl-*a* levels using the MODIS satellite data is advisable for different coral reef regions in the Gulf. The daily monitoring of these parameters can potentially be evolved in an early warning system with the aim to alert decision makers in the Gulf region about undesired trends in climate and water chemistry parameters.
- The results of chapter 2 together with recent studies by in the Coral Reef Laboratory at the University of Southampton (Wiedenmann et al., 2013 and D'Angelo and Wiedenmann, 2014; Rosset et al., 2017) have shown how levels of dissolved nutrients and phytoplankton in the water column can influence the capacity of corals to resist

bleaching during periods of elevated summer temperatures. further understanding of the involved mechanisms and refinement of techniques on how to monitor them (remote sensing vs. ground measurements) is desirable to optimise environmental monitoring programs and use them more efficient in predicting environmental conditions that endanger coral reefs.

- Further work is recommended to evaluate the potential to reduce the risk of bleaching by the reduction of nutrient enrichment of coral reefs waters through the management of coastal run-off and sewage disposal.

Appendices



Contents lists available at ScienceDirect

Marine Pollution Bulletin

journal homepage: www.elsevier.com/locate/marpolbul

Local bleaching thresholds established by remote sensing techniques vary among reefs with deviating bleaching patterns during the 2012 event in the Arabian/Persian Gulf



Dawood Shuail^a, Jörg Wiedenmann^a, Cecilia D'Angelo^a, Andrew H. Baird^b, Morgan S. Pratchett^b, Bernhard Riegl^c, John A. Burt^d, Peter Petrov^e, Carl Amos^a

^a Coral Reef Laboratory, Ocean and Earth Science, University of Southampton, SO143ZH Southampton, UK

^b ARC Centre of Excellence for Coral Reef Studies, James Cook University, Townsville, Queensland 4811, Australia

^c National Coral Reef Institute, Nova Southeastern University, Fort Lauderdale, Florida 33314-7796, USA

^d Center for Genomics and Systems Biology, New York University Abu Dhabi, Abu Dhabi, United Arab Emirates

^e Regional Organization for the Protection of the Marine Environment (ROPME), 13124 Safat, Kuwait

ARTICLE INFO

Article history:

Received 18 December 2015

Received in revised form 6 February 2016

Accepted 1 March 2016

Available online 10 March 2016

Keywords:

Coral bleaching
Threshold temperature
Extreme environment
Coral reefs
Zooxanthellae
Symbiodinium
Global change

ABSTRACT

A severe bleaching event affected coral communities off the coast of Abu Dhabi, UAE in August/September, 2012. In Saadiyat and Ras Ghanada reefs ~40% of the corals showed signs of bleaching. In contrast, only 15% of the corals were affected on Delma reef. Bleaching threshold temperatures for these sites were established using remotely sensed sea surface temperature (SST) data recorded by MODIS-Aqua. The calculated threshold temperatures varied between locations (34.48 °C, 34.55 °C, 35.05 °C), resulting in site-specific deviations in the numbers of days during which these thresholds were exceeded. Hence, the less severe bleaching of Delma reef might be explained by the lower relative heat stress experienced by this coral community. However, the dominance of *Porites* spp. that is associated with the long-term exposure of Delma reef to elevated temperatures, as well as the more pristine setting may have additionally contributed to the higher coral bleaching threshold for this site.

Crown Copyright © 2016 Published by Elsevier Ltd. This is an open access article under the CC BY license (<http://creativecommons.org/licenses/by/4.0/>).

1. Introduction

Warm water coral reefs are among the most productive and biologically diverse ecosystems on Earth. Many of these reefs are in decline due to the impact of a variety of global and local stressors (Sheppard, 2003; Baker et al., 2008; Logan et al., 2014; van Hooidonk et al., 2013; D'Angelo and Wiedenmann, 2014). Among them are heat stress episodes during which temperatures exceed a regional threshold and induce the often fatal breakdown of the coral/alga symbiosis which manifests as coral bleaching (Baker et al., 2008; Goreau and Hayes, 1994). The globally highest bleaching thresholds are found among corals of the southern Arabian/Persian Gulf, hereafter IRSA (Inner ROPME Sea Area) where they survive peak temperatures above 35 °C (Coles, 2003; Sheppard et al., 1992). However, also these corals can fall victim to bleaching and coral bleaching linked to unusually warm temperatures has been shown to affect the IRSA at least since 1996 contributing to a substantial loss of coral cover (Riegl and Purkis, 2015; Riegl, 2002). The variability of bleaching susceptibility observed among different species resulted in shifts of the coral community structure in the aftermath of bleaching events in the IRSA (Riegl and Purkis, 2015).

The IRSA is a shallow basin at high latitude and therefore, the thermal properties of the waterbody, respond quickly to local factors. Rapid

cooling by winds (Thoppil and Hogan, 2010; Cavalcante et al., 2016) or preferential heating/cooling in shallow areas or regions protected by headlands is common (Riegl and Purkis, 2012). Correspondingly, small-scale excursions of thermal stress with consequent variation in the severity of coral bleaching and mortality events have been observed. A severe bleaching event recorded in 2007 off the Iranian coast (Baker et al., 2008) was absent or had negligible impact in the south-eastern IRSA. Bleaching was observed in 2013 in Qatar, but not in eastern Abu Dhabi (B. Riegl pers. obs.). In general, coral stress events in the northern IRSA (Iran) often do not coincide with those in the southern IRSA, and the Western IRSA (Kuwait, KSA, Bahrain) appears to have suffered fewer, or at least differently-timed, events than the south-eastern IRSA. Hence, strong regional variability in the frequency and severity of bleaching events seem to be characteristic for the region.

Bleaching events are frequently characterized by high variability. On an individual level, the within-colony bleaching response can strongly vary depending on light exposure (Coles and Jokiel, 1978; Brown et al., 1994; Hoegh-Guldberg, 1999). Further variability can also arise from the bleaching susceptibility of different zooxanthellae clades/species (Baker, 2001; Pettay et al., 2015). Among them, the year-round prevalent algal partner of corals in the southern IRSA, *Symbiodinium thermophilum*, can be considered to be one of the most thermo-

<http://dx.doi.org/10.1016/j.marpolbul.2016.03.001>

0025-326X/Crown Copyright © 2016 Published by Elsevier Ltd. This is an open access article under the CC BY license (<http://creativecommons.org/licenses/by/4.0/>).

tolerant symbionts (D'Angelo et al., 2015; Hume et al., 2015). Marked regional variability is commonly encountered during bleaching events and may be caused by small-scale water-dynamics and flow patterns (Nakamura and Van Woesik, 2001; Davis et al., 2011), by greater adaptation/acclimatization due to previous stress episodes (Brown et al., 2002; Guest et al., 2012) or by differences in the species assemblage of the affected sites (Marshall and Baird, 2000). The onset of bleaching is often not synchronous across several, even nearby, reefs and neither is the severity or the effects of bleaching (Baker et al., 2008). Additional stressors, such as the disturbance of the nutrient environment, can have significant impacts on bleaching susceptibility (Wiedenmann et al., 2012; D'Angelo and Wiedenmann, 2014). In this context, the mean water column productivity, besides mean temperatures, was the best predictor of the variability of coral reef recovery across the Indo-Pacific (Riegl et al., 2015). Also, local adaptations to environmental factors other than temperature can have strong influences on the temperature tolerance of corals. D'Angelo et al. have shown that IRSA corals are characterized by a pronounced local adaptation to the high salinity of their habitat and that their superior heat tolerance is lost when they are exposed to normal oceanic salinity levels (D'Angelo et al., 2015). Global warming will expose the world's reef to positive temperature anomalies with increasing frequency (Logan et al., 2014). The prerequisite for knowledge-based coral reef management that aims to regionally mitigate the effects of climate change is a thorough understanding of how local factors modulate the response to temperature stress. Therefore, we set out to identify the causes for local differences in bleaching severity observed among coral communities in the southern IRSA off the coast of Abu Dhabi. Since remote sensing platforms offer valuable

tools to reconstruct environmental conditions prevailing during coral reef disturbance events (Andréfouët et al., 2014), we used satellite data to establish the local bleaching thresholds in the study sites.

2. Material and methods

2.1. Measuring SST using remote sensing products

The SST ($^{\circ}\text{C}$) data was extracted from the Aqua/Terra Ocean Color 3 (OC3) Moderate Resolution Imaging Spectroradiometer (MODIS) imagery downloaded from the NASA ocean color data website (<http://oceancolor.gsfc.nasa.gov/>) and by the Regional Organization for the Protection of the Marine Environment (ROPME) archived in Kuwait. MODIS data are recorded by two instruments. The first is integrated in the Terra satellite (MODIS-Terra) and launched in December, 1999. The second instrument is installed on the Aqua satellite (MODIS-Aqua), and was launched in May, 2002. Both satellites are in sun-synchronous orbits: Terra crosses the equator in a descending node at 10:00, and Aqua crosses in an ascending node at 12:00 noon. Satellite imagery was used for the periods between February, 2000 to December, 2014 (MODIS Terra) and from July, 2002 to December, 2014. (MODIS Aqua). Level-2 images were used for which the sensors were calibrated, geo-located with atmospheric corrections and bio-optical algorithms had been applied. Temperatures were determined for 1 km^2 areas covering the study sites, the highest spatial resolution provided by the MODIS product. Images were analyzed using the SeaWiFS Data Analysis System (SeaDAS) software program Version 7.2 and VISAT BEAM software Version 4.10.3. Images in which the SST signal was affected by

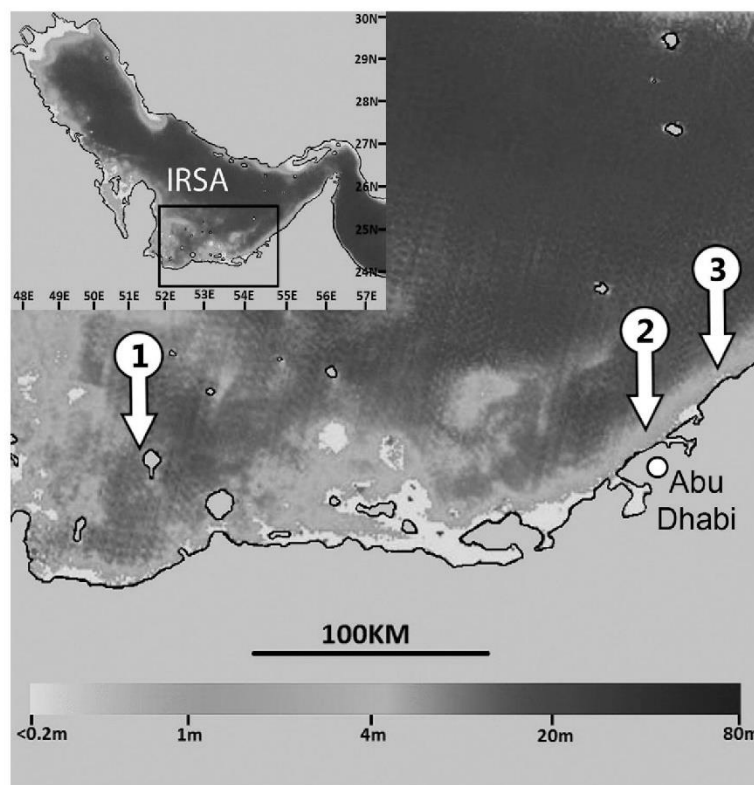


Fig. 1. Bathymetric map of the southern IRSA. Numbers identify the three study sites: (1) Delma, (2) Saadiyat and (3) Ras Ghanada. The Map was constructed using Sea-viewing Wide Field-of-view Sensor (SeaWiFS) Ocean Color Data provided by NASA Ocean Biology (OB.DAAC). Gray-level scale defines the depth in meters.

Table 1
Calculated bleaching threshold temperatures for the hottest weeks of the year.

	Delma	Saadiyat	Ras Ghanadah
Bleaching threshold temp. (01–31 Aug. 2002–2014)	34.99	34.55 ^a	34.37
Bleaching threshold temp. (15 Aug.–15 Sept. 2002–2014)	35.05	34.53	34.48

^a Highest values for each site are underlined.

cloud cover or high amounts of dust in the air were excluded from the analysis. The time of recording of the respective imagery was extracted from file names.

2.2. Reconstruction of daily temperature maxima in situ

In situ water temperature timeseries were recorded at ~7 m depth for the Saadiyat and Delma sites using Hobo temperature loggers (Tempcon, UK) at hourly intervals from January to December, 2013. Using this data set and data from August 2014, typical daily temperature variations were calculated by averaging the corresponding hourly values for the last week of August, commonly one of the hottest weeks of the year. This temperature record revealed considerable variations of the temperature over the course of the day with temperatures differing by >0.25 °C between the early morning hours and the daily temperature maximum at ~17:00 (Supplementary Fig. 1).

2.3. Reconstruction of daily temperature maxima using remote sensing data

The recording times of the analyzed MODIS Terra and Aqua imagery show considerable deviations due to the different flight paths of the satellites. Terra data were recorded between 09:30–11:45 (median 10:50) whereas Aqua images were taken in the period 12:05–14:20 (median 13:50). The Terra data provide values that can be ~0.15 °C below the daily SST maximum due to their early recording time. By contrast, MODIS Aqua records close to the *in situ* temperature maximum and its data are therefore best suited to reconstruct the SST of the IRSA. To verify this method, we selected >250 pairs of MODIS-Aqua values and corresponding *in situ* measurements (14:00 data points), from days distributed over all seasons of 2013. Then, the corresponding temperature values were plotted against each other and the coefficient of determination (R^2) for a linear regression fit was calculated (Supplementary Fig. 2b–c).

2.4. Calculation of bleaching threshold temperatures

The MODIS-Aqua SST data set was used to calculate the local threshold temperature of coral bleaching, defined as the temperature 1 °C higher than the highest monthly mean temperature (Glynn and D'Croz, 1990). Since the SST peaks are mostly in August in the southern IRSA (Supplementary Fig. 2), we used this period to determine the highest 4-weekly mean temperature using the Aqua data set for the years 2002 to 2014. However, since temperatures are also high in the first two weeks of September, the period from 15th August to 15th September was analyzed for comparison.

2.5. Field surveys

Coral communities were surveyed at three sites in the southern IRSA in UAE, Delma (latitude 24.5208/longitude 52.2781), Saadiyat (lat. 24.599/long. 54.4215) and Ras Ghanada (lat. 24.8481/long. 54.6903) (Fig. 1). At each of these sites, bleaching was recorded along three replicate transects during the period from 17th to 19th September, 2012. Transects were arranged radially around a central origin, extending for 10 m with 120 degrees separating each transect. Corals were classified to genus level on the basis of Veron (2000), with taxonomic updates from Budd et al. (2012). The genus of juvenile corals (<5 cm diameter) within a 1 m wide band were included in the dataset. The analysis of adult corals was restricted to *Platygyra* spp. and *Porites* spp. as these corals were represented in large numbers in all sites. *Porites* spp. were represented by species with massive growth forms (*Porites* cf. *lutea*, *lobata* and *harrisoni*). Underwater color scales were used to assign the degree of bleaching to three categories: 1) Bleached: The whole colony was white, 2) Partially bleached: Larger parts of the colony (>20%) lost their normal color and 3) Unbleached: The colonies showed their typical variety of colors.

Chi-square statistic (χ^2) was used to test whether the percentage of bleached, partially bleached and non-bleached coral colonies recorded in August 2012 in Delma, Saadiyat and Ras Ghanada was region-specific.

3. Results

3.1. Local temperature thresholds of coral bleaching

Using the MODIS Aqua data, the local threshold temperatures for coral bleaching (defined as 1 °C above the long-term average of the mean temperature of the 4 hottest weeks of each year) was calculated

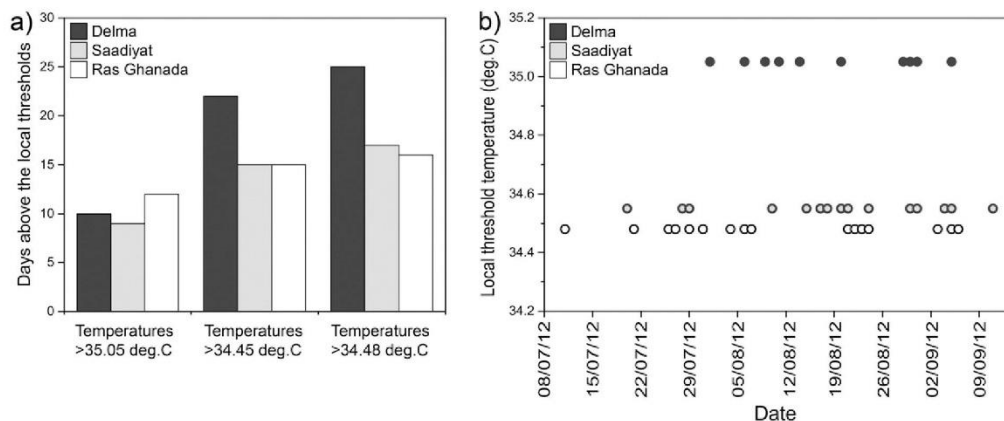


Fig. 2. Variations in heat stress exposure during the 2012 bleaching event in the southern IRSA reconstructed from MODIS-Aqua imagery. a) Number of days during which the site-specific bleaching threshold temperatures (Delma: 35.05 °C, Saadiyat 34.55 °C, Ras Ghanada: 34.8 °C) were exceeded in each of the study sites. b) Days at which the site-specific local bleaching threshold was exceeded in the corresponding study sites, indicating also the length of the positive temperature anomaly.

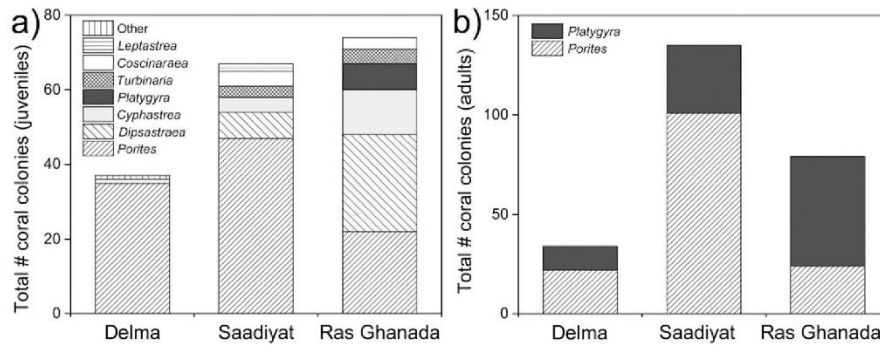


Fig. 3. Site-specific composition of the coral community. a) Total number of juvenile (species indicated in the panel legend) and b) adult (*Porites* spp. and *Platygyra* spp.) corals recorded along the transects in the three study sites.

for the time period 2002–2014. Comparably high threshold temperatures were obtained for the 4 weeks of August and for the period from the 15th of August to the 15th of September, signifying the length of

time over which IRSAs corals are exposed to elevated temperatures (Table 1). Our analysis revealed marked differences in the local temperature history of the study sites which are reflected in bleaching

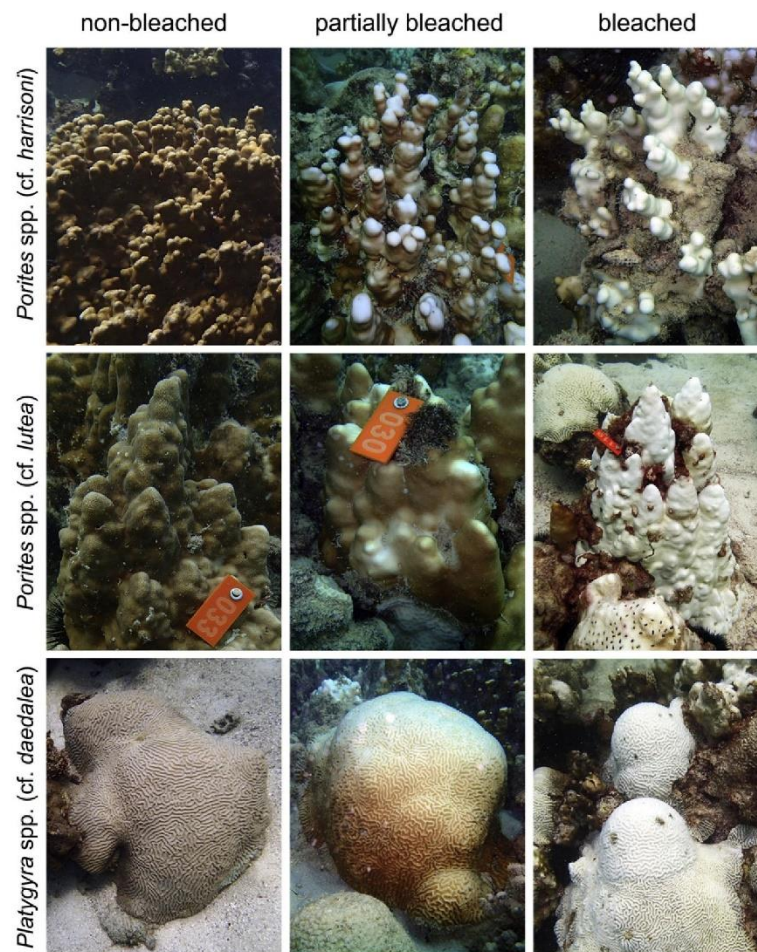


Fig. 4. Representative photographs of corals from the bleaching categories used in this study. (Image credits: J. Wiedenmann).

threshold temperatures ranging from 34.48 °C (Ras Ghanada) over 34.55 °C (Saadiyat) to 35.05 °C (Delma) (Supplementary Fig. 2, Table 1).

In summer 2012, the number of days during which temperatures exceeded 35.05 °C was comparable for the three sites (Fig. 2a). Around Delma reef, temperatures above 34.48 and 34.55 °C were recorded more frequently than for the other two sites within the same time period. However, due to the site-specific deviations of the bleaching threshold temperatures, the three locations showed considerable differences in the number of days during which their regional thresholds were exceeded (Fig. 2b). Specifically, coral communities had to endure above-threshold temperatures for 16 days in Ras Ghanada reefs and for 15 days in Saadiyat reefs. In contrast, in Delma Island reefs, the temperatures were higher than the local bleaching threshold for only 10 days (Fig. 2). Also, the period of time between the first and the last day at which the threshold temperatures were exceeded was longer in Saadiyat and Ras Ghanada compared to Delma. These data suggest that similar relative heat stress levels were experienced by corals in Saadiyat and Ras Ghanada and that these were higher than in Delma.

3.2. Site-specific severity of the 2012 bleaching event

We surveyed three coral reef sites in the southern IRSA to document the bleaching event that took place in August/September 2012. The three sites revealed pronounced differences in the abundance of genera and genus richness of juvenile corals (Fig. 3a). The overall abundance of juveniles was similar in Saadiyat and Ras Ghanada and numbers were higher than in Delma. Species richness of juvenile corals decreased from Ras Ghanada to Saadiyat and Delma, with *Porites* spp. becoming increasingly dominant. Similarly, the number of adult *Porites* spp. and *Platygyra* spp. recorded along the transects was higher in Ras Ghanada and Saadiyat than in Delma (Fig. 3b).

Within the sites, corals of the same taxonomic group were affected to variable degrees by bleaching, ranging from unaffected to partially bleached and completely bleached (Fig. 4). Partially bleached corals

lost their pigmentation often in the upper, most light-exposed parts of the colonies.

In Ras Ghanada and Saadiyat reefs, >40% of the analyzed corals (juvenile and adult *Porites*, adult *Platygyra*) were affected by bleaching (Fig. 5). An exception were juvenile *Porites* among which no partially bleached individuals were encountered in Ras Ghanada and the overall percentage of colonies showing signs of bleaching was accordingly lower. In all analyzed groups, between 20 and ~30% of the corals were completely bleached in Saadiyat and Ras Ghanada. By contrast, the corals in the Delma site were less affected and no more than 15% of the corresponding groups showed signs of bleaching. For both species, statistical analysis identified the lower bleaching severity in Delma as a significant site-specific effect (Supplementary Table 3).

Similar bleaching levels were observed for the combined numbers of recorded juveniles from other species (Supplementary Fig. 3). It has to be noted, however, that the data for Delma reef need to be considered with caution due to low number of non-*Porites* spp. juveniles encountered in this site.

4. Discussion

We studied three sites in the IRSA that experienced different levels of bleaching during the 2012 bleaching event with the purpose to establish potential causes for the patchiness of bleaching that is frequently observed during mass bleaching events. Bleaching levels for two common taxa, *Porites* spp. and *Platygyra* spp., were analyzed. Additionally, we recorded the site-specific degree of bleaching among juvenile *Porites* spp. and other less abundant corals.

Reefs in Saadiyat and Ras Ghanada were severely affected by bleaching whereas corals in Delma showed little or no signs of bleaching despite their relatively close geographic proximity and exposure to a comparable temperature regime in August–September, 2012. This trend was comparable for all the monitored species and developmental stages.

Since light exposure is known to promote heat-stress mediated bleaching (Coles and Jokiel, 1978; Brown et al., 1994, 2002; Hoegh-Guldberg, 1999; Fitt et al., 2001), the observation, that partial bleaching of adult colonies was frequently found in the upper part of the colonies, suggests that light stress was also influential in 2012 bleaching event.

In Ras Ghanada, a higher percentage of adult *Porites* spp. showed signs of bleaching compared to juveniles from the same taxon. This observation is in line with previous studies that found that juvenile corals were less affected by bleaching than adults (Mumby, 1999; Nakamura and Van Woesik, 2001; Loya et al., 2001). However, this trend was not observed in the other sites where comparable numbers of adults and juveniles suffered from bleaching.

A possible explanation for the different bleaching susceptibility across the three study sites is that the local bleaching threshold of ~35 °C at Delma reef is ~0.5 °C higher than in the other sites. Consequently, the corals experienced less relative heat stress, indicated by the smaller number of days during which the local bleaching threshold was exceeded. Still, the threshold temperature was exceeded for 10 days at Delma with little effect on the corals, setting this site among the most temperature tolerant reefs of the world (Riegl et al., 2011, 2012). The resilience of Delma reef is further underlined by the fecundity of its corals in the aftermath of the 2012 bleaching event which was significantly higher compared to those from Saadiyat and Ras Ghanada reefs (Howells et al., 2016). Previous observations from elsewhere found massive *Porites* spp. to be among the taxa with a high survival rate after bleaching events (Loya et al., 2001; Sheppard and Loughland, 2002). Therefore, the dominance of massive *Porites* spp. at Delma (Burt et al., 2011) that is reflected by the species composition of juvenile corals presented in this study, may be considered as an additional potential reason for the exceptional heat tolerance of this reef site (Marshall and Baird, 2000; Loya et al., 2001). Also, the history of

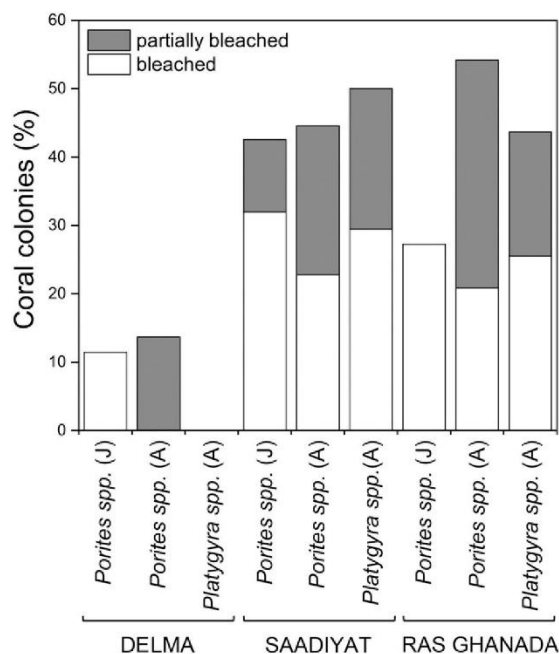


Fig. 5. Site-specific severity of bleaching. Comparison of the percentage of the total numbers of juvenile and adult *Porites* spp. colonies and other species affected by bleaching.

increased temperature stress levels in Delma may have increased the bleaching threshold of the community by a long-term selection of more resilient genotypes and/or acclimatization of corals (Brown et al., 2002). Furthermore, Delma reef is situated ~50 km off the coast in a relatively pristine environment whereas the other two sites are under the direct influence of a densely populated urban area and intense coastal construction (Sale et al., 2011; Van Lavieren et al., 2011). Since the water quality, in particular the nutrient levels, can affect bleaching thresholds (Wooldridge, 2009; Wiedenmann et al., 2012; D'Angelo and Wiedenmann, 2014), the influence of the water chemistry at the different sites should be investigated as another potential cause for the observed differences in their bleaching tolerance.

5. Conclusions

Different bleaching threshold temperatures and the composition of the coral communities at the study sites offer likely explanations for the “patchiness” of the 2012 bleaching event in the southern IRSA, but other parameters such as the water quality and light stress should also be considered. Our results suggest that the bleaching threshold of the *Porites*-dominated Delma site is only 0.5 °C higher than in the more diverse Saadiyat and Ras Ghanada sites. Hence, a long-term increase of the mean temperature of the hottest weeks in the same order of magnitude may lead to a considerable loss of coral diversity in the latter reefs.

Acknowledgment

The study was funded by NERC (Grant no. NE/K00641X/1 to JW) and the European Research Council under the European Union's Seventh Framework Program (FP/2007–2013) ERC Grant Agreement no. 311179 to JW and a scholarship by the Public Authority for Education and Training of the State of Kuwait to DS. We are grateful to NYU Abu Dhabi Institute for supporting the 2012/2013 field workshops during which data for this study were collected. We also thank Tropical Marine Centre (London) and Tropic Marin (Wartenberg) for sponsoring the NOCS Coral Reef Laboratory and acknowledge NASA Ocean Biology (OB.DAAC) for Sea-viewing Wide Field-of-view Sensor (SeaWiFS) Ocean Color Data. We extend our appreciation to ROPME for the access to their remote sensing database.

Appendix A. Supplementary data

Supplementary data to this article can be found online at <http://dx.doi.org/10.1016/j.marpolbul.2016.03.001>.

References

- Andréfouët, S., Dutheil, C., Menkes, C.E., Bador, M., Lengaigne, M., 2014. Mass mortality events in atoll lagoons: environmental control and increased future vulnerability. *Glob. Chang. Biol.* 21, 195–205.
- Baker, A.C., 2001. Reef corals bleach to survive change. *Nature* 411, 765–766.
- Baker, A.C., Glynn, P.W., Riegl, B., 2008. Climate change and coral reef bleaching: an ecological assessment of long-term impacts, recovery trends and future outlook. *Estuar. Coast. Shelf Sci.* 80, 435–471.
- Brown, B.E., Dunne, R.P., Goodson, M.S., Douglas, A.E., 2002. Experience shapes the susceptibility of a reef coral to bleaching. *Coral Reefs* 21, 119–126.
- Brown, B.E., Dunne, R.P., Scoffin, T.P., Letissier, M.D.A., 1994. Solar damage in intertidal corals. *Mar. Ecol. Prog. Ser.* 105, 219–230.
- Budd, A.F., Fukami, H., Smith, N.D., Knowlton, N., 2012. Taxonomic classification of the reef coral family Mussidae (Cnidaria: Anthozoa: Scleractinia). *Zool. J. Linnean Soc.* 166, 465–529.
- Burt, J., Al-Harthi, S., Al-Cibahy, A., 2011. Long-term impacts of coral bleaching events on the world's warmest reefs. *Mar. Environ. Res.* 72, 225–229.
- Cavalcante, G.H., Feary, D.A., Burt, J.A., 2016. The influence of extreme winds on coastal oceanography and its implications for coral population connectivity in the southern Arabian Gulf. *Mar. Pollut. Bull.* 105, 489–497.
- Coles, S.L., 2003. Coral species diversity and environmental factors in the Arabian Gulf and the Gulf of Oman: a comparison to the Indo-Pacific region. *Atoll Res. Bull.* 11–119.
- Coles, S.L., Jokiel, P.L., 1978. Synergistic effects of temperature salinity and light on the thermatypic coral *Montipora verrucosa*. *Mar. Biol.* 49, 187–195.
- D'Angelo, C., Wiedenmann, J., 2014. Impacts of nutrient enrichment on coral reefs: new perspectives and implications for coastal management and reef survival. *Curr. Opin. Environ. Sustain.* 7, 82–93.
- D'Angelo, C., Hume, B.C.C., Burt, J., Smith, E.G., Achterberg, E.P., Wiedenmann, J., 2015. Local adaptation constrains the distribution potential of heat-tolerant *Symbiodinium* from the Persian/Arabian Gulf. *ISME J.* 1–10.
- Davis, K.A., Lentz, S.J., Pineda, J., Farrar, J.T., Starczak, V.R., Churchill, J.H., 2011. Observations of the thermal environment on Red Sea platform reefs: a heat budget analysis. *Coral Reefs* 30, 25–36.
- Fitt, W.K., Brown, B.E., Warner, M.E., Dunne, R.P., 2001. Coral bleaching: interpretation of thermal tolerance limits and thermal thresholds in tropical corals. *Coral Reefs* 20, 51–65.
- Glynn, P.W., D'Croz, L., 1990. Experimental evidence for high temperature stress as the cause of El Niño-coincident coral mortality. *Coral Reefs* 8, 181–191.
- Goreau, T.J., Hayes, R.L., 1994. Coral bleaching and ocean “hot spots”. *Ambio* 23, 176–180.
- Guest, J.R., Baird, A.H., Maynard, J.A., Muttaqin, E., Edwards, A.J., Campbell, S.J., Yewdall, K., Affendi, Y.A., Chou, L.M., 2012. Contrasting patterns of coral bleaching susceptibility in 2010 suggest an adaptive response to thermal stress. *PLoS One* 7, 1–8.
- Hoegh-Guldberg, O., 1999. Climate change, coral bleaching and the future of the world's coral reefs. *Mar. Freshw. Res.* 50, 839.
- Howells, E.J., Ketchum, R.N., Bauman, A.G., Mustafa, Y., Watkins, K.D., Burt, J.A., 2016. Species-specific trends in the reproductive output of corals across environmental gradients and bleaching histories. *Mar. Pollut. Bull.* 105, 532–539.
- Hume, B.C.C., Angelo, C.D., Smith, E.G., Stevens, J.R., Burt, J., Wiedenmann, J., 2015. *Symbiodinium thermophilum* sp. nov., a thermotolerant symbiotic alga prevalent in corals of the world's hottest sea, the Persian/Arabian Gulf. *Sci. Rep.* 5, 8562.
- Logan, C., Dunne, J.P., Eakin, C.M., Donner, S.D., 2014. Incorporating adaptive responses into future projections of coral bleaching. *Glob. Chang. Biol.* 20, 125–139.
- Loya, Y., Sakai, K., Nakano, Y., Woesik, R., Van, 2001. Coral Bleaching: The Winners and The Losers 122–131.
- Marshall, P.A., Baird, A.H., 2000. Bleaching of corals on the Great Barrier Reef: differential susceptibilities among taxa. *Coral Reefs* 19, 155–163.
- Mumby, P.J., 1999. Bleaching and hurricane disturbances to populations of coral recruits in Belize. *Mar. Ecol. Prog. Ser.* 190, 27–35.
- Nakamura, T., Van Woesik, R., 2001. Water-flow rates and passive diffusion partially explain differential survival of corals during the 1998 bleaching event. *Mar. Ecol. Prog. Ser.* 212, 301–304.
- Pettay, D.T., Wham, D.C., Smith, R.T., Iglesias-Prieto, R., Lajeunesse, T.C., 2015. Microbial invasion of the Caribbean by an Indo-Pacific coral zooxanthella. *Proc. Natl. Acad. Sci. U. S. A.* 112, 7513–7518.
- Riegl, B., 2002. Effects of the 1996 and 1998 positive sea-surface temperature anomalies on corals, coral diseases and fish in the Arabian Gulf (Dubai, UAE). *Mar. Biol.* 140, 29–40.
- Riegl, B.M., Purkis, S.J., 2012. Coral reefs of the gulf: Adaptation to climatic extremes in the world's hottest sea. *Coral Reefs of the Gulf*, pp. 1–4.
- Riegl, B., Purkis, S., 2015. Coral population dynamics across consecutive mass mortality events. *Glob. Chang. Biol.* 21, 3995–4005.
- Riegl, B., Glynn, P.W., Wieters, E., Purkis, S., d'Angelo, C., Wiedenmann, J., 2015. Water column productivity and temperature predict coral reef regeneration across the Indo-Pacific. *Sci. Rep.* 5, 8273.
- Riegl, B.M., Purkis, S.J., Al-Cibahy, A.S., Abdel-Moati, M.A., Hoegh-Guldberg, O., 2011. Present limits to heat-adaptability in corals and population-level responses to climate extremes. *PLoS One* 6, e24802.
- Riegl, B.M., Purkis, S.J., Al-Cibahy, A.S., Al-Harthi, S., Grandcourt, E., Al-Sulaiti, K., Baldwin, J., Abdel-Moati, A.M., 2012. Coral bleaching and mortality thresholds in the SE Gulf: highest in the world. *Coral Reefs of the Gulf*. Springer, pp. 95–105.
- Sale, P.F., Feary, D.A., Burt, J.A., Bauman, A.G., Cavalcante, G.H., Drouillard, K.G., Kjerfve, B., Marquis, E., Trick, C.G., Usseglio, P., Van Lavieren, H., 2011. The growing need for sustainable ecological management of marine communities of the Persian Gulf. *Ambio* 40, 4–17.
- Sheppard, C.R., 2003. Predicted recurrences of mass coral mortality in the Indian Ocean. *Nature* 425, 294–297.
- Sheppard, C.R., Loughland, R., 2002. Coral mortality and recovery in response to increasing temperature in the southern Arabian Gulf. *Aquat. Ecosyst. Health Manag.* 5, 395–402.
- Sheppard, C.R., Price, A.R.G., Roberts, C.J., 1992. *Marine Ecology of the Arabian Area. Patterns and Processes in Extreme Tropical Environments*. Academic Press, London.
- Thoppil, P.G., Hogan, P.J., 2010. A modeling study of circulation and eddies in the Persian Gulf. *J. Phys. Oceanogr.* 40, 2122–2134.
- van Hooidonk, R., Maynard, J.A., Planes, S., 2013. Temporary refugia for coral reefs in a warming world. *Nat. Clim. Chang.* 3, 508–511.
- Van Lavieren, H., Burt, J., Feary, D.A., Cavalcante, G., Marquis, E., Benedetti, L., Trick, C., Kjerfve, B., Sale, P.F., 2011. Managing the growing impacts of development on fragile coastal and marine ecosystems: Lessons from the Gulf. Policy Report of the United Nations University—Institute for Water, Environment and Health, pp. 1–100.
- Veron, J.E.N., 2000. In: Stafford-Smith, M. (Ed.) *Corals of the World 1–3*. Australian Institute of Marine Science, Townsville, Australia (1382 pp.).
- Wiedenmann, J., D'Angelo, C., Smith, E.G., Hunt, A.N., Legret, F.-E., Postle, A.D., Achterberg, E.P., 2012. Nutrient enrichment can increase the susceptibility of reef corals to bleaching. *Nat. Clim. Chang.* 3, 160–164.
- Wooldridge, S.A., 2009. Water quality and coral bleaching thresholds: formalising the linkage for the inshore reefs of the Great Barrier Reef, Australia. *Mar. Pollut. Bull.* 58, 745–751.

Supplementary Material

Local bleaching thresholds established by remote sensing techniques vary among reefs with deviating bleaching patterns during the 2012 event in the Arabian/Persian Gulf

Dawood Shuail¹, Jörg Wiedenmann¹, Cecilia D'Angelo¹, Andrew H. Baird², Morgan S. Pratchett², Bernhard Riegl³, John A. Burt⁴, Peter Petrov⁵ and Carl Amos¹

¹ Coral Reef Laboratory, Ocean and Earth Science, University of Southampton, SO143ZH Southampton, UK

² ARC Centre of Excellence for Coral Reef Studies, James Cook University Townsville, Queensland 4811, Australia

³ National Coral Reef Institute, Nova Southeastern University, Fort Lauderdale, Florida 33314-7796, USA

⁴ Center for Genomics and Systems Biology, New York University Abu Dhabi, Abu Dhabi, UAE

⁵ Regional Organization for the Protection of the Marine Environment (ROPME), 13124 Safat, State of Kuwait

Correspondence: joerg.wiedenmann@noc.soton.ac.uk

Supplementary table 1: Numbers of adult *Porites* spp. and *Platygyra* corals recorded along the transects in the different study sites.

Corals	Delma	Saadiyat	Ras Ghanada
<i>Porites</i> sp. (adults) (<i>Porites</i> cf. <i>lobata</i> / <i>lutea</i> / <i>harrisoni</i>)	22	101	24
<i>Platygyra</i> sp. (adults)	12	34	55
Total (adults)	34	135	79

Supplementary table 2: Numbers of juvenile corals recorded along the transects in the different study sites.

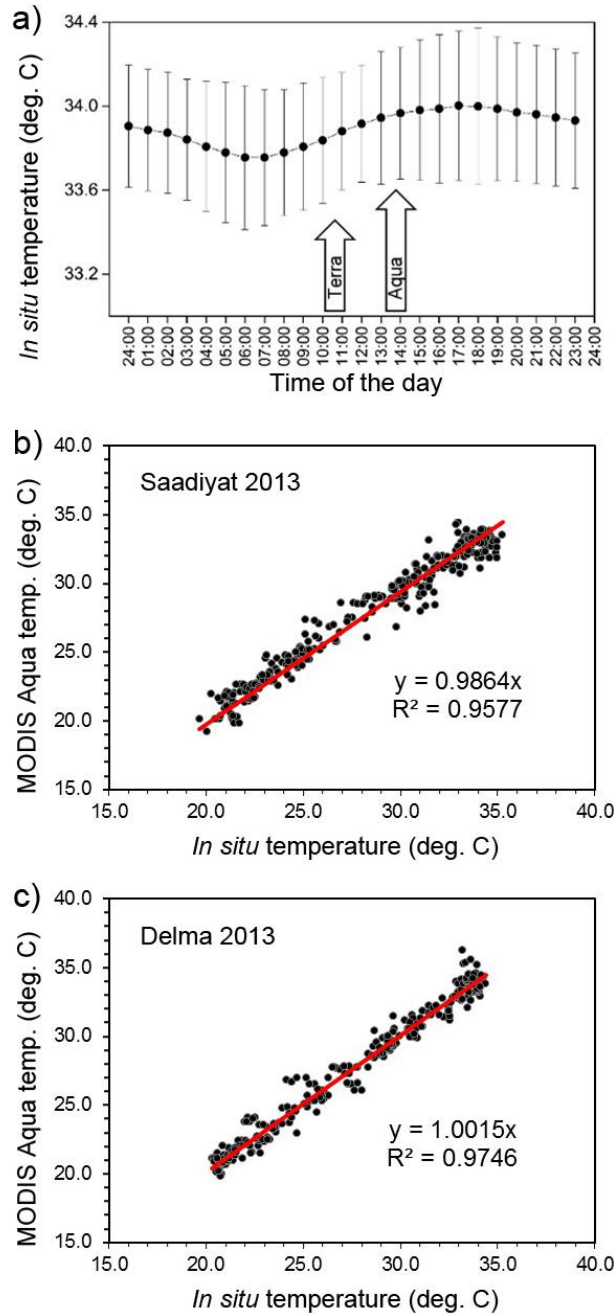
	Delma			Saadiyat			Ras Ganada		
Species	Non-bleached	Bleached	Partially Bleached	Non-bleached	Bleached	Partially Bleached	Non-bleached	Bleached	Partially Bleached
<i>Porites</i>	31	4	0	27	15	5	16	6	0
<i>Dipsastraea</i> (<i>Favia</i> *)	0	0	0	4	3	0	18	8	0
<i>Cyphastrea</i>	1	0	0	2	0	2	5	7	0
<i>Platygyra</i>	0	0	0	0	0	0	3	3	1
<i>Turbinaria</i>	0	0	0	0	3	0	1	3	0
<i>Coscinaraea</i>	0	0	0	1	3	0	0	3	0
<i>Leptastrea</i>	0	0	0	2	0	0	0	0	0
other	1	0	0	0	0	0	0	0	0
Total	33	4	0	36	24	7	43	30	1

*The genus *Favia* was replaced by *Dipsastrea* by: Budd, A.F., Fukami, H., Smith, N.D., Knowlton, N. 2012, Taxonomic classification of the reef coral family Mussidae (Cnidaria: Anthozoa: Scleractinia). Zoological Journal of the Linnean Society 166, 465-529.

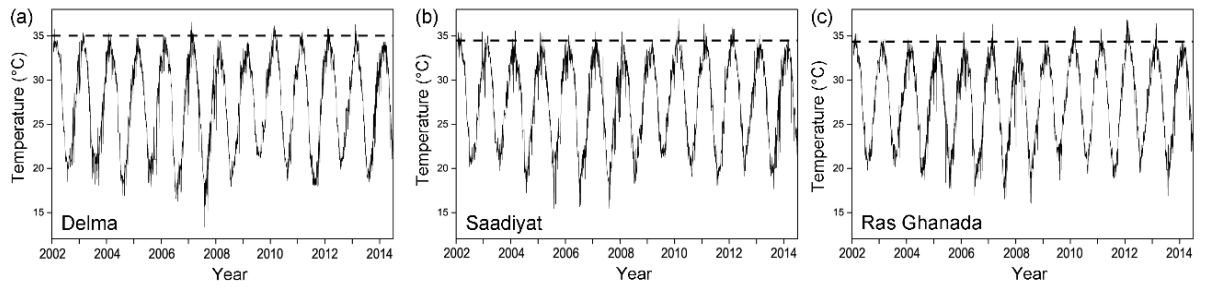
Supplementary Table 3. Statistical analysis of site-specific differences in bleaching susceptibility.

Juvenile <i>Porites</i> spp.	Bleached	Partially bleached	Non bleached	Total
Dalma	4	0	31	35
Saadiyat	15	5	27	47
Ras Ghanada	6	0	16	22
Total	25	5	74	104
$\chi^2 = 12.42867066$, df = 4, P-value = 0.014437				
Adult <i>Porites</i> spp.	Bleached	Partially bleached	Non bleached	Total
Dalma	0	3	19	22
Saadiyat	23	22	56	101
Ras Ghanada	5	8	11	24
Total	28	33	86	147
$\chi^2 = 10.75273216$, df = 4, P-value = 0.029497				
Juvenile <i>Platygyra</i> spp.	Bleached	Partially bleached	Non bleached	Total
Dalma	0	0	12	12
Saadiyat	10	7	17	34
Ras Ghanada	14	10	31	55
Total	24	17	60	101
$\chi^2 = 9.659601028$, df = 4, P-value = 0.046569				

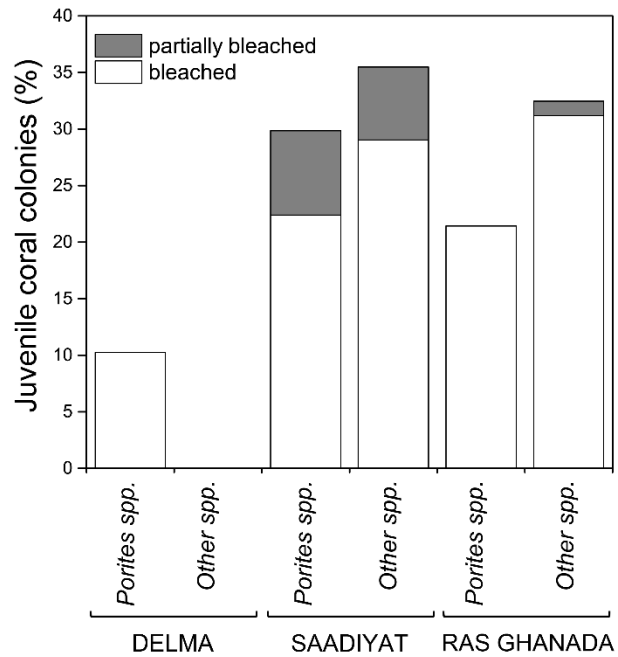
χ^2 = Chi-square value, df = degrees of freedom, P-value < 0.05 indicates that the recorded proportion of bleached, partially bleached and non-bleached colonies is significantly dependent on the region.



Supplementary Figure 1: SST data. (a) *In situ* temperature data recorded in hourly intervals at ~7m depth at the Saadiyat site. The graph shows the average temperatures and standard deviations calculated from the values obtained for the last week of August from the years 2013 and 2014. The arrows indicate the median time when the MODIS-Terra and -Aqua satellites record the IRSA region. (b-c) MODIS Aqua data and the corresponding *in situ* temperature values were plotted against each other and the coefficient of determination (R^2) for a linear regression fit was calculated. Equations are given in the graphs.



Supplementary Figure 2: Time series of regional SST in the southern IRSA. SST values were obtained from MODIS-Aqua imagery from 2002-2014 for (a) Delma, (b) Saadiyat and (c) Ras Ghanada. The local bleaching thresholds (Delma: 35.05°C, Saadiyat: 34.55°C and Ras Ghanada: 34.48°C) are indicated by horizontal dashed lines.



Supplementary Figure 3: Comparison of bleaching severity between juvenile *Porites* spp. and non-*Porites* spp. in the study sites. Numbers are provided in Supplementary table 2.

List of References

- Abdi Vishkaee, F., Flamant, C., Cuesta, J., Oolman, L., Flamant, P. and Khalesifard, H.R., 2012. Dust transport over Iraq and northwest Iran associated with winter Shamal: A case study. *Journal of Geophysical Research: Atmospheres*, 117(D3).
- Abuelgasim, A. and Alhosani, N., 2014. Mapping the seasonal variations of chlorophyll concentrations in the Arabian Gulf and the Gulf of Oman using MODIS satellite data. *The Arab World Geographer*, 17(1), pp.82-90.
- Abuelgasim, A. and Alhosani, N., 2014, July. Investigations of the seasonal and inter-annual variations of phytoplankton blooms in the Arabian Gulf using satellite data. In *Geoscience and Remote Sensing Symposium (IGARSS), 2014 IEEE International* (pp. 3874-3877). IEEE.
- Abu Dhabi Global Environmental Data Initiative, 2016. Marine and Coastal environment-of Abu Dhabi Emirate, United Arab Emirates.
- Ahmed, M., Umali, G.M., Chong, C.K., Rull, M.F. and Garcia, M.C., 2007. Valuing recreational and conservation benefits of coral reefs—The case of Bolinao, Philippines. *Ocean & Coastal Management*, 50(1), pp.103-118.
- Ainsworth, T.D., Kvennefors, E.C., Blackall, L.L., Fine, M. and Hoegh-Guldberg, O., 2007. Disease and cell death in white syndrome of Acroporid corals on the Great Barrier Reef. *Marine Biology*, 151(1), pp.19-29.
- Al-Ansi, M.A., Abdel-Moati, M.A.R. and Al-Ansari, I.S., 2002. Causes of fish mortality along the Qatari waters (Arabian Gulf). *International journal of environmental studies*, 59(1), pp.59-71.
- Al-Rashidi, T.B., 2009. *An analysis of drivers of seawater temperature in Kuwait Bay, Arabian Gulf* (Doctoral dissertation, University of Southampton).
- Al-Dousari, A.M., Al-Awadhi, J. and Ahmed, M., 2013. Dust fallout characteristics within global dust storm major trajectories. *Arabian Journal of Geosciences*, 6(10), pp.3877-3884.
- Al-Ghadban, A.N. and El-Sammak, A., 2005. Sources, distribution and composition of the suspended sediments, Kuwait Bay, Northern Arabian Gulf. *Journal of Arid Environments*, 60(4), pp.647-661.
- Almazroui, M., Islam, M.N., Jones, P.D., Athar, H. and Rahman, M.A., 2012. Recent climate change in the Arabian Peninsula: seasonal rainfall and temperature climatology of Saudi Arabia for 1979–2009. *Atmospheric Research*, 111, pp.29-45.
- Al-Rashidi, T.B., 2009. *An analysis of drivers of seawater temperature in Kuwait Bay, Arabian Gulf* (Doctoral dissertation, University of Southampton).
- Alsharhan, A.S. and Kendall, C.S.C., 2003. Holocene coastal carbonates and evaporites of the southern Arabian Gulf and their ancient analogues. *Earth-Science Reviews*, 61(3), pp.191-243.
- Al-Shehhi, M.R., Gherboudj, I. and Ghedira, H., 2012, July. A study on the effect of dust and wind on phytoplankton activities in the Arabian Gulf. In *Geoscience and Remote Sensing Symposium (IGARSS), 2012 IEEE International* (pp. 2571-2574). IEEE.
- Al-Yamani, F., Al-Ghunaim, D., Subba Rao, D.V., Khan, N., Al-Ghool, M., Muruppel, M., Al-Qatma, S. and Luis, M., 2000. Fish kills, red tides, and Kuwait's marine environment. *Kuwait Institute for Scientific Research, Kuwait*.
- Alexandridis, T.K., Lazaridou, E., Tsirika, A. and Zalidis, G.C., 2009. Using Earth

- Observation to update a Natura 2000 habitat map for a wetland in Greece. *Journal of Environmental Management*, 90(7), pp.2243-2251.
- Andréfouët, S., Dutheil, C., Menkes, C.E., Bador, M. and Lengaigne, M., 2015. Mass mortality events in atoll lagoons: environmental control and increased future vulnerability. *Global change biology*, 21(1), pp.195-205.
- Anderson, D.M., Glibert, P.M. and Burkholder, J.M., 2002. Harmful algal blooms and eutrophication: nutrient sources, composition, and consequences. *Estuaries*, 25(4), pp.704-726.
- Apel, E.C., Hornbrook, R.S., Hills, A.J., Blake, N.J., Barth, M.C., Weinheimer, A., Cantrell, C., Rutledge, S.A., Basarab, B., Crawford, J. and Diskin, G., 2015. Upper tropospheric ozone production from lightning NO_x-impacted convection: Smoke ingestion case study from the DC3 campaign. *Journal of Geophysical Research: Atmospheres*, 120(6), pp.2505-2523.
- Arimoto, R., 2001. Eolian dust and climate: relationships to sources, tropospheric chemistry, transport and deposition. *Earth-Science Reviews*, 54(1), pp.29-42.
- Arimoto, R., Duce, R.A., Ray, B.J., Ellis, W.G., Cullen, J.D. and Merrill, J.T., 1995. Trace elements in the atmosphere over the North Atlantic. *Journal of Geophysical Research: Atmospheres*, 100(D1), pp.1199-1213.
- Arimoto, R.I.C.H.A.R.D., Duce, R.A. and Ray, B.J., 1989. Concentrations, sources and air-sea exchange of trace elements in the atmosphere over the Pacific Ocean. *Chemical Oceanography*, 10, pp.107-149.
- Arnal, D. and Cortet, J.C., 1985. Nilpotent Fourier transform and applications. *letters in mathematical physics*, 9(1), pp.25-34.
- Austin, R.W. and Petzold, T.J., 1986. Spectral dependence of the diffuse attenuation coefficient of light in ocean waters. *Optical Engineering*, 25(3), pp.253471-253471.
- Ayoub, M., Ackermann, L., Skillern, A. and Strickland, J., 2016, March. 2015, A Year of Climate and Air Quality Anomalies. In *Qatar Foundation Annual Research Conference Proceedings* (Vol. 2016, No. 1, p. EEPP2916). Qatar: HBKU Press.
- Baker, A.C., 2001. Ecosystems: reef corals bleach to survive change. *Nature*, 411(6839), p.765.
- Baker, A.C., Glynn, P.W. and Riegl, B., 2008. Climate change and coral reef bleaching: An ecological assessment of long-term impacts, recovery trends and future outlook. *Estuarine, coastal and shelf science*, 80(4), pp.435-471.
- Baker, A.C., Starger, C.J., McClanahan, T.R. and Glynn, P.W., 2002. Symbiont communities in reef corals following the 1997–98 El Nino—will recovering reefs be more resistant to a subsequent bleaching event. In *Proc Int Soc Reef Studies Eur Meeting, Cambridge, Sept, Abstr* (Vol. 10).
- Barrett, E.C., 2013. *Introduction to environmental remote sensing*. Routledge.
- Bauman, A.G., Baird, A.H., Burt, J.A., Pratchett, M.S. and Feary, D.A., 2014. Patterns of coral settlement in an extreme environment: the southern Persian Gulf (Dubai, United Arab Emirates). *Marine Ecology Progress Series*, 499, pp.115-126.
- Bauman, A.G., Feary, D.A., Heron, S.F., Pratchett, M.S. and Burt, J.A., 2013. Multiple environmental factors influence the spatial distribution and structure of reef communities in the northeastern Arabian Peninsula. *Marine pollution bulletin*, 72(2), pp.302-312.
- Bauman, A.G., Pratchett, M.S., Baird, A.H., Riegl, B., Heron, S.F. and Feary, D.A., 2013.

- Variation in the size structure of corals is related to environmental extremes in the Persian Gulf. *Marine environmental research*, 84, pp.43-50.
- Bell, P.R., Lapointe, B.E. and Elmetri, I., 2007. Reevaluation of ENCORE: Support for the eutrophication threshold model for coral reefs. *AMBIO: A Journal of the Human Environment*, 36(5), pp.416-424.
- Ben-Romdhane, H., Marpu, P.R., Ouarda, T.B. and Ghedira, H., 2016. Corals & benthic habitat mapping using DubaiSat-2: a spectral-spatial approach applied to Dalma Island, UAE (Arabian Gulf). *Remote Sensing Letters*, 7(8), pp.781-789.
- Bennion, P., Hubbard, R., O'hara, S., Wiggs, G., Wegerdt, J., Lewis, S., Small, I., van der Meer, J. and Upshur, R., 2007. The impact of airborne dust on respiratory health in children living in the Aral Sea region. *International journal of epidemiology*, 36(5), pp.1103-1110.
- Berkelmans, R. and Willis, B.L., 1999. Seasonal and local spatial patterns in the upper thermal limits of corals on the inshore Central Great Barrier Reef. *Coral Reefs*, 18(3), pp.219-228.
- Berkelmans, R., 2009. Bleaching and mortality thresholds: how much is too much?. *Coral bleaching*, pp.103-119.
- Bernstein, R. and Stevens, P., 1986. Ocean remote sensing. *Space science and applications: Progress and potential*(A 87-30876 12-12). New York, IEEE Press, 1986,, pp.123-131.
- Blondeau-Patissier, D., Gower, J.F., Dekker, A.G., Phinn, S.R. and Brando, V.E., 2014. A review of ocean color remote sensing methods and statistical techniques for the detection, mapping and analysis of phytoplankton blooms in coastal and open oceans. *Progress in oceanography*, 123, pp.123-144.
- Bots, O.C.P., 2013. Understanding and modeling the process of resuspension of fines in the coastal zone; case Khalifa Port.
- Bracewell, R.N. and Bracewell, R.N., 1986. *The Fourier transform and its applications* (Vol. 31999). New York: McGraw-Hill.
- Brest, C.L. and Goward, S.N., 1987. Deriving surface albedo measurements from narrow band satellite data. *International Journal of Remote Sensing*, 8(3), pp.351-367.
- Brown, B.E., Dunne, R.P., Scoffin, T.P. and Le Tissier, M.D.A., 1994. Solar damage in intertidal corals. *Marine Ecology Progress Series*, pp.219-230.
- Brown, B.E., 1997. Coral bleaching: causes and consequences. *Coral reefs*, 16(5), pp.S129-S138.
- Brown, B., Dunne, R., Goodson, M. and Douglas, A., 2002. Experience shapes the susceptibility of a reef coral to bleaching. *Coral Reefs*, 21(2), pp.119-126.
- Brodie, J.E., Devlin, M., Haynes, D. and Waterhouse, J., 2011. Assessment of the eutrophication status of the Great Barrier Reef lagoon (Australia). *Biogeochemistry*, 106(2), pp.281-302.
- Bruno, J.F., Petes, L.E., Drew Harvell, C. and Hettinger, A., 2003. Nutrient enrichment can increase the severity of coral diseases. *Ecology letters*, 6(12), pp.1056-1061.
- Bruckner, A.W. and Hill, R.L., 2009. Ten years of change to coral communities off Mona and Desecheo Islands, Puerto Rico, from disease and bleaching. *Diseases of Aquatic Organisms*, 87(1-2), pp.19-31.
- Brzezinski, M.A. and Nelson, D.M., 1995. The annual silica cycle in the Sargasso Sea near Bermuda. *Deep Sea Research Part I: Oceanographic Research Papers*, 42(7),

- pp.1215-1237.
- Budd, A.F., Fukami, H., Smith, N.D. and Knowlton, N., 2012. Taxonomic classification of the reef coral family Mussidae (Cnidaria: Anthozoa: Scleractinia). *Zoological Journal of the Linnean Society*, 166(3), pp.465-529.
- Burt, J., Bartholomew, A. and Usseglio, P., 2008. Recovery of corals a decade after a bleaching event in Dubai, United Arab Emirates. *Marine Biology*, 154(1), pp.27-36.
- Burt, J., Al-Harthi, S. and Al-Cibahy, A., 2011. Long-term impacts of coral bleaching events on the world's warmest reefs. *Marine environmental research*, 72(4), pp.225-229.
- Burt, J., Van Lavieren, H. and Feary, D., 2014. Persian Gulf reefs: an important asset for climate science in urgent need of protection. *Ocean Challenge*, 20, pp.49-56.
- Burt, J.A., 2014. The environmental costs of coastal urbanization in the Arabian Gulf. *City*, 18(6), pp.760-770.
- Butler, A., 1998. Acquisition and utilization of transition metal ions by marine organisms. *Science*, 281(5374), pp.207-209.
- Butler, E.C.V., Butt, J.A., Lindstrom, E.J., Teldesley, P.C., Pickmere, S. and Vincent, W.F., 1992. Oceanography of the subtropical convergence zone around southern New Zealand. *New Zealand Journal of Marine and Freshwater Research*, 26(2), pp.131-154.
- Cavalcante, G.H., Feary, D.A. and Burt, J.A., 2016. The influence of extreme winds on coastal oceanography and its implications for coral population connectivity in the southern Arabian Gulf. *Marine pollution bulletin*, 105(2), pp.489-497.
- Chang, H., Richardson, K., Uddstrom, M. and Pinkerton, M., 2005. Eye in the sky: tracking harmful algal blooms with satellite remote sensing. *Water Atmos*, 13, pp.14-15.
- Chao, S.Y., Kao, T.W. and Al-Hajri, K.R., 1992. A numerical investigation of circulation in the Arabian Gulf. *Journal of Geophysical Research: Oceans*, 97(C7), pp.11219-11236.
- Chattopadhyay, J., Sarkar, R.R. and El Abdllaoui, A., 2002. A delay differential equation model on harmful algal blooms in the presence of toxic substances. *Mathematical Medicine and Biology*, 19(2), pp.137-161.
- Chu, D.A., Kaufman, Y.J., Ichoku, C., Remer, L.A., Tanré, D. and Holben, B.N., 2002. Validation of MODIS aerosol optical depth retrieval over land. *Geophysical research letters*, 29(12).
- Chung, Y.S. and Yoon, M.B., 1996. On the occurrence of yellow sand and atmospheric loadings. *Atmospheric Environment*, 30(13), pp.2387-2397.
- Claereboudt, M.R., 2006. *Reef corals and coral reefs of the Gulf of Oman*. Historical Association of Oman.
- Claustre, H. and Maritorena, S., 2003. The many shades of ocean blue. *Science*, 302(5650), pp.1514-1515.
- Clemens, S. and Prell, W., 1991. Forcing mechanisms of the Indian Ocean monsoon. *Nature*, 353(6346), p.720.
- Cole, P. and Broderick, M., 2007. Environmental Impact Assessment (EIA) and Strategic Environmental Assessment (SEA): an exploration of synergies through development of a Strategic Environmental Framework (SEF). *WIT Transactions on Ecology and the Environment*, 102.
- Coles, S.L., 2003. Coral species diversity and environmental factors in the Arabian Gulf

- and the Gulf of Oman: A comparison to the Indo-Pacific region. *Atoll Research Bulletin*, 507, 1–19
- Coles, S.L. and Fadlallah, Y.H., 1991. Reef coral survival and mortality at low temperatures in the Arabian Gulf: new species-specific lower temperature limits. *Coral Reefs*, 9(4), pp.231-237.
- Coles, S.L. and Jokiel, P.L., 1978. Synergistic effects of temperature, salinity and light on the hermatypic coral *Montipora verrucosa*. *Marine Biology*, 49(3), pp.187-195.
- Coles, S.L. and Riegl, B.M., 2013. Thermal tolerances of reef corals in the Gulf: A review of the potential for increasing coral survival and adaptation to climate change through assisted translocation. *Marine pollution bulletin*, 72(2), pp.323-332.
- Colwell, R.N., 1983. *Manual of remote sensing*. American Society of Photogrammetry.
- Connell, J.H., 1978. Diversity in tropical rain forests and coral reefs. *Science*, 199(4335), pp.1302-1310.
- Conley, D.J. and Malone, T.C., 1992. Annual cycle of dissolved silicate in Chesapeake Bay: implications for the production and fate of phytoplankton biomass. *Marine Ecology Progress Series*, pp.121-128.
- Cooper, T.F., Ridd, P.V., Ulstrup, K.E., Humphrey, C., Slivkoff, M. and Fabricius, K.E., 2008. Temporal dynamics in coral bioindicators for water quality on coastal coral reefs of the Great Barrier Reef. *Marine and Freshwater Research*, 59(8), pp.703-716.
- Crossland, C.J., 1984. Seasonal variations in the rates of calcification and productivity in the coral *Acropora formosa* on a high-latitude reef. *Marine ecology progress series*, pp.135-140.
- Cunning, R. and Baker, A.C., 2013. Excess algal symbionts increase the susceptibility of reef corals to bleaching. *Nature Climate Change*, 3(3), pp.259-262.
- Cullen, J.J., 1982. The deep chlorophyll maximum: comparing vertical profiles of chlorophyll a. *Canadian Journal of Fisheries and Aquatic Sciences*, 39(5), pp.791-803.
- Davis, T.W., Bullerjahn, G.S., Tuttle, T., McKay, R.M. and Watson, S.B., 2015. Effects of increasing nitrogen and phosphorus concentrations on phytoplankton community growth and toxicity during *Planktothrix* blooms in Sandusky Bay, Lake Erie. *Environmental science & technology*, 49(12), pp.7197-7207.
- D'angelo, C., Hume, B.C., Burt, J., Smith, E.G., Achterberg, E.P. and Wiedenmann, J., 2015. Local adaptation constrains the distribution potential of heat-tolerant *Symbiodinium* from the Persian/Arabian Gulf. *The ISME journal*, 9(12), p.2551.
- D'Angelo, C. and Wiedenmann, J., 2014. Impacts of nutrient enrichment on coral reefs: new perspectives and implications for coastal management and reef survival. *Current Opinion in Environmental Sustainability*, 7, pp.82-93.
- D'Angelo, C., Smith, E.G., Oswald, F., Burt, J., Tchernov, D. and Wiedenmann, J., 2012. Locally accelerated growth is part of the innate immune response and repair mechanisms in reef-building corals as detected by green fluorescent protein (GFP)-like pigments. *Coral reefs*, 31(4), pp.1045-1056.
- Davis, K.A., Lentz, S.J., Pineda, J., Farrar, J.T., Starczak, V.R., Churchill, J.H., 2011. Observations of the thermal environment on Red Sea platform reefs: a heat budget analysis. *Coral Reefs* 30, 25–36.
- Dawson, T.P., Jackson, S.T., House, J.I., Prentice, I.C. and Mace, G.M., 2011. Beyond predictions: biodiversity conservation in a changing climate. *science*, 332(6025),

- pp.53-58.
- Dayan, U., Heffter, J., Miller, J. and Gutman, G., 1991. Dust intrusion events into the Mediterranean basin. *Journal of Applied Meteorology*, 30(8), pp.1185-1199.
- Dennison, W.C. and Barnes, D.J., 1988. Effect of water motion on coral photosynthesis and calcification. *Journal of Experimental Marine Biology and Ecology*, 115(1), pp.67-77.
- Denner, E.B., Smith, G.W., Busse, H.J., Schumann, P., Narzt, T., Polson, S.W., Lubitz, W. and Richardson, L.L., 2003. *Aurantimonas coralicida* gen. nov., sp. nov., the causative agent of white plague type II on Caribbean scleractinian corals. *International journal of systematic and evolutionary microbiology*, 53(4), pp.1115-1122.
- Devara, P.C.S. and Manoj, M.G., 2013. Aerosol–cloud–precipitation interactions: A challenging problem in regional environment and climate research. *Particuology*, 11(1), pp.25-33.
- Douglas, A.E., 2003. Coral bleaching—how and why?. *Marine Pollution Bulletin*, 46(4), pp.385-392.
- Downing, N. and Roberts, C., 1993. Has the Gulf War affected coral reefs of the northwestern Gulf?. *Marine Pollution Bulletin*, 27, pp.149-156.
- Dubinsky, Z. and Falkowski, P., 2011. Light as a source of information and energy in zooxanthellate corals. In *Coral Reefs: An Ecosystem in Transition*(pp. 107-118). Springer Netherlands.
- Dubinsky, Z. and Jokiel, P.L., 1994. Ratio of energy and nutrient fluxes regulates symbiosis between zooxanthellae and corals.
- Duce, R.A., Ray, B.J., Hoffman, G.L. and Walsh, P.R., 1976. Trace metal concentration as a function of particle size in marine aerosols from Bermuda. *Geophysical Research Letters*, 3(6), pp.339-342.
- Duce, R.A. and Tindale, N.W., 1991. Atmospheric transport of iron and its deposition in the ocean. *Limnology and Oceanography*, 36(8), pp.1715-1726.
- Dugdale, R.C., Wilkerson, F.P. and Minas, H.J., 1995. The role of a silicate pump in driving new production. *Deep Sea Research Part I: Oceanographic Research Papers*, 42(5), pp.697-719.
- Environmental Agency Abu Dhabi, UAE, 2015. Marine water quality 2nd Quarterly Report 2015.
- Esmail, M.A., Fathallah, H. and Alouini, M.S., 2016. An experimental study of FSO link performance in desert environment. *IEEE Communications Letters*, 20(9), pp.1888-1891.
- Fabricius, K.E., Cooper, T.F., Humphrey, C., Uthicke, S., De'ath, G., Davidson, J., LeGrand, H., Thompson, A. and Schaffelke, B., 2012. A bioindicator system for water quality on inshore coral reefs of the Great Barrier Reef. *Marine Pollution Bulletin*, 65(4), pp.320-332.
- Fabricius, K.E., Cséke, S., Humphrey, C. and De'ath, G., 2013. Does Trophic Status Enhance or Reduce the Thermal Tolerance of Scleractinian Corals. *A Review*.
- Fabricius, K.E., Okaji, K. and De'Ath, G., 2010. Three lines of evidence to link outbreaks of the crown-of-thorns seastar *Acanthaster planci* to the release of larval food limitation. *Coral Reefs*, 29(3), pp.593-605.
- Fadlallah, Y.H., Allen, K.W. and Estudillo, R.A., 1995. Mortality of shallow reef corals in the western Arabian Gulf following aerial exposure in winter. *Coral Reefs*, 14(2), pp.99-107.

- Feldman, G., Kuring, N., Ng, C., Esaias, W., McClain, C., Elrod, J., Maynard, N., Endres, D., Evans, R., Brown, J. and Walsh, S., 1989. Ocean color: availability of the global data set. *Eos, Transactions American Geophysical Union*, 70(23), pp.634-641.
- Feldman, G. and Halpern, D., 1984. Satellite color observations of the phytoplankton distribution in the eastern equatorial Pacific during the 1982-1983 El Nino. *Science*, 226, pp.1069-1072.
- Fitt, W.K., Brown, B.E., Warner, M.E. and Dunne, R.P., 2001. Coral bleaching: interpretation of thermal tolerance limits and thermal thresholds in tropical corals. *Coral reefs*, 20(1), pp.51-65.
- Foster, K., Foster, G., Al-Cibahy, A.S., Al-Harthi, S., Purkis, S.J. and Riegl, B.M., 2012. Environmental setting and temporal trends in southeastern Gulf coral communities. In *Coral Reefs of the Gulf* (pp. 51-70). Springer Netherlands.
- Franz, B.A., Werdell, P.J., Meister, G., Bailey, S.W., Eplee, R.E., Feldman, G.C., Kwiatkowskaa, E., McClain, C.R., Patt, F.S. and Thomas, D., 2005, July. The continuity of ocean color measurements from SeaWiFS to MODIS. In *Proc. SPIE* (Vol. 5882, No. 1, p. 68820W).
- Fryrear, D.W., 1981. Long-term effect of erosion and cropping on soil productivity. *Geological Society of America Special Papers*, 186, pp.253-260.
- Furman, H.K.H., 2003. Dust storms in the Middle East: sources of origin and their temporal characteristics. *Indoor and Built Environment*, 12(6), pp.419-426.
- Furnas, M., Mitchell, A., Skuza, M. and Brodie, J., 2005. In the other 90%: phytoplankton responses to enhanced nutrient availability in the Great Barrier Reef Lagoon. *Marine pollution bulletin*, 51(1), pp.253-265.
- Furnas, M.J., Mitchell, A.W. and Skuza, M., 1995. *Nitrogen and phosphorus budgets for the central Great Barrier Reef shelf*. Great Barrier Reef Marine Park Authority.
- Gardner, S.G., Nielsen, D.A., Laczka, O., Shimmon, R., Beltran, V.H., Ralph, P.J. and Petrou, K., 2016, February. Dimethylsulfoniopropionate, superoxide dismutase and glutathione as stress response indicators in three corals under short-term hyposalinity stress. In *Proc. R. Soc. B* (Vol. 283, No. 1824, p. 20152418). The Royal Society.
- Garrison, V.H., Shinn, E.A., Foreman, W.T., Griffin, D.W., Holmes, C.W., Kellogg, C.A., Majewski, M.S., Richardson, L.L., Ritchie, K.B. and Smith, G.W., 2003. African and Asian dust: from desert soils to coral reefs. *AIBS Bulletin*, 53(5), pp.469-480.
- Garrison, T.S., 2012. *Essentials of oceanography*. Cengage Learning.
- Genin, A., Lazar, B. and Brenner, S., 1995. Vertical mixing and coral death in the Red Sea following the eruption of Mount Pinatubo. *Nature*, 377(6549), pp.507-510.
- George, J.D. and John, D.M., 2000, April. The coral reefs of Abu Dhabi, United Arab Emirates: past, present and future. In *Proc 2nd Arab Int Conf Exhib Environment Biotechnol (Coastal Habitats), Abu Dhabi*.
- George, J.D. and John, D.M., 1999. High sea temperatures along the coast of Abu Dhabi (UAE), Arabian Gulf—their impact upon corals and macroalgae. *Reef Encounter*, 25, pp.21-23.
- George, J.D. and John, D.M., 1998. A preliminary report on the condition of the coral reefs at Bu Tini shoals and at other locations in Abu Dhabi. A report for His Highness Sheikh Hamdan bin Zayed Al Nahyan. *The Natural History Museum, London*, 15pp.
- George, J.D., John, D.M., Abuzinada, A.H., Joubert, E. and Krupp, F., 2005. The status of coral reefs and associated macroalgae in Abu Dhabi (UAE) after recent coral

- bleaching events.
- Ginoux, P., Chin, M., Tegen, I., Prospero, J.M., Holben, B., Dubovik, O. and Lin, S.J., 2001. Sources and distributions of dust aerosols simulated with the GOCART model. *Journal of Geophysical Research: Atmospheres*, 106(D17), pp.20255-20273.
- Glibert, P.M., Landsberg, J.H., Evans, J.J., Al-Sarawi, M.A., Faraj, M., Al-Jarallah, M.A., Haywood, A., Ibrahim, S., Klesius, P., Powell, C. and Shoemaker, C., 2002. A fish kill of massive proportion in Kuwait Bay, Arabian Gulf, 2001: the roles of bacterial disease, harmful algae, and eutrophication. *Harmful Algae*, 1(2), pp.215-231.
- Glynn, P.W. and D'croz, L., 1990. Experimental evidence for high temperature stress as the cause of El Nino-coincident coral mortality. *Coral reefs*, 8(4), pp.181-191.
- Gong, S.L., Zhang, X.Y., Zhao, T.L., McKendry, I.G., Jaffe, D.A. and Lu, N.M., 2003. Characterization of soil dust aerosol in China and its transport and distribution during 2001 ACE-Asia: 2. Model simulation and validation. *Journal of Geophysical Research: Atmospheres*, 108(D9).
- Goreau, T., McClanahan, T., Hayes, R. and Strong, A.L., 2000. Conservation of coral reefs after the 1998 global bleaching event. *Conservation Biology*, 14(1), pp.5-15.
- Goreau, T.J. and Hayes, R.L., 1994. Coral bleaching and ocean "hot spots". *Ambio-Journal of Human Environment Research and Management*, 23(3), pp.176-180.
- Gordon, H.R., Clark, D.K., Brown, J.W., Brown, O.B., Evans, R.H. and Broenkow, W.W., 1983. Phytoplankton pigment concentrations in the Middle Atlantic Bight: comparison of ship determinations and CZCS estimates. *Applied optics*, 22(1), pp.20-36.
- Graedel, T.E., Mandich, M.L. and Weschler, C.J., 1986. Kinetic model studies of atmospheric droplet chemistry: 2. Homogeneous transition metal chemistry in raindrops. *Journal of Geophysical Research: Atmospheres*, 91(D4), pp.5205-5221.
- Gregg, W.W. and Casey, N.W., 2007. Sampling biases in MODIS and SeaWiFS ocean chlorophyll data. *Remote Sensing of Environment*, 111(1), pp.25-35.
- Guerzoni, S., Chester, R., Dulac, F., Herut, B., Loÿe-Pilot, M.D., Measures, C., Migon, C., Molinaroli, E., Moulin, C., Rossini, P. and Saydam, C., 1999. The role of atmospheric deposition in the biogeochemistry of the Mediterranean Sea. *Progress in Oceanography*, 44(1), pp.147-190.
- Guest, J.R., Baird, A.H., Maynard, J.A., Muttaqin, E., Edwards, A.J., Campbell, S.J., Yewdall, K., Affendi, Y.A. and Chou, L.M., 2012. Contrasting patterns of coral bleaching susceptibility in 2010 suggest an adaptive response to thermal stress. *PloS one*, 7(3), p.e33353.
- Hallegraeff, G.M., 1993. A review of harmful algal blooms and their apparent global increase. *Phycologia*, 32(2), pp.79-99.
- Hamza, W., Enan, M.R., Al-Hassini, H., Stuut, J.B. and de-Beer, D., 2011. Dust storms over the Arabian Gulf: a possible indicator of climate changes consequences. *Aquatic ecosystem health & management*, 14(3), pp.260-268.
- Hamza, W., 2008. Nutritive contribution of Sahara dust to aquatic environment productivity: A laboratory experimental approach. *Verhandlungen der Internationalen Vereinigung für Theoretische und Angewandte Limnologie*, 30(1), p.82.
- Hagen, L.J. and Woodruff, N.P., 1973. Air pollution from duststorms in the Great Plains. *Atmospheric Environment (1967)*, 7(3), pp.323-332.

- Hodgson, G. and Carpenter, K.E., 1995. Scleractinian corals of Kuwait. *Pacific Science*, 49(3).
- Hoegh-Guldberg, O., 1999. Climate change, coral bleaching and the future of the world's coral reefs. *Marine and freshwater research*, 50(8), pp.839-866.
- Hoegh-Guldberg, O., Mumby, P.J., Hooten, A.J., Steneck, R.S., Greenfield, P., Gomez, E., Harvell, C.D., Sale, P.F., Edwards, A.J., Caldeira, K. and Knowlton, N., 2007. Coral reefs under rapid climate change and ocean acidification. *science*, 318(5857), pp.1737-1742.
- Hovis, W.A., Clark, D.K., Anderson, F., Austin, R.W., Wilson, W.H., Baker, E.T., Ball, D., Gordon, H.R., Mueller, J.L., El-Sayed, S.Z. and Sturm, B., 1980. Nimbus-7 Coastal Zone Color Scanner: system description and initial imagery. *Science*, 210(4465), pp.60-63.
- Howells, E.J., Ketchum, R.N., Bauman, A.G., Mustafa, Y., Watkins, K.D. and Burt, J.A., 2016. Species-specific trends in the reproductive output of corals across environmental gradients and bleaching histories. *Marine pollution bulletin*, 105(2), pp.532-539.
- Hu, C., Carder, K.L. and Muller-Karger, F.E., 2001. How precise are SeaWiFS ocean color estimates? Implications of digitization-noise errors. *Remote Sensing of Environment*, 76(2), pp.239-249.
- Hughes, T.P., Baird, A.H., Bellwood, D.R., Card, M., Connolly, S.R., Folke, C., Grosberg, R., Hoegh-Guldberg, O., Jackson, J.B.C., Kleypas, J. and Lough, J.M., 2003. Climate change, human impacts, and the resilience of coral reefs. *science*, 301(5635), pp.929-933.
- Hume, B.C., Voolstra, C.R., Arif, C., D'Angelo, C., Burt, J.A., Eyal, G., Loya, Y. and Wiedenmann, J., 2016. Ancestral genetic diversity associated with the rapid spread of stress-tolerant coral symbionts in response to Holocene climate change. *Proceedings of the National Academy of Sciences*, 113(16), pp.4416-4421.
- Hume, B.C., D'Angelo, C., Smith, E.G., Stevens, J.R., Burt, J. and Wiedenmann, J., 2015. *Symbiodinium thermophilum* sp. nov., a thermotolerant symbiotic alga prevalent in corals of the world's hottest sea, the Persian/Arabian Gulf. *Scientific reports*, 5.
- Hunter, J.R., 1982, February. The physical oceanography of the Arabian Gulf: a review and theoretical interpretation of previous observations. In *The first Arabian Gulf conference on environment and pollution*. Kuwait University, Faculty of Science, Kuwait (pp. 1-23).
- Husar, R.B., Prospero, J.M. and Stowe, L.L., 1997. Characterization of tropospheric aerosols over the oceans with the NOAA advanced very high resolution radiometer optical thickness operational product. *Journal of Geophysical Research: Atmospheres*, 102(D14), pp.16889-16909.
- Husar, R.B., Tratt, D.M., Schichtel, B.A., Falke, S.R., Li, F., Jaffe, D., Gasso, S., Gill, T., Laulainen, N.S., Lu, F. and Reheis, M.C., 2001. Asian dust events of April 1998. *Journal of Geophysical Research: Atmospheres*, 106(D16), pp.18317-18330.
- Islam, S., 2015. Modelling the effects of cyclonic storm surge and wave action on selected coastal embankments.
- Jerlov, N.G., 1976. Marine optics, Elsevier Oceanography Series 14.
- Jickells, T.D., 1999. The inputs of dust derived elements to the Sargasso Sea; a synthesis. *Marine Chemistry*, 68(1), pp.5-14.

- Jickells, T.D., An, Z.S., Andersen, K.K., Baker, A.R., Bergametti, G., Brooks, N., Cao, J.J., Boyd, P.W., Duce, R.A., Hunter, K.A. and Kawahata, H., 2005. Global iron connections between desert dust, ocean biogeochemistry, and climate. *science*, 308(5718), pp.67-71.
- John, V.C., Coles, S.L. and Abozed, A.I., 1990. Seasonal cycles of temperature, salinity and water masses of the western Arabian Gulf. *Oceanologica Acta*, 13(3), pp.273-281.
- Jokiel, P.L., 1978. Effects of water motion on reef corals. *Journal of Experimental Marine Biology and Ecology*, 35(1), pp.87-97.
- Jokiel, P.L. and Coles, S.L., 1977. Effects of temperature on the mortality and growth of Hawaiian reef corals. *Marine Biology*, 43(3), pp.201-208.
- Kaimal, J.C. and Finnigan, J.J., 1994. *Atmospheric boundary layer flows: their structure and measurement*. Oxford university press.
- Kaufman, Y.J., Tanre, D. and Boucher, O., 2002. A satellite view of aerosols in the climate system. *Nature* 419, 215e223.
- Kavouras, I.G., Etyemezian, V., DuBois, D.W., Xu, J. and Pitchford, M., 2009. Source reconciliation of atmospheric dust causing visibility impairment in Class I areas of the western United States. *Journal of Geophysical Research: Atmospheres*, 114(D2).
- Kendell, C.S.C., Lakshmi, V., Althausen, J. and Alsharhan, A.S., 2003. Changes in microclimate tracked by the evolving vegetation cover of the Holocene beach ridges of the United Arab Emirates. *Desertification in the Third Millennium*, pp.91-98.
- Kendall, J.J., Powell, E.N., Connor, S.J., Bright, T.J. and Zastrow, C.E., 1985. Effects of turbidity on calcification rate, protein concentration and the free amino acid pool of the coral *Acropora cervicornis*. *Marine Biology*, 87(1), pp.33-46.
- Khan, N.N.Y., Munawar, M. and Price, A.R. eds., 2002. *The gulf ecosystem: Health and sustainability*. Backhuys.
- Kidder, S.Q. and Haar, T.H.V., 1995. *Satellite meteorology: an introduction*. Gulf Professional Publishing.
- Kinsman, D.J.J., 1964. Reef coral tolerance of high temperatures and salinities. *Nature*, 202(4939), pp.1280-1282.
- Kirk, J.T., 1994. *Light and photosynthesis in aquatic ecosystems*. Cambridge university press.
- Knowlton, N. and Jackson, J.B., 2008. Shifting baselines, local impacts, and global change on coral reefs. *PLoS biology*, 6(2), p.e54.
- Korrubel, J.L. and Riegl, B., 1998. A new coral disease from the southern Arabian Gulf. *Coral reefs*, 17(1), pp.22-22.
- Kukal, Z. and Saadallah, A., 1973. Aeolian admixtures in the sediments of the northern Persian Gulf. In *The Persian Gulf* (pp. 115-121). Springer Berlin Heidelberg.
- Kushmaro, A., Banin, E., Loya, Y., Stackebrandt, E. and Rosenberg, E., 2001. *Vibrio shiloi* sp. nov., the causative agent of bleaching of the coral *Oculina patagonica*. *International journal of systematic and evolutionary microbiology*, 51(4), pp.1383-1388.
- Kuta, K. and Richardson, L., 2002. Ecological aspects of black band disease of corals: relationships between disease incidence and environmental factors. *Coral Reefs*, 21(4), pp.393-398.
- Landsberg, J.H., 2002. The effects of harmful algal blooms on aquatic organisms. *Reviews*

- in *Fisheries Science*, 10(2), pp.113-390.
- Lau, K.M. and Kim, K.M., 2006. Observational relationships between aerosol and Asian monsoon rainfall, and circulation. *Geophysical Research Letters*, 33(21).
- Lesser, M.P., 2004. Experimental biology of coral reef ecosystems. *Journal of Experimental Marine Biology and Ecology*, 300(1), pp.217-252.
- Lesser, M.P., 1996. Elevated temperatures and ultraviolet radiation cause oxidative stress and inhibit photosynthesis in symbiotic dinoflagellates. *Limnology and oceanography*, 41(2), pp.271-283.
- Lesser, M.P., Weis, V.M., Patterson, M.R. and Jokiel, P.L., 1994. Effects of morphology and water motion on carbon delivery and productivity in the reef coral, *Pocillopora damicornis* (Linnaeus): diffusion barriers, inorganic carbon limitation, and biochemical plasticity. *Journal of Experimental Marine Biology and Ecology*, 178(2), pp.153-179.
- Lesser, M.P., 2006. Oxidative stress in marine environments: biochemistry and physiological ecology. *Annu. Rev. Physiol.*, 68, pp.253-278.
- Liu, G., Heron, S.F., Eakin, C.M., Muller-Karger, F.E., Vega-Rodriguez, M., Guild, L.S., De La Cour, J.L., Geiger, E.F., Skirving, W.J., Burgess, T.F. and Strong, A.E., 2014. Reef-scale thermal stress monitoring of coral ecosystems: new 5-km global products from NOAA Coral Reef Watch. *Remote Sensing*, 6(11), pp.11579-11606.
- Logan, C.A., Dunne, J.P., Eakin, C.M. and Donner, S.D., 2014. Incorporating adaptive responses into future projections of coral bleaching. *Global Change Biology*, 20(1), pp.125-139.
- Loya, Y., Sakai, K., Yamazato, K., Nakano, Y., Sambali, H. and van Woesik, R., 2001. Coral bleaching: the winners and the losers. *Ecology letters*, 4(2), pp.122-131.
- Lyle, M.W., Prahl, F.G. and Sparrow, M.A., 1992. Upwelling and productivity changes inferred from a temperature record in the central equatorial Pacific. *Nature*, 355(6363), pp.812-815.
- Mahowald, N.M., Baker, A.R., Bergametti, G., Brooks, N., Duce, R.A., Jickells, T.D., Kubilay, N., Prospero, J.M. and Tegen, I., 2005. Atmospheric global dust cycle and iron inputs to the ocean. *Global biogeochemical cycles*, 19(4).
- Mahowald, N.M. and Luo, C., 2003. A less dusty future?. *Geophysical Research Letters*, 30(17).
- Maina, J., Venus, V., McClanahan, T.R. and Ateweberhan, M., 2008. Modelling susceptibility of coral reefs to environmental stress using remote sensing data and GIS models. *Ecological modelling*, 212(3), pp.180-199.
- Malone, T.C., Crocker, L.H., Pike, S.E. and Wendler, B.W., 1988. Influences of river flow on the dynamics of phytoplankton production in a partially stratified estuary. *Marine Ecology Progress Series*, pp.235-249.
- Manzello, D., Enochs, I., Musielewicz, S., Carlton, R. and Gledhill, D., 2013. Tropical cyclones cause CaCO₃ undersaturation of coral reef seawater in a high-CO₂ world. *Journal of Geophysical Research: Oceans*, 118(10), pp.5312-5321.
- Martin, J.H., 1990. Glacial-interglacial CO₂ change: The iron hypothesis. *Paleoceanography*, 5(1), pp.1-13.
- Martin, J.H., Coale, K.H., Johnson, K.S., Fitzwater, S.E., Gordon, R.M., Tanner, S.J., Hunter, C.N., Elrod, V.A., Nowicki, J.L., Coley, T.L. and Barber, R.T., 1994. Testing the iron hypothesis in ecosystems of the equatorial Pacific Ocean. *Nature*, 371(6493),

- pp.123-129.
- Marcello, J., Eugenio, F. and Hernández, A., 2004, September. Validation of MODIS and AVHRR/3 sea surface temperature retrieval algorithms. In *Geoscience and Remote Sensing Symposium, 2004. IGARSS'04. Proceedings. 2004 IEEE International* (Vol. 2, pp. 839-842). IEEE.
- Martin, J.H., 1990. Glacial-interglacial CO₂ change: The iron hypothesis. *Paleoceanography*, 5(1), pp.1-13.
- Martin, S., 2014. *An introduction to ocean remote sensing*. Cambridge University Press.
- Marshall, P.A., Baird, A.H., 2000. Bleaching of corals on the Great Barrier Reef: differential susceptibilities among taxa. *Coral Reefs* 19, 155–163.
- Markaki, Z., Oikonomou, K., Kocak, M., Kouvarakis, G., Chaniotaki, A., Kubilay, N. and Mihalopoulos, N., 2003. Atmospheric deposition of inorganic phosphorus in the Levantine Basin, eastern Mediterranean: Spatial and temporal variability and its role in productivity. *Limnology and Oceanography*, 48(4), pp.1557-1568.
- Mayor, A.G., 1914. *The effects of temperature upon tropical marine animals*. Carnegie Institution of Washington.
- Maynard, J.A., Turner, P.J., Anthony, K., Baird, A.H., Berkelmans, R., Eakin, C.M., Johnson, J., Marshall, P.A., Packer, G.R., Rea, A. and Willis, B.L., 2008. ReefTemp: An interactive monitoring system for coral bleaching using high-resolution SST and improved stress predictors. *Geophysical Research Letters*, 35(5).
- Maynard, J.A., Anthony, K.R.N., Marshall, P.A. and Masiri, I., 2008. Major bleaching events can lead to increased thermal tolerance in corals. *Marine Biology*, 155(2), pp.173-182.
- Mcallister, D.E., 1991. What is the status of the world's coral reef fishes. *Sea Wind*, 5(1), pp.14-18.
- McTainsh, G., 1980. Harmattan dust deposition in northern Nigeria. *Nature*, 286(5773), pp.587-588.
- Moberg, F. and Folke, C., 1999. Ecological goods and services of coral reef ecosystems. *Ecological economics*, 29(2), pp.215-233.
- Middleton, N.J. and Chaudhary, Q.Z., 1988. Severe dust storm at Karachi, 31 May 1986. *Weather*, 43(8), pp.298-301.
- Miller, D.J. and Yellowlees, D., 1989. Inorganic nitrogen uptake by symbiotic marine cnidarians: a critical review. *Proceedings of the Royal Society of London B: Biological Sciences*, 237(1286), pp.109-125.
- Miller, J., Muller, E., Rogers, C., Waara, R., Atkinson, A., Whelan, K.R.T., Patterson, M. and Witcher, B., 2009. Coral disease following massive bleaching in 2005 causes 60% decline in coral cover on reefs in the US Virgin Islands. *Coral Reefs*, 28(4), p.925.
- Miller, J., Waara, R., Muller, E. and Rogers, C., 2006. Coral bleaching and disease combine to cause extensive mortality on reefs in US Virgin Islands. *Coral Reefs*, 25(3), pp.418-418.
- Mitchell, J.M., 1971. The effect of atmospheric particles on radiation and temperature. *Man's Inspection on the Climate, edited by: Mathews WH, Kellogg WW and Robinson GD, MIT Press, Cambridge*, pp.295-301.

- Mohammadizadeh, M., Tavakoli-Kolour, P. and Rezai, H., 2013. Coral reefs and community around Iarak Island (Persian Gulf). *Caspian Journal of Applied Sciences Research*, 2(11).
- Moradi, M. and Kabiri, K., 2015. Spatio-temporal variability of SST and Chlorophyll-a from MODIS data in the Persian Gulf. *Marine pollution bulletin*, 98(1), pp.14-25.
- Morales, C., 1979. Saharan dust. *Scope*, 14, pp.298-301.
- Moriarty, D.J.W., Pollard, P.C., Hunt, W.G., Moriarty, C.M. and Wassenberg, T.J., 1985. Productivity of bacteria and microalgae and the effect of grazing by holothurians in sediments on a coral reef flat. *Marine Biology*, 85(3), pp.293-300.
- Muller-Parker, G., D'elia, C.F. and Cook, C.B., 2015. Interactions between corals and their symbiotic algae. In *Coral Reefs in the Anthropocene* (pp. 99-116). Springer Netherlands.
- Mumby, P.J., 1999. Bleaching and hurricane disturbances to populations of coral recruits in Belize. *Marine Ecology Progress Series*, pp.27-35.
- Murty, T.S. and El-Sabh, M.I., 1984. Storm tracks, storm surges and sea state in the Arabian Gulf, Strait of Hormuz and the Gulf of Oman. *UNESCO reports in Marine Sciences*, 28, pp.12-24.
- Muscantine, L., Falkowski, P.G., Porter, J.W. and Dubinsky, Z., 1984. Fate of photosynthetic fixed carbon in light-and shade-adapted colonies of the symbiotic coral *Stylophora pistillata*. *Proceedings of the Royal Society of London B: Biological Sciences*, 222(1227), pp.181-202.
- Muscantine, L., Falkowski, P.G., Dubinsky, Z., Cook, P.A. and McCloskey, L.R., 1989. The effect of external nutrient resources on the population dynamics of zooxanthellae in a reef coral. *Proceedings of the Royal Society of London B: Biological Sciences*, 236(1284), pp.311-324.
- Muscantine, L., 1990. The role of symbiotic algae in carbon and energy flux in reef corals. *Coral reefs*.
- Nakamura, T. and Van Woesik, R., 2001. Water-flow rates and passive diffusion partially explain differential survival of corals during the 1998 bleaching event. *Marine Ecology Progress Series*, 212, pp.301-304.
- Nakamura, T., Van Woesik, R. and Yamasaki, H., 2005. Photoinhibition of photosynthesis is reduced by water flow in the reef-building coral *Acropora digitifera*. *Marine Ecology Progress Series*, 301, pp.109-118.
- Nakamura, T., Yamasaki, H. and Van Woesik, R., 2003. Water flow facilitates recovery from bleaching in the coral *Stylophora pistillata*. *Marine Ecology Progress Series*, 256, pp.287-291.
- NASA Goddard Space Flight Center, Ocean Ecology Laboratory, Ocean Biology Processing Group. Sea-viewing Wide Field-of-view Sensor (SeaWiFS NASA OB. DAAC, Greenbelt, MD, USA. Accessed on 06/07/2017
- Nasrallah, H.A., Nieplova, E. and Ramadan, E., 2004. Warm season extreme temperature events in Kuwait. *Journal of Arid Environments*, 56(2), pp.357-371.
- Neuer, S., Torres-Padrón, M.E., Gelado-Caballero, M.D., Rueda, M.J., Hernández-Brito, J., Davenport, R. and Wefer, G., 2004. Dust deposition pulses to the eastern subtropical North Atlantic gyre: Does ocean's biogeochemistry respond?. *Global Biogeochemical Cycles*, 18(4).
- Nezlin, N.P. and Li, B.L., 2003. Time-series analysis of remote-sensed chlorophyll and

- environmental factors in the Santa Monica–San Pedro Basin off Southern California. *Journal of Marine Systems*, 39(3), pp.185-202.
- Nezlin, N.P., Polikarpov, I.G. and Al-Yamani, F., 2007. Satellite-measured chlorophyll distribution in the Arabian Gulf: spatial, seasonal and inter-annual variability. *International Journal of Oceans and Oceanography*, 2(1), pp.139-156.
- Nezlin, N.P., Polikarpov, I.G., Al-Yamani, F.Y., Rao, D.S. and Ignatov, A.M., 2010. Satellite monitoring of climatic factors regulating phytoplankton variability in the Arabian (Persian) Gulf. *Journal of Marine Systems*, 82(1), pp.47-60.
- Nicholls, N., Glantz, M.H. and Katz, R.W. eds., 1991. *Teleconnections Linking Worldwide Climate Anomalies: Scientific Basis and Societal Impact*. Cambridge University Press.
- Nishino, S., Kawaguchi, Y., Inoue, J., Hirawake, T., Fujiwara, A., Futsuki, R., Onodera, J. and Aoyama, M., 2015. Nutrient supply and biological response to wind-induced mixing, inertial motion, internal waves, and currents in the northern Chukchi Sea. *Journal of Geophysical Research: Oceans*, 120(3), pp.1975-1992.
- O'Reilly, J.E., Maritorena, S., Mitchell, B.G., Siegel, D.A., Carder, K.L., Garver, S.A., Kahru, M. and McClain, C., 1998. Ocean color chlorophyll algorithms for SeaWiFS. *Journal of Geophysical Research: Oceans*, 103(C11), pp.24937-24953.
- Paasche, E., 1973. Silicon and the ecology of marine plankton diatoms. I. *Thalassiosira pseudonana* (*Cyclotella nana*) grown in a chemostat with silicate as limiting nutrient. *Marine biology*, 19(2), pp.117-126.
- Paerl, H.W., 1997. Coastal eutrophication and harmful algal blooms: Importance of atmospheric deposition and groundwater as “new” nitrogen and other nutrient sources. *Limnology and oceanography*, 42(5part2), pp.1154-1165.
- Park, S.U. and In, H.J., 2003. Parameterization of dust emission for the simulation of the yellow sand (Asian dust) event observed in March 2002 in Korea. *Journal of Geophysical Research: Atmospheres*, 108(D19).
- Prakash, P.J., Stenchikov, G., Kalenderski, S., Osipov, S. and Bangalath, H., 2014. The impact of dust storms on the Arabian Peninsula and the Red Sea. *Atmospheric Chemistry & Physics Discussions*, 14(13).
- Parkhill, J.P., Maillet, G. and Cullen, J.J., 2001. Fluorescence-based maximal quantum yield for PSII as a diagnostic of nutrient stress. *Journal of Phycology*, 37(4), pp.517-529.
- Parkinson, C.L., Ward, A. and King, M.D., 2006. Earth science reference handbook: a guide to NASA's earth science program and earth observing satellite missions. *National Aeronautics and Space Administration*, p.277.
- Patterson, M.R., 1992. A mass transfer explanation of metabolic scaling relations in some aquatic invertebrates and algae. *Science*, pp.1421-1423.
- Patterson, K.L., Porter, J.W., Ritchie, K.B., Polson, S.W., Mueller, E., Peters, E.C., Santavy, D.L. and Smith, G.W., 2002. The etiology of white pox, a lethal disease of the Caribbean elkhorn coral, *Acropora palmata*. *Proceedings of the National Academy of Sciences*, 99(13), pp.8725-8730.
- Pettay, D.T., Wham, D.C., Smith, R.T., Iglesias-Prieto, R. and LaJeunesse, T.C., 2015. Microbial invasion of the Caribbean by an Indo-Pacific coral zooxanthella. *Proceedings of the National Academy of Sciences*, 112(24), pp.7513-7518.

- Perry, K.D., Cahill, T.A., Eldred, R.A., Dutcher, D.D. and Gill, T.E., 1997. Long-range transport of North African dust to the eastern United States. *Journal of Geophysical Research: Atmospheres*, 102(D10), pp.11225-11238.
- Perrone, T.J., 1979. *Winter shamal in the Persian Gulf* (No. NEPRF-TR-79-06). Naval Environmental Prediction Research Facility Monterey CA.
- Pettorelli, N., Laurance, W.F., O'Brien, T.G., Wegmann, M., Nagendra, H. and Turner, W., 2014. Satellite remote sensing for applied ecologists: opportunities and challenges. *Journal of Applied Ecology*, 51(4), pp.839-848.
- Phlips, E.J. and Mitsui, A., 1983. Role of light intensity and temperature in the regulation of hydrogen photoproduction by the marine cyanobacterium *Oscillatoria* sp. strain Miami BG7. *Applied and environmental microbiology*, 45(4), pp.1212-1220.
- Pitta, P., Kanakidou, M., Mihalopoulos, N., Christodoulaki, S., Dimitriou, P.D., Frangoulis, C., Giannakourou, A., Kagiorgi, M., Lagaria, A., Nikolaou, P. and Papageorgiou, N., 2017. Saharan Dust Deposition Effects on the Microbial Food Web in the Eastern Mediterranean: A Study Based on a Mesocosm Experiment. *Frontiers in Marine Science*, 4, p.117.
- Porter, J.W., Battey, J.F. and Smith, G.J., 1982. Perturbation and change in coral reef communities. *Proceedings of the National Academy of Sciences*, 79(5), pp.1678-1681.
- Prospero, J.M., 1996. The atmospheric transport of particles to the ocean. *Scope-scientific committee on problems of the environment international council of Scientific unions*, 57, pp.19-52.
- Prospero, J.M., Glaccum, R.A. and Nees, R.T., 1981. Atmospheric transport of soil dust from Africa to South America. *Nature*, 289(5798), pp.570-572.
- Prospero, J.M., Nees, R.T. and Uematsu, M., 1987. Deposition rate of particulate and dissolved aluminum derived from Saharan dust in precipitation at Miami, Florida. *Journal of Geophysical Research: Atmospheres*, 92(D12), pp.14723-14731.
- Purkis, S.J. and Riegl, B.M., 2012. Geomorphology and reef building in the SE Gulf. In *Coral Reefs of the Gulf* (pp. 33-50). Springer Netherlands.
- Purser, B.H. and Seibold, E., 1973. The principal environmental factors influencing Holocene sedimentation and diagenesis in the Persian Gulf. In *The Persian Gulf* (pp. 1-9). Springer, Berlin, Heidelberg.
- Pye, K., 2015. *Aeolian dust and dust deposits*. Elsevier.
- Rabalais, N.N., Turner, R.E., Justić, D., Dortch, Q., Wiseman, W.J. and Gupta, B.K.S., 1996. Nutrient changes in the Mississippi River and system responses on the adjacent continental shelf. *Estuaries*, 19(2), pp.386-407.
- Ransom, K.P. and Mangi, S.C., 2010. Valuing recreational benefits of coral reefs: the case of Mombasa Marine National Park and Reserve, Kenya. *Environmental management*, 45(1), pp.145-154.
- Rees, W.G., 2013. *Physical principles of remote sensing*. Cambridge University Press.
- Redfield, A.C., 1958. The biological control of chemical factors in the environment. *American scientist*, 46(3), pp.230A-221.
- Reynolds, C.S., 1984. *The ecology of freshwater phytoplankton*. Cambridge University Press.
- Reynolds, R.M., 1993. Physical oceanography of the Gulf, Strait of Hormuz, and the Gulf of Oman—Results from the Mt Mitchell expedition. *Marine Pollution Bulletin*, 27,

- pp.35-59.
- Rezai, H., Wilson, S., Claereboudt, M. and Riegl, B., 2004. Coral reef status in the ROPME sea area: Arabian/Persian Gulf, Gulf of Oman and Arabian Sea. *Status of coral reefs of the world, 1*, pp.155-170.
- Richardson, L.L., 1998. Coral diseases: what is really known?. *Trends in Ecology & Evolution, 13*(11), pp.438-443.
- Richardson, L.L., 1997. Occurrence of the black band disease cyanobacterium on healthy corals of the Florida Keys. *Bulletin of Marine Science, 61*(2), pp.485-490.
- Richlen, M.L., Morton, S.L., Jamali, E.A., Rajan, A. and Anderson, D.M., 2010. The catastrophic 2008–2009 red tide in the Arabian Gulf region, with observations on the identification and phylogeny of the fish-killing dinoflagellate *Cochlodinium polykrikoides*. *Harmful algae, 9*(2), pp.163-172.
- Riegl, B., 2003. Climate change and coral reefs: different effects in two high-latitude areas (Arabian Gulf, South Africa). *Coral reefs, 22*(4), pp.433-446.
- Riegl, B., 2002. Effects of the 1996 and 1998 positive sea-surface temperature anomalies on corals, coral diseases and fish in the Arabian Gulf (Dubai, UAE). *Marine biology, 140*(1), pp.29-40.
- Riegl, B., 1999. Corals in a non-reef setting in the southern Arabian Gulf (Dubai, UAE): fauna and community structure in response to recurring mass mortality. *Coral Reefs, 18*(1), pp.63-73.
- Riegl, B. and Purkis, S., 2015. Coral population dynamics across consecutive mass mortality events. *Global change biology, 21*(11), pp.3995-4005.
- Riegl, B.M., Purkis, S.J., Al-Cibahy, A.S., Al-Harthi, S., Grandcourt, E., Al-Sulaiti, K., Baldwin, J. and Abdel-Moati, A.M., 2012. Coral bleaching and mortality thresholds in the SE Gulf: highest in the world. In *Coral Reefs of the Gulf* (pp. 95-105). Springer Netherlands.
- Riegl, B.M. and Purkis, S.J., 2012. Dynamics of Gulf coral communities: observations and models from the world's hottest coral sea. In *Coral Reefs of the Gulf* (pp. 71-93). Springer Netherlands.
- Riegl, B.M., Bruckner, A.W., Samimi-Namin, K. and Purkis, S.J., 2012. Diseases, harmful algae blooms (HABs) and their effects on Gulf coral populations and communities. In *Coral Reefs of the Gulf* (pp. 107-125). Springer Netherlands.
- Riegl, B.M. and Purkis, S.J., 2012. Coral reefs of the Gulf: adaptation to climatic extremes in the world's hottest sea. In *Coral Reefs of the Gulf* (pp. 1-4). Springer Netherlands.
- Riegl, B.M. and Purkis, S.J., 2012. Environmental constraints for reef building in the Gulf. In *Coral Reefs of the Gulf* (pp. 5-32). Springer Netherlands.
- Riegl, B.M., Purkis, S.J., Al-Cibahy, A.S., Abdel-Moati, M.A. and Hoegh-Guldberg, O., 2011. Present limits to heat-adaptability in corals and population-level responses to climate extremes. *PloS one, 6*(9), p.e24802.
- Riegl, B.M. and Purkis, S.J., 2009. Model of coral population response to accelerated bleaching and mass mortality in a changing climate. *ecological modelling, 220*(2), pp.192-208.
- Riegl, B., Glynn, P.W., Wieters, E., Purkis, S., d'Angelo, C. and Wiedenmann, J., 2015. Water column productivity and temperature predict coral reef regeneration across the Indo-Pacific. *Scientific reports, 5*.
- Robarts, R.D. and Zohary, T., 1987. Temperature effects on photosynthetic capacity,

- respiration, and growth rates of bloom-forming cyanobacteria. *New Zealand Journal of Marine and Freshwater Research*, 21(3), pp.391-399.
- Robinson, A.R., 2006. *The global coastal ocean: interdisciplinary regional studies and syntheses* (Vol. 14). Harvard University Press.
- ROPME, 2012. ROPME Oceanographic Cruise - Winter 2006, Technical Report : No. 4, Spatial Distribution of Chlorophyll-a in the ROPME Sea Area. Kuwait Inst. Sci. Res. KISR Rep. 8655, 1–59.
- Rosenberg, E. and Ben-Haim, Y., 2002. Microbial diseases of corals and global warming. *Environmental microbiology*, 4(6), pp.318-326.
- Rosset, S., Wiedenmann, J., Reed, A.J. and D'Angelo, C., 2017. Phosphate deficiency promotes coral bleaching and is reflected by the ultrastructure of symbiotic dinoflagellates. *Marine Pollution Bulletin*, 118(1), pp.180-187.
- Rowan, R., 1998. Diversity and ecology of zooxanthellae on coral reefs. *Journal of Phycology*, 34(3), pp.407-417.
- Roy, S., Bhattacharya, S., Das, P. and Chattopadhyay, J., 2007. Interaction among non-toxic phytoplankton, toxic phytoplankton and zooplankton: inferences from field observations. *Journal of Biological physics*, 33(1), pp.1-17.
- Sabine, A.M., Smith, T.B., Williams, D.E. and Brandt, M.E., 2015. Environmental conditions influence tissue regeneration rates in scleractinian corals. *Marine pollution bulletin*, 95(1), pp.253-264.
- Sahay, A., Mishra, M.K., Chauhan, P. and Ajai, 2014. Absorption characteristics of ocean water in the Arabian Sea during winter bloom from in situ measurements and Oceansat 2 OCM and MODIS data. *International journal of remote sensing*, 35(9), pp.2982-2995.
- Sale, P.F., Feary, D.A., Burt, J.A., Bauman, A.G., Cavalcante, G.H., Drouillard, K.G., Kjerfve, B., Marquis, E., Trick, C.G., Usseglio, P. and Lavieren, H.V., 2011. The growing need for sustainable ecological management of marine communities of the Persian Gulf. *AMBIO: A Journal of the Human Environment*, 40(1), pp.4-17.
- Saydam, A.C. and Senyuva, H.Z., 2002. Deserts: Can they be the potential suppliers of bioavailable iron?. *Geophysical research letters*, 29(11).
- Schultz, G.A. and Engman, E.T. eds., 2012. *Remote sensing in hydrology and water management*. Springer Science & Business Media.
- Schowengerdt, R.A., 2006. *Remote sensing: models and methods for image processing*. Academic press.
- Seibold, E., 1973. Sedimentation in the Persian Gulf. *J Mar Biol Ass India*, 15(2), pp.621-624.
- Sedigh Marvasti, S., Gnanadesikan, A., Bidokhti, A.A., Dunne, J.P. and Ghader, S., 2016. Challenges in modeling spatiotemporally varying phytoplankton blooms in the Northwestern Arabian Sea and Gulf of Oman. *Biogeosciences*, 13(4), pp.1049-1069.
- Sharifinia, M., Penchah, M.M., Mahmoudifard, A., Gheibi, A. and Zare, R., 2015. Monthly variability of chlorophyll- α concentration in Persian Gulf using remote sensing techniques. *Sains Malaysiana*, 44(3), pp.387-397.
- Sheppard, C., Al-Husiani, M., Al-Jamali, F., Al-Yamani, F., Baldwin, R., Bishop, J., Benzoni, F., Dutrieux, E., Dulvy, N.K., Durvasula, S.R.V. and Jones, D.A., 2010. The Gulf: a young sea in decline. *Marine Pollution Bulletin*, 60(1), pp.13-38.
- Sheppard, C. and Loughland, R., 2002. Coral mortality and recovery in response to

- increasing temperature in the southern Arabian Gulf. *Aquatic Ecosystem Health & Management*, 5(4), pp.395-402.
- Sheppard, C., Price, A. and Roberts, C., 1992. Marine ecology of the Arabian region: patterns and processes in extreme tropical environments.
- Sheppard, C. and Rayner, N.A., 2002. Utility of the Hadley Centre sea ice and sea surface temperature data set (HadISST1) in two widely contrasting coral reef areas. *Marine pollution bulletin*, 44(4), pp.303-308.
- Sheppard, C.R., 2003. Predicted recurrences of mass coral mortality in the Indian Ocean. *Nature*, 425(6955), p.294.
- Sheppard, C.R., 1993. Physical environment of the Gulf relevant to marine pollution: an overview. *Marine Pollution Bulletin*, 27, pp.3-8.
- Shick, J.M., Iglic, K., Wells, M.L., Trick, C.G., Doyle, J. and Dunlap, W.C., 2011. Responses to iron limitation in two colonies of *Stylophora pistillata* exposed to high temperature: Implications for coral bleaching. *Limnology and Oceanography*, 56(3), pp.813-828.
- Shinn, E.A., 1976. Coral reef recovery in Florida and the Persian Gulf. *Environmental Geology*, 1(4), p.241.
- Shinn, E.A., 1973. Sedimentary accretion along the leeward, SE coast of Qatar Peninsula, Persian Gulf. In *The Persian Gulf* (pp. 199-209). Springer, Berlin, Heidelberg.
- Shinn, E.A., Smith, G.W., Prospero, J.M., Betzer, P., Hayes, M.L., Garrison, V. and Barber, R.T., 2000. African dust and the demise of Caribbean coral reefs. *Geophysical Research Letters*, 27(19), pp.3029-3032.
- Shuail, D., Wiedenmann, J., D'angelo, C., Baird, A.H., Pratchett, M.S., Riegl, B., Burt, J.A., Petrov, P. and Amos, C., 2016. Local bleaching thresholds established by remote sensing techniques vary among reefs with deviating bleaching patterns during the 2012 event in the Arabian/Persian Gulf. *Marine pollution bulletin*, 105(2), pp.654-659.
- Singh, R.P., Prasad, A.K., Kayetha, V.K. and Kafatos, M., 2008. Enhancement of oceanic parameters associated with dust storms using satellite data. *Journal of Geophysical Research: Oceans*, 113(C11).
- Smayda, T.J., 1997. Harmful algal blooms: their ecophysiology and general relevance to phytoplankton blooms in the sea. *Limnology and oceanography*, 42(5part2), pp.1137-1153.
- Smith, G.W., Ives, L.D., Nagelkerken, I.A. and Ritchie, K.B., 1996. Caribbean sea-fan mortalities. *Nature*, 383(6600), pp.487-487.
- Smith, S.V., Kimmerer, W.J., Laws, E.A., Brock, R.E. and Walsh, T.W., 1981. Kaneohe Bay sewage diversion experiment: perspectives on ecosystem responses to nutritional perturbation. *Pacific Science*, 35(4), pp.279-395.
- Spalding, M.D. and Grenfell, A.M., 1997. New estimates of global and regional coral reef areas. *Coral Reefs*, 16(4), pp.225-230.
- Spalding, M., Ravilious, C. and Green, E.P., 2001. *World atlas of coral reefs*. Univ of California Press.
- Stanhill, G. and Cohen, S., 2001. Global dimming: a review of the evidence for a widespread and significant reduction in global radiation with discussion of its probable causes and possible agricultural consequences. *Agricultural and forest meteorology*, 107(4), pp.255-278.

- Stumpf, R.P., Arnone, R.A., Gould, R.W., Martinolich, P.M. and Ransibrahmanakul, V., 2003. A partially coupled ocean-atmosphere model for retrieval of water-leaving radiance from SeaWiFS in coastal waters. *NASA Tech. Memo*, 206892, pp.51-59.
- Survey, U.S.G., 2005. Landsat 8 (L8) Data Users Handbook. America (NY). 8, 1993–1993.
- Szmant, A.M., 2002. Nutrient enrichment on coral reefs: is it a major cause of coral reef decline?. *Estuaries*, 25(4), pp.743-766.
- Taft, J.L., Taylor, W.R., Hartwig, E.O. and Loftus, R., 1980. Seasonal oxygen depletion in Chesapeake Bay. *Estuaries and Coasts*, 3(4), pp.242-247.
- Taylor, D.L., 1974. Symbiotic marine algae: taxonomy and biological fitness. *Symbiosis in the Sea*, pp.245-262.
- Tegen, I., Werner, M., Harrison, S.P. and Kohfeld, K.E., 2004. Relative importance of climate and land use in determining present and future global soil dust emission. *Geophysical Research Letters*, 31(5).
- Tchernov, D., Gorbunov, M.Y., de Vargas, C., Yadav, S.N., Milligan, A.J., Häggblom, M. and Falkowski, P.G., 2004. Membrane lipids of symbiotic algae are diagnostic of sensitivity to thermal bleaching in corals. *Proceedings of the National Academy of Sciences of the United States of America*, 101(37), pp.13531-13535.
- Tchernov, D., Kvitt, H., Haramaty, L., Bibby, T.S., Gorbunov, M.Y., Rosenfeld, H. and Falkowski, P.G., 2011. Apoptosis and the selective survival of host animals following thermal bleaching in zooxanthellate corals. *Proceedings of the National Academy of Sciences*, 108(24), pp.9905-9909.
- Thompson, S., 2008. Globalization, Economics and Museums: Saadiyat Island's Cultural District in Abu Dhabi, UAE. *International Journal of the Arts in Society*, 3(3), pp.21-26.
- Thoppil, P.G. and Hogan, P.J., 2010. Persian Gulf response to a wintertime Shamal wind event. *Deep Sea Research Part I: Oceanographic Research Papers*, 57(8), pp.946-955.
- Thoppil, P.G. and Hogan, P.J., 2010. A modeling study of circulation and eddies in the Persian Gulf. *Journal of Physical Oceanography*, 40(9), pp.2122-2134.
- Titgen, R., 1983. The systematic and ecology of the decapods of Dubai, and their zoogeographic relationships to the Arabian Gulf and the Western Indian Ocean (United Arab Emirates).
- Tratt, D.M., Frouin, R.J. and Westphal, D.L., 2001. April 1998 Asian dust event: A southern California perspective. *Journal of Geophysical Research: Atmospheres*, 106(D16), pp.18371-18379.
- Trench, R.K., 1993. Microalgal-invertebrate symbioses-a review. *Endocytobiosis and Cell Research*, 9(2-3), pp.135-175.
- Trench, R.K., 1979. The cell biology of plant-animal symbiosis. *Annual Review of Plant Physiology*, 30(1), pp.485-531.
- Turner, S.M., Nightingale, P.D., Spokes, L.J., Liddicoat, M.I. and Liss, P.S., 1996. Increased dimethyl sulphide concentrations in sea water from in situ iron enrichment. *Nature*, 383(6600), pp.513-517.
- Uno, I., Amano, H., Emori, S., Kinoshita, K., Matsui, I. and Sugimoto, N., 2001. Trans-Pacific yellow sand transport observed in April 1998: a numerical simulation. *Journal of Geophysical Research: Atmospheres*, 106(D16), pp.18331-18344.
- Uno, I., Harada, K., Satake, S., Hara, Y. and Wang, Z., 2005. Meteorological

- characteristics and dust distribution of the Tarim Basin simulated by the nesting RAMS/CFORS dust model. *Journal of the Meteorological Society of Japan. Ser. II*, 83, pp.219-239.
- Van Hooedonk, R., Maynard, J.A. and Planes, S., 2013. Temporary refugia for coral reefs in a warming world. *Nature Climate Change*, 3(5), pp.508-511.
- Van Lavieren, H., Burt, J., Feary, D.A., Cavalcante, G., Marquis, E., Benedetti, L., Trick, C., Kjerfve, B. and Sale, P.F., 2011. Managing the growing impacts of development on fragile coastal and marine ecosystems: Lessons from the Gulf.
- Van Mol, B., Ruddick, K., Astoreca, R., Park, Y. and Nechad, B., 2007. Optical detection of a *Noctiluca scintillans* bloom. *EARSeL eProceedings*, 6(2), p.130.
- Van Woesik, R. and Koksai, S., 2006. A coral population response (CPR) model for thermal stress. *Coral Reefs and Climate Change: Science and Management*, pp.129-144.
- Veron, J.E.N., 2000. Coral of the World, 3 vols. *Australia Institute of Marine Sciences, Townsville, Australia*.
- Volpe, G., Santoleri, R., Vellucci, V., d'Alcalà, M.R., Marullo, S. and d'Ortenzio, F., 2007. The colour of the Mediterranean Sea: Global versus regional bio-optical algorithms evaluation and implication for satellite chlorophyll estimates. *Remote Sensing of Environment*, 107(4), pp.625-638.
- Wang, Z., Ueda, H. and Huang, M., 2000. A deflation module for use in modeling long-range transport of yellow sand over East Asia. *Journal of Geophysical Research: Atmospheres*, 105(D22), pp.26947-26959.
- Wang, C., 2013. Impact of anthropogenic absorbing aerosols on clouds and precipitation: A review of recent progresses. *Atmospheric research*, 122, pp.237-249.
- Wang, M., 1999. A sensitivity study of the SeaWiFS atmospheric correction algorithm: effects of spectral band variations. *Remote sensing of environment*, 67(3), pp.348-359.
- Wang, J. and Christopher, S.A., 2003. Intercomparison between satellite-derived aerosol optical thickness and PM_{2.5} mass: implications for air quality studies. *Geophysical research letters*, 30(21).
- Wang, M., Son, S. and Harding, L.W., 2009. Retrieval of diffuse attenuation coefficient in the Chesapeake Bay and turbid ocean regions for satellite ocean color applications. *Journal of Geophysical Research: Oceans*, 114(C10).
- Wang, C., 2013. Impact of anthropogenic absorbing aerosols on clouds and precipitation: A review of recent progresses. *Atmospheric research*, 122, pp.237-249.
- Walker, J.C. and Brimblecombe, P., 1985. Iron and sulfur in the pre-biologic ocean. *Precambrian Research*, 28(3-4), pp.205-222.
- Weir-Brush, J.R., Garrison, V.H., Smith, G.W. and Shinn, E.A., 2004. The relationship between gorgonian coral (Cnidaria: Gorgonacea) diseases and African dust storms. *Aerobiologia*, 20(2), pp.119-126.
- Werdell, P.J., Fargion, G.S., McClain, C.R. and Bailey, S.W., 2002. The SeaWiFS bio-optical archive and storage system (SeaBASS): Current architecture and implementation.
- West, J.M. and Salm, R.V., 2003. Resistance and resilience to coral bleaching: implications for coral reef conservation and management. *Conservation Biology*, 17(4), pp.956-967.

- Wiedenmann, J., D'angelo, C., Smith, E.G., Hunt, A.N., Legiret, F.E., Postle, A.D. and Achterberg, E.P., 2013. Nutrient enrichment can increase the susceptibility of reef corals to bleaching. *Nature Climate Change*, 3(2), p.160.
- Wilkinson, C.R. and Buddemeier, R.W., 1994. *Global Climate Change and Coral Reefs: Implications for People and Reefs: Report of the UNEP-IOC-ASPEI-IUCN Global Task Team on the Implications of Climate Change on Coral Reefs*. IUCN.
- Wilkinson, C., 2000. *Status of coral reefs of the world: 2000*.
- Wilkinson, C.R. and Souther, D.N. eds., 2008. *Status of Caribbean coral reefs after bleaching and hurricanes in 2005* (Vol. 148). Global Coral Reef Monitoring Network.
- Wilkinson, C.C., 2004. *Status of coral reefs of the world: 2004*. Australian Institute of Marine Science (AIMS).
- Wilkinson, C.C., 2001. The 1997-1998 mass bleaching event around the world. *Status coral reefs world 1998* 15–38.
- Wilkinson, C.R., 1999. Global and local threats to coral reef functioning and existence: review and predictions. *Marine and Freshwater Research*, 50(8), pp.867-878.
- Wong, C.S. and Matear, R.J., 1999. Sporadic silicate limitation of phytoplankton productivity in the subarctic NE Pacific. *Deep Sea Research Part II: Topical Studies in Oceanography*, 46(11), pp.2539-2555.
- Wooldridge, S.A., 2009. Water quality and coral bleaching thresholds: Formalising the linkage for the inshore reefs of the Great Barrier Reef, Australia. *Marine Pollution Bulletin*, 58(5), pp.745-751.
- Young, R.W., Carder, K.L., Betzer, P.R., Costello, D.K., Duce, R.A., DiTullio, G.R., Tindale, N.W., Laws, E.A., Uematsu, M., Merrill, J.T. and Feely, R.A., 1991. Atmospheric iron inputs and primary productivity: Phytoplankton responses in the North Pacific. *Global Biogeochemical Cycles*, 5(2), pp.119-134.
- Zanter, K., 2005. Landsat 8 (L8) data users handbook. *LSDS-1574 Version, 1*.
- Zhang, C., Hu, C., Shang, S., Müller-Karger, F.E., Li, Y., Dai, M., Huang, B., Ning, X. and Hong, H., 2006. Bridging between SeaWiFS and MODIS for continuity of chlorophyll-a concentration assessments off Southeastern China. *Remote Sensing of Environment*, 102(3), pp.250-263.
- Zhang, X.Y., Gong, S.L., Shen, Z.X., Mei, F.M., Xi, X.X., Liu, L.C., Zhou, Z.J., Wang, D., Wang, Y.Q. and Cheng, Y., 2003. Characterization of soil dust aerosol in China and its transport and distribution during 2001 ACE-Asia: 1. Network observations. *Journal of Geophysical Research: Atmospheres*, 108(D9).
- Zhao, J. and Ghedira, H., 2014. Monitoring red tide with satellite imagery and numerical models: A case study in the Arabian Gulf. *Marine pollution bulletin*, 79(1), pp.305-313.
- Zhuang, G., Yi, Z., Duce, R. A., Brown, P.R., 1992. Link between iron and sulphur cycles suggested by detection of Fe(II) in remote marine aerosols. *Nature* 355(6360), p.537.

